UNCLASSIFIED

AD NUMBER

AD821628

NEW LIMITATION CHANGE

TO

Approved for public release, distribution unlimited

FROM

Distribution authorized to U.S. Gov't. agencies and their contractors; Critical Technology; SEP 1967. Other requests shall be referred to Air Force Materials Lab., AFSC, Wright-Patterson AFB, OH 45433.

AUTHORITY

AFML ltr, 12 Jan 1972

THIS PAGE IS UNCLASSIFIED

DEVELOPMENT OF COATINGS FOR COLUMBIUM BASE ALLOYS PART I–BASIC PROPERTY MEASUREMENTS AND COATING SYSTEM DEVELOPMENT

AD821628

A. R. Stetson and A. G. Metcalfe
Solar Division of International Harvester Company

TECHNICAL REPORT AFML-TR-67-139, Part I

September 1967

This document is subject to special export controls and each transmittal to foreign governments or foreign nationals may be made only with prior approval of the Metals and Ceramics Division (MAM), Air Force Materials Laboratory, Wright-Patterson Air Force Base, Ohio 45433.

Air Force Materials Laboratory
Research and Technology Division
Air Force Systems Command
Wright-Patterson Air Force Base, Ohio

NOTICES

When Government drawings, specifications, or other data are used for any purpose other than in connection with a definitely related Government procurement operation, the United States Government thereby incurs no responsibility nor any obligation whatsoever; and the fact that the Government may have formulated, furnished, or in any way supplied the said drawings, specifications, or other data, is not to be regarded by implication or otherwise as in any manner licensing the holder or any other person or corporation, or conveying any rights or permission to manufacture, use, or sell any patented invention that may in any way be related thereto.

DDC release to CFSTI not authorized.

Copies of this report should not be returned unless return is required by security considerations, contractual obligations, or notice on a specific document.

AFML-TR-67-139, Part I

DEVELOPMENT OF COATINGS FOR COLUMBIUM BASE ALLOYS PART I–BASIC PROPERTY MEASUREMENTS AND COATING SYSTEM DEVELOPMENT

A. R. Stetson and A. G. Metcalfe
Solar Division of International Harvester Company

TECHNICAL REPORT AFML-TR-67-139, Part I

September 1967

This document is subject to special export controls and each transmittal to foreign governments or foreign nationals may be made only with prior approval of the Metals and Ceramics Division (MAM), Air Force Materials Laboratory, Wright-Patterson Air Force Base, Ohio 45433.

Air Force Materials Laboratory
Research and Technology Division
Air Force Systems Command
Wright-Patterson Air Force Base, Ohio

FOREWORD

This Final Summary Report was prepared by the Research Laboratories at the Solar Division of International Harvester Company, under Air Force Contract AF33(615)-1598. The program was administered by the Air Force Materials Laboratory, with Mr. Norman M. Geyer (MAMP) acting as Project Engineer.

This report covers work conducted from 1 July 1964 to 31 October 1966. The report was released by the authors for publication in March 1967.

The program was divided into three phases:

- Phase I – Basic Property Studies and Coating System Development
- Phase II – Evaluation of a Selected Coating for Reentry Vehicles
- Phase III – Evaluation of Selected Coatings for Gas Turbine Engines

The data generated in each of these phases is presented in separate parts, but the Summary (Section II) in each part covers the entire program to provide every reader with the program scope.

The I. I. T. Research Institute (IITRI) cooperated with Solar in the program. The program at IITRI covered coating concepts and property data generation in systems deriving protection from an aluminum-containing reservoir. Mr. J. J. Rausch was the Program Manager at IITRI.

The program was jointly directed at Solar by A. R. Stetson and Dr. A. G. Metcalfe. The following personnel were major contributors to the experimental effort:

- At IITRI - J. J. Rausch, Project Manager; V. L. Hill, Research Metallurgist; and M. Zoiss, Project Technician.

- At Solar - Dr. A. G. Metcalfe, basic concepts and program coordination; A. R. Stetson, basic concepts and coating process development; Dr. Knut Osthagen, interdiffusion studies and property measurement; V. S. Moore, Phase II and III coating evaluations; W. D. Brentnall, basic studies on silicide systems; P. J. Mazzei, metallurgical analysis and fused salt deposition; D. Crociani, pack cementation; C. Antonick, oxidation and expansion measurements; R. Hutting, metallography.

Solar's internal report number is RDR-1380-6 Parts I, II, and III.

This technical report has been reviewed and is approved.

I. Perlmutter
Chief, Metals Branch
Air Force Materials Laboratory

[redacted]

ABSTRACT

The program was designed to originate protective coating concepts for columbium-base alloys for applications in aerospace environments and gas turbine engines. Thermal expansion and oxidation resistance was determined on potential ductile sublayer alloys, MAl and MAL_3 aluminides, and MSi_2 and M_5Si_3 silicides. Diffusion barriers between the Ti-Cr modifier and substrate were also evaluated. Coating systems evolved from the studies included the V-(80Cr-20Ti)-Si, (95Mo-5Ti)-Si, Mo-Cr-(Fe-25Cr-5Al) ductile all bcc system, V-(Cr-Ti)-Al-Si and other systems of lesser importance. The V-(80Cr-20Ti)-Si system was the most extensively studied. It exhibited the potential for 500 plus hours of protection at 1600 and 2400 F. This system was extensively evaluated for reentry (Part II) and turbojet (Part III) applications.

This abstract is subject to special export controls and each transmittal to foreign governments or foreign nationals may be made only with prior approval of the Metals and Ceramics Division (MAM), Air Force Materials Laboratory, Wright-Patterson AFB, Ohio 45433.

CONTENTS

SECTION		PAGE
I	INTRODUCTION	1
II	SUMMARY	5
	2.1 Summary of Phase I Work	8
	2.2 Phase II - Evaluation of the V-(Cr-Ti)-Si Coating for Aerospace Applications	15
	2.3 Phase III - Evaluation of the V-(Cr-Ti)-Si Coating for Gas Turbines	19
III	DEVELOPMENT OF COATING CONCEPTS	23
	3.1 Background	24
	3.2 Evaluation of Sublayer Properties	36
	3.3 Evaluation of Primary Oxidation Barriers	91
	3.4 Evaluation of all Body Centered Cubic System	128
	3.5 Selection of Coating Systems	136
IV	EXAMINATION OF SPECIAL NEW COATING SYSTEM	139
	4.1 Coating Containing Major Additions of Aluminum	140
	4.2 Aluminum-Containing Silicide Coatings	155
	4.3 The Silicide-Ceramic System	176
	4.4 Discussion of Special New Coating Systems	188
V	DEVELOPMENT OF SILICIDE COATING PROCESS	191
	5.1 The (Ti-Mo)-Si System	192
	5.2 The V-(Cr-Ti)-Si System	222
	5.3 Application of the V-(Cr-Ti)-Si Coating to Phase II and III Specimens	265
VI	CONCLUSIONS	275
	6.1 Diffusion Barrier for the Ti-Cr Modifier	275
	6.2 Substitution of Molybdenum for Chromium in the Ti-Cr Modifier Layer	275
	6.3 Substitution of Vanadium for Titanium in the Ti-Cr Modifier Layer	276
	6.4 Vanadium Modified Coatings	276

CONTENTS (Cont)

SECTION		PAGE
VI	CONCLUSIONS (Cont)	
	6.5 Gamma Sublayer Aluminide Coatings	277
	6.6 Ductile Metallic Coating System	277
	6.7 The Combination Aluminum-Silicon Coating	278
	6.8 The Ceramic Coating Overlay	278
	6.9 General Conclusions on Property Measurement Relative to Coating Performance	279
	REFERENCES	281
	APPENDIX	283

ILLUSTRATIONS

FIGURE		PAGE
1	Comparison of Cyclic Oxidation Life at 2400 F; Solar V-(Cr-Ti)-Si Coating and TRW (Ti-Cr)-Si Coating	6
2	Cyclic Oxidation Life at 2400 F; Solar V-(Cr-Ti)-Si Coating	7
3	Concentration-Penetration Profile of TRW D Coating on L-6 Alloy	26
4	Chromium-Titanium Binary System	27
5	Microstructure of the Heat Treated (Ti-Cr)-Si Coated B66 Specimens; Phase A	28
6	Partial Molal Free Energy of Formation of Solution of Oxygen with Various Transition Metals	29
7	Partial Molal Free Energies at 1500 K; Carbon in Transition Metals	31
8	Ratio of Disilicide Thermal Expansion to Expansion of Typical Columbium-Base Alloys	31
9	Oxidation Resistance of the Components of the (Ti-Cr)-Si Coating for Columbium Alloys	32
10	Commercial Columbium-Base Alloys Oxidized at 1600 F	40
11	Oxidation Rate Plots of Several Uncoated Substrate Alloys; 1600 F in Air	43
12	Columbium-Titanium-Chromium Alloys Oxidized at 1600 F	45
13	Columbium-Titanium-Molybdenum Alloys Oxidized at 1600 F	46
14	Columbium-Vanadium-Chromium Alloys Oxidized at 1600 F	47
15	Weight Gain After Two Hours at 1600 F in Air; Cb-Ti-Cr, Cb-Ti-Mo, and Cb-V-Cr Alloys	48
16	Columbium-Titanium-Chromium Alloys Arc Melted and Annealed Four Hours at 2300 F	49
17	Columbium, Titanium, Molybdenum Alloys Arc Melted and Annealed Four Hours at 2300 F	50
18	Columbium-Vanadium-Chromium Alloys Arc Melted and Annealed Four Hours at 2300 F	51
19	Microstructure of Various Columbium Alloys Containing Titanium, Vanadium and Chromium	52
20	Specimens of Sublayer Alloys Q1 through Q7 After Oxidation Testing at 1600 F	54

ILLUSTRATIONS (Cont)

FIGURE		PAGE
21	Oxidation Rate of Various Sublayer Alloys	56
22	Microstructure of Various Titanium, Vanadium, Chromium, and Columbium Alloys After Oxidation at 1600 F for 16 Hours	57
23	Summary Plot of Oxidation Rates at 1600 F of Sublayers and Substrates	58
24	Oxidation Rate of Columbium, Aluminum, and Titanium Solid Solutions at 1600 F in Air	62
25	Oxidation Rate of Columbium-Titanium-Chromium-Aluminum Alloy; One-Hour Cycles at 1600 to 2400 F	63
26	Oxidation Rate of Columbium-Titanium-Chromium Alloy; One-Hour Cycles at 1600 to 2400 F	63
27	Oxidation Rate of Columbium-Titanium-Aluminum Alloy; One-Hour Cycles at 1600 to 2400 F	64
28	Oxidation Rate Versus Temperature of Columbium Alloys for First One-Hour Cycle	65
29	Summary of the Most Oxidation Resistant Ductile Columbium Alloy Evaluated	68
30	Expansion of Titanium-Chromium Alloys	71
31	Diffusion Couples of Cb752, D43, and B66 Versus Ti-33Cr With Diffusion Barriers of Tantalum, Molybdenum, and Tungsten	73
32	Diffusion Couples of Cb752 Versus Titanium-Molybdenum and Titanium-Tungsten Alloys	78
33	Diffusion Couples of B66 Versus Titanium-Molybdenum and Titanium-Tungsten Alloys	79
34	Diffusion Couples of D43 Versus Titanium-Molybdenum and Titanium-Tungsten Alloys	80
35	Diffusion Couples of Cb752 Versus Titanium-Chromium and Vanadium-Chromium Alloys	81
36	Diffusion Couples of B66 Versus Titanium-Chromium and Vanadium-Chromium Alloys	32
37	Diffusion Couples of D43 Versus Titanium-Chromium and Vanadium-Chromium Alloys	83
38	Transverse and Longitudinal Sections of As-Received Cb132M Alloy	90
39	As-Bonded Cb132M-Titanium Diffusion Couple	90
40	Cb132M-Titanium Annealed 15 Hours at 2400 F	91

ILLUSTRATIONS (Cont)

FIGURE		PAGE
41	1500 F Oxidation of Various Disilicides	95
42	2400 F Oxidation of Various Disilicides	96
43	The Binary M_5Si_3 Silicides; Arc Melted and Annealed	98
44	The Ternary M_5Si_3 Silicides; Arc Melted and Annealed	99
45	The Quarternary M_5Si_3 Silicides; Arc Melted and Annealed	100
46	M_5Si_3 Silicides After 101 Hours at 1500 F in Air	102
47	M_5Si_3 Silicides After 101 Hours at 2400 F in Air	103
48	Microstructure of $(Ti_{0.9}, Mo_{0.1})_{0.45}$ $Al_{0.55}$ Alloy Oxidized 12 Hours at 2500 F	113
49	Microstructure of $(Ti_{0.8}, Mo_{0.2})_{0.45}Al_{0.55}$ Alloy Oxidized 12 Hours at 2500 F	113
50	Comparison of Craze Cracking in $MoSi_2$ and (Ti-Cr)-Si Coated Cb 752 Alloy	127
51	Microhardness Traverse Data for V-(Fe-25Cr-5Al) and Cr-(Fe-25Cr-5Al) Diffusion Couples	130
52	Hardness Traverse Data for Specimens Annealed in Vacuum at 2300 F	132
53	Hardness Traverse of Diffusion Bonded Specimens Oxidized in Static Air Eight Hours	133
54	Diffusion Bonded Specimen Oxidized Eight Hours at 2300 F	134
55	Diffusion Bonded Specimen Oxidized 10 Hours at 2450 F	134
56	Aluminized Cb-75 Atomic Percent Titanium Alloy Oxidized at 2300 F for 16 Hours	142
57	Cb-75 Atomic Percent Titanium Alloy Oxidized at 2300 F for One Hour	142
58	Cb-15Mo Alloy After Titanizing and Aluminizing	145
59	Cb-15Mo Alloy After Titanizing and Aluminizing	145
60	Specific Weight Gain Versus Time for the (Cb-15Mo)-Ti-Al Coating (2400 F)	146
61	Coating Formed on Cb-752 Using Cu-40Ti-10Mo-10Al Slurry	147
62	Coating Formed on Cb-752 Using Cu-44Ti-11Mo-4Al Slurry	148
63	Columbium Alloys Coated with Titanium and Aluminum and Annealed at 2400 F for 15 Hours	150
64	Columbium Alloys Coated with Aluminum and Annealed at 2400 F for 15 Hours	151
65	Titanium + Aluminum Coated Columbium Alloys	152

ILLUSTRATIONS (Cont)

FIGURE		PAGE
66	Yield Strength of Columbium Alloys at 2000 F	153
67	Silicided Cb-5Ti-4Al; IITRI13	158
68	Silicided Cb-10Ti-5Al; IITRI33	158
69	Silicided Cb-30Ti-5Al; IITRI35	158
70	Silicided Cb-40Ti-5Al; IITRI37	159
71	Silicided Cb-60Ti-10Al; IITRI38	159
72	Silicided Cb-20Ti-5Al; IITRI34	159
73	Electron Microprobe Scan of Cb-4Al-5Ti Alloy	160
74	Electron Microprobe Scan of Cb-5Al-10Ti Alloy	161
75	Electron Microprobe Scan of Cb-5Al-20Ti Alloy	162
76	Electron Microprobe Scan of Cb-5Al-30Ti Alloy	163
77	V-(Cr-Ti)-Al-Si Coating on D43 Alloy	170
78	D43 and Cb752 Specimens After 93 Hours at 2400 F	173
79	D43 Specimen After Additional 40 Hours (133 Total) at 2400 F	173
80	Cb752 Coated With V-(Cr-Ti)-Al-Si (14.0 mg/cm^2 Si) Oxidation Tested 83 Hours at 2400 F	174
81	D43 Coated With V-(Cr-Ti)-Al-Si (180 mg/cm^2 Si); 100 hrs at 2400 F	175
82	D43 and Cb752 Samples After 500 Hours at 1600 F; 16-Hour Cycles	176
83	V-(Cr-Ti)-Al-Si Coating on Cb752 Alloy: Oxidation Tested 509 Hours at 1600 F, 16-Hour Cycles	177
84	Typical As-Coated Appearance of Ceramic-Coated Cb752 Alloy	180
85	Typical Ceramic-Coated Specimen After Three Four-Hour Cycles at 2400 F	184
86	Typical Contact Area Failures of Ceramic Coatings After Three Four-Hour Cycles at 2400 F	185
87	Weight Change After Cyclic Oxidation	186
88	Typical Microstructure of Ceramic-Coated 0.012-Inch Cb752 Alloy	186
89	Typical Ceramic-Coated Cb752 Alloy After the 2400 F Test	187
90	Typical Graphite-Lined Inconel Retort	195
91	Cycle Purging and Pressure Control Fixtures	196
92	Retort Pressure Control System	196
93	Deposition from Mo-25Ti and Pure Molybdenum Packs of Two Grit Sizes Using NaCl Activator	197

ILLUSTRATIONS (Cont)

FIGURE		PAGE
94	Plot of Effective Deposition Rate Coefficients for the Mo-25Ti Pack With NaCl Activator	199
95	Deposit from 50Mo-50Ti Pack	204
96	Deposit from 25Mo-75Ti Pack	205
97	Probable Form of the Pb-Mo Equilibrium Phase Diagram	208
98	Microstructure of Pb-10Mo Alloy; Quenched From 3000 F	209
99	Molybdenum Coating Deposited on Pure Columbium Substrate From Pb-15Mo Liquid Bath	210
100	Tungsten and Molybdenum Coated B66	212
101	Schematic Drawing of a High Pressure Retort	214
102	Microstructure of Several Molybdenum-Titanium Modifier Coatings	215
103	Microstructure of the Silicided Molybdenum-Titanium Coatings	216
104	Microstructure of the Modified Molybdenum-Titanium Coatings Before and After Siliciding	217
105	Microstructure of Failed (Mo-Ti)-Si Coatings	220
106	Microhardness of Selected Slurry Coatings After 2400 F Oxidation	221
107	Sintering During Vanadium Deposition	225
108	Vanadium Coated Cb752 Alloy; Series I Specimens	227
109	As-Vanadized Cb752 and D43 Alloys; Series II Specimens	229
110	Vanadized and Annealed Cb752 and D43 Alloys; Series II Specimens	230
111	Schematic Arrangement of a Low-Pressure Retort	232
112	As-Coated Surface Finish of Chromium-Titanium Vanadized Cb752 Alloy	234
113	Chromium-Titanium Coated Vanadized Cb752 Alloy; Series I Specimens	235
114	Microstructure Comparison of V-(60Cr-40Ti)-Si and V-(80Cr-40Ti)-Si Coatings	237
115	Cb752 Alloy After Coating With Vanadium and (Cr-Ti); Series III Specimens	240
116	D43 Alloy After Coating With Vanadium and (Cr-Ti); Series III Specimens	240
117	Vanadized Specimens Coated With 80Cr-20Ti Using Low-Pressure Techniques; Series II	242
118	V-(Cr-Ti)-Si Coated Cb752 Specimen; Series II	244
119	V-(Cr-Ti)-Si Coated D43 Specimen; Series II	244

ILLUSTRATIONS (Cont)

FIGURE		PAGE
120	V-(Cr-Ti)-Si Coated Cb752 Specimen; Series III	248
121	V-(Cr-Ti)-Si Coated D43 Specimen; Series III	248
122	Unidentified Phase in V-(Cr-Ti)-Si Coated D43 Alloy	249
123	Weibull Cumulative Failure Plot of V-(Cr-Ti)-Si Coated Cb752 Specimens After Oxidation Testing at 2400 F; Series II One-Hour Cycles	250
124	Weight Change Versus Time for V-(Cr-Ti)-Si Coating on Cb752 Alloy at 2400 F In Air	251
125	V-(Cr-Ti)-Si Coated Cb752 Alloy; Series I Edge Failure at 150 Hours	252
126	V-(Cr-Ti)-Si Coated Cb752 Alloy Surface After 106 One-Hour Cycles at 2400 F; Series III	252
127	Electron Microprobe Analysis of Vanadium and Columbium in Vanadized Cb752 Alloy	254
128	Electron Microprobe Analysis of Vanadium and Columbium in Vanadized D43 Alloy	255
129	Electron Microprobe Analysis of Chromium, Titanium, Vanadium, and Columbium in (Cr-Ti)-V Coated Cb752 Alloy	256
130	Electron Microprobe Analysis of Chromium, Titanium, Vanadium, and Columbium in (Cr-Ti)-V Coated D43 Alloy	257
131	Electron Microprobe Analysis of Silicon, Chromium, Titanium, Vanadium, and Columbium in Si-(Cr-Ti)-V Coated Cb752 Alloy	258
132	Electron Microprobe Analysis of Silicon, Chromium, Titanium, Vanadium, and Columbium in Si-(Cr-Ti)-V Coated D43 Alloy	259
133	Cb752 Alloy Coated With 80Cr-20Ti and Silicon	261
134	Vanadized and Silicided Cb752 Alloy	261
135	Vanadized and Siliconized Cb752 Alloy; Oxidation Tested 131 Hours at 2400 F	262
136	Weight Change Versus Time for V-(Cr-Ti)-Si and V-Si Coatings on Cb752 Alloy at 2400 F In Air	263
137	Surface Defects in D43 Columbium Alloy Sheet	267
138	Vacuum Coating Retort; Cb-1Zr Material	269
139	Vacuum Vanadium Coating Retort Specimens and Pack Material	269
140	Evacuated and Sealed Retort Ready for Vacuum Furnace	270
141	Dendritic Vanadium Deposit on D43 Alloy From Large Low-Pressure Pack	270
142	High-Pressure Argon Retorts for Coating Phase II and III Specimens	271

FIGURE		PAGE
143	Hardness Versus Oxygen Content in Arc-Melted V-50Cr Alloy	285
144	Deoxidizing Effect of Meschmetal in Arc-Melted 50V-50Cr Alloy	286
145	Arc-Melted V-50Cr Alloy	287
146	Arc-Melted V-49.8Cr-0.5 MM Alloy	287
147	Arc-Melted V-49.5Cr-1.0 MM Alloy	287
148	Arc-Melted V-49Cr-2.0 MM Alloy	288
149	Arc-Melted V-47.5Cr-5.0 MM Alloy	288
150	Arc-Melted V-45Cr-10 MM Alloy	288
151	Partial Molal Free Energy of Solution of Oxygen in Titanium and Columbium at 2200 F	289
152	Arc-Melted V-45Cr-10Ti Alloy	290
153	Schematic Diagram of Fused Salt Plating Cell	293
154	Oxidation Rate of Vanadium and Chromium Surface Modified Cb752 Substrate Alloy	300

TABLES

TABLE		PAGE
I	Summary of Oxidation Tests V-(Cr-Ti)-Si Coating on 0.012-Inch D43 and Cb752 Alloys	16
II	Summary of Oxidation Tests V-(Cr-Ti)-Si Coating on 0.030-Inch D43 and Cb752 Alloys	20
III	Experimental Program and Schedule for Phase I	34
IV	Nominal Compositions of Commercial Substrate Alloys Oxidation Tested	38
V	Nominal Composition of Arc-Melted Sublayer Alloys for Oxidation Studies at Solar	39
VI	Oxidation of Uncoated Substrate Alloys - 1600 F In Air	42
VII	Oxidation in Air at 1600 F of Several Cb-Ti-Cr, Cb-Ti-Mo, and Cb-V-Cr Ternary Alloys	44
VIII	Oxidation In Air at 1600 F of Several Ti-V-Cr-Cb Alloys	55
IX	Oxidation of Cb-Al-Ti Alloys	61
X	Oxidation at 1600 F In Air of Some Beryllium-Containing Columbium Alloys	66
XI	Thermal Expansion of Binary Alloys	70
XII	Diffusion Studies of Columbium Alloys Versus Ti-33Cr Foil With Diffusion Barriers of Tantalum, Molybdenum, and Tungsten Annealed 100 Hours 2400 F	74
XIII	Weight Ratios of Possible Diffusion Barriers for 100 Hours Protection at 2400 F	76
XIV	Nominal Composition of the Binary Alloys Used in the Diffusion Studies	77
XV	Diffusion Penetration Into Columbium Alloys After 100 Hours at 2200 F	84
XVI	Ultimate Tensile Strength at 2200 F	86
XVII	Elongation at 2200 F	86
XVIII	Stability of Duplex Heat-Treated Cb752 Alloy After Various Anneals	88
XIX	Stability of Duplex Heat-Treated D43 Alloy After Various Anneals	89

TABLES (Cont)

TABLE		PAGE
XX	Calculated Partition of Carbon and Oxygen at 1500 K	89
XXI	Oxidation Test Results on Several MSi_2 Compositions	94
XXII	Oxidation Test Results on Several M_5Si_3 Compositions	101
XXIII	Oxidation Data for Trialuminide Compounds Exposed at 2200 F	105
XXIV	Oxidation Data for Trialuminide Compounds Exposed at 2500 F	105
XXV	Oxidation Data for Selected Trialuminide Compounds Exposed at 1600 F	106
XXVI	Oxidation Data for (Cb-Ti-Mo)Al_3 Compounds Exposed at 1600 F	107
XXVII	Oxidation Data for (Cb-Ti-Mo)Al_3 Compounds Exposed at 2400 F	108
XXVIII	Oxidation Data for Selected Gamma Compoisitions Exposed at 2200 F	110
XXIX	Oxidation Data for Selected Gamma Compositions Exposed at 2500 F	110
XXX	Oxidation Data for Selected Gamma Alloys Exposed at 1600 F	111
XXXI	Oxidation Data for Selected Gamma Alloys Exposed at 2500 F	112
XXXII	Oxidation Data for Gamma Alloys	115
XXXIII	Summary of Oxidation Data for Cb-Al Base Solid-Solution Alloys Exposed at 2200 F	116
XXXIV	Summary of Oxidation Data for Cb-Al Base Solid-Solution Alloys Exposed at 2500 F	117
XXXV	Weight Gain Data For Cb-Al Base Solid-Solution Alloys Exposed at 2400 F	118
XXXVI	Thermal Expansion of Various Disilicides (MSi_2)	121
XXXVII	Thermal Expansion of Various Trisilicides (M_5Si_3)	122
XXXVIII	Coefficients of Thermal Expansion for Selected Gamma Alloys	124
XXXIX	Retained Stress in Hypothetical Coatings on Cb752 Alloy	125
XL	Oxidation Data for Aluminized Alloys Exposed at 2400 F	143
XLI	Oxidation Test Results at 1600 F on Aluminized and Titanized Plus Aluminized Columbium Alloy	149
XLII	Mechanical Properties at 2200 F of Aluminized and Titanized and Aluminized Columbium-Base Alloys	154
XLIII	Silicide Formation on Cb-Ti-Al Alloy	156
XLIV	Electron Microprobe Results	164

TABLES (Cont)

TABLE		PAGE
XLV	Deposition Parameters for the (80Cr-20Ti)-Al-Si and Ti-Al-Si Coating Systems	166
XLVI	Oxidation Tests of the (80Cr-20Ti)-Al-Si and Ti-Al-Si Coatings at 1600 F	167
XLVII	Cyclic Oxidation Tests of the (80Cr-20Ti)-Al-Si and Ti-Al-Si Coatings at 2400 F	168
XLVIII	2400 F Oxidation Test Data of the V-(Cr-Ti)-Al-Si Coating	171
XLIX	1600 F Oxidation Test Data on the V-(Cr-Ti)-Al-Si Coating	171
L	Coating Compositions - Parts by Weights	180
LI	Coating Properties	181
LII	Ceramic Coating Cyclic Oxidation In Air	183
LIII	Chemical Analysis of Ti and Mo Material for Pack Preparation	193
LIV	Analysis of Arc-Melted Ti-Mo Alloys	193
LV	Effective Deposition Rate Coefficient for the 75Mo-25Ti Pack on B66 Alloy	200
LVI	Pack Deposition Results - 75Mo-25Ti Alloy	201
LVII	Pack Deposition Results - 50Mo-50Ti Alloy	203
LVIII	Pack Deposition Results - 25Mo-75Ti Alloy	206
LIX	X-Ray Counts of a Coated B66 Specimen	212
LX	Materials Used for Slurry Coating Cb752	213
LXI	Deposition of the Mo-Ti Modifiers and Silicon	214
LXII	Oxidation Performance of the (Mo-Ti)-Si and (Mo-Ti-X)-Si Coating Systems on 0.030-Inch Cb752 Alloy	218
LXIII	Deposition of the Iron-, Manganese-, Boron-Containing Modifiers and Silicon	219
LXIV	Series II Vanadium Deposition	228
LXV	X-Ray Fluorescent Analyses of the Cr-Ti Coated Specimens	228
LXVI	Chrome-Titanium Pack Media	233
LXVII	Preliminary Summary of Oxidation Data on the V-(60Cr-40Ti-Si and V-(80Cr-20Ti)-Si Coatings	238
LXVIII	Deposition History of Series I and III Specimens Through the 80Cr-20Ti Cycles	239
LXIX	Deposition and Chemical Analyses for the Low-Pressure Pack Deposition on Series II Vanadized Specimens	245

TABLES (Cont)

TABLE		PAGE
LXX	Deposition Weight Gains and Oxidation Performance of the Preliminary V-(Cr-Ti)-Si Coated Specimens	246
LXXI	Deposition Results and Oxidation Performance of Additional Silicide Coating Systems	262
LXXII	Compositions Phase II and III Alloys	265
LXXIII	Deposition Weight Gains for V-(Cr-Ti)-Si Coated Phase II and III Specimens	273
LXXIV	Typical Purities and Cost Comparison for Various Grades of Vanadium and Chromium	284
LXXV	Arc-Melted, Nominal 50V-50Cr Alloys Showing Effect of Gettering Agents on Residual Oxygen Content and Hardness of As-Cast Structure	285
LXXVI	Coating Results with Vanadium/Chromium Powders on Cb752 Substrate at 2200 F	291
LXXVII	Chemical Analyses of the Metal Anode Materials and Cb752 Substrate Alloys	295
LXXVIII	Fused Salt Deposition of Chromium on Cb752 Alloy	298
LXXIX	Oxidation Test Results of Vanadium and Chromium Surface Modified Cb752 Substrate Alloy at 1600 F	299

I. INTRODUCTION

Refractory metal alloys represent a desirable approach to a number of future Air Force high-temperature structural requirements, but their application has been limited, pending discovery of completely satisfactory solutions to the problem of oxidation protection. Although the considerable effort devoted to coating development over the past fifteen years has resulted in identifying several promising coatings for columbium alloys, rigorous testing had disclosed weaknesses in nearly all the coatings which had been devised prior to institution of this program in July 1964. A good demonstration of the problems was provided by work at Solar under Contract AF33(657)-9443, where it was found that the number of candidate coatings for columbium alloys was gradually reduced to one as more and more severe tests were added to the program. When reentry simulation test was introduced even this showed weakness under slow thermal cycling.

A basic limitation, common in varying degree to all the available coatings, has been the lack of coating ductility. Thermal expansion matching of coatings and substrates appears to be impractical, so coating systems must have a mechanism to tolerate the effects of thermal strains induced by thermal cycling. An even more imperative requirement is ductility to avoid damage as a result of strains of external origin. These strains may be the result of assembling the component parts of a structure or, at the other extreme, may be caused by the impact of a foreign body. The concept pursued in this program was to provide at least one layer in the coating with reasonable ductility. Outer coatings of brittle materials such as ceramics and silicides were to be considered so long as the underlying layer had sufficient oxidation resistance and ductility to sustain impact damage and yet complete the mission. This approach has been termed effective ductility.

Reentry vehicles and gas turbines are two of the most urgent yet demanding fields where system development is held up by lack of completely adequate solutions to

this coating problem. To focus attention on the special needs of each of these fields, the program was divided into three phases:

- **Phase I** Measurement of basic property data on components of coating systems and development of application techniques for new protective coating systems for columbium alloys.
- **Phase II** The evaluation of a selected coating from Phase I on foil gage columbium alloys in tests critical to reentry and hypersonic vehicle applications.
- **Phase III** The evaluation of selected coating compositions from Phase I on columbium-base alloys of potential use in turbojet engines.

In order not to burden the reader with details of the entire program, this work is reported in three parts corresponding to the three phases. The parts will have special interest to the coating developer and materials specialist (Part I); to those with interest in aerospace vehicle applications (Part II); and to the engineer concerned with powerplants (Part III). However, to make available the complete results to each field of activity, each report contains a complete summary of the overall program.

The Phase I activities were conducted jointly by the I. I. T. Research Institute (IITRI) and by the Solar Division of International Harvester Company (Solar). The general division of studies was for IITRI to investigate aluminide systems and for Solar to study silicide and ceramic coatings. Ductile layers with aluminum-containing systems were to be based on the moderately oxidation resistance columbium/aluminum alloys; the somewhat more oxidation resistant and ductile gamma phase in the titanium/aluminum system; and the body centered cubic alloys of good oxidation resistance based on the Fe-Cr-Al alloy. In the cases of work on silicides at Solar, moderately ductile sublayers were to be formed by pre-alloying to form alloys such as Cb-V-Cr, Cb-Ti-Mo, Cb-Ti-W, and Cb-Ti-Cr. In addition to specific coating development, studies were undertaken to develop physical property data that would assist in making the selection of coating systems. Data generated included:

- Interdiffusion rates with and without diffusion barriers
- Oxidation resistance of aluminides, silicides, and ductile sublayers
- Coefficient of thermal expansion of aluminides and silicides.

On selected coating compositions, preliminary application studies were undertaken using D43 and Cb752 substrate alloys. The prime application technique

used was high-pressure pack cementation, although some limited special studies using other techniques were also included.

In Phase II, properties were measured on 0.012-inch Cb752 and D43 alloys after application of the V-(Cr-Ti)-Si coating. The test program emphasized those properties that would limit the use of coated refractory metals in lightweight, structural applications in hypersonic and reentry vehicles. Evaluation methods included room-temperature bend; oxidation (cyclic with and without prestrain, step-down, low-pressure, and high-velocity plasma torch); reentry simulation, i.e., slow cycle with applied stress; mechanical properties (creep and mechanical fatigue).

Phase III, was likewise application oriented but with emphasis on the use of coated columbium alloys in high-performance gas turbines. Two alloys were used throughout the test program, Cb752 and D43; one additional alloy, Cb132M, was used in specialized tests for blade applications. Evaluation was conducted on 0.030-inch sheet and 0.5-inch diameter bar specimens and included: cyclic oxidation with and without impact damage; bend ductility; thermal fatigue (0.030-inch material); oxidation erosion (burner rig); thermal fatigue (burner rig, wedge specimens); and mechanical fatigue (0.030-inch material only). The V-(Cr-Ti)-Si coating was evaluated on all alloys and specimens; the (95Mo-5Ti)-Si coating was included in erosion rig tests on the D43 alloy only. Late development of this latter coating did not permit complete evaluation. The coating is, however, continuing to undergo tests on another AFML program (Ref. 1).

II. SUMMARY

The objectives of the program were:

- The development of new coating approaches to give better reliability than existing coatings.
- The development of coatings with effective ductility; namely, coatings with ability to withstand some deformation.
- The evaluation of these coatings for gas turbine and aerospace application.

In view of the large number of empirical approaches conducted in the past, more knowledge was essential as a basis for new coating concepts. The approach was taken that data should be measured on each of the components of a coating system so that better coating systems could be synthesized using the most desirable and compatible components. Oxidation behavior, expansion, and interdiffusion were the principal properties studied. This work led to several concepts, particularly the molybdenum-rich disilicide coating applied by slurry techniques that achieves a close expansion match with the columbium alloy substrate, and to the V-(Cr-Ti)-Si coating that reduces the Laves phase formation and the severity of the interstitial sink effect.

The effective-ductility concept was intended to provide some means of avoiding catastrophic failures and to provide a protection mechanism against thermal cycling cracks. It required a sublayer with adequate ductility to resist impact damage and sufficient oxidation resistance to withstand failure of the primary oxidation barrier (silicide, aluminide, or other brittle phase). Two types of primary barrier failure were considered; local failure such as craze cracking caused by thermal cycling, and gross spalling. Considerable success was achieved in the development of coatings with resistance to local failure by a combination of oxidation-resistant sublayers and better coating repair mechanisms. The V-(Cr-Ti)-Si coating, an example of this type, is compared in Figures 1 and 2 with an earlier coating based on (Ti-Cr)-Si. The need to develop coatings to withstand gross spalling of the primary barrier was predicated on the requirement that a coated columbium alloy component should have sufficient oxidation resistance to complete a mission even after failure of the primary barrier.

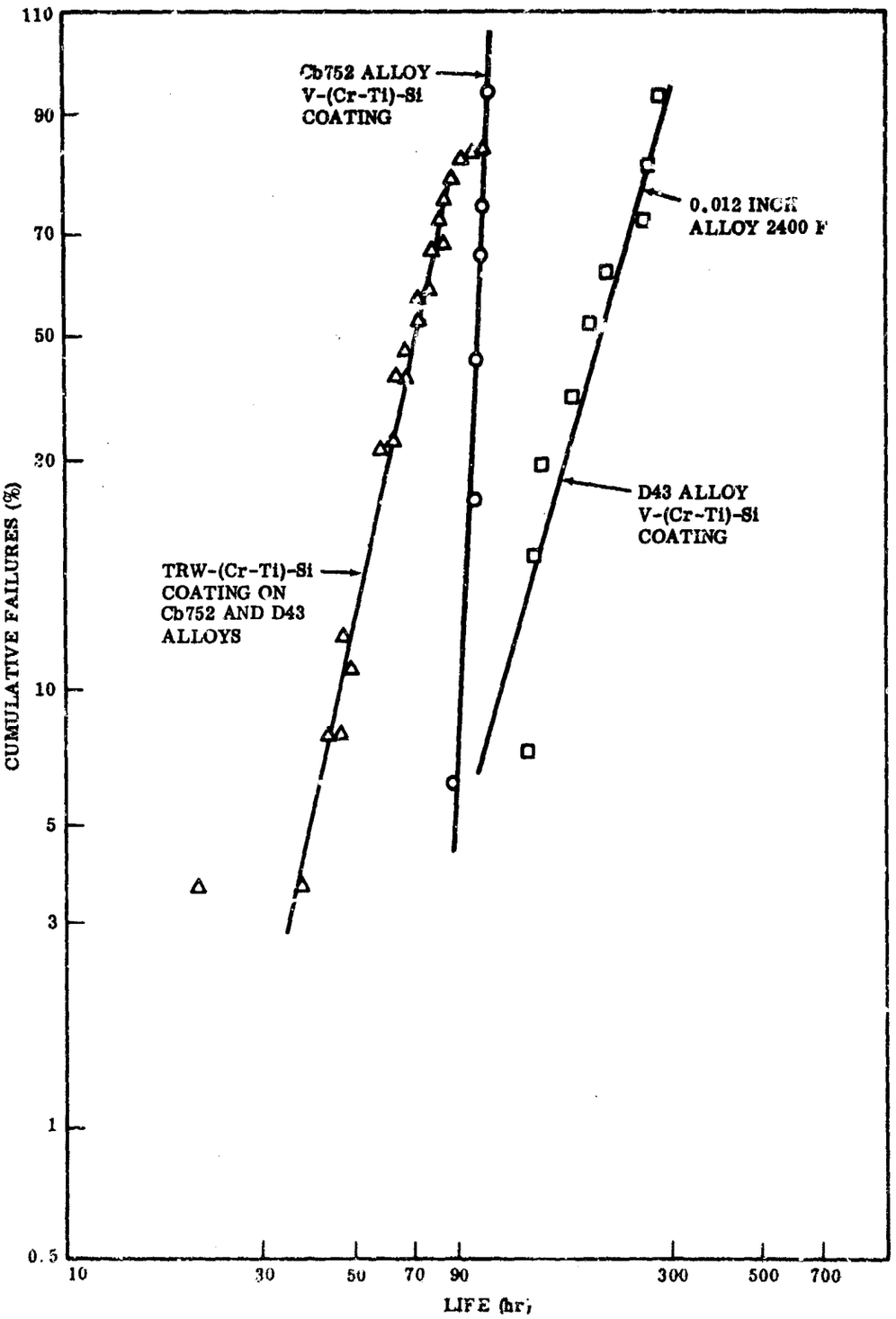

FIGURE 1. COMPARISON OF CYCLIC OXIDATION LIFE AT 2400 F; Solar V-(Cr-Ti)-Si Coating and TRW (Ti-Cr)-Si Coating

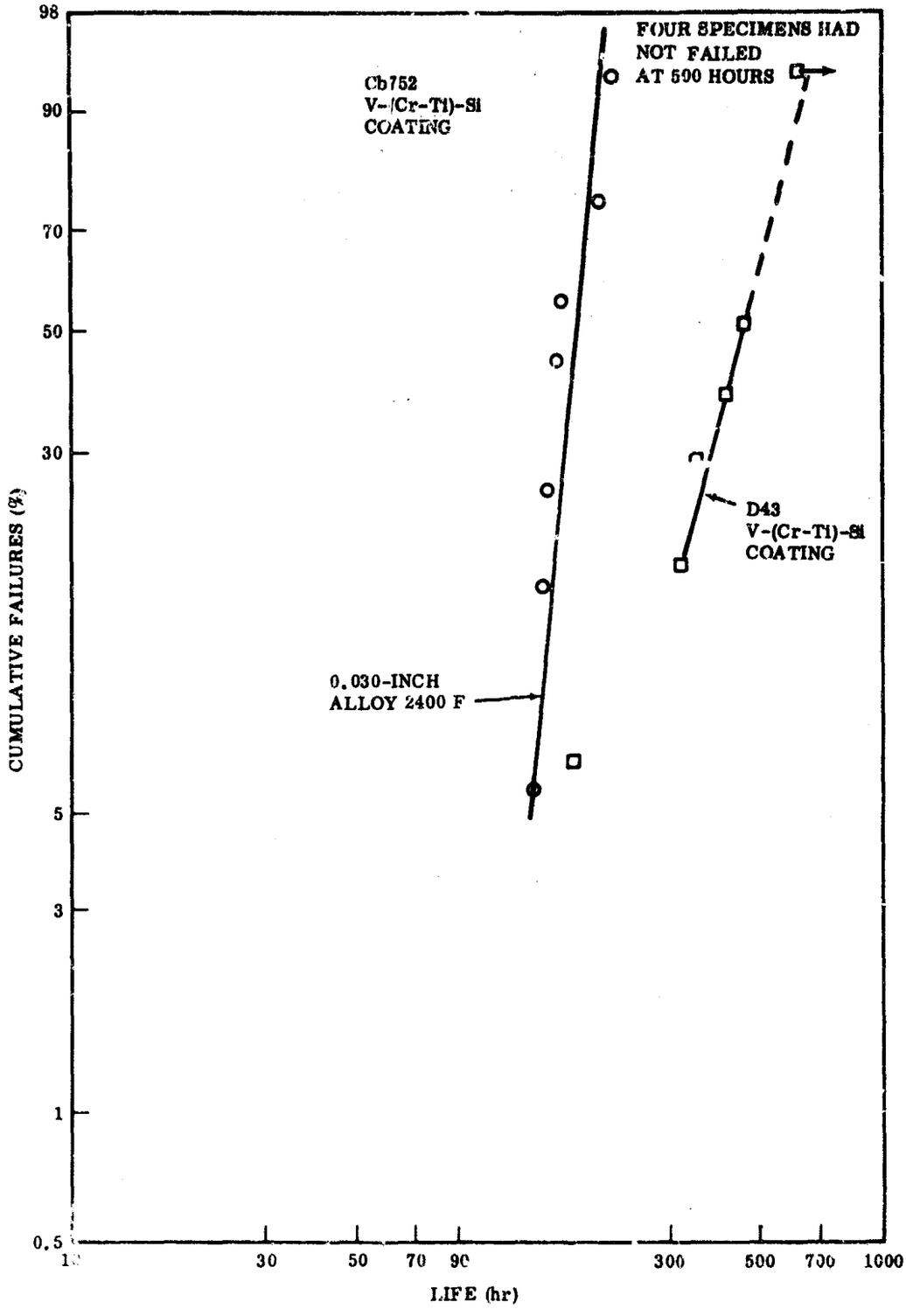

FIGURE 2. CYCLIC OXIDATION LIFE AT 2400 F; Solar V-(Cr-Ti)-Si Coating

Adequate oxidation resistance was defined as resistance for one hour at 2400 F, but this goal could not be achieved within the limits of ductile, columbium-rich alloys. Another approach was tried to achieve full ductility which employed iron-base alloys. These were bonded to the columbium substrate through an all body centered cubic sequence, such as Cb-Mo-Cr-(Fe-Cr-Al). Diffusion studies on such systems showed hardening to 800 VHN at the chromium-molybdenum interface after 200 hours at 2300 F, so that the coating system appeared to be limited in life. Further development of this concept may be warranted for short-life coatings.

Major effort was spent on development of coating methods for the V-(Cr-Ti)-Si composition and evaluation of this coating for aerospace and gas turbine applications. The optimum deposit was:

Vanadium – 5 to 9 mg/cm^2
80Cr-20Ti – 8 to 11 mg/cm^2
Silicon – 10 to 13 mg/cm^2

This coating provides 200 plus hours protection at 1600 F and 100 plus hours protection at 2400 F to D43, Cb752, and Cb132M alloys. Evaluation tests included tensile, creep, fatigue, and oxidation for all alloys, with reentry simulation for aerospace applications, and with rig and thermal shock/erosion tests to evaluate the coating for gas turbine applications. Results in every category of test showed performance that was remarkably uniform and better than other available coatings. Consistency of results was excellent; for example, after low-pressure exposure, five Cb752 specimens had cyclic oxidation lives of 96, 96, 97, 98, and 99 hours at 2400 F.

2.1 SUMMARY OF PHASE I WORK

2.1.1 Ductile Sublayer Oxidation Resistance

The alloy sublayer systems studied were:

- Cb-V-Cr
- Cb-Ti-V-Cr
- Cb-Ti-Mo
- Cb-Ti-Cr
- Cb-Ti-Al
- Cb-Mo-V

These systems showed that marked improvements over the oxidation resistance of columbium metal at 1600 F can be achieved by additions of titanium (to at least 40 weight percent), vanadium (to at least 5 weight percent), molybdenum (to at least 10 weight percent), titanium plus chromium (to at least 38 weight percent), vanadium plus molybdenum (to at least 10 weight percent), titanium plus aluminum (to at least 70 weight percent), and vanadium plus titanium plus chromium (to at least 35 weight percent). The Cb-Ti-Al alloys with or without additions of molybdenum or chromium provided the most oxidation-resistant alloys; however, none of the alloys could be considered oxidation resistant enough to withstand 2400 F without a primary barrier. Ductile alloy layers may provide adequate protection at the base of craze cracks in silicide or aluminide coatings and, thus, minimize some low-temperature oxidation problems. The alloys will not, however, afford significant protection as an undercoat if the outer oxidation barrier is grossly damaged. Only silicides and aluminides were found sufficiently oxidation resistant to afford oxidation protection at 2400 F for at least one hour.

The concept of effective ductility could not be fully developed because sublayers were not found which would provide the requisite short-time, high-temperature oxidation resistance. Resistance to impact failure with a known system would have to be attained by a combination of sublayer modification and self-healing outer layer (liquid phase oxide formation).

A modestly oxidation resistant ductile sublayer for non-damage performance can, however, be considered extremely advantageous when considered in light of the marked difference in the coefficient of thermal expansion of silicides and aluminides from that of columbium alloys. This differential expansion produces craze cracking at the lower temperature in which the sublayers are particularly oxidation resistant.

The Ti-Al and Ti-Cr alloy provided the most oxidation-resistant sublayers. Both of these alloy systems are objectionable because of the effect of titanium on carbide- (or oxide-) strengthened alloys. The use of vanadium in the program was primarily as a diluent to titanium to lower its activity and permit higher chromium concentrations while minimizing formation of $CbCr_2$ and $TiCr_2$. Some sacrifice in sublayer oxidation had to be accepted, but this sacrifice should have been compensated somewhat by the advantages of V_2O_5 formation in modifying the silica glass formed on silicides.

2.1.2 Oxidation Resistance of M_5Si_3 and MAl Compounds.

M_5Si_3 Compounds

The M_5Si_3 silicides provide an intermediate layer between the disilicide and the columbium substrate or sublayer. As the disilicide is consumed, this phase can become the actual protective coating. Oxidation tests at 1500 and 2400 F of the following compounds showed that Cb_5Si_3 had the highest oxidation rate at both temperatures.

Cb_5Si_3	$(Ti-Cr)_5Si_3$	$(Ti-Cr-Cb)_5Si_3$
Ti_5Si_3	$(Ti-Mo)_5Si_3$	$(Ti-Mo-Cb)_5Si_3$
Cr_5Si_3	$(V-Cr)_5Si_3$	$(V-Cr-Cb)_5Si_3$
V_5Si_3		
Mo_5Si_3		

The Mo_5Si_3 composition and a combination of molybdenum and columbium had the next highest rates. The outstanding compositions for low rates at both temperatures were $(Ti-Cr)_5Si_3$ and $(Ti-Cr-Cb)_5Si_3$ followed closely by Cr_5Si_3 and $(V-Cr)_5Si_3$. The $(Ti-Cr-Cb)_5Si_3$ composition was unique in the study being the only columbium-containing M_5Si_3 silicide with outstanding oxidation resistance at 2400 F for 100 hours, actually being equivalent to the disilicide.

Although the significance of the M_5Si_3 silicide in the oxidation resistance of coated alloys was not determined in this investigation, it was shown that any of the elements under study as modifiers form more oxidation resistant M_5Si_3 silicides than columbium. The most effective elements in improving oxidation resistance are chromium and titanium in combination with each other.

MAl Compounds

The TiAl compounds were modified with solid solution additions of zirconium, hafnium, vanadium, columbium, tantalum, chromium, molybdenum, and tungsten. At 2200 and 2500 F, zirconium, hafnium, and vanadium had an adverse effect; tungsten slowed the oxidation rate for short times only, then accelerated it; the other elements all decreased the oxidation rate. Increasing the aluminum content within the solubility range increased oxidation resistance. The most oxidation resistant MAl compound had small quantities of molybdenum and columbium substituted for titanium. A number of the (Ti-Cb-Mo)Al compounds showed only minor oxidation at both 1600 and

2400 F in 16 hours; however, some internal oxidation of the alloys was observed at 2400 F to a depth of 0.010 inch, indicating inadequacy as a primary oxygen barrier.

2.1.3 Oxidation Resistance of MSi_2 and MAl_3 Compounds

MSi_2 Compounds

The primary protection in silicide coatings is provided by the MSi_2 silicide. The oxidation resistance of a large number of disilicide compositions was, therefore, determined in the program. Included were compositions from the following systems:

Mo-Si	Mo-Ti-Si	Mo-Ti-Cb-Si
W-Si	W-Ti-Si	W-Ti-Cb-Si
V-Si	Cr-Ti-Si	Cr-Ti-Cb-Si
Ti-Si	V-Cr-Si	V-Ti-Cb-Si
Cr-Si	V-Cb-Si	V-Ti-Cr-Si
Cb-Si		V-Ti-Cr-Cb-Si

Test temperatures were 1500 and 2400 F for 100 hours.

At 1500 F, $CbSi_2$ and WSi_2 exhibited extremely rapid oxidation as did almost all ternary or quaternary compositions containing tungsten alone or in combination with columbium and other elements. The majority of the combinations free of tungsten and columbium were outstanding, showing a metallic luster after 100 hours.

Tests results at 2400 F, as assessed by a retention of a metallic appearance after 100 hours, indicated the following systems to be the most oxidation resistant:

V-Si	Ti-Mo-Si	Cb-Ti-Mo-Si
Mo-Si	Ti-W-Si	Cb-Ti-W-Si
W-Si	V-Cb-Si	

With few exceptions, however, the disilicides as a group had outstanding oxidation resistance even though a dark modified silica glass formed on the surface. Notably poor were $CbSi_2$ and Ti-Cr-Si. The Ti-Cr containing disilicides are remarkably poor in oxidation when contrasted to any of the other systems noted. Additions of columbium, unlike most other systems, appear to improve the oxidation resistance of the Ti-Cr composition. Chromium in combination with vanadium and the combination of V-Cr-Ti both produced more oxidation-resistant disilicides than the Ti-Cr composition

MAl_3 Compounds

Compositions studied in the MAl_3 system included: $TiAl_3$, $CbAl_3$, a modification of $CbAl_3$ with titanium, chromium, molybdenum, and tantalum; and $TiAl_3$ modified with molybdenum. With few exceptions, the MAl_3 composition underwent pest-type attack at 1600 F. Small additions of chromium and molybdenum appeared to mitigate the attack. At 2400 F small additions of molybdenum or large additions of titanium to $CbAl_3$ appeared to provide the most resistant compositions, being equivalent to some disilicides.

2.1.4 Thermal Expansion of Various Potential Coating System Components

Extensive thermal expansion measurements were made on M_5Si_3 and MSi_2 silicides, on aluminides, and on selected sublayer alloys. With the exception of silicides high in tungsten or molybdenum, the expansion of aluminides and silicides was sufficiently higher than the columbium alloys to ensure the formation of craze cracks in coatings on cooldown from equilibration at an elevated temperature. All MAl and MAl_3 compounds tested and all silicides containing appreciable quantities of vanadium, chromium, or titanium had coefficients of thermal expansion at least 50 percent higher than the Cb752 alloy in the temperature range from 100 to 1800 F.

2.1.5 Selection of Coating Compositions From the Basic Property Study

If the (Ti-Cr)-Si coating system had not already been developed, the basic property study would probably have resulted in its selection as one of the leading candidates, primarily based on the unusually good oxidation resistance of the $(Cr-Ti-Cb)_5Si_3$ silicide and the (Ti-Cr-Cb) sublayer; however, such a selection would have been tempered by the interstitial sink effect resulting from the presence of large quantities of titanium. The second choice was the (Ti-Mo)-Si system with a high molybdenum content. This selection was predicated on the fair sublayer oxidation resistance of Cb-Ti alloys, the outstanding oxidation resistance of the $(Ti-Mo)Si_2$ silicide, and the close expansion match of $MoSi_2$ and the columbium alloys. The third selection was the (V-Cr)-Si system based on a negligible interstitial sink problem, good oxidation resistance of the disilicide, and potential ease of application.

The outstanding oxidation resistance of the Cb-Ti-Al solid solution alloys made these alloys potential sublayer candidates, but the aluminide systems as a group did not have the potential of the silicide. Internal oxidation was a serious problem with these intermetallics. Titanium-molybdenum-aluminum combinations provided the most satisfactory performance and were tentatively selected as coating candidates.

2.1.6 Application of Selected Coating Systems

Phase II and III of this program initially required the development and evaluation of coatings for reentry and turbojet engine applications, respectively. The development activity was transferred to Phase I to retain the majority of the research activity in this phase. The application studies were concentrated in the deposition of the V-(Cr-Ti)-Si composition with less extensive effort in the (Mo-Ti)-Si, (V-Cr-Ti-Al)-Si, and (Cb-Mo-Ti)-Al coatings.

For the majority of the program, pack deposition was the application technique used, but in the latter stages sintered slurries were included, particularly in the application of the (Mo-Ti) modifier and fugitive vehicle slurries for the application of (Ti-Mo-Al). A number of other techniques were also considered briefly, e.g., fused salt deposition of vanadium, precipitation of molybdenum from a molten metal, and chemical substitution of molybdenum for silicon.

The V-(Cr-Ti)-Si Coating

Initial studies in the (V-Cr)-Si coating showed two deficiencies in the deposition of pure chromium over vanadized D43 and Cb752 alloys:

- The deposition rate of chromium was extremely slow at the maximum practical temperature for high-pressure packs (2300 F).
- The substrate was embrittled by the transport of oxygen unless iodide chromium was used.

To overcome these problems a chromium-titanium alloy was used to alloy the vanadized layers. Studies showed that an 80Cr-20Ti alloy provided the most satisfactory oxidation resistance at 1600 and 2400 F. A deposit of the following compositions appears to provide optimum protection:

Vanadium—5 to 9 mg/cm^2
80Cr-20Ti—8 to 11 mg/cm^2
Silicon — 10 to 13 mg/cm^2

A coating of the above compositions appears to be capable of providing 200 plus hours of protection at 1600 F and 100 plus hours of protection at 2400 F to D43, Cb752, and Cb132M alloys.

The most severe problem in the deposition of the coating is in sintering vanadium to the specimen. The use of two 5-hour runs at 2250 F instead of one

10-hour cycle was essential in reducing sintering, but this problem was never completely overcome during the program.

The (Ti-Mo)-Si Coating System

The development of a pack deposition process for the (Ti-Mo) modifier layer was found to be essentially impossible. Arc-melted alloys containing as much as 75 percent molybdenum deposited only titanium. Molybdenum could be deposited from packs by sulfide and oxide transport and by displacement with the silicide, but all of the techniques yielded coatings of poor quality and an embrittled substrate.

Vacuum sintering of Ti-Mo slurries, a process developed at Solar under NASA Contract NAS3-7276, provided a feasible route to molybdenum modification. Compositions up to 95 percent molybdenum could be readily applied. Oxidation tests showed that the coatings could protect the Cb752 alloy for 130 plus hours at 2400 F, but protection at 1600 F was poor; however, by glass impregnation the 1600 F life was extended to greater than 552 hours and the 2400 F life to a minimum of 222 hours. The addition of 10 percent iron to the (95Mo-5Ti) composition provided lives comparable to the glass impregnated (95Mo-5Ti)-Si coating.

Other Coating Systems

To use the highly oxidation resistant and slightly ductile Ti-Al and (Ti-Cr-Al) alloys, the systems were investigated as a basis for silicide coating. Vanadium was also included to enable the deposition of the 80Cr-20Ti coating prior to depositing aluminum. With the V-(Cr-Ti)-Al-Si coatings, lives comparable to the V-(Cr-Ti)-Si coating were obtained; but because of the increased complexity of the system, it was not considered for additional study. All other aluminum-containing sublayers for silicides provided less protection than the V-(Cr-Ti)-Si coating.

2.1.7 Selection of Coatings for Phase II and III

The V-(Cr-Ti)-Si coating was the only one selected for evaluation in Phase II and III. The selection was based primarily on the state of development of the process at the outset of the phases. The logical second choice was the (95Mo-5Ti)-Si coating with glass impregnation. The late development of the coating, however, precluded its inclusion except in selected tests in Phase III.

2.2 PHASE II - EVALUATION OF THE V-(Cr-Ti)-Si COATING FOR AEROSPACE APPLICATIONS

Seven types of oxidation tests were performed in evaluating the performance of the V-(Cr-Ti)-Si coating on 0.12-inch Cb752 and D43 alloys. Five of the tests were furnace cyclic oxidation tests, generally using the procedures and techniques specified in MAB-201-M. The other two tests were specifically designed to evaluate the performance of the coating under simulated reentry conditions for aerospace vehicles. The tests were:

- Oxidation in the pest-temperature region
- Temperature step-down test
- Cyclic oxidation test
- Low-pressure exposure tests
- Oxidation after coating damage
- Reentry simulation tests
- Plasma torch tests

Four other tests were included to evaluate the effects of the coating and/or processing conditions on mechanical properties of the alloys. These tests were:

- Tensile tests
- Fatigue tests
- Bend tests
- Creep tests

A brief summary of the results of the tests are discussed in the following paragraphs.

2.2.1 Test Results

The results of the furnace oxidation tests are summarized in Table I.

Pest Oxidation Tests

Results of the tests at 1600 F show that the coating does not have a low-temperature problem. Of the 10 specimens tested, no failures were observed and the specimens were removed from test after 212 hours of exposure.

TABLE I

SUMMARY OF OXIDATION TESTS V-(Cr-Ti)-Si COATING ON 0.012-INCH D43 AND Cb752 ALLOYS

Type of Test	Temperature (F)	Alloy	Thickness (in.)	Number of Test Specimens	Oxidation Performance (hours to failure for each specimen)(2)
Pest Test(1)	1600	D43	0.012	5	+212 (all)
Pest Test(1)	1600	Cb752	0.012	5	+212 (all)
Cyclic Oxidation(3)	2400	D43	0.012	10	150, 153, 156, 185, 192, 217, 257, 269, 283, +310
Cyclic Oxidation	2400	Cb752	0.012	10	84, 101, 101, 102, 102, 105, 105, 112, 114, 114
Low Pressure(4)	2400	D43	0.012	5	188, +274, +274, +274, +274
Low Pressure(4)	2400	Cb752	0.012	5	96, 96, 97, 98, 99
Step-Down Oxidation(5)		D43	0.012	5	No failures. 2400 F for 10 cycles +2600 F for 5 cycles
Step-Down Oxidation(5)		Cb752	0.012	5	1 failure at 15 cycles. 2400 F for 10 cycles +2600 F for 5 cycles
Oxidation After Coating Damage(6)	2400	Cb752	0.012	5	40, 102, 106, 106, 106
Oxidation After Coating Damage(6)	2400	D43	0.012	5	+108 (all)

1. Standard MAB-201-M test at 1600 F
2. + denotes specimen did not fail
3. Standard MAB-201-M test at 2400 F
4. One hour exposure at 0.1 Torr pressure and 2400 F, followed by cyclic oxidation at 2400 F and atmospheric pressure
5. Standard MAB-201-M step-down test. 2400, 2200, 1400 F, and ambient 30 minute cycles. Ten cycles run using 2400 F maximum and five cycles using 2600 F maximum temperature
6. Specimens bent to a permanent bend angle of 19 degrees 30 minutes.

Temperature Step-Down Tests

The second type of oxidation test used in the program was the standard MAB step-down type of test. In this evaluation, five specimens of each alloy were subjected to 10 cycles of 2400, 2200, and 1400 F using the procedures specified in MAB-201-M. At the conclusion of 10 cycles of exposure, the specimens showed no evidence of oxidation; hence, the top temperature was increased to 2600 F. One Cb752 specimen showed evidence of edge oxidation and the test was terminated after five additional cycles using 2600 F as the maximum temperature.

Cyclic Oxidation Tests

To evaluate the high-temperature protection afforded to the 0.012-inch Cb752 and D43 alloys, ten specimens of each alloy and thickness were subjected to a standard MAB cyclic oxidation test at 2400 F. The test results are shown in Table I and a Weibull cumulative failure plot of the results of the tests on the 0.012-inch Cb752 and D43 alloys is shown in Figure 1. At 2400 F, the maximum coating life was exhibited by the coated D43 alloy. Maximum probable oxidation life was 375 hours and the slope of the curve was 2.7. The coated Cb752 alloy exhibited a maximum probable oxidation life of only 115 hours; however, the slope was 45. At an 80 percent reliability level, oxidation life was 100 hours, and only decreased to 95 hours at a reliability level of 95 percent. All failures were initiated along the edges and were quite small.

Low-Pressure Exposure Tests

The fourth test was selected to simulate the low-pressure high-temperature conditions encountered during reentry. Coated specimens of both alloys and thickness were exposed to 2400 F at 0.1 Torr pressure for one hour, and then cyclic oxidation tested at the same temperature at atmospheric pressure. Results of the tests (Table I) show that the low-pressure exposure had no deleterious effects on the oxidation life of the coating. Only 6 of the 10 specimens subjected to the test showed evidence of oxidation, and these failure times were in agreement with specimens that had not been exposed at low pressure.

Oxidation After Coating Damage

Assessment of the relative room-temperature ductility of the V-(Cr-Ti)-Si coating, and its ability to provide substrate protection after plastic deformation was made by intentionally damaging specimens by bending into the plastic region. After damaging, the specimens were subjected to furnace cyclic oxidation at 2400 F. There

was no gross or catastrophic oxidation during the test. All failures (the coated Cb752 specimens only) were initiated along the bend line at the edges of the specimens.

Reentry Simulation

Performance of the V-(Cr-Ti)-Si coating in simulated reentry tests (slow cycle 800 to 2500 to 800 F under stress) was variable. The ability of the coating to retain its overall protective properties during elastic and plastic deformation under the continuous temperature cycling conditions on Cb752 alloy was excellent. The coated Cb752 specimens did not fail in 22 cycles and consequently performed as well as any coating ever tested in the reentry simulators. Four out of six coated D43 specimens, however, exhibited severe edge oxidation during the test, indicating problems in the silicon deposition cycle on these specimens.

Tensile Tests

Retention of yield and ultimate tensile strengths of the V-(Cr-Ti)-Si coated Cb752 and D43 alloys tested at room temperature was good, averaging approximately 80 percent of baseline data. Results of the tensile tests at 2200 F showed a reduction in strength of 20 percent for the Cb752 alloy and 30 percent for the D43 alloy. This reduction in strength is less than that exhibited by these same alloys coated with (Ti-Cr)-Si. With the duplex heat-treated Cb752 and D43 alloys, the (Ti-Cr)-Si coating reduces the yield and tensile strengths by 33 and 50 percent, respectively.

Fatigue Tests

Results of the fatigue tests performed at room temperature on the coated alloys showed a reduction in fatigue strength of approximately 50 percent at one million cycles. Specimens tested after isothermal oxidation exposure at 2400 F for 15 hours showed no appreciable further reduction in fatigue strength.

Creep Tests

The results of creep tests show that the V-(Cr-Ti)-Si coatings can withstand up to five percent creep at 2200 and 2400 F. Most specimens, however, exhibited evidence of edge oxidation at the conclusion of the test (generally 24 hours exposure) similar to that exhibited by the environmental test specimens. In general, the creep rate for the coated Cb752 alloy was higher than the coated D43 alloy.

Plasma Torch Tests

Plasma torch tests on V-(Cr-Ti)-Si coated Cb752 and D43 alloys showed the coating performed satisfactorily. There was no oxidation, warpage, or other deleterious effects after eight 15-minute exposures with a test temperature of 2400 F.

Bend Tests

Room temperature bend tests were performed on triplicate specimens of each alloy using the procedures specified in MAB-176-M. All coated D43 specimens passed the 90-degree bend test with only a minor loss of coating on the tension and compression sides of the specimens. The Cb752 alloy was embrittled by the coating process and failed to pass the bend test.

2.3 PHASE III - EVALUATION OF THE V-(Cr-Ti)-Si COATING FOR GAS TURBINES

The primary objective of Phase III was to demonstrate the relative potentials of protective coating systems, developed in Phase I, for application to advanced jet engine components. Combustion cans and liners, nozzle vanes, afterburner parts, blades, and vanes fabricated from the columbium alloys will require an extremely reliable coating system.

In Phase III, the test program was designed to simulate, as closely as possible, the severity of actual engine tests on heavy sheet stock and bar materials. Tests were performed on V-(Cr-Ti)-Si coated 0.030-inch Cb752 and D43 alloys, and on wedge specimens fabricated from 0.5-inch diameter bar stock of Cb132M and D43 alloys. Limited tests were performed on the glass impregnated TNV-7[1] and TNV-12[1] coatings. The Phase III tests were:

- Furnace Cyclic Oxidation
- Low-Pressure Exposure
- Thermal Fatigue (hole-in-plate)
- Oxidation-Erosion Rig Tests
- Thermal Fatigue Rig Tests
- Oxidation After Coating Damage
- Fatigue Tests
- Bend Tests

A brief summary of the test results is included in the following paragraphs.

1. The TNV-7 and TNV-12 coatings were developed under NASA Contract NAS3-7276 on the T222 tantalum alloy, but were included in this program because the compositions fit the program goals. The coatings are applied by sintering on the modifier, 35W-35Mo-15V-15Ti(TNV-7) and 95Mo-5Ti(TNV-12), at 2760 F and pack siliciding. Glass impregnation is used as a final process.

2.3.1 Test Results

Cyclic Oxidation Tests

The furnace oxidation test results on the 0.030-inch Cb752 and D43 alloys are summarized in Table II. A Weibull cumulative plot of the 2400 F results at atmospheric pressure are shown in Figure 2. For the Cb752 alloy, oxidation life ranged from 155 to 229 hours. The slope of the curve was 10 and maximum probable oxidation life was 245 hours. All specimens failed along the edges. In all cases, oxidation sites were quite small and never resulted in catastrophic oxidation of the substrate. For the D43 alloy, five specimens out of nine tested failed in the oxidation test at 176, 323, 361, 437, and 461 hours. The remaining four specimens were removed from test at 500 hours without any evidence of substrate oxidation.

Low-Pressure Tests

Results of the tests at low pressure were similar to those on the coated 0.012-inch specimens. Except for two premature failures on each alloy, specimens were still good when removed from test after several hundred hours exposure (Table II).

TABLE II

SUMMARY OF OXIDATION TESTS V-(Cr-Ti)-Si COATING ON 0.030-INCH D43 AND Cb752 ALLOYS

Type of Test	Temperature (F)	Alloy	Number of Test Specimens	Oxidation Performance (hours to failure for each specimen) (1)
Cyclic Oxidation (2)	2400	D43	9	176, 323, 361, 437, 461, +500, +500, +500, +500
Cyclic Oxidation (2)	2400	Cb752	10	155, 155, 163, 164, 182, 182, 187, 204, 229, 229
Low Pressure (3)	2400	D43	5	88, 94, +277, +277, +277
Low Pressure (3)	2400	Cb752	5	217, 217, +231, +231, +231

1. + denotes specimen did not fail.
2. Standard MAB-201-M test at 2400 F
3. One-hour exposure at 0.1 Torr pressure and 2400 F, followed by cyclic oxidation at 2400 F and atmospheric pressure.

Thermal Fatigue Tests

Thermal fatigue testing of the V-(Cr-Ti)-Si coating involved exposing the periphery of a 0.750-inch diameter hole in the center of the specimen (0.030-inch thick Cb752 and D43 alloys) to direct impingement of an oxygen-methane flame for one minute, followed by quenching in a controlled flow of ambient temperature air for a similar period.

Results of the tests at 1800 F show that the coating has no severe low-temperature problem in this type of test. Duplicate specimens of each alloy were tested for over 1400 thermal cycles without evidence of substrate oxidation. The specimens showed varying amounts of macro craze cracking in the coating, extending away from the hole approximately 0.125 inch, but no cracks were apparent in the substrate. Slight glassing of the coating was apparent at the 1800 F test temperature.

Duplicate specimens of each alloy were also tested at 2400 F. All specimens successfully passed over 1000 thermal cycles without evidence of thermal fatigue cracks or gross oxidation. Minor craze cracking was apparent in the silicide around the periphery of the hole, and some warpage also occurred around the hole.

Erosion-Oxidation and Thermal Shock Rig Tests

Oxidation-erosion and thermal shock tests were performed at 2400 F on one set each of V-(Cr-Ti)-Si coated Cb132M and D43 wedge shaped test specimens. Eight specimens of each alloy were tested together for 50 hours duration (250 cycles) in a combusted JP-5 fuel and air stream. Nozzle exit gas velocity was maintained at 0.85 Mach throughout testing. Specimens were alternately heated to the test temperature for 10 minutes, and rapidly cooled in an 600 F air blast for two minutes. On the D43 alloy specimens, three failures were observed during the test. The failure sites, however, were quite small and were generally attributed to coating defects observed prior to test. The remaining five specimens were in excellent condition after test. Four of the eight Cb132M specimens exhibited spot failures in the 50-hour, erosion-oxidation test. These failures were slightly more severe than on the D43 alloy specimens and were all on the trailing edges of the specimens.

Thermal fatigue type rig tests were also performed on V-(Cr-Ti)-Si coated Cb132M specimens and on D43 alloy specimens coated with the TNV-7 and TNV-12 glass-impregnated coatings. Specimens were alternately heated to 2400 F for three minutes followed by air blast cooling for two minutes. Specimens were tested for

1000 cycles without evidence of thermal fatigue cracking or oxidation of the substrate. The TNV-7 and TNV-12 impregnated coatings showed some glass flow toward the trailing edge of the bars.

Oxidation After Coating Damage Tests

The ability of the V-(Cr-Ti)-Si, TNV-7, and TNV-12 coatings to provide substrate protection after plastic deformation was evaluated. Specimens of each of the three coatings on 0.030-inch D43 alloy were damaged at room temperature using the falling ball technique. These specimens were impacted at 12 foot-pounds (using a one-inch diameter ball) on the edge and in the center. Triplicate specimens of each coating impact combination were then cyclic oxidation tested at 1600 and 2400 F.

Results of the tests at 1600 F showed that all three coatings impacted in the center region, provided substrate protection for up to five hours (the limit of the test). The TNV-7 and TNV-12 coatings, impacted on the edges, provided protection for one hour; whereas, the V-(Cr-Ti)-Si coated specimens were adequately protected. At 2400 F, there was no gross or catastrophic oxidation after five hours exposure of any of the three coatings impacted on the edges or in the center. There was minor spalling of the coating on the edges and center portions of the specimens and oxidation was confined to these areas.

Fatigue Tests

Results of the fatigue tests on the V-(Cr-Ti)-Si coated 0.030-inch Cb752 and D43 alloys showed a reduction in fatigue strength from baseline data of approximately 50 percent. This reduction in strength was approximately the same as that exhibited by the coated 0.012-inch Cb752 and D43 alloys in Phase II.

The effects of diffusion and oxidation exposure on the fatigue life of the coated D43 and Cb752 alloys were evaluated by subjecting coated specimens of each alloy to isothermal oxidation at 2400 F for 15 hours and then fatigue testing the specimens. The tests showed that the oxidation exposure of 15 hours had no deleterious effects on the fatigue strength of the V-(Cr-Ti)-Si coated alloys.

Bend Tests

The bend tests on as-coated 0.030-inch Cb752 and D43 alloys were similar to those on the 0.012-inch alloys. Again, the Cb752 alloy was embrittled during coating and failed to pass the 90-degree bend test. The D43 specimens were ductile.

III. DEVELOPMENT OF COATING CONCEPTS

The basic problems experienced with coatings for refractory metals have been related to their lack of ductility. Two lines of development have been followed to achieve adequate ductility in coatings. One has been through the use of ductile claddings such as the recent work on platinum cladding of columbium alloys (Ref. 2). The other has been through the effective-ductility approach in which a sublayer of the coating has ductility coupled with some oxidation resistance. According to the effective-ductility concept, the ductility of the sublayer would prevent brittle failure in the event of failure of the outer layer, and the oxidation resistance of the sublayer would be adequate to complete a mission. The (Ti-Cr)-Si coating was identified as the best available coating for thin gage columbium alloys, resulting from an extensive survey conducted in 1963-64 (Ref. 3), and this coating has the characteristics of an effective-ductility coating. However, the performance of this coating was marginal for multiple reentry use so that reliable performance was not achieved for up to 22 reentry cycles of one hour each with slow heating and cooling (T_{max} 2500 F). Its superior performance led to studies to characterize its behavior, and it was on the basis of the strengths and weaknesses of this coating that the philosophy for this program was developed. The strong points noted in tests of this coating were:

- Silicide has excellent oxidation resistance
- Excellent repair mechanism in spite of extensive coating cracking that forms on thermal cycling
- Excellent performance in MAB cyclic oxidation tests (fast heating and cooling cycle)

On the other hand, several weak points were noted:

- Performance in slow cycling tests is not reproducible
- Brittle Laves phase MCr_2 forms beneath silicide
- Interstitial sink effect may cause strength loss of columbium alloy (especially duplex heat treated). May reach 50 percent loss of strength.
- Solution and reprecipitation of Laves phase may occur on heating and cooling.

Because the course of development in the work to be described was influenced so heavily by these observations, the first section presents a detailed review of the (Ti-Cr)-Si system. Although the points summarized above were the ones from which the present program started, the review includes additional data on this chemistry gathered during the course of the present program. Oxidation resistance and expansivities of individual components of the coating are examples of such data.

The general approach taken in this work has been to overcome the problems identified with the (Ti-Cr)-Si system by modification of the chemistry, yet retain the desirable characteristics of the coating. The approach is discussed in Paragraph 3.1.2. It includes detailed studies of the individual components that were believed to act independently. Oxidation, stability, thermal expansion, and structure were some of the areas where studies were made of massive specimens of alloyed sublayers, subsilicides (M_5Si_3), and disilicides. Where coating components act in concert, as in interdiffusion, study was made of materials in pairs such as diffusion couples. Finally, studies were made of complete coating systems where complete interaction is involved as in repair mechanisms. Details of the individual studies are reported in Paragraphs 3.2 (sublayers) and 3.3 (aluminides and silicides). These studies led to the selection of potential coating systems reported in Paragraph 3.4.

3.1 BACKGROUND

Data obtained from the (Ti-Cr)-Si coating formed the starting point for this development. An analysis of factors affecting the performance of this coating was made prior to start of work on the program. On this basis an experimental approach was developed. Data on the (Ti-Cr)-Si coating was incomplete at the time the program was initiated, and some of the missing data have been generated during the course of the present program. It was decided to give as complete an account of this coating as possible at this point in the report, although details of the methods by which the data were generated are not presented until later. The reason for this decision is that a better appreciation of the lines of research can be obtained when viewed against this background.

3.1.1 Analysis of the (Ti-Cr)-Si Coating

This coating is applied by TRW in a double-cycle process. Typical cycles are:

- Eight hours at 2300 F using a halide-activated 60Cr-40Ti pack in a reduced pressure environment.
- Four hours at 2050 F using a halide-activated pure silicon pack in a reduced pressure environment.

The (Ti-Cr)-Si coating on columbium alloys (as applied by TRW) produces a modified alloy layer beneath the coating that is composed of Laves phase (MCr_2) and beta solid solution. Figure 3 shows that the titanium content reaches a maximum of 40 percent with enough of the beta formers, Cr and Cb, to stabilize the beta phase. Columbium stabilizes the Laves phase to the melting point, but Figure 4 is believed to represent the essential features of this portion of the coating. Dissolution and precipitation of the Laves phase in the beta solid solution as the temperature is increased or decreased characterize a wide range of composition within the Ti-Cr system. Available evidence supports a similar dissolution in coated columbium alloys. The temperature at which this dissolution is pronounced may be significant because of the damage that can result in the silicide coating due to the volume change resulting from the dissolution reaction. Figure 5 shows photomicrographs of the (Ti-Cr)-Si coating, before and after various heat treatments, and illustrates the Laves phase dissolution which occurs at temperatures between 1750 and 2500 F. In slow heating, particularly, this dissolution and precipitation could be more disruptive to silicide coatings because of the sluggishness of the processes. In slow-cycle tests at Solar (Ref. 3), the oxidation life of many batches of the (Ti-Cr)-Si coating on various columbium alloys has been reduced to less than a few minutes at 2500 F when the cycle time, to and from this temperature, is on the order of 30 minutes compared to 50 plus hours during rapid heating.

Application of titanium-chromium alloys by pack techniques in the composition range in excess of 67 weight percent chromium (β + $TiCr_2$) is made more complex by two problem areas:

- The stability of $CbCr_2$ Laves phase
- The transport of oxygen from the pack alloy if commercial chromium is used in the pack.

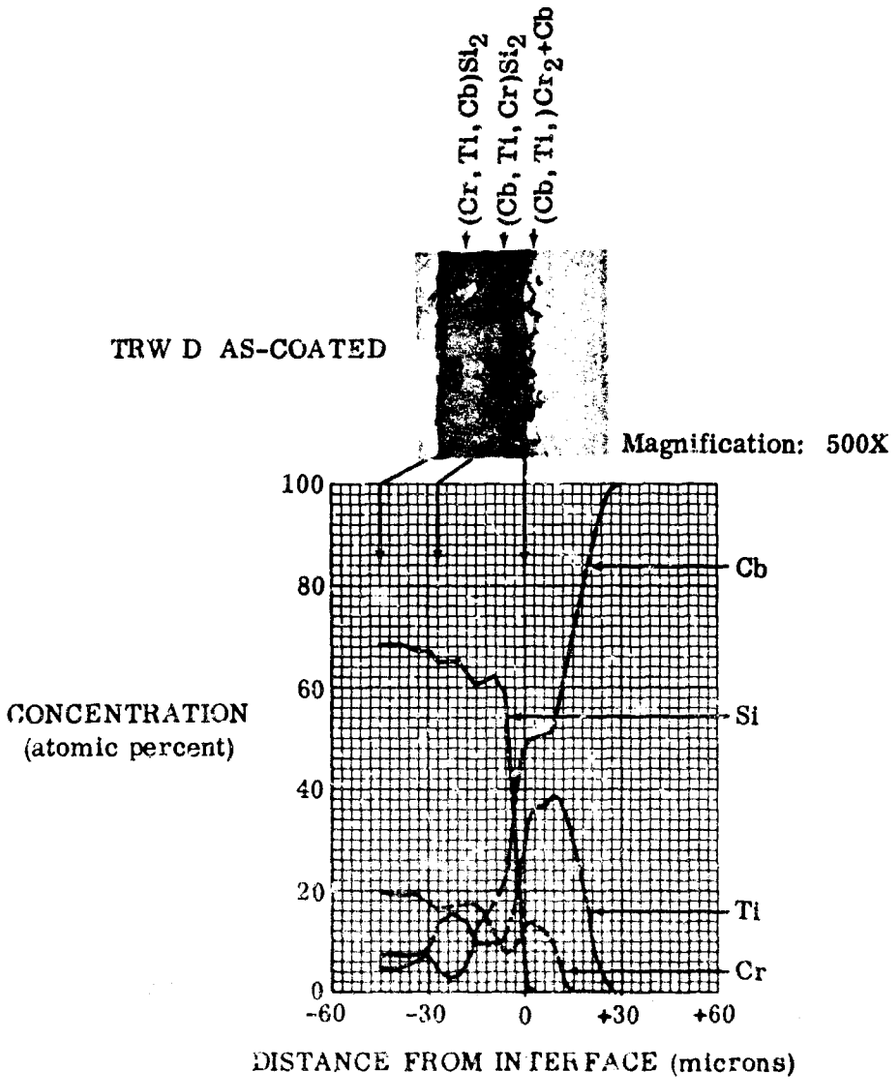

FIGURE 3. CONCENTRATION-PENETRATION PROFILE OF TRW D COATING ON B66 ALLOY

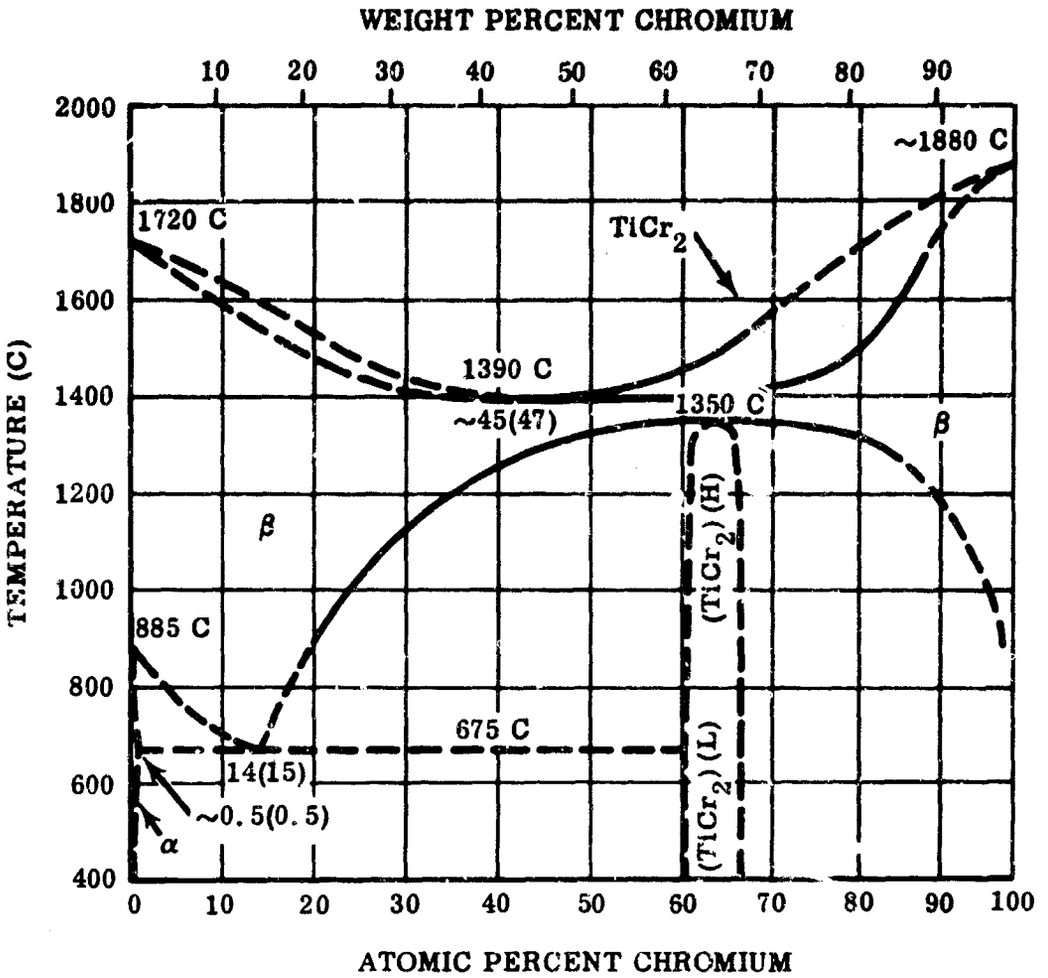

FIGURE 4. CHROMIUM-TITANIUM BINARY SYSTEM

A typical difference in deposition rates on the Cb752 alloy between 60Cr-40Ti[1] and 80Cr-20Ti[1] alloys using identical pack deposition conditions is:

Alloy	Coating Cycle	Deposition Rate
60Cr-40Ti	5 hours at 2300 F	12 mg/cm^2
80Cr-20Ti	5 hours at 2300 F	2.5 mg/cm^2

These pack alloys typically contain 2000 to 3000 ppm oxygen. A 60Cr-40Ti[1] does not transport oxygen to columbium alloys, even with this high oxygen content, due to the high concentration of titanium and the high negative free energy of formation of solutions of oxygen in titanium (Fig. 6). Reducing the titanium and increasing the chromium concentration, as in the 80Cr-20Ti[1] pack alloy, can, however,

1. All compositions are in weight percent unless otherwise noted.

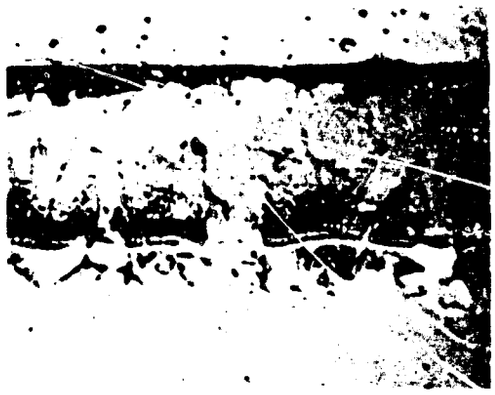

As Coated

One Hour at 2500 F + Water Quench (WQ)

One Hour at 2500 F + WQ + One hour at 1750 F

One Hour at 1750 F + WQ

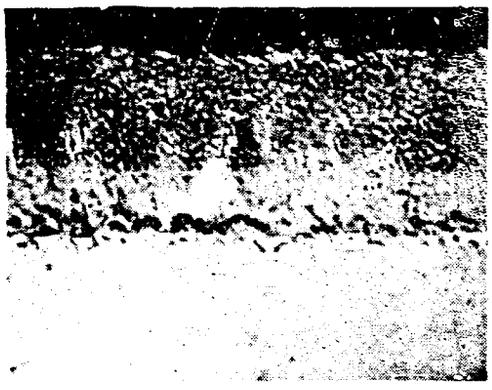

One Hour at 2500 F + Furnace Cool (FC)

One Hour at 2500 F + FC + One Hour at 1750 F

FIGURE 5. MICROSTRUCTURE OF THE HEAT TREATED (Ti-Cr)-Si COATED B66 SPECIMENS; Phase A

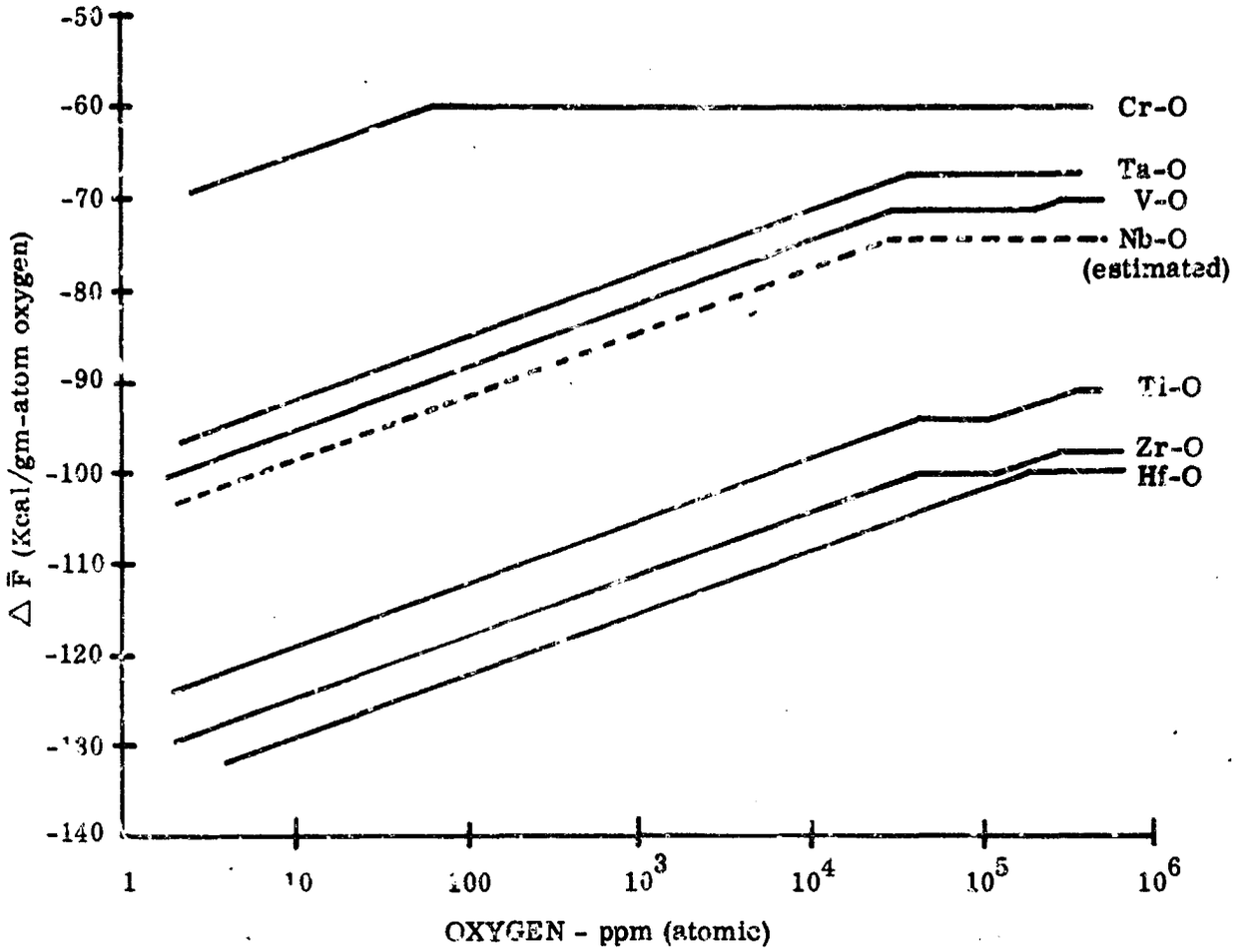

FIGURE 6. PARTIAL MOLAL FREE ENERGY OF FORMATION OF SOLUTION OF OXYGEN WITH VARIOUS TRANSITION METALS

result in transport of oxygen and embrittlement of columbium alloys. For example, the Cb752 (Cb-10W-2.5Zr) alloy has the ductile-brittle bend transition temperature increased to above room temperature by coating with the 80Cr-20Ti pack, whereas the D43 (Cb-10W-1Zr-0.1C) alloy is not embrittled. The difference in response to this coating is believed to be due to the available zirconium in the alloys. The D43 alloy has almost all the zirconium tied up as carbide and oxide; whereas, the Cb752 alloy has considerable zirconium that is uncombined in solid solution in the matrix. The large negative free energy of formation of ZrO_2 and grain boundary diffusion are responsible for the transfer of oxygen. Stein and Lisagor (Ref. 5) observed a similar embrittlement of the D36 (Cb-10Ti-5Zr) alloy when coated with the (60Cr-40Ti)-Si coating, indicating again the importance of zirconium on oxygen transport and embrittlement.

The slow deposition rate of the high-chromium chromium-titanium pack on columbium is a direct result of the greater stability of the $CbCr_2$ phase. This Laves phase is stable according to Hansen (Ref. 4) to at least 1850 C compared to 1350 C for $TiCr_2$ (Fig. 4). Diffusion of chromium or columbium through this high melting phase is extremely slow. One function of titanium in the chromium-titanium modified layer is the destabilization of the $CbCr_2$ Laves phase, thus increasing the deposition rate of chromium. Although the titanium provides destabilization of the $CbCr_2$ Laves phase, allowing reasonably high deposition rates of chromium, it provides two disadvantages:

- It lowers the solidus of the (Ti-Cr)-Si coating to approximately 2500 F.
- It weakens substrate alloys that are strengthened with carbon or oxygen.

The latter point is particularly significant since the third generation of columbium alloys rely on dispersions of carbides or oxides for at least part of their strength (e.g., D43 (0.1 percent carbon), Cb132M (0.1 percent carbon), and Cb752). The loss in strength of the duplex annealed (solution treatment, cold reduction, and aging) D43 alloy after application of the (Ti-Cr)-Si coating has been extensively discussed in other papers (Ref. 6 and 7) and conclusive proof has been developed that titanium is responsible for the carbon migration. The high negative free energy of formation of solution of carbon in titanium is the driving force for carbon migration (Fig. 7). Duplex annealed Cb752 alloy, when coated, shows comparable loss in strength (30 to 50 percent) after coating (Ref. 7) but strength loss is due to the migration of oxygen. The oxygen loss would be expected from the free energy data shown in Figure 6. Further reduction of titanium below the 40 percent level appears imperative if carbide or oxide strengthened columbium-base alloys are to be used effectively.

Another factor that must be considered when evaluating the (Ti-Cr)-Si coating is the relative expansions of the various phases. The microstructures shown in Figure 5 are typical. Crack free areas were selected in most cases. The cracks are not a result of metallographic preparation methods. Thermally cycled specimens for example show a network of cracks on the free surface and the cracks become progressively worse with time. Because of this observation, thermal expansion measurements have been made on coatings and are summarized here to complete the discussion of the (Ti-Cr)-Si coating. Figure 8 shows the thermal expansion of disilicides in the ternary system, $TiSi_2$-$CrSi_2$-$CbSi_2$, compared with a typical columbium alloy. An expansion bar formed from disilicides removed from TRW

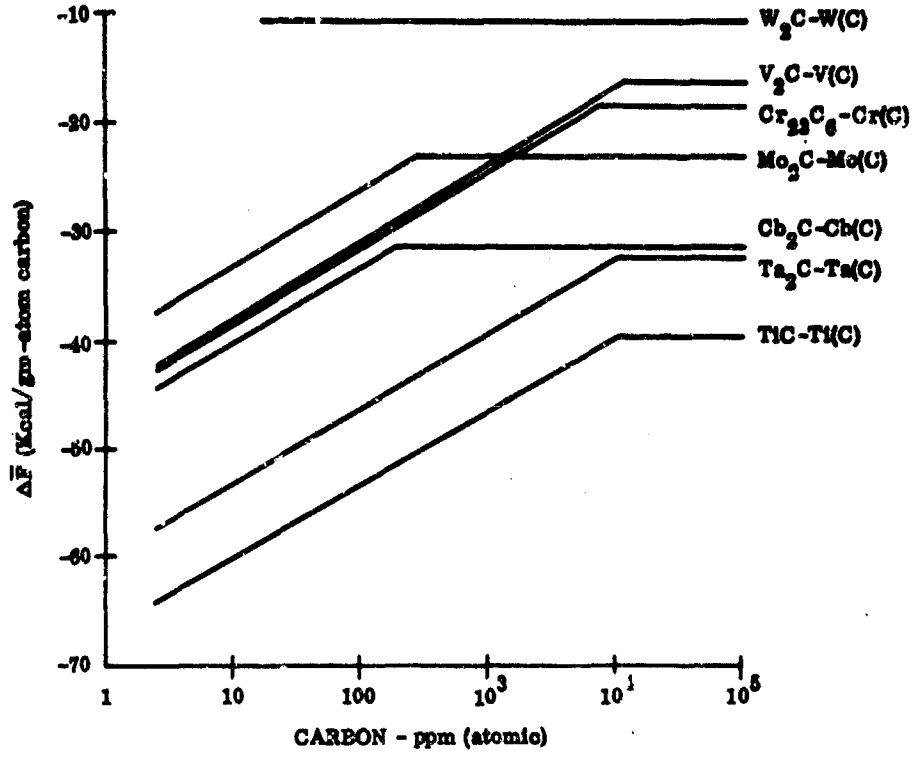

FIGURE 7. PARTIAL MOLAL FREE ENERGIES AT 1500 K; Carbon in Transition Metals

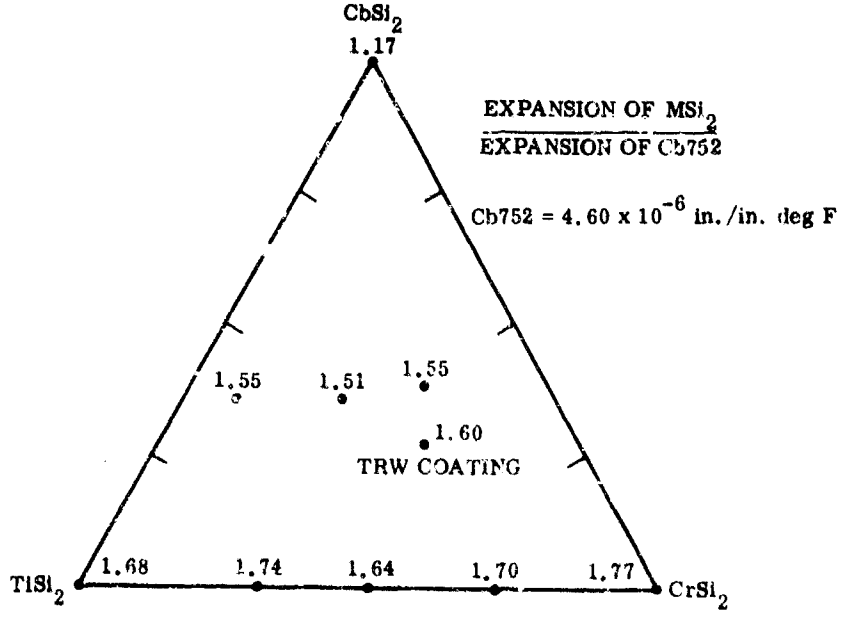

FIGURE 8. RATIO OF DISILICIDE THERMAL EXPANSION TO EXPANSION OF TYPICAL COLUMBIUM-BASE ALLOYS

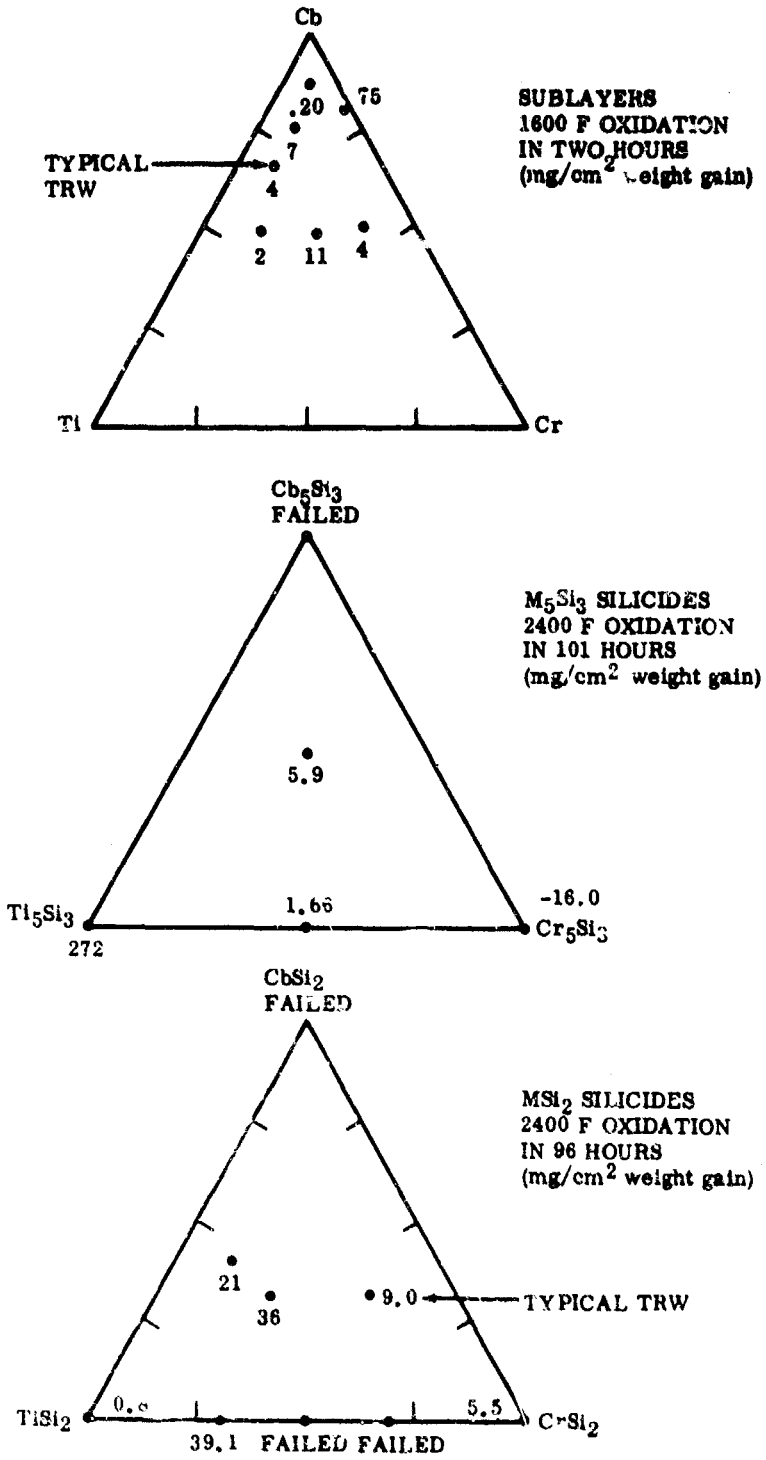

FIGURE 9. OXIDATION RESISTANCE OF THE COMPONENTS OF THE (Ti-Cr)-Si COATING FOR COLUMBIUM ALLOYS

coated specimens is shown at the typical composition in Figure 8. The cause of cracking on thermal cycling is immediately apparent. Figure 9 shows also the oxidation resistance of sublayers at 1600 F, and of subsilicides and disilicides at 2400 F. The oxidation resistance of the sublayer appeared to be important at 1600 F because the higher expansion silicide would be expected to crack and form openings at a temperature of 1600 to 1800 F on cooldown. The results show a strong feature of the (Ti-Cr)-Si chemistry, that of good oxidation resistance of all components of the coating.

5.1.2 General Approach

The original plan of attack called for studies of systems designed to circumvent specific problems noted in the model system, (Ti-Cr)-Si. Table III summarizes the general lines of experimental work planned. Specific reasons for selection of individual systems were based on their contributions to identified problems in the (Ti-Cr)-Si system. For example:

- V-Cr-Si Coating - Vanadium reduces stability of Laves phase; reduces tendency to form interstitial sink.
- Ti-Mo-Si Coating - To reduce evaporation of chromium that occurs at low pressure, to avoid Laves phase.
- Mo-Cr-(Fe, Al) Coating - All ductile, body centered cubic phases.

However, it was realized that a study of final coating chemistries was not the most efficient way to proceed because time and effort may be expended in application of a coating chemistry that is not effective, and, in addition, little is learned that can be applied to a different chemistry. Further, the working hypothesis was adopted that silicides and aluminides tend to be plastic at service temperature e.g., 2500 F), but crack at intermediate temperatures when they become brittle and are subject to differential contraction stresses. It was assumed that an ideal system would be one where the sublayer exposed at the root of the crack in the more brittle aluminide or silicide must be sufficiently oxidation resistant to avoid failure. Development of systems based on such a hypothesis would require data such as sublayer oxidation rates and expansivities of the various coating components. Following this line of reasoning, the general approach was to determine such properties before attempting to develop coating methods to apply such chemistries, on the grounds that early detection of inadequacy would avoid time-consuming efforts on coating application.

TABLE III

EXPERIMENTAL PROGRAM AND SCHEDULE FOR PHASE I

Experimental Program	Primary Objective	Experimental Approach
Diffusion barrier to limit Cr and Ti diffusion into substrate.	To avoid rapid Cr and Ti diffusion from the TRW coating into Cb alloy substrates.	Diffusion bond W or Mo to Cb alloys and apply Cr-Ti-Si coating. Perform metallographic, microhardness and, if necessary, microprobe analyses of diffusion zones after high-temperature anneals.
Substitution of Mo or W for Cr in the Cr-Ti-Si coating.	To avoid rapid Cr and Ti diffusion into Cb alloy substrates with accompanying loss in mechanical properties.	Diffusion studies on the Cb-Ti-Mo or Cb-Ti-W systems compared to Ti-Cr diffusion in TRW coating.
		Determine expansion and oxidation behavior of $(Ti-Mo)Si_2$ and $(Cb-Ti-Mo)Si_2$ or $(Ti-W)Si_2$ and $(Cb-Ti-W)Si_2$ Make necessary modifications consistent with realistic coating methods to provide oxidation resistance.
Substitution of V for Ti in the Cr-Ti-Si coating.	To avoid rapid Cr diffusion--avoid formation of $(Cb-Ti)Cr_2$.	Diffusion bond V-Cr alloys to Cb alloys and determine diffusion rates.
		Determine expansion and oxidation behavior of $(V-Cr)Si_2$ and $(Cb-V-Cr)Si_2$. Make necessary modifications consistent with realistic coating methods to provide oxidation resistance.
Vanadium-modified silicide coatings.	To produce (V-Cb) silicide coatings on Cb alloys and demonstrate the degree of protection afforded by the very fluid glass oxidation products.	Siliconize Cb alloys in a duplex V-Si pack. Compare behavior to best coated Cb alloys in a series of simple comparative oxidation tests.

TABLE III (Cont)

EXPERIMENTAL PROGRAM AND SCHEDULE FOR PHASE I

Experimental Program	Primary Objective	Experimental Approach
Gamma sublayer aluminide coatings.	To attempt to utilize a relatively ductile, oxidation resistant, intermetallic compound as the primary constituent of a coating system.	Diffuse Al and Ti into Cb alloys. Conditions required to form a preponderance of the (Cb-Ti)Al phase as a continuous layer will be determined. Modification with Cr and Si will be considered.
V-Cb aluminide coatings.	To produce effective-ductility coating similar to TRW, Cr-Ti-Si, based on aluminides.	Co-plate Al and V on Cb alloys. Determine oxidation behavior and expansion of the compounds $(V-Cb)Al_3$ and $(Ti-Cb0V)Al_3$.
Ductile metallic coating systems.	To produce a continuous BCC coating system composed of compatible layers which are effective diffusion barriers.	Determine rate of interdiffusion between Cr and each of the alloys Fe-Al, Fe-Cr-Al, Fe-Cr-Y, Fe-Cr-Al-Y. If interdiffusion is too rapid, determine influence of Ni additions to alloys in decreasing Al diffusion rate. Confirm interdiffusion rates in the systems Cr-(Mo or W)-Cb alloy. If a satisfactory minimum diffusion life can be established, specimens suitable for oxidation and mechanical property studies will be prepared and evaluated.
Enamel coating for prealloyed Substrates.	To permit better control of surface oxide composition and improve thermal cycling characteristic and resistance to pest-type failure.	Application of commercial ceramic coatings to Cb alloys prediffusion coated with Ti-Cr. If oxygen barrier performance and cycle performance appears promising, new, more refractory ceramic coatings will be developed specifically for 2300 to 2500 F service.

Examination of certain problems is not possible by single component specimens. Formation of a subsilicide by interdiffusion of disilicide and columbium alloy, and the interstitial sink effect are two examples of problems that must be solved by means of diffusion couples or of actual coatings.

The most difficult problem is selection of compositions for study. Use of noble or scarce metals was not considered in view of potential requirements for USAF applications.

Another point to be considered in selecting compositions for development was the environment and its influence. The coating on aerospace structures will be exposed to low pressure under both static and high aerodynamic shear conditions. The turbine components, excluding such applications as combustion chamber liners, will be exposed to extremely high mass flows and/or centrifugal forces. Coatings having appreciable fluidity or high volatility were, therefore, not included in the program. Prior work (Ref. 3) on coated specimens tested in a plasma arc torch at 2500 F, illustrated the problem. The aluminum-tin type of coating and the silicide coating generating very fluid oxides both failed in short periods of time; whereas, the more refractory coatings held up very well. For vane, blade, and reentry surface areas, fluid silicide, conventional aluminum-tin, or zinc coatings were not considered.

In summary, the approach consisted of a study of suitable alloys for use beneath silicides or aluminides as primary oxidation-resistant barriers. Work on the sublayers included oxidation resistance, expansion, interdiffusion with columbium substrate, and effect on the mechanical properties of the substrate, this work is reported in Paragraph 3.2. Work on the primary oxidation barriers was largely a study of silicides and aluminides and is reported in Paragraph 3.3. In addition, single-layer coatings of ductile alloys were studied based on the all body centered cubic lattice concept (Table III); this work is reported in Paragraph 3.4.

3.2 EVALUATION OF SUBLAYER PROPERTIES

The general purpose of the work described in this section was to develop a ductile sublayer with oxidation resistance sufficiently better than that of the basic columbium alloy so that it would provide protection at the base of cracks in the primary oxidation barrier (e.g., silicide or aluminide). At the same time, the possibility of development of an oxidation resistant alloy that would permit complete failure of the primary barrier, yet allow completion of a mission, was regarded as a definite

secondary objective. These approaches represent the effective-ductility concept. However, attainment of the first objective requires oxidation resistance at the temperature where the primary barrier might crack on cooldown; this temperature was selected to be 1600 F. The basis for this temperature was that it allows at least 600 degrees F cooling below the temperature where the primary barrier possesses some plasticity (assumed to be 2200 F). If cracking occurs above 1600 F, additional cooling to 1600 F would allow the cracks to open wider when oxidation protection will be even more necessary; whereas, if cracking occurs below 1600 F (because of good expansion match, for example), the kinetics of oxidation will not require such a good oxidation-resistant substrate.

Attainment of the second objective requires that the sublayer have good oxidation resistance at the service temperature. The approach was taken that if good oxidation resistance was found at 1600 F, meeting the first objective, the sublayer would be investigated up to 2400 F.

Other properties that need to be studied are expansion of the sublayer composition, interdiffusion between sublayer and columbium alloy, and the effect of the sublayer on the mechanical properties of the columbium alloy. Each of these problem areas is discussed in the following sections.

3.2.1 Oxidation Resistance

The determination of the oxidation resistance of potential sublayers was a major experimental effort in the program. Included in the study were various substrate alloys that would indicate a trend in oxidation resistance of solid solution alloys; alloys in the Cb-Ti-Cr, Cb-Ti-Mo, Cr-V, and Cb-Ti-Cr-V systems; alloys in the Cb-Ti-Al; and several systems containing beryllium. The nominal compositions of the sheet alloys investigated are shown in Table IV and the potential sublayer alloys prepared on this program in Table V.

The sublayer alloys were prepared by cold pressing, followed by arc melting in a water-cooled copper crucible with a tungsten electrode in gettered argon at 0.5 atmosphere. To ensure complete melting, the specimens were melted on both sides. After melting, the specimens were homogenized in gettered argon at 2300 F for four hours. The oxidation specimens were diamond sawed from the arc-melted buttons. The alloys that were prepared during the investigation are listed in Table V.

TABLE IV

NOMINAL COMPOSITIONS OF COMMERCIAL SUBSTRATE ALLOYS OXIDATION TESTED

Alloy Designation	Source	Thickness (in.)	Composition (Nominal) (wt %)
D14	du Pont	0.041	Cb-5Zr
D36	du Pont	0.125	Cb-10Ti-5Zr
D31	du Pont	0.103	Cb-10Ti-10Mo-0.1C
Cb752	Union Carbide	0.125	Cb-10W-2.5Zr
Cb753	Union Carbide	0.022	Cb-5V
D43	du Pont	0.030	Cb-10W-1Zr-0.1C
C129	Wah Chang	0.0123	Cb-10W-10Hf
C129Y	Wah Chang	0.0305	Cb-10W-10Hf plus Y
B66	Westinghouse	0.050	Cb-5V-5Mo-1Zr
Cb (pure)		0.021	100Cb

Oxidation tests were conducted in air for 1, 2, 4, and 16 hours at 1600 F. Initially, the specimens were measured and weighed before the tests with the intention of scraping off the oxide after the tests to measure the surface recession rate of alloys. However, this was feasible for most of the specimens after the one-hour test only. It could be done for a few specimens after the two-hour test, but the oxidation was catastrophic after 4 and 16 hours for almost all of the initial alloy specimens (Alloys 101 through 127). For subsequent alloys, the specimen plus all of its oxide was weighed after each cycle to generate rate plots from the data.

Oxidation of Commercial Alloys

The 1600 F oxidation test results on ten commercial columbium-base alloys are shown in Table VI, and specimens exposed 1 and 16 hours are shown in Figure 10. The oxidation test results are plotted in Figure 11, and show that the alloys fall into two groups in their resistance to oxidation. All of the alloys underwent diffusion controlled, i.e., parabolic oxidation; however, the rate constants were markedly different for the two groups. The rate constant, k, is given by the relation between weight gain, W, and time t:

$$W = kt^{1/2}$$

TABLE V

NOMINAL COMPOSITION OF ARC-MELTED SUBLAYER ALLOYS FOR OXIDATION STUDIES AT SOLAR

Alloy Designation	Nominal Composition (wt %)						
	Cb	Ti	Cr	Mo	V	Al	Be
101	65.7	27.0	7.3	--	--	--	--
102	65.0	16.8	18.2	--	--	--	--
103	64.4	6.7	28.9	--	--	--	--
104	74.0	19.1	6.9	--	--	--	--
105	73.6	12.7	13.7	--	--	--	--
106	73.2	6.3	20.5	--	--	--	--
107	85.1	11.7	3.2	--	--	--	--
108	84.5	2.9	12.6	--	--	--	--
109	88.1	2.7	9.2	--	--	--	--
110	61.8	25.5	--	12.7	--	--	--
111	56.4	14.5	--	29.1	--	--	--
112	51.8	5.4	--	42.8	--	--	--
113	70.0	18.0	--	12.0	--	--	--
114	--	11.3	--	22.7	--	--	--
115	--	5.4	--	32.2	--	--	--
116	--	11.4	--	5.7	--	--	--
117	--	2.6	--	21.0	--	--	--
118	--	2.6	--	5.3	--	--	--
119	--	--	7.2	--	28.3	--	--
120	--	--	18.0	--	17.6	--	--
121	--	--	28.7	--	7.0	--	--
122	--	--	6.8	--	20.1	--	--
123	--	--	13.6	--	13.4	--	--
124	--	--	20.4	--	6.7	--	--
125	--	--	3.1	--	12.4	--	--
126	--	--	12.6	--	3.1	--	--
127	--	--	2.9	--	2.9	--	--
Q_1	64.6	6.87	21.7	--	7.1	--	--
Q_2	64.2	--	28.7	--	7.0	--	--
Q_3	65.2	27.1	7.3	--	--	--	--
Q_4	65.2	23.2	11.0	--	3.6	--	--
Q_5	65.0	13.4	14.5	--	7.1	--	--
Q_6	65.7	27.1	--	--	7.2	--	--
Q_7	65.4	26.2	7.3	--	1.2	--	--
IITRI[1] 13	91	5	--	--	--	4	--
IITRI 33	85	10	--	--	--	5	--
IITRI 34	75	20	--	--	--	5	--
IITRI 35	65	30	--	--	--	5	--
IITRI 36	40	50	--	--	--	10	--
IITRI 37	55	40	--	--	--	5	--
IITRI 38	30	60	--	--	--	10	--
--	45	40	10	--	--	5	--
Be-1	99.75	--	--	--	--	--	0.25
Be-2	99.5	--	--	--	--	--	0.5
Be-3	99.0	--	--	--	--	--	1.0
Be-4	95.0	--	--	--	--	--	5.0
Be-5	89.5	10.0	--	--	--	--	0.5
Be-6	89.5	10.0	--	--	--	--	0.5
Be-7	55.0	39.0	10.0	--	--	--	5.0
Be-8	59.5	30.0	10.0	--	--	--	9.5

1. Alloys IITRI 13 through IITRI 38 were prepared at IITRI and oxidation tested at Solar.

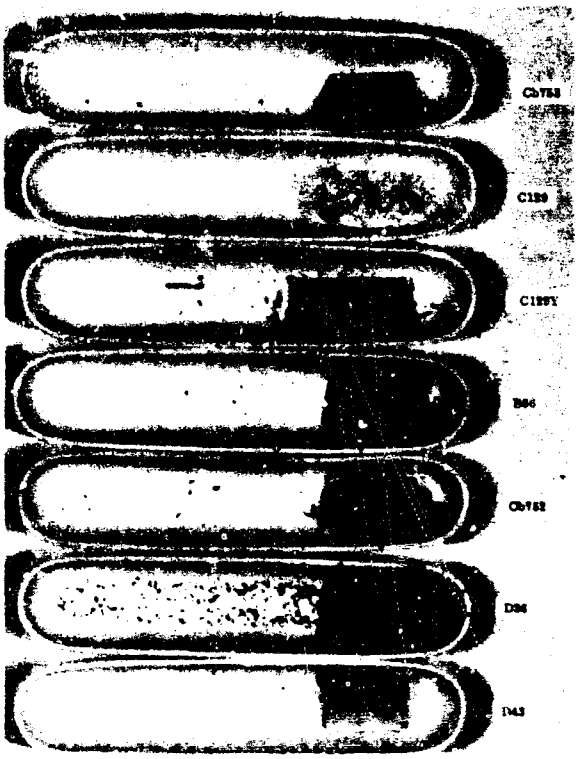

1 Hour

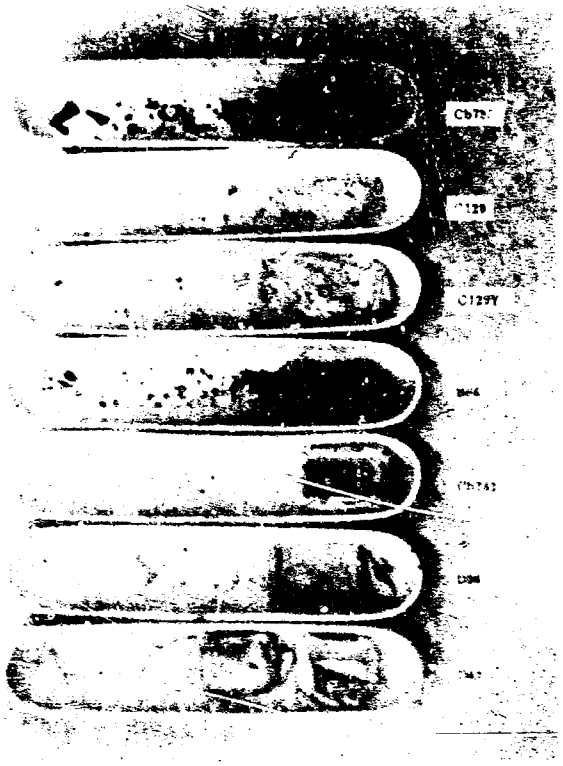

16 Hours

FIGURE 10. COMMERCIAL COLUMBIUM-BASE ALLOYS OXIDIZED AT 1600 F
(Sheet 1 of 2)

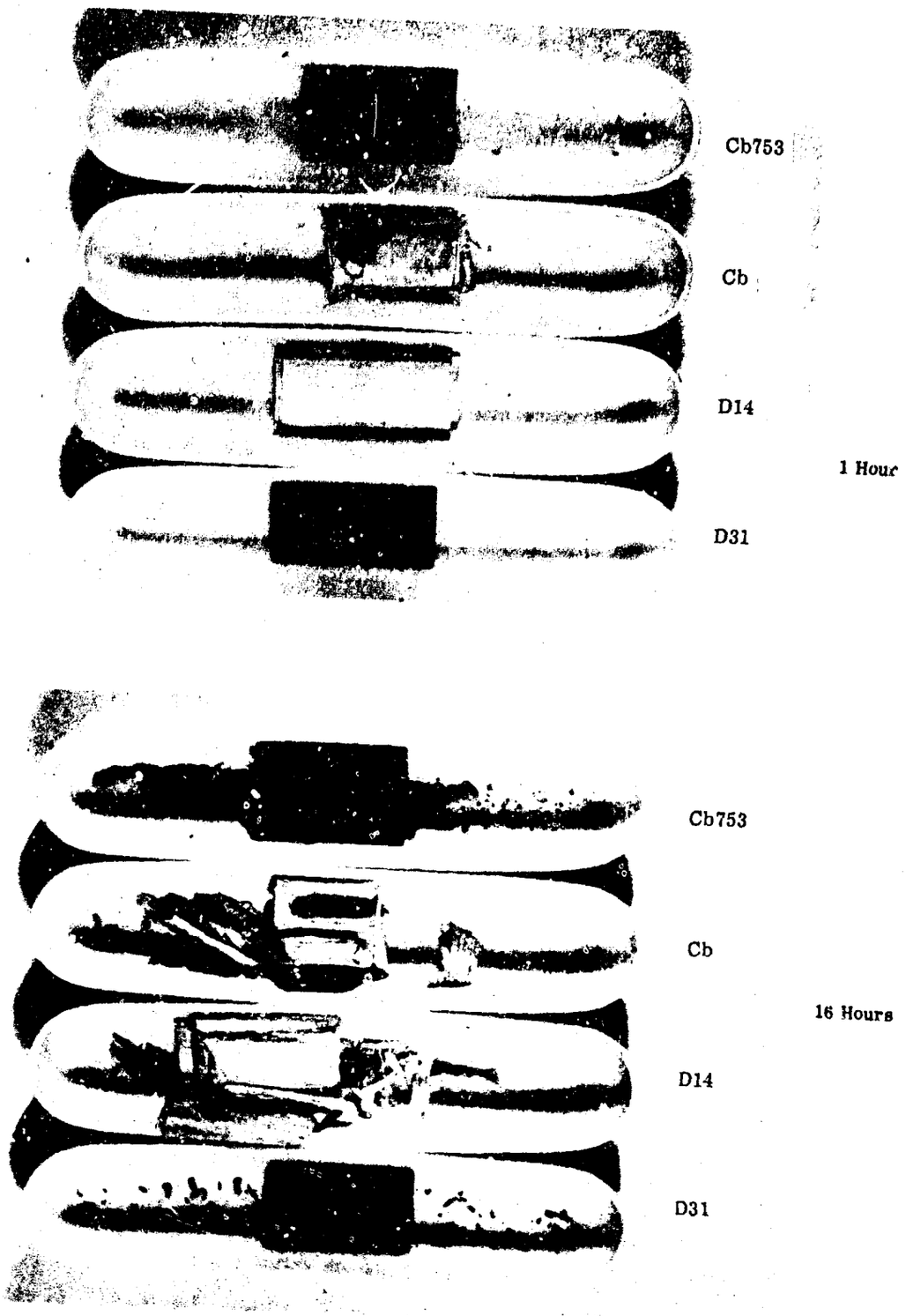

FIGURE 10. COMMERCIAL COLUMBIUM-BASE ALLOYS OXIDIZED AT 1600 F
(Sheet 2 of 2)

TABLE VI

OXIDAT)N OF UNCOATED SUBSTRATE ALLOYS - 1600 F IN AIR

Alloy	Nominal Composition (weight percent)	Weight Gain (mg/cm^2)				Comments
		1 hr	2 hr	4 hr	16 hr	
D36	Cb-10Ti-5Zr	5.2	5.5	13.9	26.8	Third best; white, non-adherent oxide.
Cb753	Cb-5V	12.8 11.4	15.5 16.8	16.1 14.5	27.5 17.6	Fourth best; dark oxide.
B66	Cb-5V-5Mo-1Zr	6.4	8.5	10.3	19.4	Second best; dark oxide.
Cb752	Cb-10W-2.5Zr	32.1	39.7	44.0	126.0	Poor; fast oxidation; white oxide.
D43	Cb-10W-1Zr-0.1C	27.4	35.4	51.4	109.6	Poor; fast oxidation; white oxide.
C129	Cb-10W-10Hf	49.5	-	-	-	Poor; fast oxidation; white oxide.
C129Y	Cb-10W-10Hf + Y	25.3	36.3	68.6	129.6	Poor fast oxidation; white oxide.
D14	Cb-5Zr	61.0	95.8	162.8	Complete oxide	Poor; very fast oxidation.
D31	Cb-10Ti-10Mo-0.1C	3.7	4.8	6.5	13.0	Best of series; dark oxide.
Pure Cb	100Cb	41.5	57.0	Complete oxide	Complete oxide	Poor; very fast oxidation.

This constant varied from more than 27.5 $mg/cm^2/hr^{1/2}$ for the high group to less than 6.9 $mg/cm^2/hr^{1/2}$ for the low group. The high oxidation rate group contained pure columbium, D14, C129, C129Y, Cb752, and D43 alloys; the low group contained Cb753, D36, B66, and D31 alloys.

Duplicate oxidation tests were run on the Cb753 alloy because of the unusual oxidation resistance results (Table VI and Figure 11). The parabolic oxidation rate constant of this alloy appeared to change with time. Up to two hours, the constant was 11.5 $mg/cm^2/hr^{1/2}$; from 2 to 16 hours the rate constant was the lowest displayed by any one of the commercial alloys, i.e., 3.47 $mg/cm^2/hr^{1/2}$ or lower depending on the data used. Both runs confirmed this effect.

It appeared significant that the commercial alloys exhibiting good oxidation resistance when uncoated, i.e., Cb753, D36, B66, and D31, are the alloys that have the most oxidation resistance when silicided with a straight silicide coating. The oxidation resistance of the substrate undoubtedly is a significant factor in the performance of such coatings.

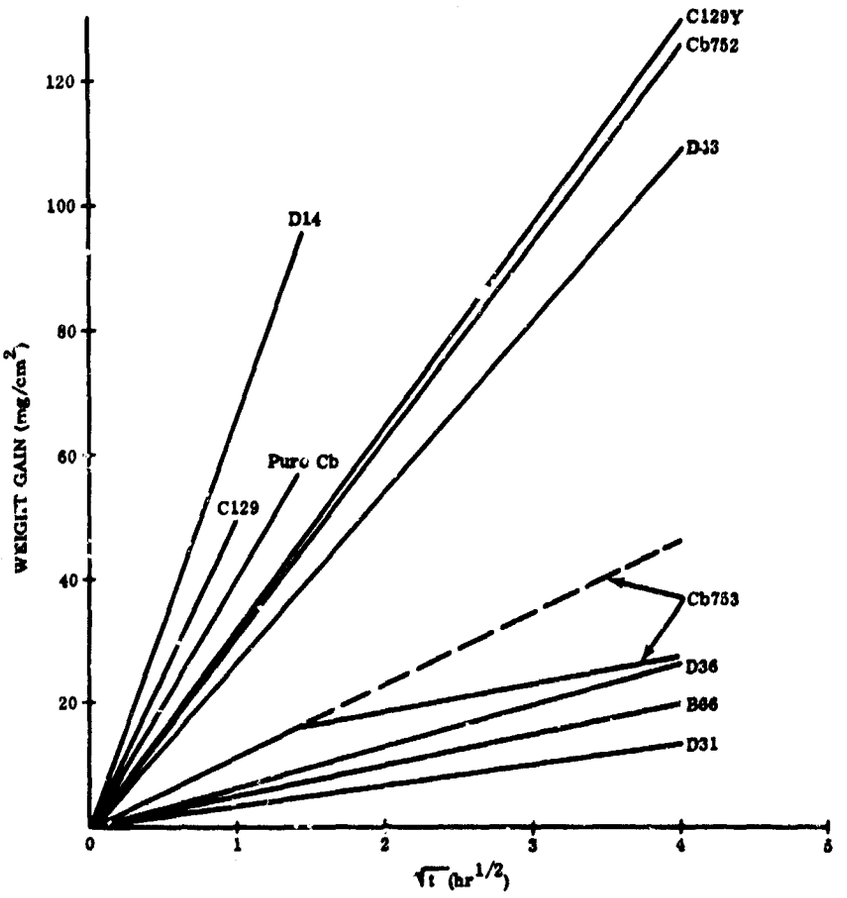

FIGURE 11. OXIDATION RATE PLOTS OF SEVERAL UNCOATED SUBSTRATE ALLOYS; 1600 F in Air

Oxidation of Cb-Ti-Cr, Cb-Ti-Mo, and Cb-V-Cr Ternary Alloys

The 1600 F oxidation test results on the above ternary alloys are summarized in Table VII. The weight increase is related to the original surface area. In many cases, however, the specimens exfoliate during tests, and as a result the actual surface area becomes very large. In Figures 12 through 14, the specimens are shown arranged according to nominal composition, after 4- and 16-hour tests. Weight gain data after two hours at 1600 F are shown in Figure 15. The same alloys are shown in Figures 12B, 13B, and 14B.

TABLE VII

OXIDATION IN AIR AT 1600 F OF SEVERAL Cb-Ti-Cr, Cb-Ti-Mo, AND Cb-V-Cr TERNARY ALLOYS

Composition Number	Nominal Composition		Weight Increase (mg/cm^2)				Thickness (in.)	
	(wt %)	(at %)	1 hr	2 hr	4 hr	16 hr	Original	After 4 hr
101	Cb-27.0Ti-7.3Cr	50Cb-40Ti-10Cr	1.01	1.82	4.84	-- (1)	0.1440	0.1435
102	Cb-16.8Ti-16.2Cr	50Cb-25Ti-25Cr	6.31	11.07	11.61	12.66	0.1285	0.1270
103	Cb-6.7Ti-28.9Cr	50Cb-10Ti-40Cr	1.76	4.08	--	comp ox	0.1450	0.1435
104	Cb-19.1Ti-6.9Cr	60Cb-30Ti-10Cr	2.32	2.91	--	8.56	0.1070	0.1070
105	Cb-12.7Ti-13.7Cr	60Cb-20Ti-20Cr	12.24	--	--	38.16	0.1325	0.1320
106	Cb-6.3Ti-20.5Cr	60Cb-10Ti-30Cr	13.13	--	13.18	--	- -	- -
107	Cb-11.7Ti-3.2Cr	75Cb-20Ti-5Cr	4.02	5.00	--	--	0.1040	0.1035
108	Cb-2.9Ti-12.6Cr	75Cb-5Ti-20Cr	3.88	6.15	--	--	- -	- -
109	Cb-2.7Ti-8.2Cr	90Cb-5Ti-5Cr	--	19.90	--	75.20	- -	- -
110	Cb-25.5Ti-12.7Mo	50Cb-40Ti-10Mo	6.64	--	9.78	16.69	0.1232	0.1232
111	Cb-14.5Ti-29.1Mo	50Cb-25Ti-25Mo	4.46	5.58	31.87	129.16	0.1393	- -
112	Cb-5.4Ti-42.8Mo	50Cb-10Ti-40Mo	23.38	39.18	comp ox	comp ox	0.1055	---
113	Cb-18.0Ti-12.0Mo	60Cb-30Ti-10Mo	9.11	8.29	16.07	16.07	0.1368	0.1345
114	Cb-11.3Ti-22.7Mo	60Cb-20Ti-20Mo	4.59	6.13	12.42	67.53	0.1315	0.1300
115	Cb-5.4Ti-32.2Mo	60Cb-10Ti-30Mo	17.76	23.66	42.97	119.82	0.1239	0.0955
116	Cb-11.4Ti-5.7Mo	75Cb-20Ti-5Mo	4.90	8.27	16.03	20.41	0.1150	0.1150
117	Cb-2.6Ti-21.0Mo	75Cb-5Ti-20Mo	much ox	much ox	much ox	comp ox	0.1618	0.1570
118	Cb-2.6Ti-5.3Mo	90Cb-5Ti-5Mo	5.72	--	much ox	comp ox	0.1235	0.1213
119	Cb-28.3V-7.2Cr	50Cb-40V-10Cr	64.80	94.20	126.77	162.93	0.1395	- -
120	Cb-17.6V-12.0Cr	50Cb-25V-25Cr	24.41	39.92	117.57	comp ox	0.1220	0.1110
121	Cb-7.0V-28.7Cr	50Cb-10V-40Cr	3.38	7.54	10.55	23.90	0.1412	0 1391
122	Cb-20.1V-6.8Cr	60Cb-30V-10Cr	47.06	--	58.08	159.26	0.1175	- -
123	Cb-13.4V-13.6Cr	60Cb-20V-20Cr	9.13	42.75	97.22	119.90	0.1513	0.1476
124	Cb-6.7V-20.4Cr	60Cb-10V-30Cr	13.90	--	30.70	76.37	0.1355	0.1335
125	Cb-12.4V-3.1Cr	75Cb-20V-5Cr	12.34	32.6	71.69	332.84	0.1000	0.0971
126	Cb-3.1V-12.6Cr	75Cb-5V-20Cr	very good	good	good	fair	0.1065	0.1050
127	Cb-2.9V-2.9Cr	90Cb-5V-5Cr	very good	good	good	fair	0.1503	0.1465

1. Values not shown due to excessive spalling

Note: comp ox - complete oxidation
much ox - much oxidation

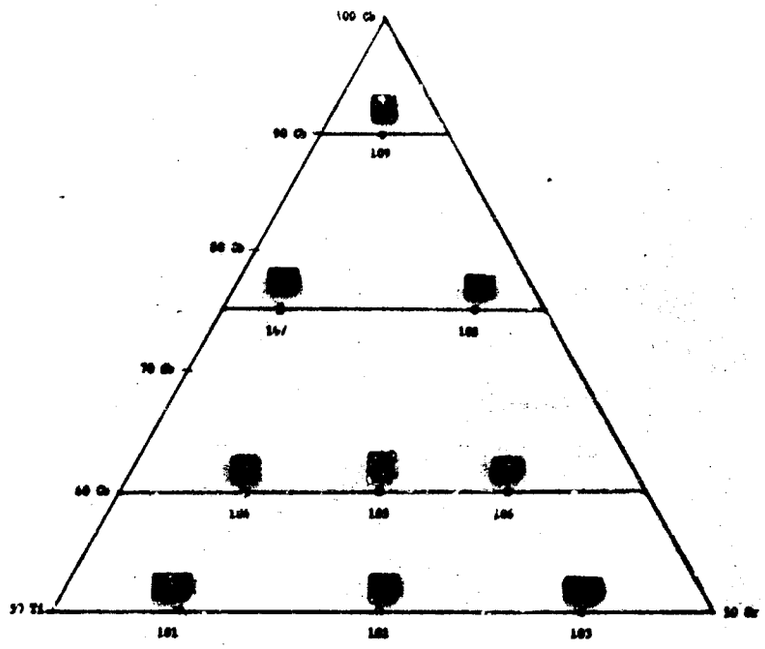

A. Oxidized Four Hours

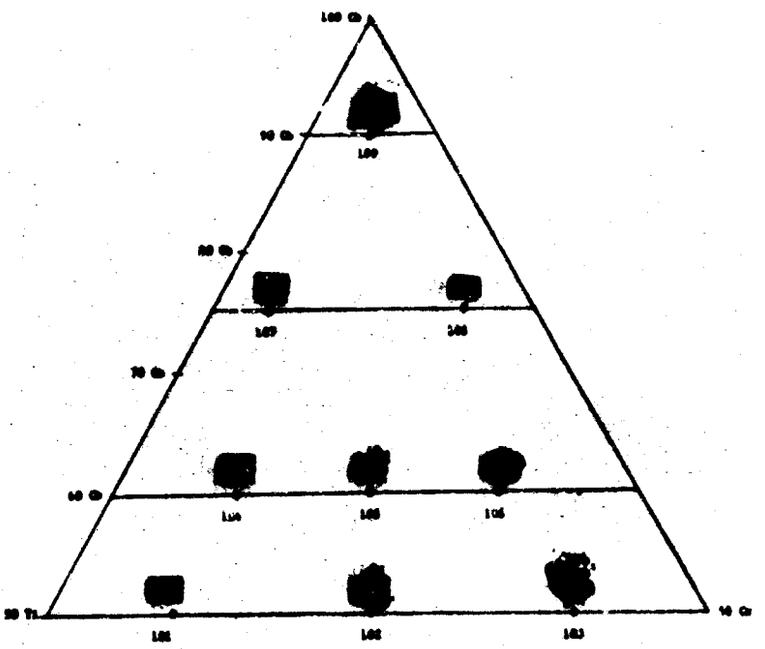

B. Oxidized Sixteen Hours

FIGURE 12. COLUMBIUM-TITANIUM-CHROMIUM ALLOYS OXIDIZED AT 1600 F

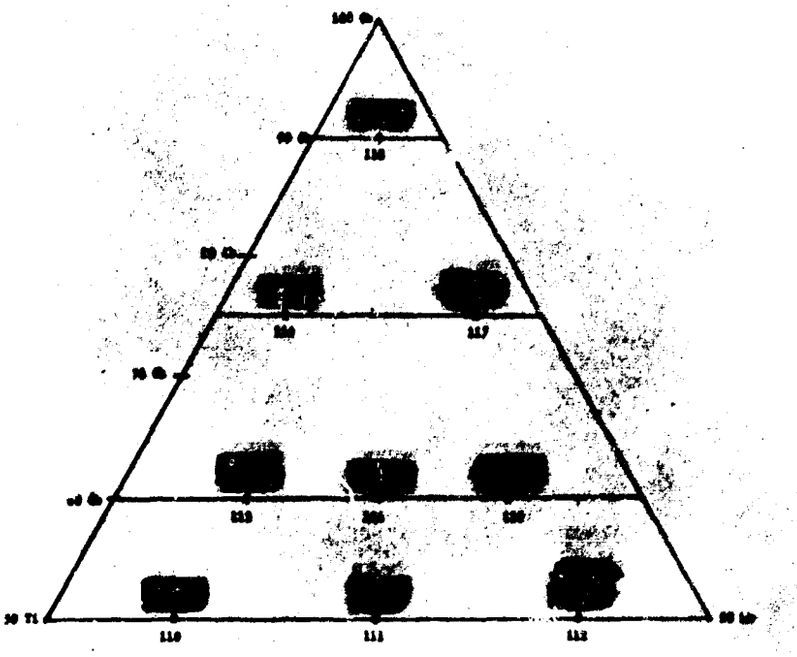

A. Oxidized Four Hours

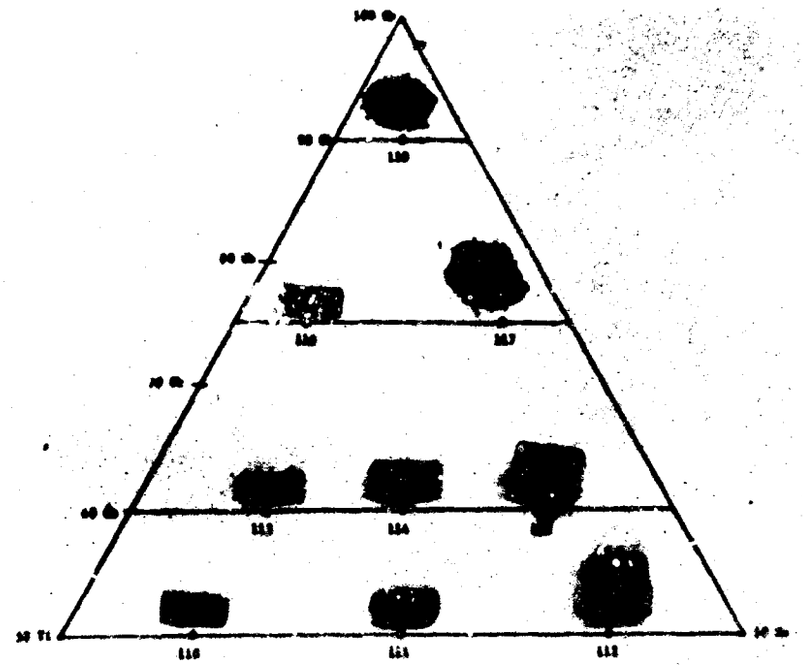

B. Oxidized Sixteen Hours

FIGURE 13. COLUMBIUM-TITANIUM-MOLYBDENUM ALLOYS OXIDIZED AT 1600 F

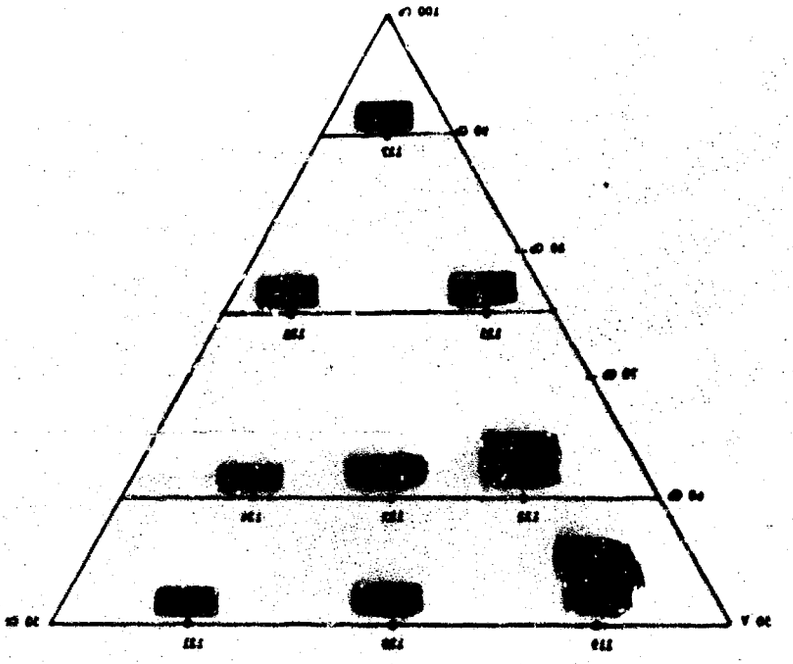

A. Oxidized Four Hours

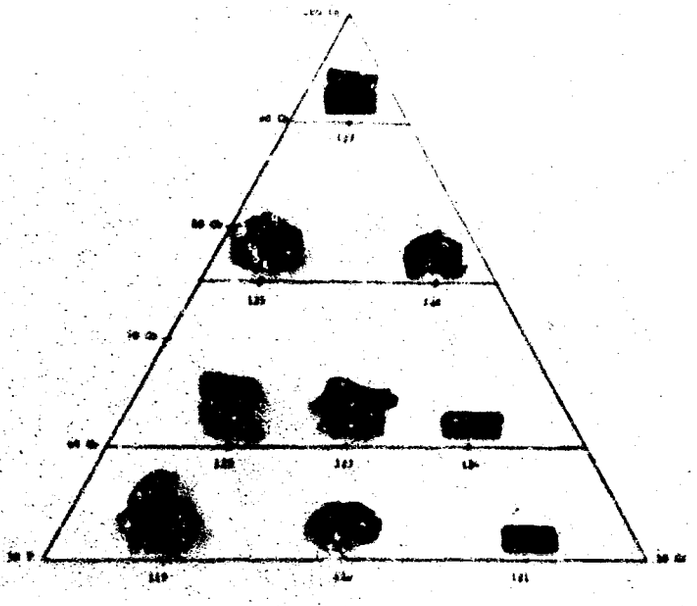

B. Oxidized Sixteen Hours

FIGURE 14. COLUMBIUM-VANADIUM-CHROMIUM ALLOYS OXIDIZED AT 1600 F

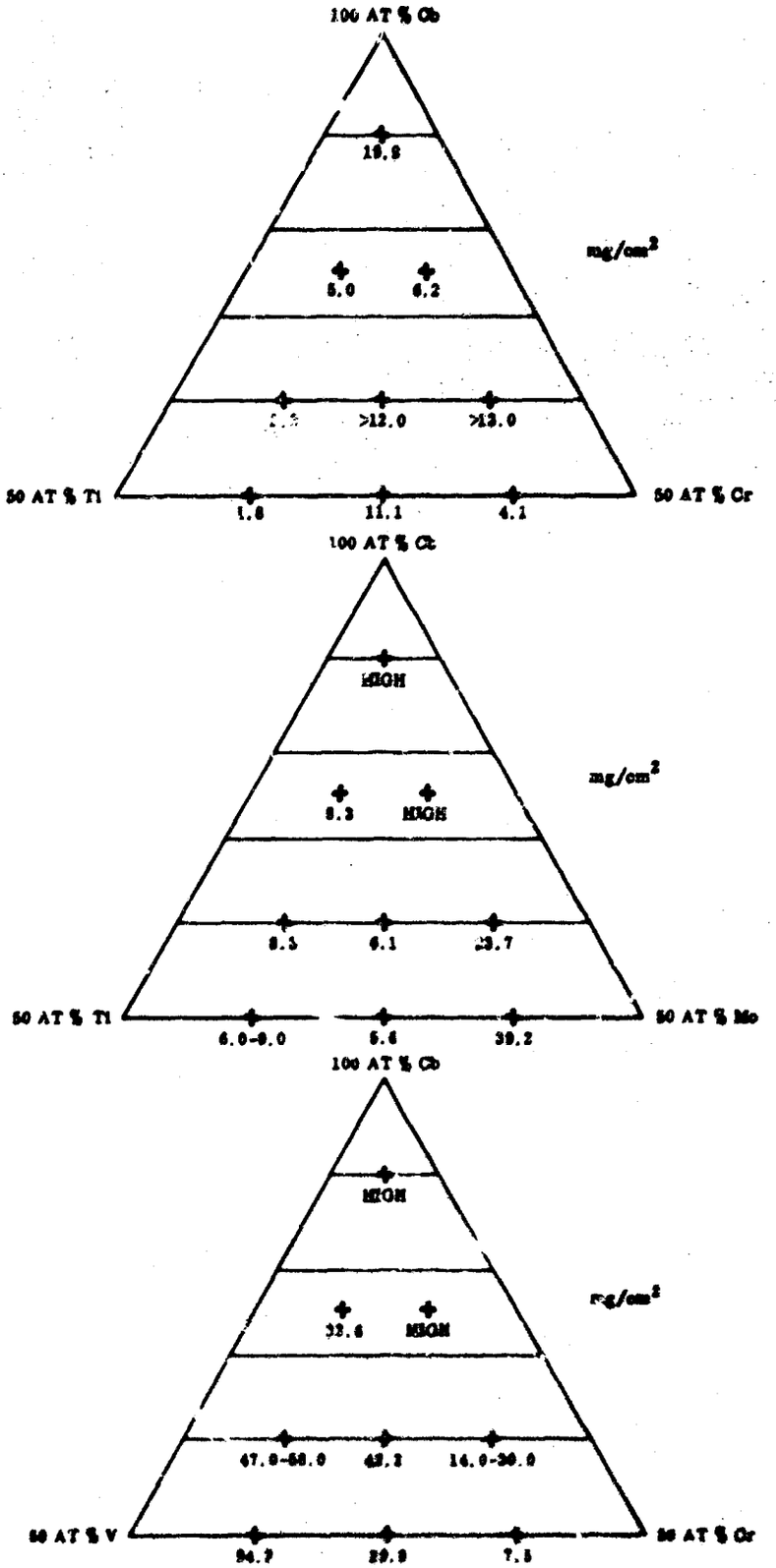

FIGURE 15. WEIGHT GAIN AFTER TWO HOURS AT 1600 F IN AIR; Cb-Ti-Cr, Cb-Ti-Mo, and Cb-V-Cr Alloys

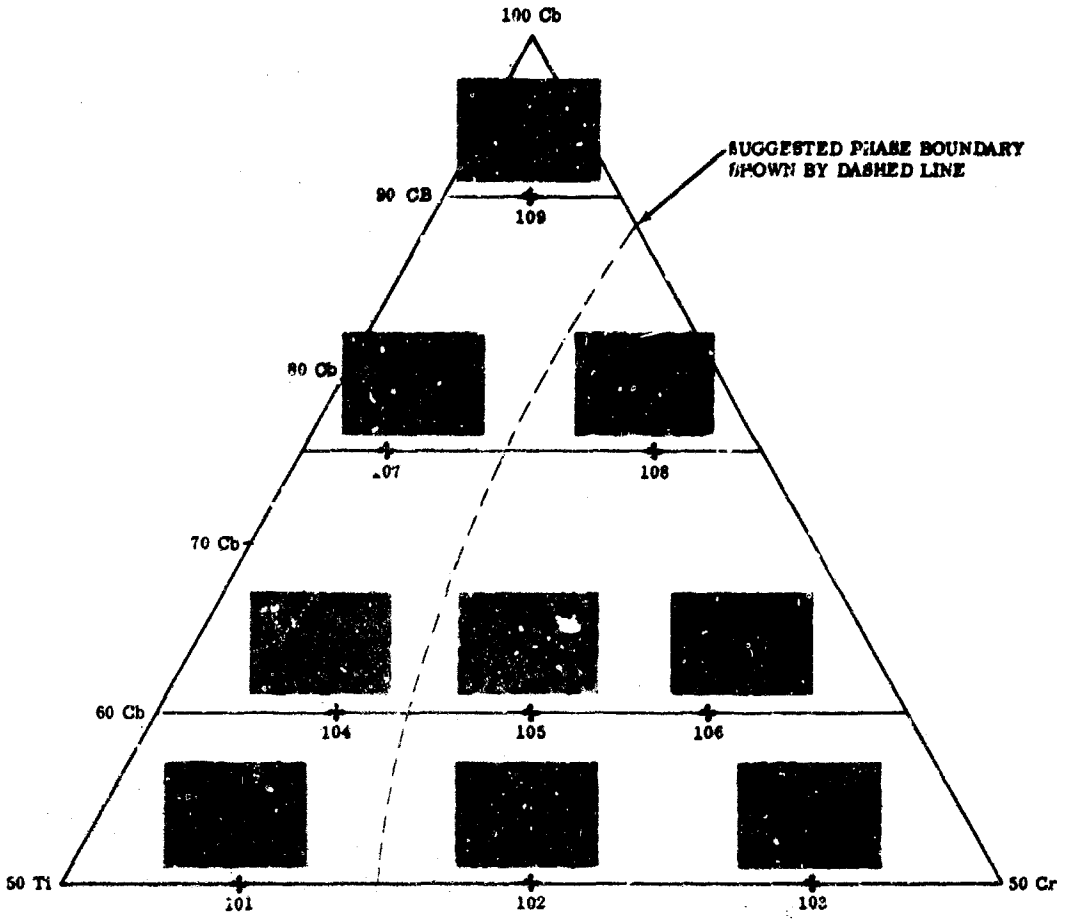

FIGURE 16. COLUMBIUM-TITANIUM-CHROMIUM ALLOYS ARC MELTED AND ANNEALED FOUR HOURS AT 2300 F

Metallographic investigations of the alloys after four-hour homogenizing at 2300 F showed the low-chromium samples of the Cb-Ti-Cr and Cb-V-Cr systems to be one-phase solid solution; the higher chromium alloys were two-phase structures. The Cb-Ti-Mo alloys were all solid solutions. Figures 16 through 18 show the microstructures of the alloys after annealing at 2300 F and suggested one- and two-phase regions for the Cb-Ti-Cr and Cb-V-Cr systems.

Interpreting the significance of the limited test series, there appeared to be some definite trends in the data that were traceable to composition. For example, zirconium, hafnium, and tungsten either did not improve the oxidation resistance of columbium or were deleterious to it; titanium and vanadium markedly improve the

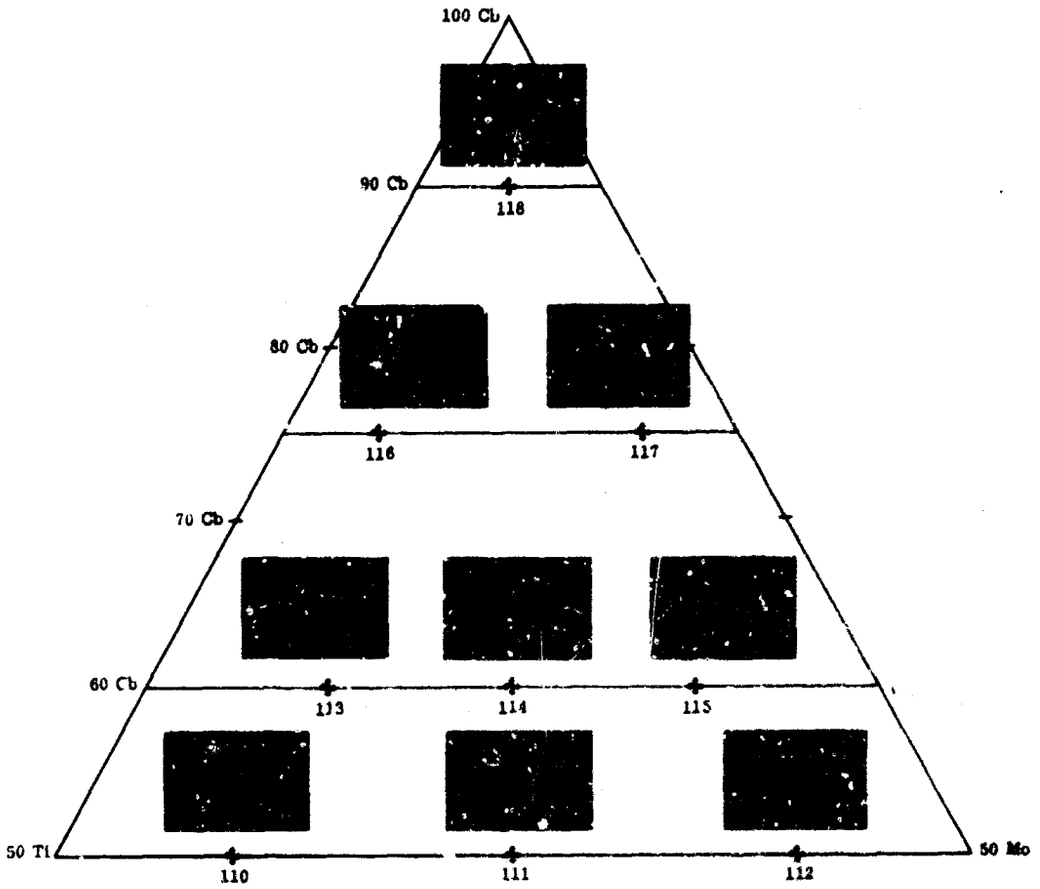

FIGURE 17. COLUMBIUM, TITANIUM, MOLYBDENUM ALLOYS ARC MELTED AND ANNEALED FOUR HOURS AT 2300 F

oxidation resistance of columbium; and the combination of molybdenum with vanadium or titanium offered further improvement in oxidation resistance over the single-element additions.

Based on the experimental results presented in this section, it was concluded that the alloys tested in the Cb-Ti-Cr system show higher oxidation resistance at 1600 F than the Cb-Ti-Mo and Cb-V-Cr alloys.

In the Cb-Ti-Cr system, good oxidation resistance occurred in the alloys of low- and medium-columbium content. By replacing the chromium with molybdenum, the oxidation resistance decreased, and the most oxidation-resistant alloys were those in which the molybdenum concentration was low. This oxidation resistance was expected, since molybdenum was known to cause catastrophic oxidation. Vanadium was

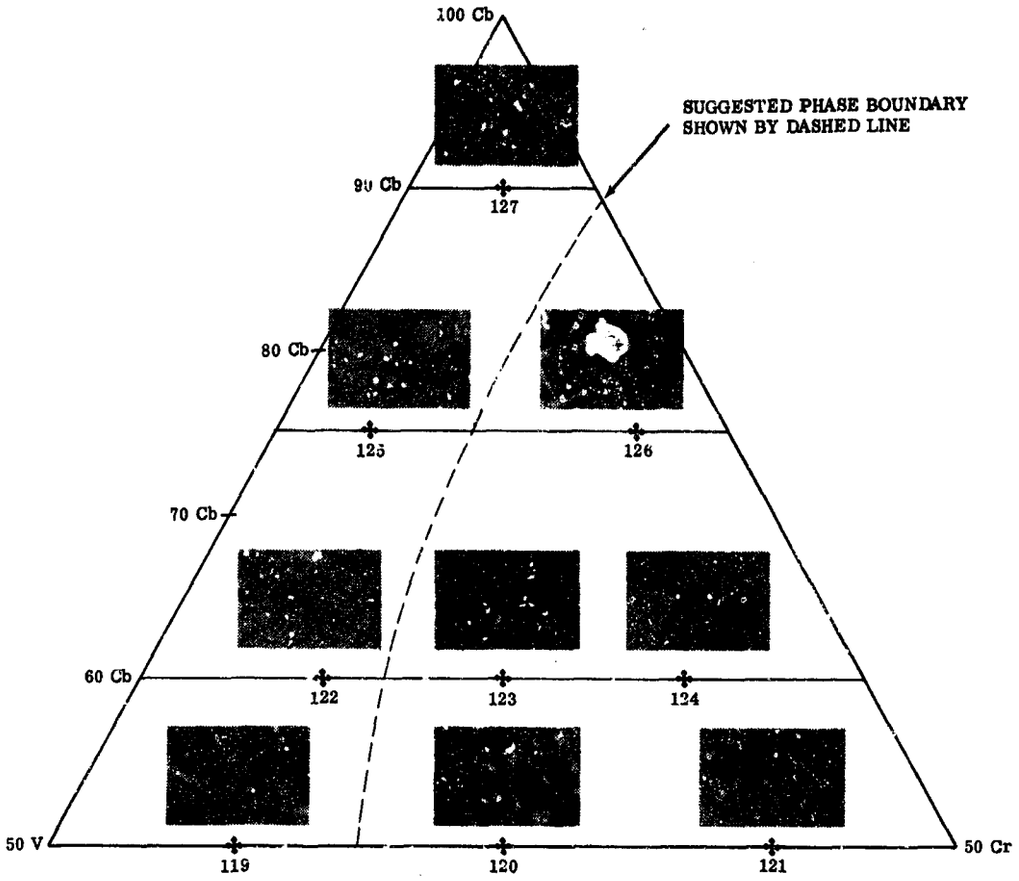

FIGURE 18. COLUMBIUM-VANADIUM-CHROMIUM ALLOYS ARC MELTED AND ANNEALED FOUR HOURS AT 2300 F

also known to cause catastrophic oxidation and, consequently, substituting vanadium for titanium was expected to cause some deterioration of the oxidation properties. This deterioration was clearly observed in this study.

The Cb-V-Cr alloys generally exhibited very poor oxidation resistance except for the one with the highest chromium content. This alloy (50Cb-10V-40Cr) was comparable to the best Cb-Ti-Mo alloys and to many of the Cb-Ti-Cr alloys, and it is conceivable that an even higher chromium content would improve the oxidation properties further.

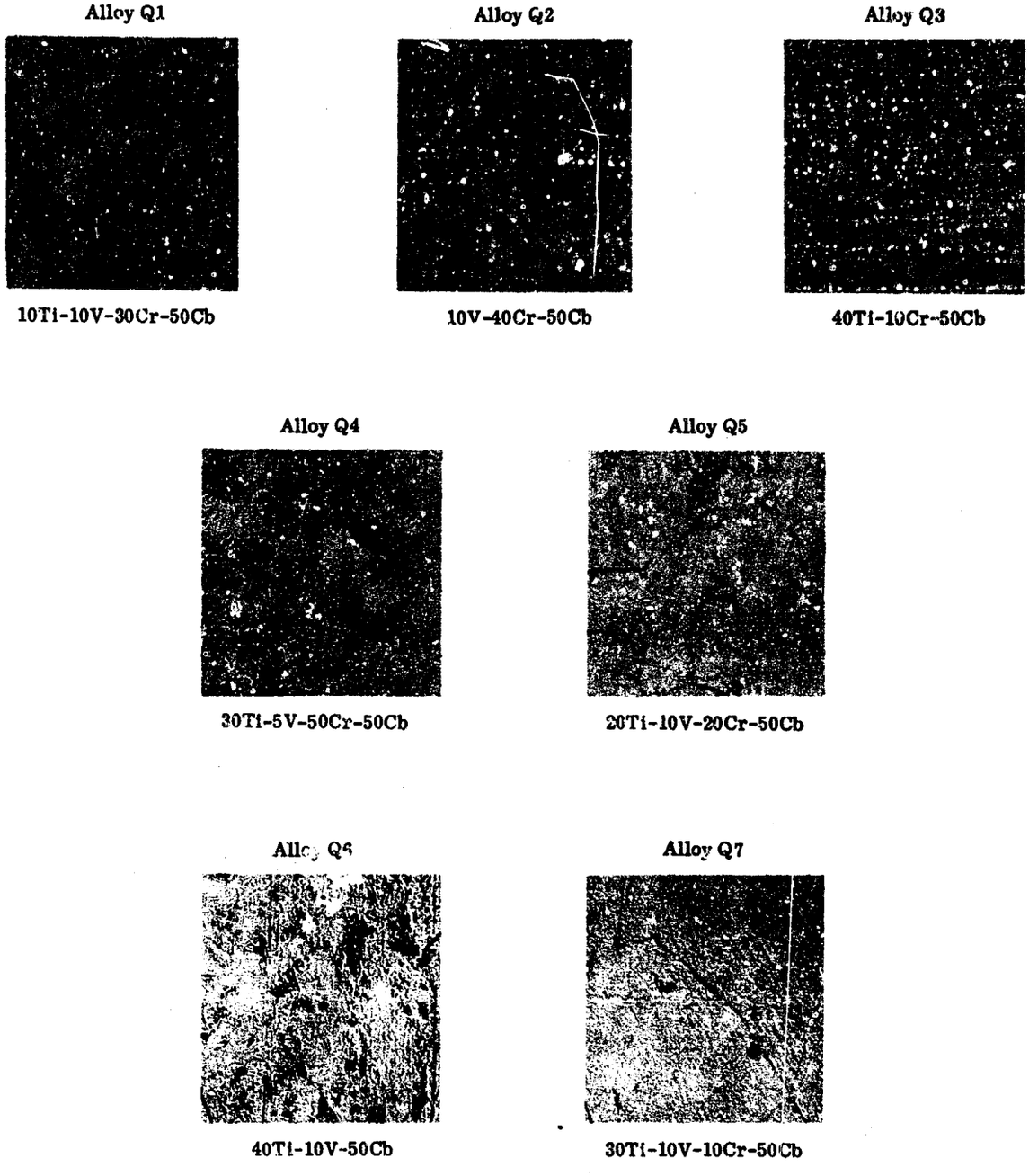

Magnification: 250X

FIGURE 19. MICROSTRUCTURE OF VARIOUS COLUMBIUM ALLOYS CONTAINING TITANIUM, VANADIUM, AND CHROMIUM

Oxidation of Alloys of Cb-Ti-V-Cr

The oxidation resistance of the ternary alloys indicated that oxidation in the Cb-Ti-Mo and Cb-Ti-Cr alloys improved with increasing ratios of titanium/molybdenum or titanium/chromium for alloys containing 50 to 90 atomic percent of columbium. With the Cb-V-Cr system, the oxidation resistance showed improvement with increasing chromium/vanadium ratios. No general trend in oxidation resistance as a function of total chromium or titanium content was noted in the Cb-Ti-Cr system; whereas, in the Cb-V-Cr and Cb-Ti-Mo system, oxidation resistance improved with decreasing vanadium and molybdenum content, respectively. The two chromium-containing systems showed some tendency to improve in oxidation resistance in the single-phase region. It was decided, therefore, to explore the single-phase regions of these systems primarily with the emphasis on the effect of substitution of titanium for chromium in the V-Cb system while retaining the columbium percentage constant. The microstructure of the arc-melted alloys are shown in Figure 19. Two of the alloys, Q1 and Q2, with the highest chromium content were definitely two phased. Alloys with 10 atomic percent chromium or less (Q3, Q6, and Q7) were single phased; whereas, alloys with 15 to 20 percent chromium had minor secondary phases (Q4 and Q5) that are probably Laves phase (MCr_2). A comparison of the microstructure of alloys Q4 and Q5 illustrated the pronounced effect that vanadium had on the solubility of chromium. The Q4 composition with 15 percent chromium and 5 percent vanadium had considerably more Laves phase than Q5 which contained 20 percent chromium and 10 percent vanadium.

Oxidation test results with the oxidation rate and retained ductility after 16 hours are contained in Table VIII. The results indicated that the single-phase alloys, Q3, Q6, and Q7, had the best oxidation resistance and retained ductility. The Q3 composition containing 40Ti-10Cr-50Cb (atomic percent) was by far the most oxidation resistant composition, but on a combination of oxidation resistance and retained ductility, the Q6 composition (40Ti-10V-50Cb) was rated equally with the Q3 alloy. Chromium had a marked adverse effect on ductility.

The specimens after 4 and 16 hours of test are shown in Figure 20. All alloys had tightly adhering oxides that showed negligible spall on cooling to room temperature after four hours. After 16 hours, only high-chromium alloys, Q1 and Q2, which showed some of the highest weight gains, retained their oxide. The most oxidation-resistant composition, Q3, spalled essentially to the base metal after the 16-hour cycle.

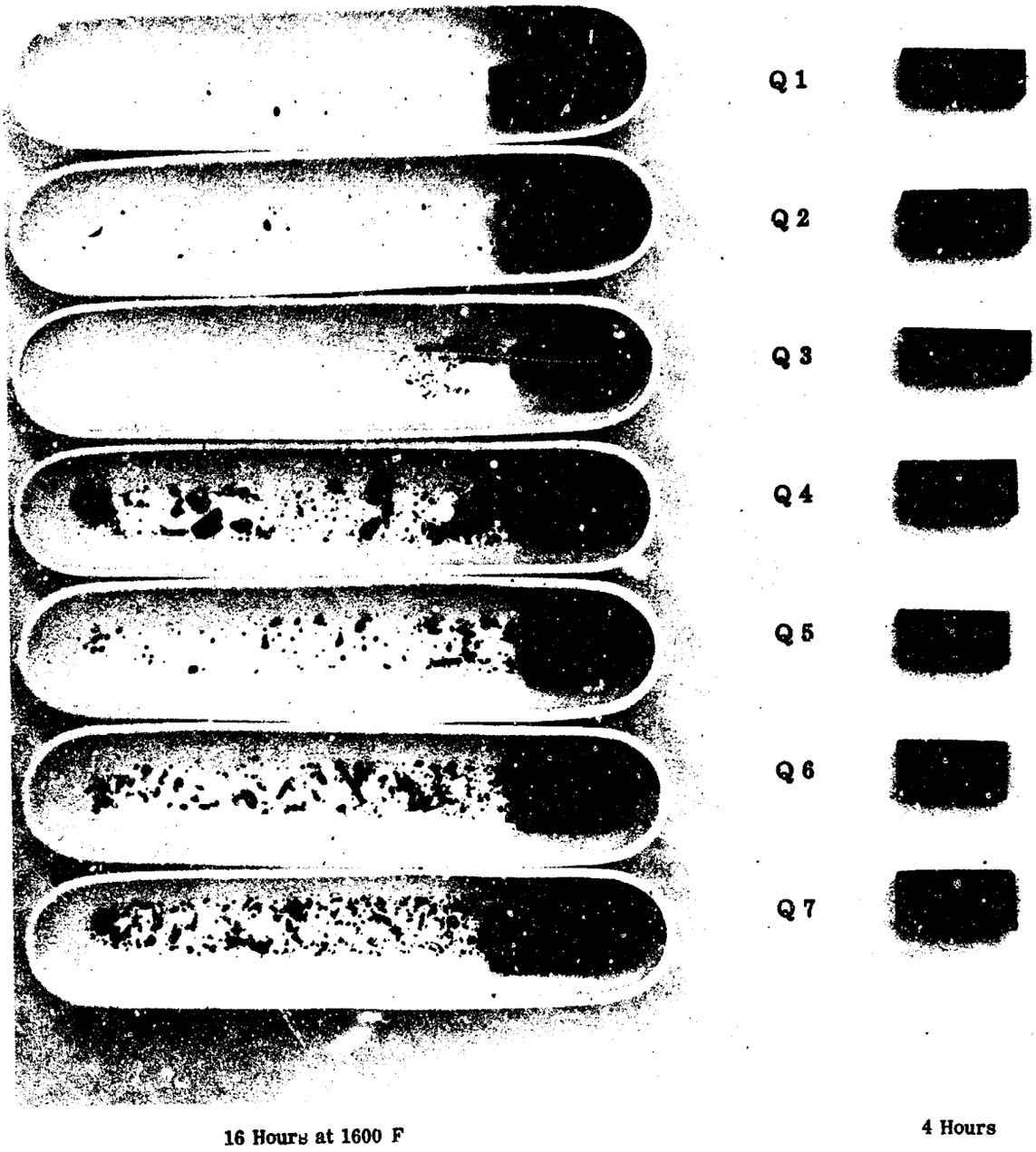

FIGURE 20. SPECIMENS OF SUBLAYER ALLOYS Q1 THROUGH Q7 AFTER OXIDATION TESTING AT 1600 F

TABLE VIII

OXIDATION IN AIR AT 1600 F OF SEVERAL Ti-V-Cr-Cb ALLOYS

Alloy Number	Nominal Composition (atomic percent)	Weight Increase (mg/cm^2)				Rating	
		1 hr	2 hr	4 hr	16 hr	Oxidation Resistance(1)	Ductility After Test(2)
Q1	10Ti-10V-30Cr-50Cb	2.4	6.4	5.15	24.7	4	6
Q2	10V-40Cr-50Cb	3.3	4.2	8.33	24.6	5	7
Q3	40Ti-10Cr-50Cb	1.6	1.8	2.65	2.4	1	2
Q4	30Ti-5V-15Cr-50Cb	3.1	3.0	9.48	24.4	6	4
Q5	20Ti-10V-20Cr-50Cb	5.9	7.3	8.97	32.9	7	5
Q6	40Ti-10V-50Cb	3.3	4.3	6.29	11.4	2	1
Q7	30Ti-10V-10Cr-50Cb	2.8	6.1	7.63	14.1	3	3

1. 1 best to 7 poorest (assessed on weight gain and appearance)
2. 1 best to 7 poorest (assessed by bending after 16 hours at temperature)

The plots of the weight change data versus time (Fig. 21) indicated that the three most oxidation-resistant alloys, Q3, Q6, and Q7, had parabolic rate constants, k, (W weight gain = $kt^{1/2}$) of 1.05, 2.87, and 3.5 ($mg/cm^2/hr^{1/2}$), respectively. The other alloys showed a breakaway type of oxidation at four hours or less.

Microstructures of the alloys after oxidation for 16 hours are shown in Figure 22. Only the titanium-free, high-chromium alloy, Q2, showed no change in structure after oxidation. The alloy exhibiting the greatest capacity to absorb oxygen without extensive grain boundary oxygen precipitation was the chromium-free alloy, Q6. The retained ductility of this alloy (note rating in Table VIII) may result from the fact that the alloy has a high solubility for oxygen and was not saturated during exposure.

A summary of the oxidation rates of the more oxidation-resistant commercial alloy substrates previously described, and the sublayer alloys described to this point is presented in Figure 23. The outstanding compositions were in the Cb-Ti-Cr systems, but the oxidation resistance was very composition dependent. The compositions in the high-titanium region, 30 to 40 atomic percent (19 to 27 weight percent), and low-chromium region, 10 atomic percent (7.2 weight percent), gave the lowest oxidation rates and most consistent performance. Alloys in the Cb-Mo-Ti system were the next most oxidation resistant with compositions in the relatively high titanium range (20 to 40 atomic percent) performing best. Molybdenum must be kept at 10 atomic percent or lower. The Cb-V, Cb-V-Mo, Cb-V-Cr, and Cb-Ti-V systems also produced compositions that exhibited lower oxidation rates than pure columbium and alloys such as D43, Cb752, and C129Y.

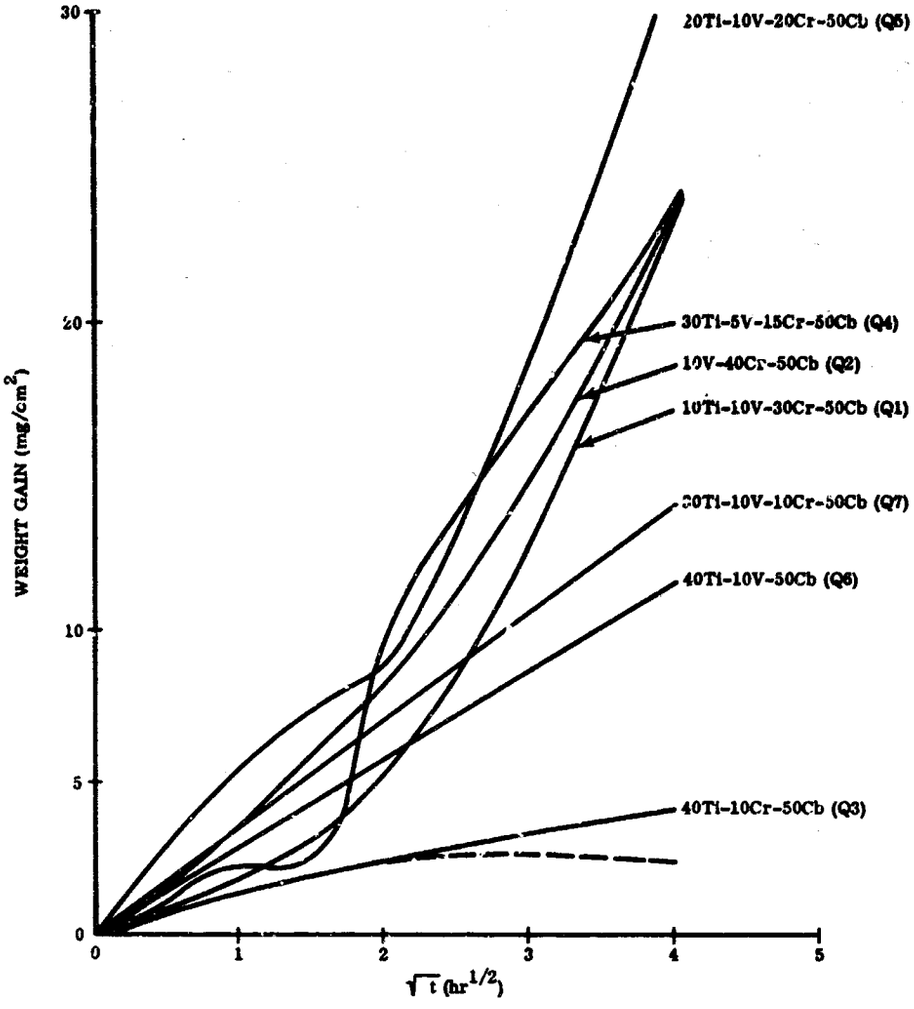

FIGURE 21. OXIDATION RATE OF VARIOUS SUBLAYER ALLOYS

All factors being equal, developing the most oxidation-resistant sublayer should yield the most satisfactory coating. Thus, a sublayer of Cb-40 at. % Ti-10 at. % Cr appeared optimum. The coating developed by TRW has a sublayer of nearly this composition and has performed commendably well in oxidation tests although not with acceptable reliability (Ref. 6). It was shown in Paragraph 3.1.1 that the high-expansion silicide cracks on cooldown so that a highly oxidation-resistant sublayer is required to protect the substrate. This requirement assumes that oxidation resistance is the most important factor. On the other hand, a porous or somewhat fluid oxide that has lower oxidation resistance, may be better able to seal a crack in the disilide, particularly if it fluxes the silica formed by oxidation of the walls of the crack. This point is mentioned because it illustrates the difficulty of separating the components of a coating

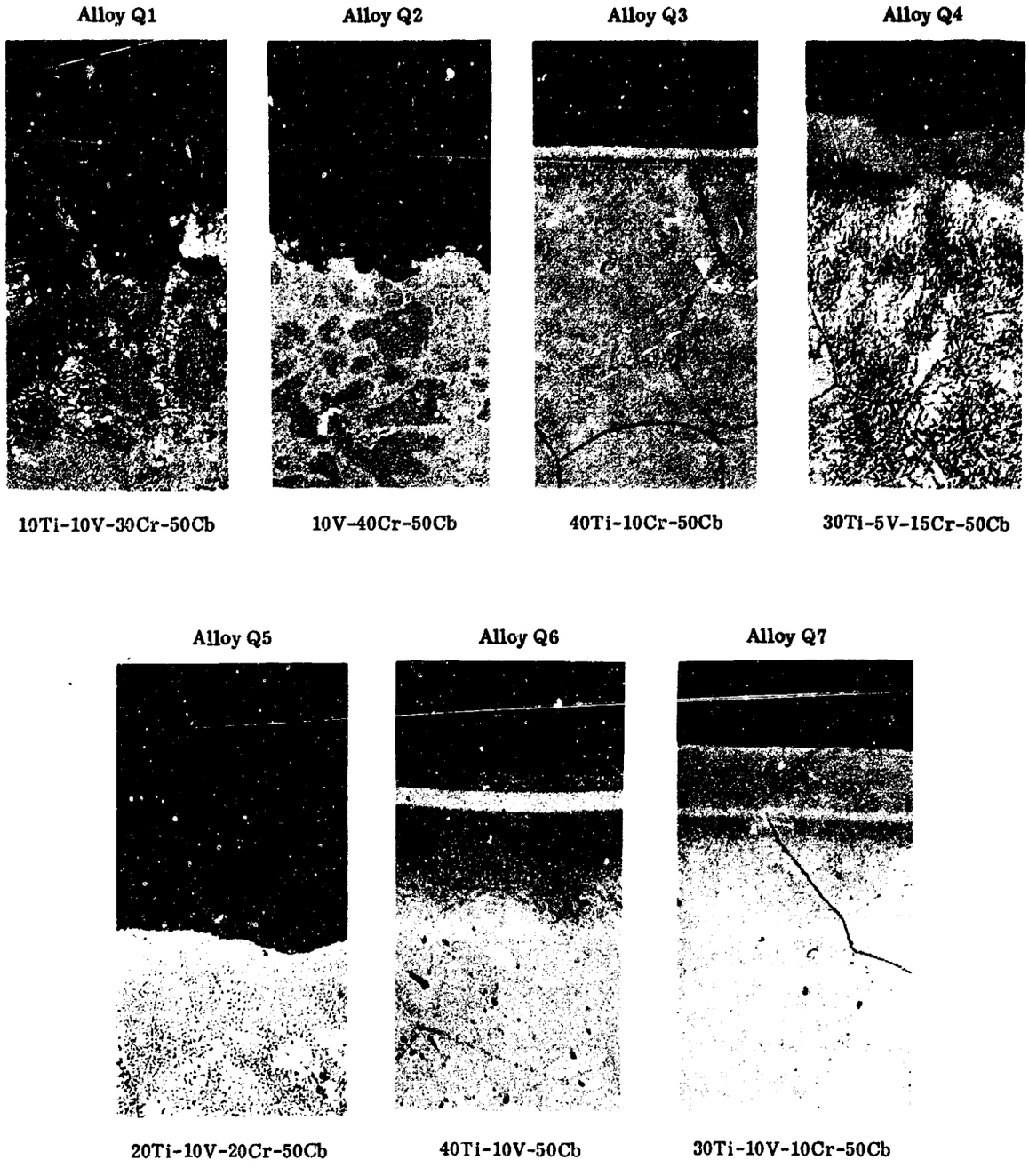

FIGURE 22. MICROSTRUCTURE OF VARIOUS TITANIUM, VANADIUM, CHROMIUM, AND COLUMBIUM ALLOYS AFTER OXIDATION AT 1600 F FOR 16 HOURS

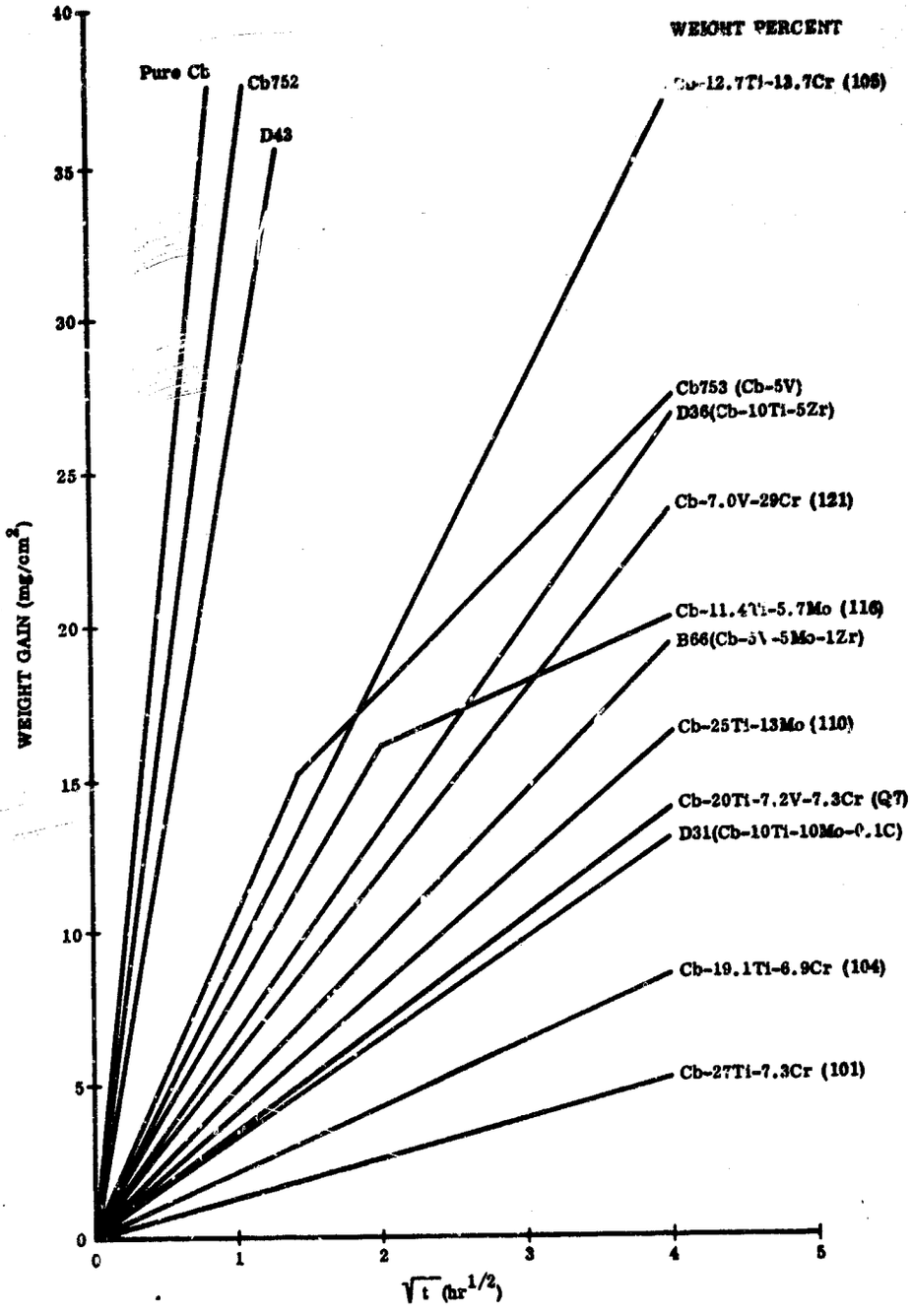

FIGURE 23. SUMMARY PLOT OF OXIDATION RATES AT 1600 F OF SUBLAYERS AND SUBSTRATES

and because it led to a decision to study V-Cr-Si coatings in spite of the low-oxidation resistance of Cb-V-Cr alloys compared with Cb-Ti-Cr, because of other advantages anticipated.

Lowering the titanium content or eliminating titanium from the surface alloy should minimize or eliminate the migration of oxygen and carbon to the coating, and thus minimize the effect of the coating on the substrate mechanical properties (Ref. 6 and 7). This factor alone justified a more serious look at the low titanium modifier compositions because all current columbium-base structural alloys derive at least a part of their strength from the dispersion of compounds formed from the interstitial elements (carbon, oxygen, and nitrogen) with zirconium and hafnium. The application studies (Section V) in the Ti-Mo and V-Cr systems include the lower concentration ranges.

The sublayer and substrate study emphasized gross oxidation of alloys only. Interdiffusion of oxygen with the alloys was not considered as a criterion because:

- It was not believed practical to develop ductile oxygen barriers except layers that could hold oxygen in solution.
- The major deficiency in silicide coatings was believed to be the result of oxide growth in craze cracks that produced fracture stresses within the coating upon thermal cycling and not substrate embrittlement by the diffusion of oxygen or nitrogen. In the case of gross mechanical damage to the silicide and loss of this primary oxygen barrier, permanent damage would result in a relatively short time. A solution to this gross damage problem appeared beyond the scope of the silicide coating phase of the program.

Oxidation of Cb-Ti-Al Solid Solution Alloys

Columbium alloy development has proceeded independently of coating development. This independent development has led to the rejection of certain alloying elements. For example, available data indicated that aluminum additions caused difficulty in working at the five percent level. Thus, Sheely and Wilson (Ref. 8) reported Cb-5Al-5V to be difficult to work and adopted Cb-3Al-3V as a base for further study. But these small additions were inadequate for oxidation resistance at typical operating temperatures, and did not lead to high-strength alloys so that work on aluminum-containing alloys was stopped.

However, when the goal of oxidation resistance at intermediate temperatures is substituted, the position must be reexamined. Aluminum appeared to be less deleterious to the strength of columbium alloys than titanium. Siliciding of aluminum containing alloys does not cause adverse reactions because microprobe analyses by Hubbard and Minton (Ref. 9) showed that aluminum did not enter the disilicide to any appreciable extent:

- Outer layer (disilicide type) 66Cb-30.5Si-3.5Al
- Inner layer 60.5Cb-35Al-4.5Si

From these results it was concluded that aluminum-containing substrates could be compatible with disilicide coatings, and would have no marked adverse effects on columbium alloys.

The following steps were taken to investigate aluminum-containing sublayers:

- Oxidation tests at 1600 F of arc-melted solid solution alloys prepared by IITRI.
- Determination of the effect of aluminum and (Ti + Al) coatings on the mechanical properties and oxidation resistance of columbium alloys.

Seven arc-melted alloys from the Cb-Ti-Al system were supplied by IITRI. The alloys were prepared as 30-gram melts by nonconsumable arc melting, and homogenized at 2500 F for one hour at 10^{-5} Torr.

The seven Cb-Ti-Al alloys were oxidation tested at 1600 F in air for 1, 2, 4, and 16 hours (separate specimens were used for each test). The test results are contained in Table IX and displayed in a parabolic plot in Figure 24. Oxidation test results for the Cb-40Ti-10Cr composition are also displayed in Figure 24.

At a constant aluminum concentration of four to five weight percent, the oxidation rate was inversely proportional to the titanium content. With a titanium concentration higher than 30 weight percent, the oxidation rate was lower than for the Cb-40Ti-10Cr alloy.

At the higher titanium concentration, it is possible to introduce more aluminum into solid solution. Two compositions were, therefore, tested at 10 weight percent aluminum with 50 and 60 weight percent titanium. The results in Table IX and Figure 24 showed that these compositions were the most oxidation resistant of the series at 1600 F, experiencing about one-fourth the weight loss in 16 hours of the Cb-40Ti-10Cr composition.

TABLE IX

OXIDATION OF Cb-Al-Ti ALLOYS

Specimen Number	Nominal Composition (wt %)	Weight Gain (mg/cm^2)				Comments	Rating Worse 7 Best 1
		1 hr	2 hr	4 hr	16 hr		
IITRI 13	Cb-4Al-8Ti	3.76	5.59	14.79	22.18	Heavy white oxide film. Complete flake-off on cooldown. Sharp corners. Rated poor due to oxide separation and weight gain.	7
IITRI 33	Cb-5Al-10Ti	2.92	3.82	5.08	9.11	Yellow gray oxide. Slight flake-off. Slight tendency to spall on corner. Good.	5
IITRI 34	Cb-5Al-20Ti	1.42	1.98	2.84	5.78	Yellow gray oxide film. Slight tendency to spall on sharp corners. Not completely homogeneous. Preferential oxide build-up; otherwise good.	4
IITRI 35	Cb-5Al-30Ti	0.75	0.94	1.33	2.62	Yellow gray oxide film. Very light, even coat. Very good to excellent. Low weight gain.	3
IITRI 36	Cb-10Al-50Ti	1.95	1.75	0.45(1)	1.13	Dark blue with trace of yellow oxide. Slight glaze. Weight gain so low that open pores and weeping oxide causes weight gain to be erratic. Excellent.	2
IITRI 37	Cb-5Al-40Ti	3.19(1)	1.10	1.66	1.62	Yellow gray oxide film. Slight whiskering. Spalling on sharp corners. Specimen not homogeneous. Slightly less than good. Better than fair.	6
IITRI 38	Cb-10Al-60Ti	1.89(1)	0.32	0.47	1.0	Blue black and glazing. No spalling. Sharp corners. Weight gain for 1-hour run. Excellent.	1

1. Results are not representative (not used in plotting Fig. 24).

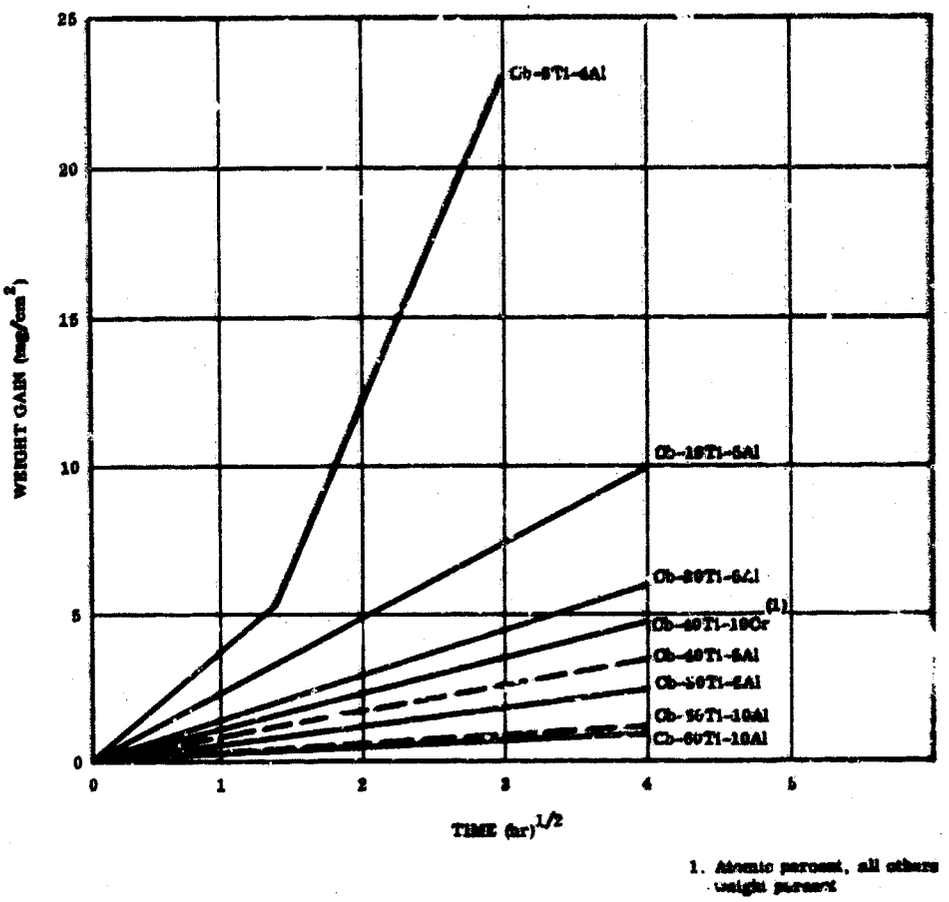

FIGURE 24. OXIDATION RATE OF COLUMBIUM, ALUMINUM, AND TITANIUM SOLID SOLUTIONS AT 1600 F IN AIR

(Some of the erratic weight gains noted in Table IX are the result of the porosity and perhaps heterogeneity of the arc-melted alloys. The values used to plot Figure 24 are believed to be the most reliable, because oxidation was uniform and free of small areas of excessive attack associated with nonuniformity of the arc-melted buttons.)

Oxidation Behavior of Cb-Ti-Cr-Al Alloys

A series of solid solutions based on Cb-27.0 wt % Ti-7.3 wt % Cr-5 wt % al, were prepared by arc-melting. Metallographic examination showed them to be homogenous solid solutions. They were then tested for oxidation resistance in air at 1600, 1800, 2000, 2200, and 2400 F for times sufficient to characterize oxidation rates. These data are shown in Figures 25 through 27 with weight gains plotted against a linear time scale. The weight gains represent the weight of the specimens plus any loose oxide which spalled from the specimen surface.

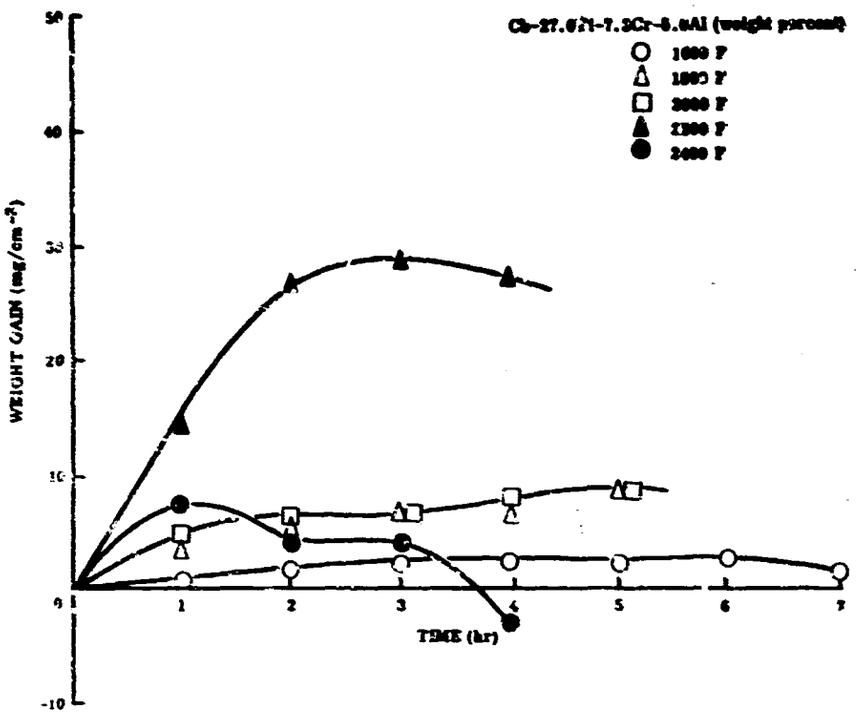

FIGURE 25. OXIDATION RATE OF COLUMBIUM-TITANIUM-CHROMIUM-ALUMINUM ALLOY; One-Hour Cycles at 1600 to 2400 F

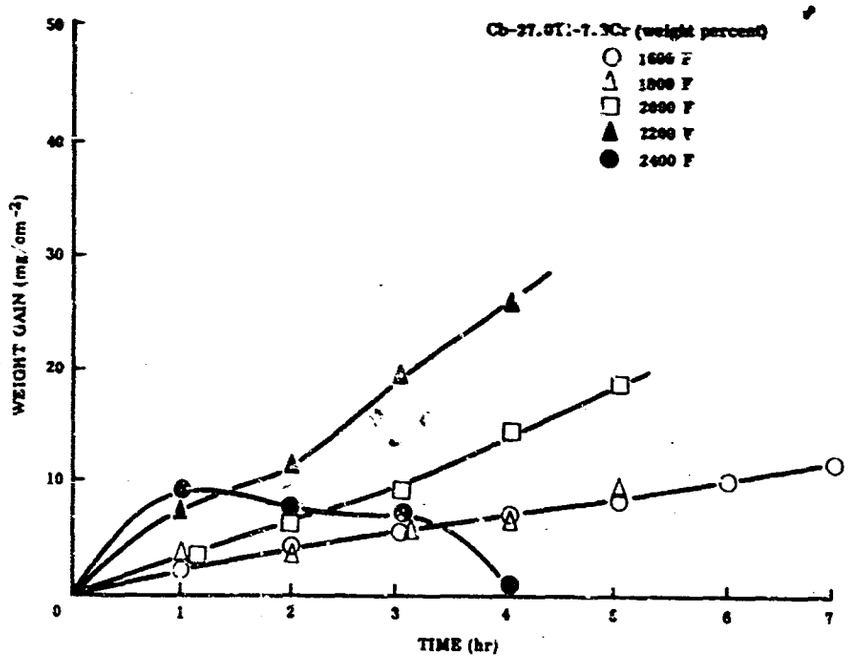

FIGURE 26. OXIDATION RATE OF COLUMBIUM-TITANIUM-CHROMIUM ALLOY; One-Hour Cycles at 1600 to 2400 F

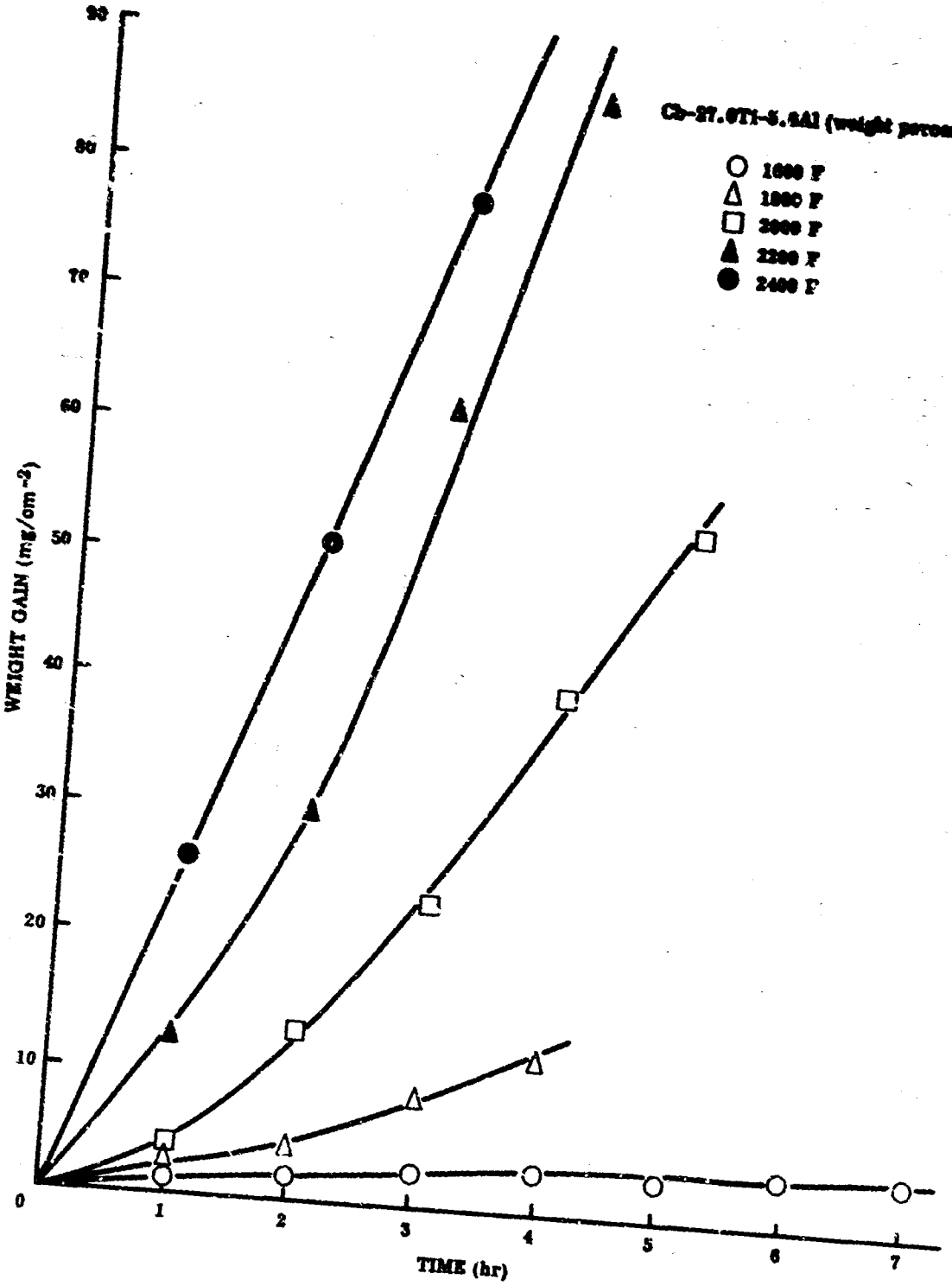

FIGURE 27. OXIDATION RATE OF COLUMBIUM–TITANIUM–ALUMINUM ALLOY; One-Hour Cycles at 1600 to 2400 F

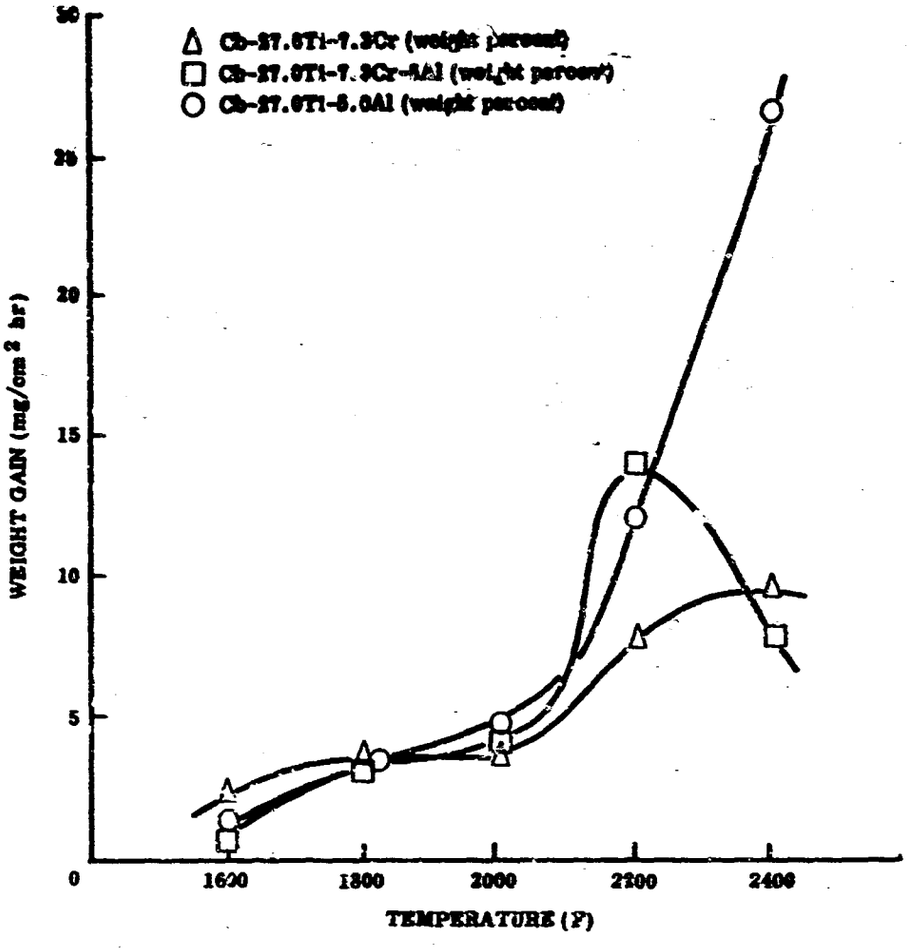

FIGURE 28. OXIDATION RATE VERSUS TEMPERATURE CF COLUMBIUM ALLOYS FOR FIRST ONE-HOUR CYCLE

After the first one-hour cycle, all specimens showed a progressive increase in weight gain with temperature, but with subsequent cycles, the two alloys containing chromium exhibited a weight loss at 2400 F. This loss was attributed to the formation of a volatile oxide and possibly indicated that at lower temperatures the true oxidation rate was masked, to some extent, by this reaction.

Figure 28 shows that similar oxidation rates for the first one-hour cycle were experienced with all three alloys for temperatures up to 2000 F. Above this temperature, deviations in observed weight gains occurred which were probably partly due to the formation of a volatile oxide species. However, from visual examination, the Cb-Ti-Cr-Al alloy had the best oxidation resistance, retaining sharp corners after four hours at 2400 F. In addition, total weight losses at 2400 F, after removal of all surface oxide, were higher by a factor of 4 in the case of the Cb-Ti-Al alloy.

Oxidation of Beryllium-Containing Columbium Alloys

A series of columbium-base alloys containing beryllium was prepared to determine the contribution of this element to the oxidation resistance of binary and ternary columbium alloys

Six alloys containing up to one weight percent beryllium were prepared by arc melting. Oxidation test results at 1600 F are presented in Table X.

When compared to similar alloys containing equivalent atomic percentages of aluminum, these results indicated that beryllium was less effective in improving oxidation resistance. Also, additions of 0.25, 0.5, and 1.0 weight percent beryllium to pure columbium had an adverse effect on oxidation behavior.

TABLE X

OXIDATION AT 1600 F IN AIR OF SOME BERYLLIUM-CONTAINING COLUMBIUM ALLOYS

Alloy Number	Nominal Composition (wt %)	Weight Increase (mg/cm^2)		Comments
		1 Hour	2 Hours	
--	Cb	41.50	57.00	
Be-1	Cb-0.25Be	42.41	66.63	Rapid oxidation - loose flaky oxide
Be-2	Cb-0.50Be	47.70	56.81	More rapid oxidation - oxide spalling loss
Be-3	Cb-1.00Be	51.15	69.25	Thick loose oxide
Be-4	Cb-5.00Al	19.84	40.31	Loose flaky oxide
Be-5	Cb-10.0Ti-0.5Be	4.92	3.31	Good corners and surface
Be-6	Cb-30.00Ti-0.5Be	8.43	9.76	Porosity cause of high weight gain
Be-7	Cb-30.0Ti-5.0Al-10.0Cr	Porosity 2.28	1.35	Excellent, sharp corners
Be-8	Cb-30.0Ti-10.0Cr-0.5Be	Porosity	Porosity	Extensive porosity

Discussion of Sublayers

Oxidation data were generated for a number of commercial columbium alloy substrates, and compared with potential ductile sublayers from the systems:

- Cb-V-Cr
- Cb-Ti-V-Cr
- Cb-Ti-Mo
- Cb-Ti-W
- Cb-Ti-Cr
- Cb-Ti-Al
- Cb-Ti-Cr-Al
- Beryllium-containing columbium alloys

A marked improvement in the oxidation resistance of columbium metal at 1600 F can be effected by alloying; however, as can be seen in the summary presentation of oxidation data for the most oxidation resistant alloy in each system (Fig. 29), the oxidation rates are relatively high even at this low temperature. At the projected use temperature of columbium alloys, 2200 F or higher, the oxidation rates are sufficiently high to consume a 0.001-inch sublayer in less than one hour. The ductile-sublayer approach based on surface modification of columbium does not have the potential for providing short-time protection in the event of catastrophic impact damage to a brittle protective aluminide or silicide.

The more oxidation-resistant modifier alloys appear to offer the greatest promise in minimizing severe oxidation at the base of craze cracks during heatup and cooldown of coated alloys. The oxidation at the base of this crack will only be severe as the temperature is reduced to between 800 and 1800 F, where the thermal strains are sufficiently high to open the crack.

The most oxidation-resistant columbium alloys were in the Cb-Ti-Cr and Cb-Ti-Al systems. Unfortunately, the most resistant alloys occurred at high titanium contents (27 to 60 weight percent) which, as discussed in other sections of this report, disturb the oxide and carbide dispersoid stability in precipitation-strengthened alloys (interstitial sink effect) and develop the highest expansion silicides and aluminides. Alloys of Cb-V-Cr and Cb-Mo-Ti are less oxidation resistant than the Cb-Ti-Cr alloys, but offer a better silicide and aluminide expansion match and have less effect on dispersoid stability. They appear to be the better selection for overall sublayer performance.

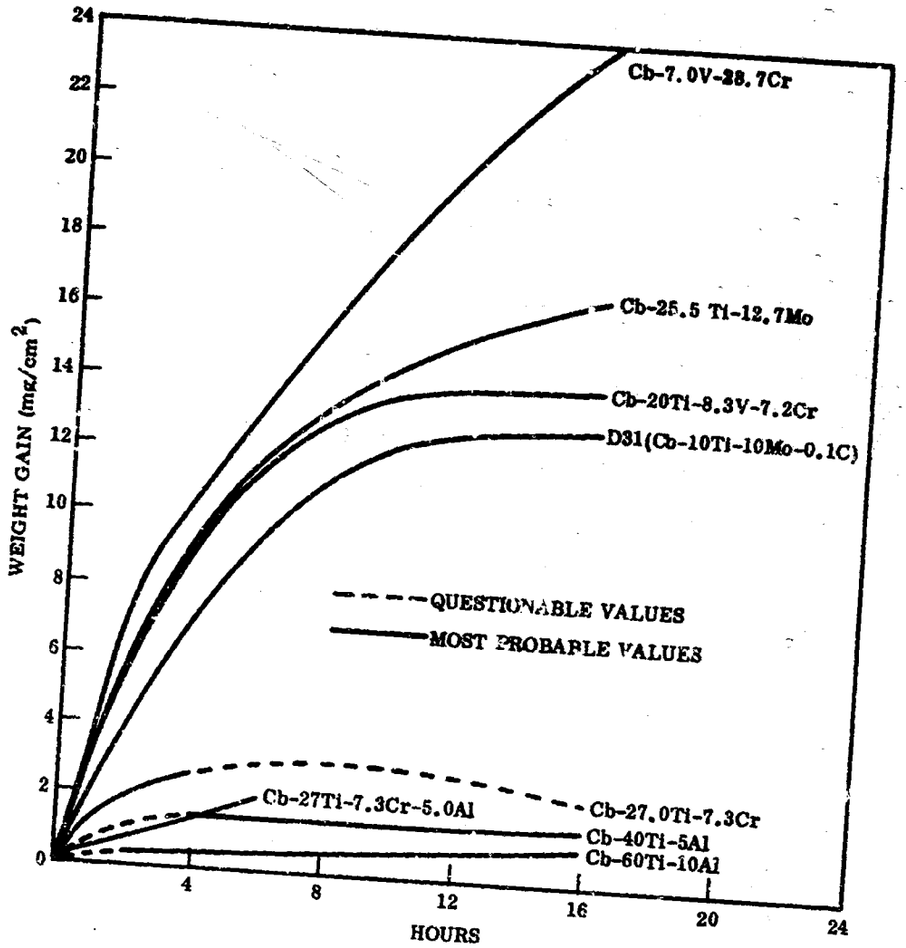

FIGURE 29. SUMMARY OF THE MOST OXIDATION RESISTANT DUCTILE COLUMBIUM ALLOY EVALUATED

Because none of the alloys studied have adequate oxidation resistance, if applied in a practical thickness of 0.001 inch, to provide even a one-hour life at 2200 F without a silicide or aluminide overlay, the effect of the individual elements on the performance of the aluminide and silicide at both low and high temperatures will probably have to be weighed far more heavily than oxidation resistance per se of the ductile sublayers.

3.2.2 Thermal Expansion of Sublayers

The concept of effective ductility was predicated upon the development of a two-component coating. That is, a sublayer of moderate oxidation resistance and moderate ductility, and an overlay of an oxidation-resistant, but hard and brittle substance. The sublayer would primarily consist of a solid solution alloy with possible dispersed phases of chromides or other intermetallics. The expansion match of the sublayer was never considered a critical problem because of its inherent ductility, and ideally would have a thermal expansion intermediate between that of the substrate and of the outer oxidation-resistant layer.

To avoid the extensive investigation of the potentially ductile sublayers, only binary alloys that had potential use for surface alloying were investigated. Systems included were binaries of Ti-Mo, Ti-W, V-Cr, and Ti-Cr.

The specimens were prepared by arc melting the specific composition in a nonconsumable arc melter. The specimens were then annealed at 2200 F for 16 hours. After this treatment, specimens approximately 1 to 1.5 inches long by 0.25 inch square were eloxed from the arc melt. The coefficient of expansion was measured in argon using a Gaertner D-1200 quartz tube dilatometer. Measurements were made between 100 and 1800 F. If the expansion was uniform over this entire temperature range, the expansion coefficient was reported as constant. Otherwise, an instantaneous expansion coefficient was determined at 400 and at 1800 F.

The thermal expansion coefficients on the binary alloys are shown in Table XI. As would be expected, the alloys high in molybdenum and tungsten had the lowest expansion. The alloys high in chromium, vanadium, and titanium showed higher coefficients of expansion. With few exceptions, the coefficient of expansion of the binary alloys studied varied quite rapidly with increase in temperature. Only the approximately 50Ti-50Mo alloy and the Ti-77Cr alloy had a constant coefficient over the entire test range.

The comparison of the V-Cr and the Ti-Cr alloys are of interest. The V-Cr alloys had markedly lower coefficients of expansion at 400 F; whereas, at 1800 F the difference was relatively minor, with Ti-Cr perhaps having the lower coefficient of expansion. A true comparison of the Ti-Cr and the V-Cr systems is quite difficult, particularly in the alloys containing relatively high percentages of titanium. The eutectoid transformation at 670 C involves an expansion in going from the alpha to

beta phase. This expansion (Fig. 30) shows the expansion of both a high and low titanium Ti-Cr alloy. Examination of the Ti-Cr phase diagram shows that contraction should occur above 670 C as a result of dissolution of $TiCr_2$ in beta. Thus, the decrease in expansion with temperature may, in part, be due to this dissolution process. At the higher chromium content, the alloys are essentially all beta and the dissolution reaction and eutectoid transformation do not occur. One advantage that can be noted for the V-Cr system over the Ti-Cr system would be the lack of Laves phase formation, which would minimize the thermal stresses that could develop in the dissolution of the MCr_2 Laves phase. Vanadium, forming solid solutions with both columbium and chromium, should minimize the formation of Laves phases and hence the problem of dissolution.

TABLE XI

THERMAL EXPANSION OF BINARY ALLOYS

Alloy Composition (at. %)	Coefficient of Expansion/Degree F x 10^6		
	400 F	Constant	1800 F
52.9Ti-47.1Mo		4.95	
79.0Ti-21.0Mo	4.02		5.36
36.6Ti-43.4W	3.59		5.87
81.3Ti-18.7W	3.85		5.84
22.7V-77.3Cr	4.85		7.93
55.3V-44.7Cr	5.69		7.05
83.2V-16.8Cr	4.98		8.26
23.0Ti-77.0Cr(1)		7.78	
71.6Ti-28.4Cr(1)	5.45		5.73
B66 alloy		4.52 at 2000 F	
D43 alloy		4.30 at 2000 F	

1. See Figure 30.

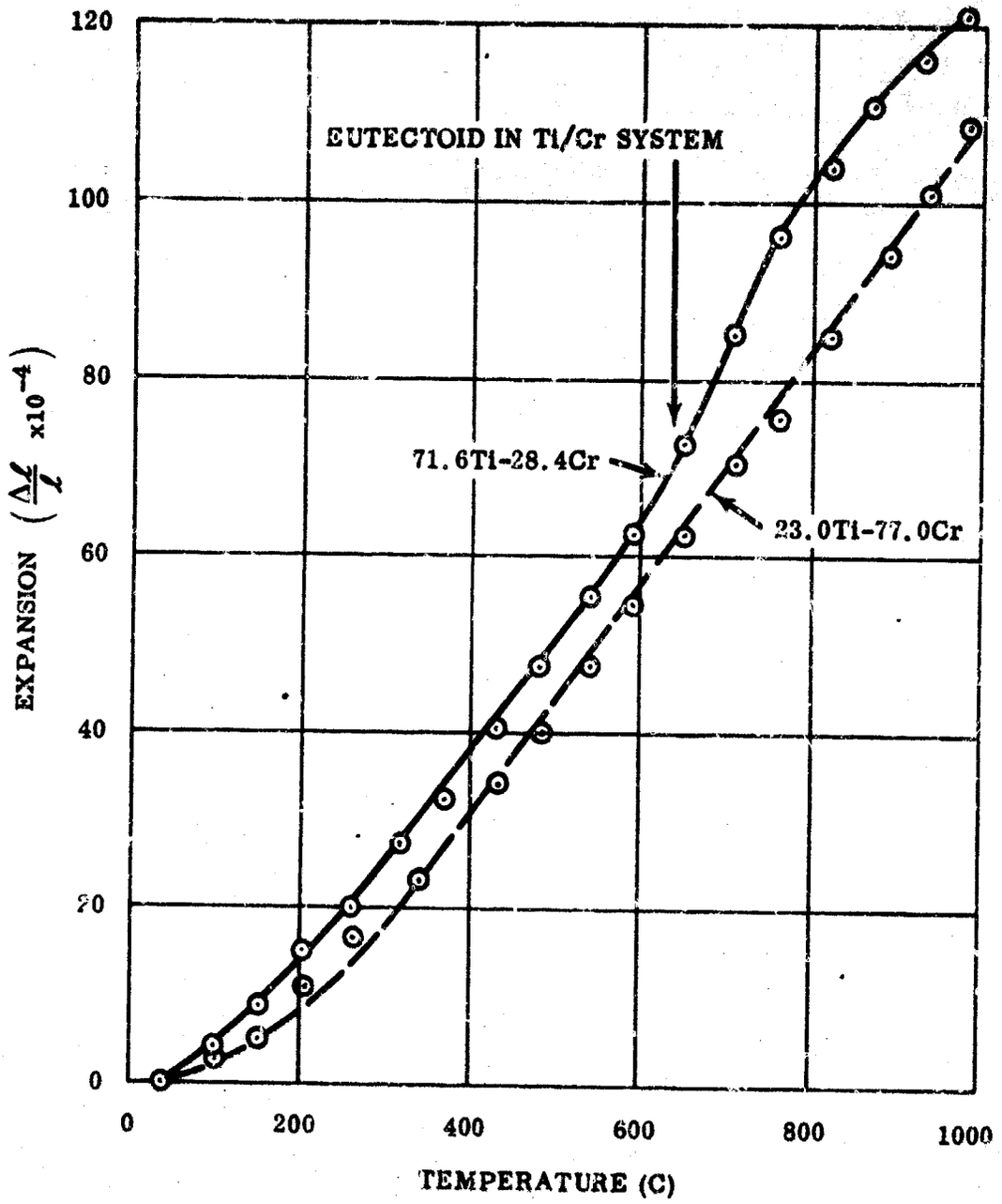

FIGURE 30. EXPANSION OF TITANIUM-CHROMIUM ALLOYS

3.2.3 Interdiffusion Barrier

Prealloyed sublayers such as the Cb-Ti-Cr alloys interdiffuse with the columbium alloy as well as with the primary oxidation barrier. Interdiffusion with the columbium alloy has several adverse effects:

- Loss of mechanical properties of the columbium alloy by alloying (e.g., Cb-Ti alloys are weak) or by the interstitial sink effect (Ref. 7)
- Loss of oxidation-resistant sublayer by diffusion
- Introduction of increasing amounts of undersirable columbium into the primary barrier

Because such effects would be undesirable with any prealloyed sublayer, diffusion barriers were studied as one way to separate the columbium alloy from the coating system.

Development of Diffusion Barrier for Cb-Ti-Cr Sublayer

To determine the magnitude of the problem, diffusion couples of Cb752, B66, and D43 alloys versus Ti-33Cr foil were run for 100 hours at 2400 F. The results were compared to diffusion couples with a diffusion barrier between the columbium alloys and the Ti-33Cr foil. The objective of this study was to find some way of avoiding the rapid chromium and titanium diffusion from the (Ti-Cr)-Si coating into the columbium alloy substrates and thereby avoid the accompanying loss of mechanical properties. Figure 31 shows Cb752, D43, and B66 alloys with tantalum, molybdenum, and tungsten, respectively, as diffusion barriers. Also shown in Figure 31 are the columbium alloys in direct contact with the Ti-33Cr foil without any diffusion barrier for use as standards.

The results of this study are contained in Table XII. Residual thicknesses of the columbium alloys after 100 hours at 2400 F are listed; under Diffusion Zone, data are included for decreased thickness of the columbium alloy plus the thickness of the diffusion barrier, if the latter is completely dissolved. Metallography was used to estimate the extent of diffusion.

Vanadium was in one case tested as the diffusion barrier for the Cb752 alloy, but the interdiffusion between the columbium alloy and pure vanadium is apparently so much faster than the diffusion with any of the above mentioned diffusion barriers that vanadium was excluded.

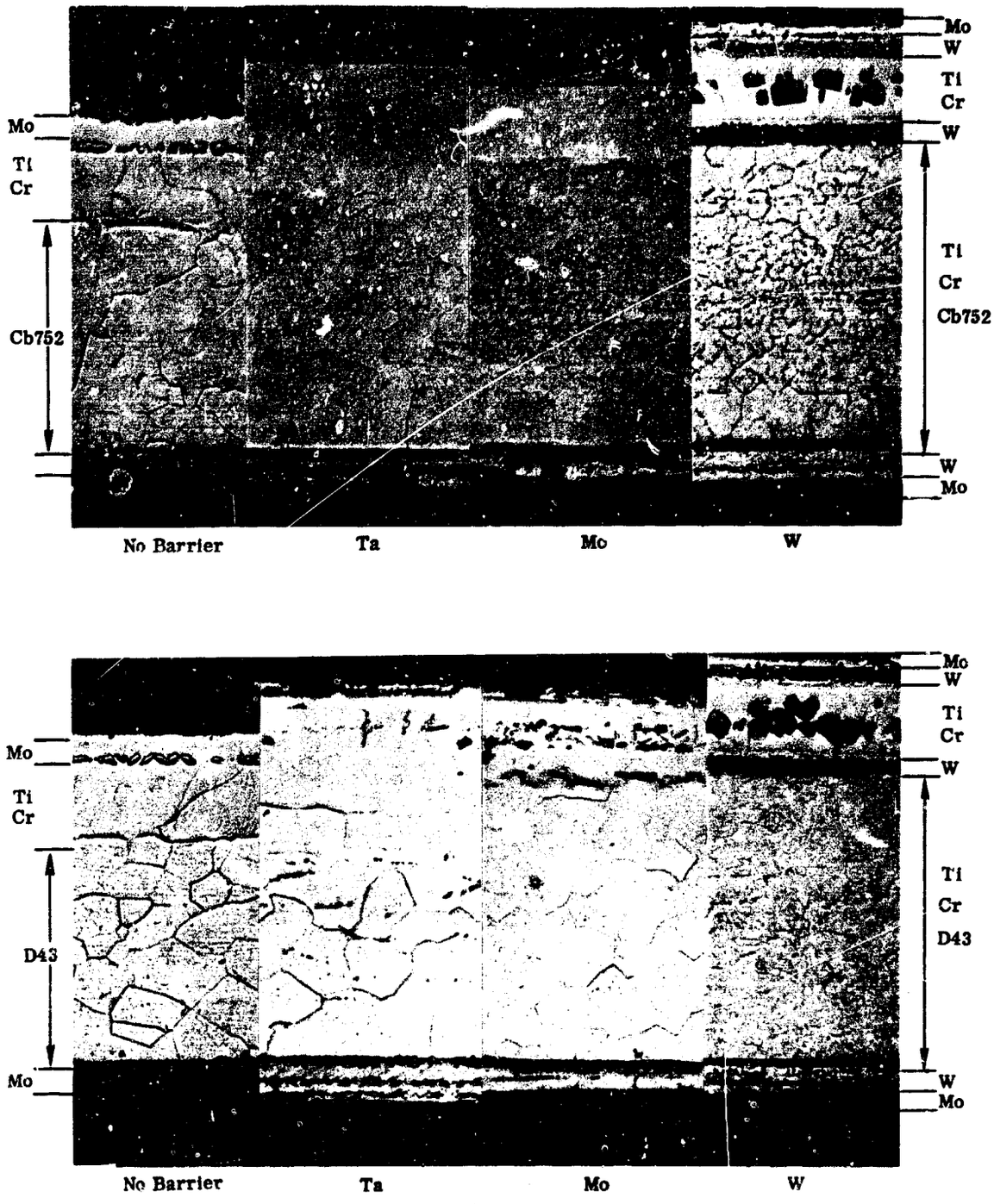

Annealed for 100 Hours at 2400 F in Argon

Magnification: 150X

FIGURE 31. DIFFUSION COUPLES OF Cb752, D43, AND B66 VERSUS Ti-33Cr WITH DIFFUSION BARRIERS OF TANTALUM, MOLYBDENUM, AND TUNGSTEN (Sheet 1 of 2)

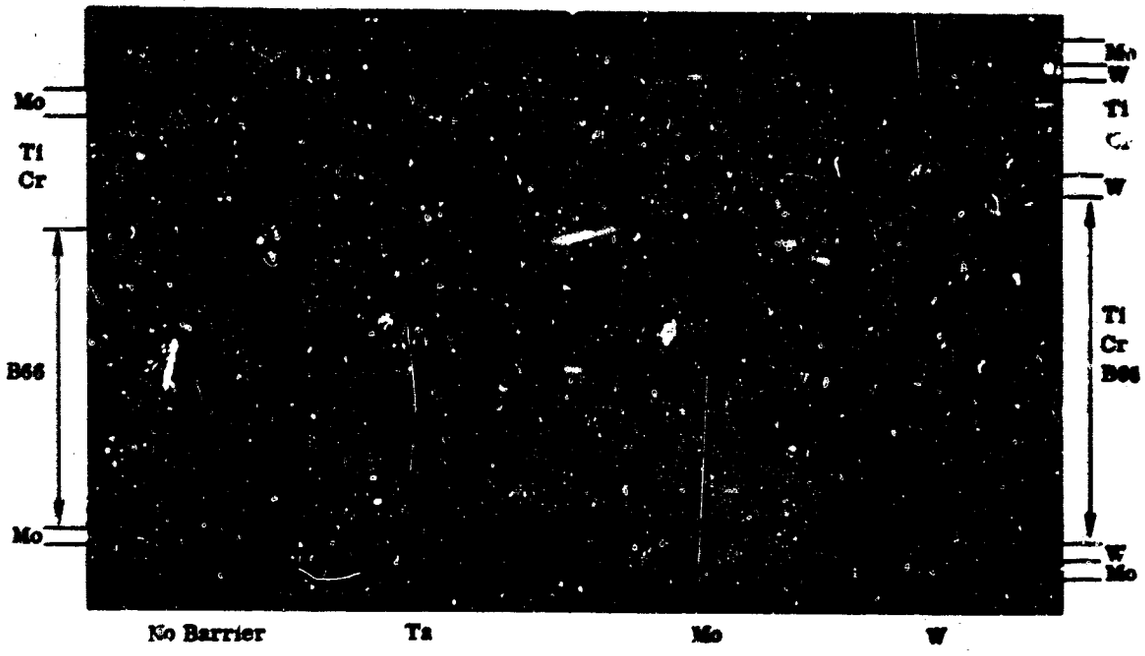

Annealed for 100 Hours at 2400 F in Argon

Magnification: 150X

FIGURE 31. DIFFUSION COUPLES OF Cb752, D43, AND B66 VERSUS Ti-33Cr WITH DIFFUSION BARRIERS OF TANTALUM, MOLYBDENUM, AND TUNGSTEN (Sheet 2 of 2)

TABLE XII

DIFFUSION STUDIES OF COLUMBIUM ALLOYS VERSUS Ti-33Cr FOIL WITH DIFFUSION BARRIERS OF TANTALUM, MOLYBDENUM, AND TUNGSTEN ANNEALED 100 HOURS 2400 F

Material	Thickness of Cb752 (in.)	Diffusion Zone (in.)	Thickness of D43 (in.)	Diffusion Zone (in.)	Thickness of B66 (in.)	Diffusion Zone (in.)
As Received	0.0126	—	0.0119	—	0.0135	—
No diffusion barrier	0.0094	0.0032	0.0091	0.0028	0.0103	0.0032
Tantalum as diffusion barrier	0.0110	0.0024	0.0103	0.0024	0.0118	0.0025
Molybdenum as diffusion barrier	0.0123	0.0010	0.0117	0.0009	0.0130	0.0012
Tungsten as diffusion barrier	0.0126	<0.0002	0.0119	<0.0002	0.0130	0.0015

Table XII indicated tungsten as an excellent diffusion barrier for the Cb752 and D43 alloys. For the B66 alloy, however, tungsten was inferior to molybdenum. Molybdenum was, aside from being the best diffusion barrier for B66, also a fairly good barrier for the Cb752 and D43 alloys. The diffusion zone with molybdenum as the diffusion barrier was about one-third of the diffusion zone of the unprotected alloy for all three columbium alloys.

Tantalum afforded a slight decrease in diffusion rate over the substrate alloy compared to the unprotected alloys. However, molybdenum was from 2 to 2.5 times better than tantalum.

It was concluded from these diffusion experiments that tungsten was the best diffusion barrier for the Cb752 and D43 alloys, while molybdenum was best for the B66 alloy. The difference between molybdenum and tungsten decreases when the weight penalty of using tungsten is taken into account. Tungsten is 2.25 times heavier than columbium, while molybdenum was only about 1.2 times heavier than columbium. This made molybdenum superior for use with B66, but tungsten was still the best of the two as a diffusion barrier for the Cb752 and D43 alloys. To get a rough numerical rating of the three diffusion barriers, the following approach was adopted.

Tungsten, 0.0002 inch thick, is necessary to protect the Cb752 alloy when annealed 100 hours at 2400 F. The same effect could be achieved by increasing the thickness of the Cb752 foil by 0.0032 inch. The weight ratio between the two possibilities is:

$$P_W = \frac{0.697 \times 0.0002}{0.326 \times 0.0032} = 0.14$$

The value (0.14) establishes tungsten as a more desirable barrier than could be obtained by increasing the thickness of the Cb752 foil.

In the case of molybdenum, the entire 0.0007-inch foil was consumed in addition to 0.0003 inch of the Cb752 foil. In this case, the weight of the two consumed materials was compared to the weight of the necessary amount of Cb752 alloy.

$$P_{Mo} = \frac{0.0007 \times 0.369 + 0.0003 \times 0.326}{0.0032 \times 0.326} = 0.34$$

This value was not quite accurate, because the 0.003-inch Cb752 alloy may be substituted by a smaller amount of molybdenum which may decrease the weight of the protective barrier and consequently the weight value. However, this decrease would not lead to any major change, so the approach outlined above was believed to give satisfactory results.

It was concluded from the weight ratios in Table XIII that tungsten was the best metal for use as a diffusion barrier for the Cb752 and D43 alloys, but molybdenum was also highly acceptable as a diffusion barrier for these alloys. The superiority of molybdenum for use with the B66 alloy is clearly illustrated in the table.

Tantalum did not offer any advantage for use as a diffusion barrier for any of the columbium alloys investigated.

TABLE XIII

WEIGHT RATIOS OF POSSIBLE DIFFUSION BARRIERS FOR 100 HOURS PROTECTION AT 2400 F

$\frac{W}{Cb752}$	0.14	$\frac{W}{B66}$	0.87	$\frac{W}{D43}$	0.15
$\frac{Mo}{Cb752}$	0.34	$\frac{Mo}{B66}$	0.42	$\frac{Mo}{D43}$	0.35
$\frac{Ta}{Cb752}$	0.96	$\frac{Ta}{B66}$	1.02	$\frac{Ta}{D43}$	1.10

Development of Diffusion Barriers for Other Sublayers

Good oxidation resistance for a sublayer was found in the Cb-Ti-Mo, Cb-Ti-W, and, to a lesser extent, in the Cb-V-Cr systems. The diffusion barrier study was therefore extended to these systems. Table XIV shows the binary alloys investigated.

A diffusion cycle of 100 hours at 2200 F was employed. Photomicrographs of the diffusion couples are shown in Figures 32 through 37. The photomicrographs show that the diffusion, as measured by the amount of the columbium alloys transferred into a solid solution with the binary alloy, is considerably retarded by substituting tungsten and molybdenum for chromium. At the same time, an increase in titanium content increases the diffusion zone into the columbium alloys.

TABLE XIV

NOMINAL COMPOSITION OF THE BINARY ALLOYS USED IN THE DIFFUSION STUDIES

Number	Composition (at. %)	Composition (wt %)
1-A	52.9Ti-47.1Mo	36.0Ti-64.0Mo
2-A	79.0Ti-21.0Mo	65.3Ti-34.7Mo
3-A	56.6Ti-43.4W	25.4Ti-74.6W
4-A	81.3Ti-18.7W	53.2Ti-46.8W
5-A	71.6Ti-28.4Cr	69.9Ti-30.0Cr
6-A	48.1Ti-51.9Cr	46.3Ti-53.7Cr
7-A	23.0Ti-77.0Cr	21.7Ti-78.4Cr
8-A	55.3V-44.7Cr	54.6V-45.1Cr
9-A	83.2V-16.8Cr	82.9V-17.1Cr
10-A	22.7V-77.3Cr	22.4V-77.7Cr

The combination of titanium and chromium seems to be especially harmful in respect to diffusion. This is in accordance with melting point considerations. All the titanium/chromium alloys have melting points around 2550 F. The titanium/tungsten and the titanium/molybdenum alloys used in this investigation have melting points well above 3200 F.

The photomicrographs also indicate that titanium is the fastest diffusing species in these alloys. The low-chromium alloy, 71.6Ti-28.4Cr, shown in Figures 35, 36, and 37 was a homogeneous alloy. The 48.1Ti-51.9Cr alloy, on the other hand, consisted of about equal amounts of the Laves phase, $TiCr_2$, and an alloy of 65Ti-35Cr. The high chromium-containing alloy, 23Ti-77Cr, shown in Figures 35, 36 and 37 had a low-titanium (10Ti-90Cr) alloy in equilibrium with the Laves phase.

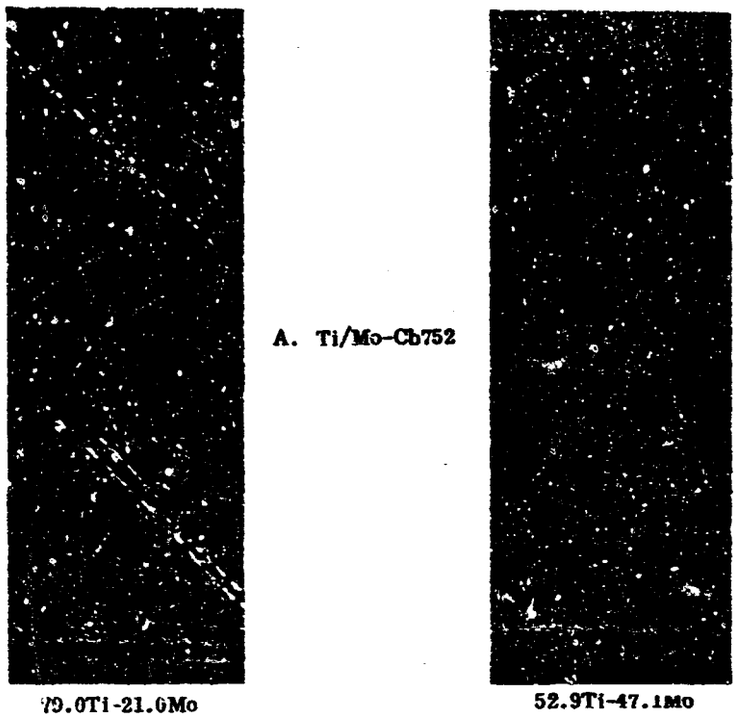

79.0Ti-21.0Mo

A. Ti/Mo-Cb752

52.9Ti-47.1Mo

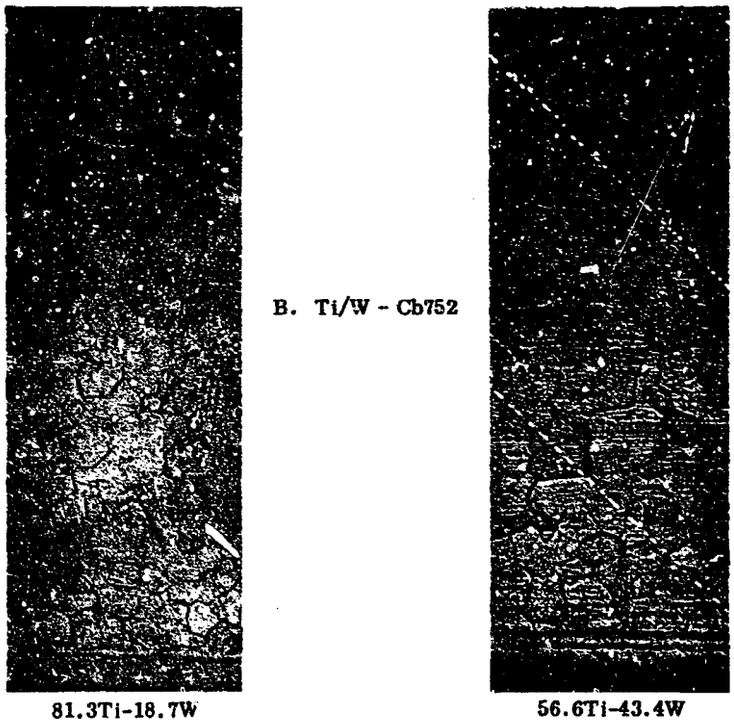

81.3Ti-18.7W

B. Ti/W - Cb752

56.6Ti-43.4W

Annealed for 100 Hours at 2200 F
Magnification: 250X

FIGURE 32. DIFFUSION COUPLES OF Cb752 VERSUS TITANIUM-MOLYBDENUM AND TITANIUM-TUNGSTEN ALLOYS

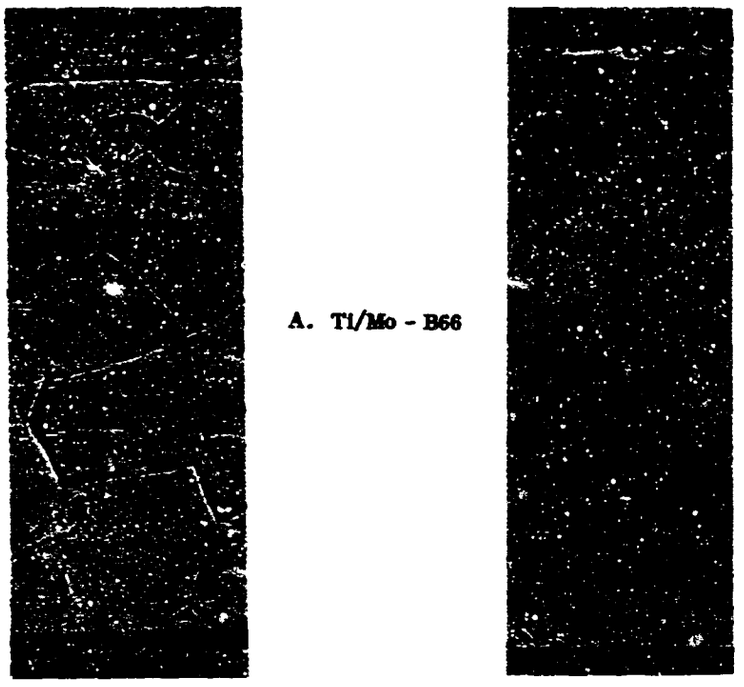

A. Ti/Mo - B66

79.0-21.0Mo

52.9Ti-47.1Mo

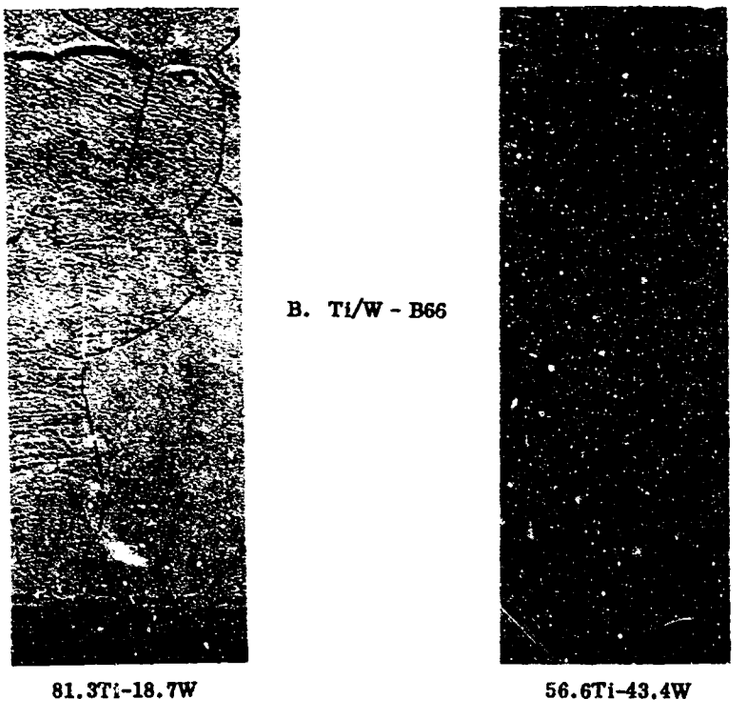

B. Ti/W - B66

81.3Ti-18.7W

56.6Ti-43.4W

Annealed for 100 Hours at 2200 F

Magnification: 250X

FIGURE 33. DIFFUSION COUPLES OF B66 VERSUS TITANIUM-MOLYBDENUM AND TITANIUM-TUNGSTEN ALLOYS

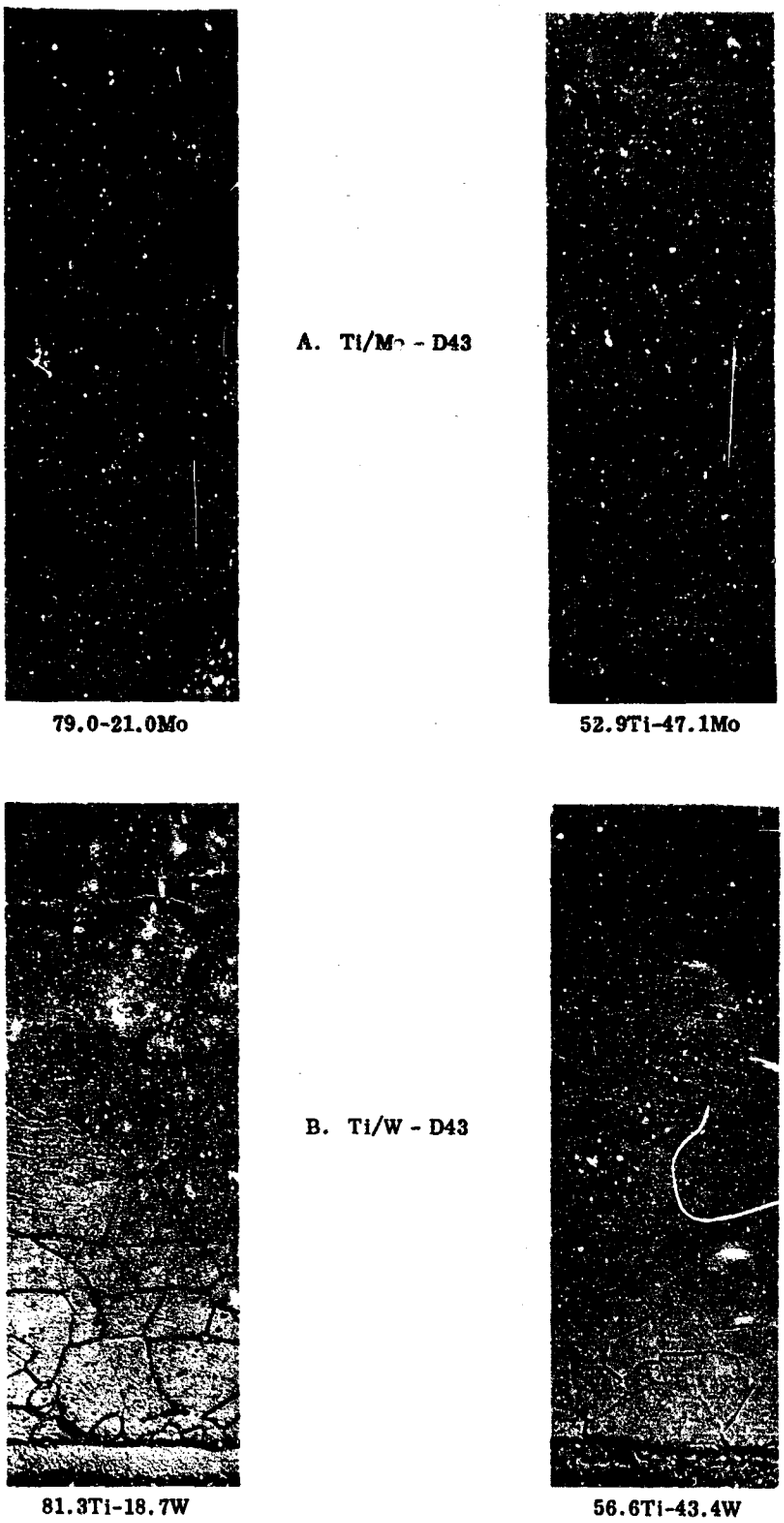

Annealed for 100 Hours at 2200 F
Magnification: 250X

FIGURE 34. DIFFUSION COUPLES OF D43 VERSUS TITANIUM-MOLYBDENUM AND TITANIUM-TUNGSTEN ALLOYS

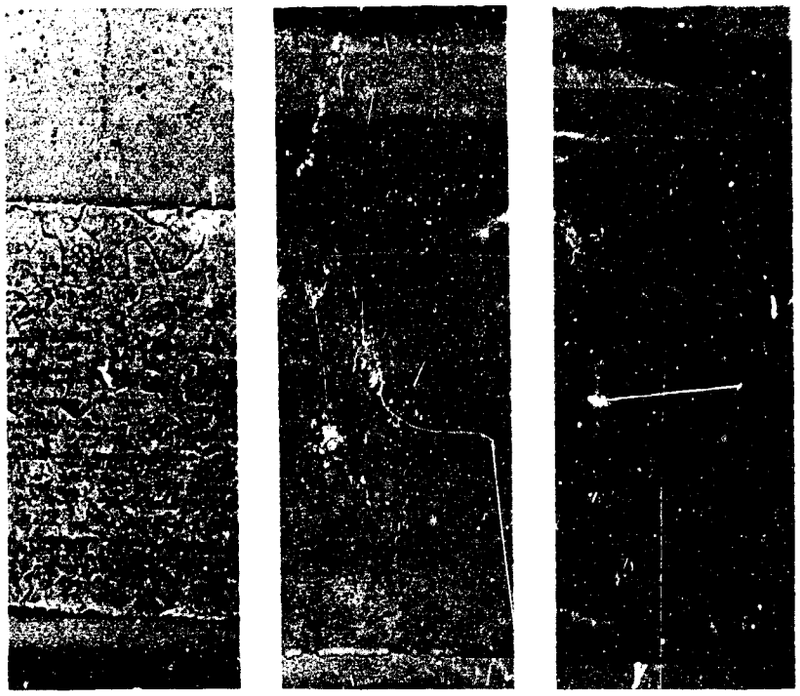

A. Ti/Cr - Cb752

71.6Ti-28.4Cr 48.1Ti-51.9Cr 23.0Ti-77.0Cr

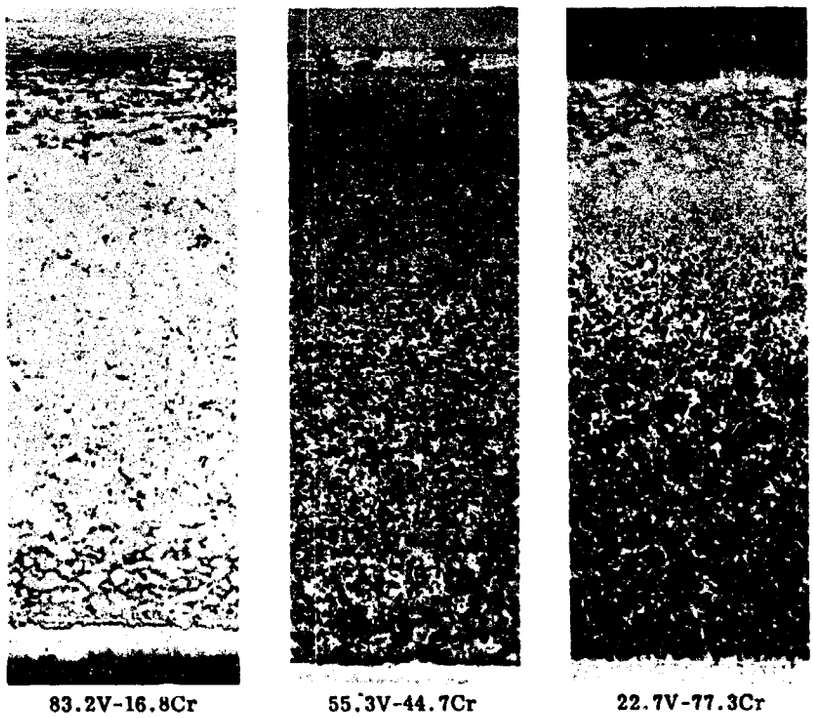

B. V/Cr - Cb752

Annealed 100 Hours at 2200 F
Magnification: 250X

83.2V-16.8Cr 55.3V-44.7Cr 22.7V-77.3Cr

FIGURE 35. DIFFUSION COUPLES OF Cb752 VERSUS TITANIUM-CHROMIUM AND VANADIUM-CHROMIUM ALLOYS

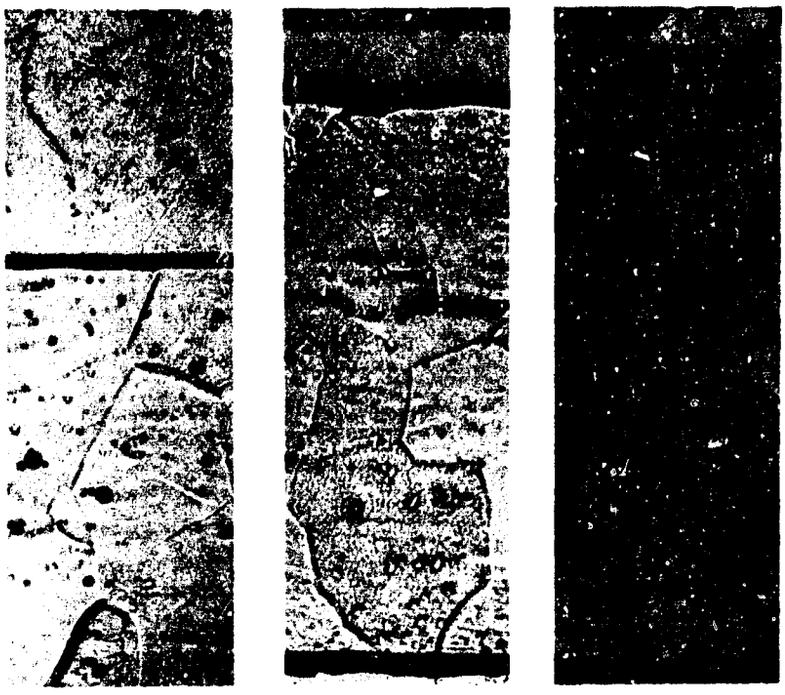

71.6Ti-28.4Cr 48.1Ti-51.9Cr 23.0Ti-77.0Cr

A. Ti/Cr - B66

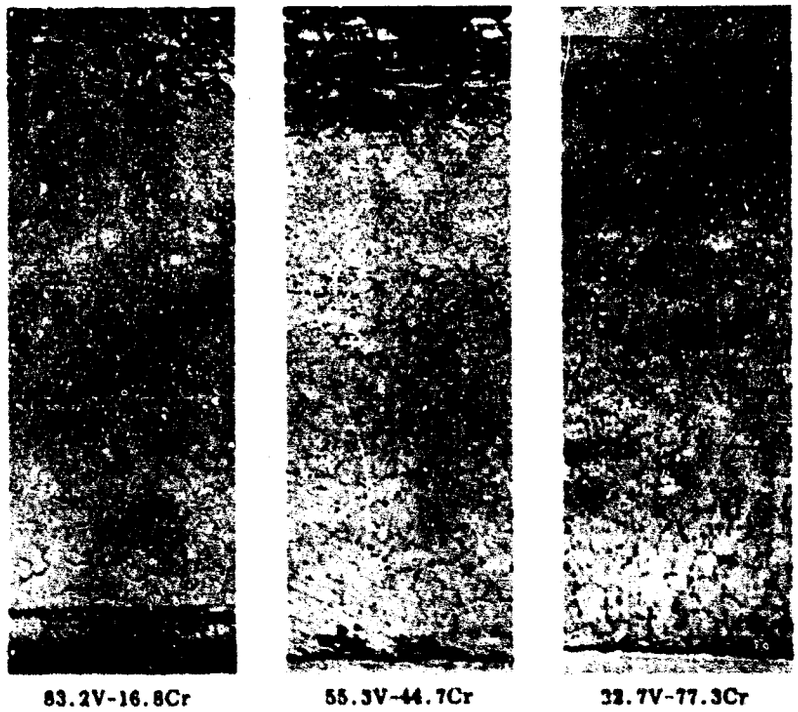

B. V/Cr - B66

83.2V-16.8Cr 55.3V-44.7Cr 32.7V-77.3Cr

Annealed 100 Hours at 2200 F

Magnification: 250X

FIGURE 36. DIFFUSION COUPLES OF B66 VERSUS TITANIUM-CHROMIUM AND VANADIUM-CHROMIUM ALLOYS

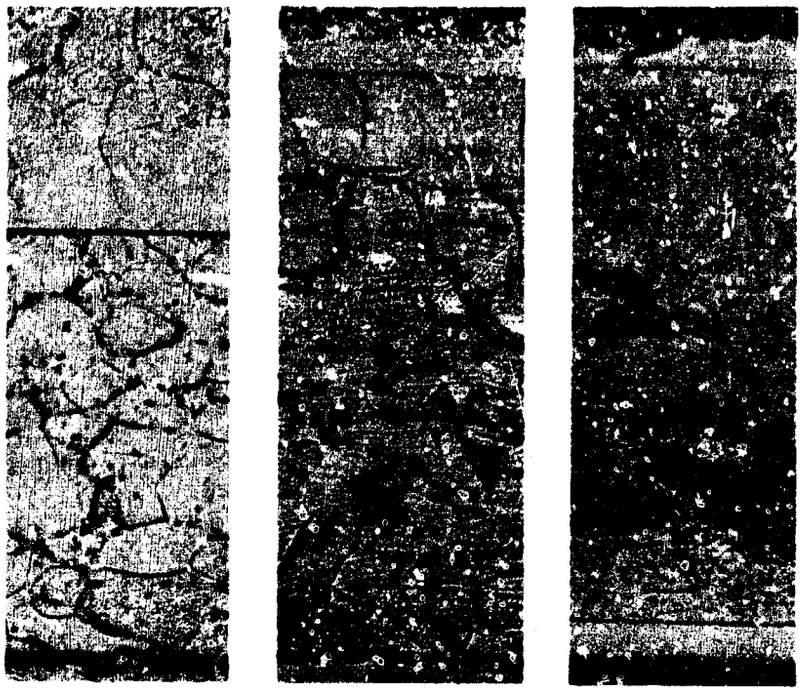

71.6Ti-28.4Cr | 48.1Ti-51.9Cr | 23.0Ti-77.0Cr

A. Ti-Cr - D43

B. V/Cr - D43

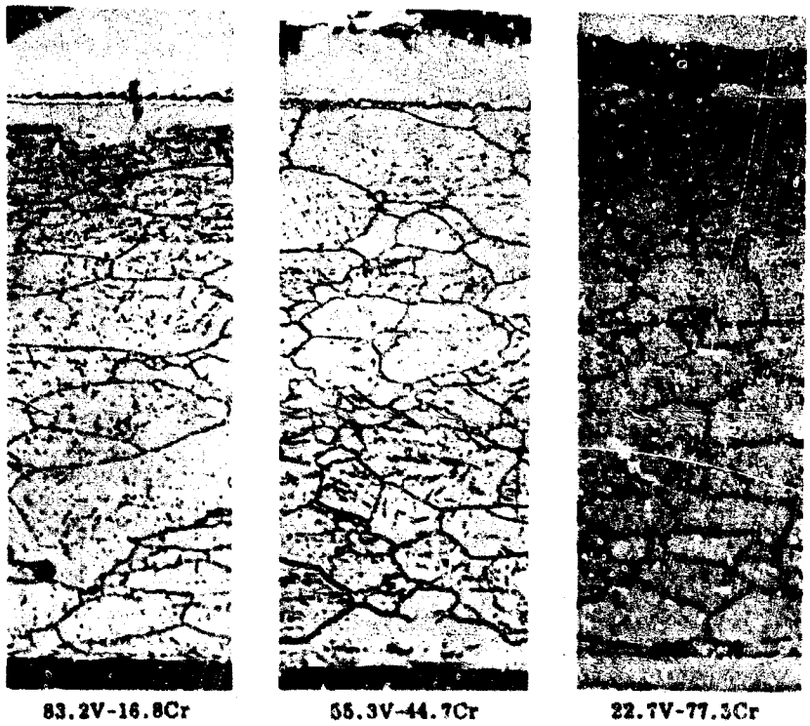

83.2V-16.8Cr | 55.3V-44.7Cr | 22.7V-77.3Cr

Annealed 100 Hours at 2200 F
Magnification: 250X

FIGURE 37. DIFFUSION COUPLES OF D43 VERSUS TITANIUM-CHROMIUM AND VANADIUM-CHROMIUM ALLOYS

To compare diffusion rates in the various alloys, the amount of dissolved columbium alloy is tabulated in Table XV for the diffusion couples shown in Figures 32 through 37.

TABLE XV

DIFFUSION PENETRATION INTO COLUMBIUM ALLOYS AFTER 100 HOURS AT 2200 F

Composition (at. %)	Penetration in inches into		
	Cb752	B66	D43
56.6Ti-43.4W	0	0.0001	0
81.3Ti-18.7W	0.0011	0.0012	0.0005
52.9Ti-47.1Mo	0	0.0002	0
79.0Ti-21.0Mo	0.0007	0.0010	0.0005
23.0Ti-77.0Cr	0	0.0003	0.0001
48.1Ti-51.9Cr	0.0011	0.0015	0.0015
71.6Ti-28.4Cr	0.0037	0.0041	0.0027

The photomicrographs also indicated the influence of the binary alloys on the columbium alloy substrates. It was particularly interesting to note how the chromium alloys contaminated the substrates. The chromium used in this study contained about 0.5 percent oxygen. The oxygen diffused into the columbium alloys and prevented grain growth. When chromium was replaced with tungsten and molybdenum, the columbium alloys exhibited a much cleaner structure with large grains.

The rate of chromium diffusion in the Ti-Cr-Si coating was believed to be accelerated by the rapid diffusion of titanium which apparently increased the solubility of chromium in columbium. By replacing titanium with the slower diffusing vanadium, retention of useful mechanical properties of the substrate could possibly be accomplished for a longer period of time.

Diffusion couples of Cb752, B66, and D43 alloys versus binary alloys of vanadium/chromium were run for 100 hours at 2200 F. Compositions of the binary alloys are shown in Table XIV. Micrographs of the diffusion couples are shown in Figures 35 through 37.

Except for one case, there is no measurable diffusion zone into any of the columbium alloys after 100 hours at 2200 F. Thus, it must be concluded that vanadium retards the overall diffusion into the columbium alloys. This holds for all the vanadium/chromium alloys independent of the vanadium concentration. The only case where a narrow diffusion zone possibly can be observed is in the D43 alloy in contact with the 83.2V-17.3Cr alloy.

An interesting feature is the effect of the vanadium/chromium alloys on the microstructure of the columbium substrate. Because of the high oxygen concentration of the chromium and the vanadium, the contamination of the columbium alloys is significant. Figure 37B shows clearly the tendency of oxides to precipitate in the grain boundaries in D43 alloy.

3.2.4 Effect of Sublayer on Mechanical Properties

The interstitial sink effect has been discussed in relation to the effect of the (Ti-Cr)-Si coating on the properties of duplex heat-treated D43 alloy (para. 3.1.1 and Ref. 6 and 7). Briefly, this effect arises when the partial molal free energy of an interstitial element in solution is lower in the coating composition than in the columbium alloy. Loss of interstitial element X to the coating causes solution of the interstitial compound ZrX (or HfX) and loss of strength of the columbium alloy. Thermochemical calculations were made to predict which elements could be tolerated in the prealloyed sublayer and which elements would act as interstitial sinks. These calculations predicted that tantalum and titanium would provide sinks for carbon-containing alloys such as D43, but only titanium would be a sink for alloys with a predominant oxide dispersion, such as the ZrO_2 in Cb752 (see Figures 6 and 7). The effect of this sink is known to be most marked for alloys in the duplex heat-treated condition, and is more marked on elevated temperature properties than on room temperature properties since dispersions contribute more to high-temperature strengths.

A series of experiments was conducted to determine the individual effects of titanium, tantalum, tungsten, and molybdenum. Foils 0.001 inch thick of each element were bonded to 0.012-inch columbium alloy test specimens. The Cb752 and B66 alloys were stress relieved; whereas, the D43 alloy had been given the duplex heat treatment. The composite specimens were annealed for 15 hours in gettered argon at 2400 F. After annealing, the foils were ground off and the columbium substrates were tensile tested at 2200 F. Tables XVI and XVII show that titanium and tantalum cause loss of strength of carbon-strengthened D43 alloy in the duplex heat-treated condition, as predicted.

TABLE XVI

ULTIMATE TENSILE STRENGTH AT 2200 F

Metal Bonded to Columbium alloys	Cb752 (ksi)	B66 (ksi)	D43 (ksi)
Uncoated	31	40	32
Titanium	30	36	20
Tungsten	39	40	31
Molybdenum	34	36	32
Tantalum	29	37	22

TABLE XVII

ELONGATION AT 2200 F

Metal Bonded to Columbium alloys	Cb752 (%)	B66 (%)	D43 (%)
Uncoated	55	20	20
Titanium	20	30	30
Tungsten	10	No data	10
Molybdenum	10	30	10
Tantalum	35	25	20

A second series of experiments was undertaken to compare D43 (carbon strengthened) and Cb752 (predominantly oxide dispersion) alloys in the duplex heat-treated condition. The same experimental procedure was used except that annealing was performed in a vacuum of 10^{-6} Torr for 15 hours at 2400 F. After annealing, the diffusion-bonded foils were removed by grinding and tensile tests were performed. In the case of titanium-coated alloys, the diffusion zone was extensive and complete removal was not achieved in every case.

Tables XVIII and XIX show the effect of these anneals on duplex processed Cb752 and D43 alloys. In agreement with predictions, only titanium caused loss of strength of the duplex processed Cb752 alloy. These calculations are presented in a different form in Table XX where the partition between pure columbium and four elements is presented for a temperature of 1500 K.

The difference in behavior of tantalum in the two cases is in line with predictions. Analysis of the D43 alloy after removal of the tantalum confirmed that this element was a sink for carbon.

- D43 - as received, 900 ppm carbon
- D43 - after anneal in contact with tantalum, 106 ppm carbon

It can be concluded that the thermodynamic calculations are reliable, therefore, and can be used to examine problems with other alloys and other coating elements. The columbium alloy, Cb132M, was being considered for coating work for eventual use in gas turbines. This alloy contains carbon so that a potential problem was thought to exist. The effect of titanium on this alloy was studied by metallography.

A diffusion couple was made by sandwiching a 0.010-inch thick foil of titanium between 1/32-inch thick pieces of Cb132M alloy. The couple was subsequently annealed at 2400 F for 5 hours.

Microstructures of as-received (extruded), as-diffusion-bonded, and diffusion-bonded and annealed materials are shown in Figures 38 through 40.

After annealing, most of the fine carbide precipitate in the columbium alloy was removed and massive carbides were formed in the titanium. Some grain growth occurred in the Cb132M alloy and the diamond pyramid hardness dropped from 315 (as-received) to 275. Considerable interdiffusion of columbium and titanium occurred, as evidenced by migration of the columbium alloy/titanium alloy interface into the Cb132M alloy.

The high-temperature creep strength properties of this alloy are derived from a combination of high solid solution alloying, and the presence of finely dispersed carbides which stabilize dislocation networks. It was concluded, therefore, that coatings high in titanium content would have a serious weakening effect on the high-temperature mechanical properties of this alloy.

TABLE XVIII

STABILITY OF DUPLEX HEAT-TREATED Cb752 ALLOY AFTER VARIOUS ANNEALS

Mechanical Properties at 2200 F (0.050 inch/inch/minute)

Specimen Condition	Tests	Yield[1] Strength (psi)	Ultimate Tensile Strength (psi)	Elongation (%)
As received	Longitudinal 2	28,200	35,100	28
	Transverse 4	30,100	33,800	22
Annealed 2400 F 15 hr	Longitudinal 4	26,200	30,000	30
	Transverse 2	27,600	34,700	30
Molybdenum foil + anneal	Longitudinal 1	28,000	30,500	35
	Transverse 3	24,700	30,900	33
Tantalum foil + anneal	Transverse 2	28,000	33,600	18
Titanium foil + anneal	Longitudinal 3	21,300	22,700	26
	Transverse 2	16,100	23,400	22
No heat treat + anneal	2	-	31,000	55
No heat treat + titanium foil + anneal	2	-	30,000	20

Cb752 Composition Heat No. 52342	Tungsten	10.0 nominal
	Zirconium	2.5 nominal
	Oxygen	65 ppm (80 ppm)[2]
	Carbon	60 ppm (65 ppm)
	Nitrogen	78 ppm (40 ppm)
Heat Treatment	Solution treated	2800 F
	Reduction	40%
	Aging	2400 F

1. Thickness 0.012 inch.
2. Analyses in parentheses were made on 0.012-inch sheets. Supplier's analyses were made on 0.050-inch sheet.

TABLE XIX

STABILITY OF DUPLEX HEAT-TREATED D43 ALLOY AFTER VARIOUS ANNEALS

Mechanical Properties at 2200 F (0.050 inch/inch/minute)

Specimen Condition (All Transverse)	Tests	Yield Strength (psi)	Ultimate Tensile Strength (psi)	Elongation (%)
As received	2	33,000	35,460	14
Annealed 2400 F - 15 hours	4	-	30,800	20
Tungsten foil + anneal	2	-	31,000	10
Molybdenum foil + anneal	2	-	32,000	10
Tantalum foil + anneal	4	16,600	20,800	20
Titanium foil + anneal	2	-	20,000	30

Composition (Heat No. 283	Tungsten	9.6%
Thickness 0.012 inch	Zirconium	0.98%
	Carbon	860 ppm
Heat Treatment		
Solution treat	3000 F	
Reduction	25%	
Aging	2600 F - 1 hour	

TABLE XX

CALCULATED PARTITION OF CARBON AND OXYGEN AT 1500 K

Metal X	Calculated Carbon (ppm)		Calculated Oxygen (ppm)	
	Cb	X	Cb	X
Molybdenum	100	<1	100	<1
Tungsten	100	<1	100	<1
Tantalum	100	270	100	(10)
Titanium	100	16,800	100	100,000

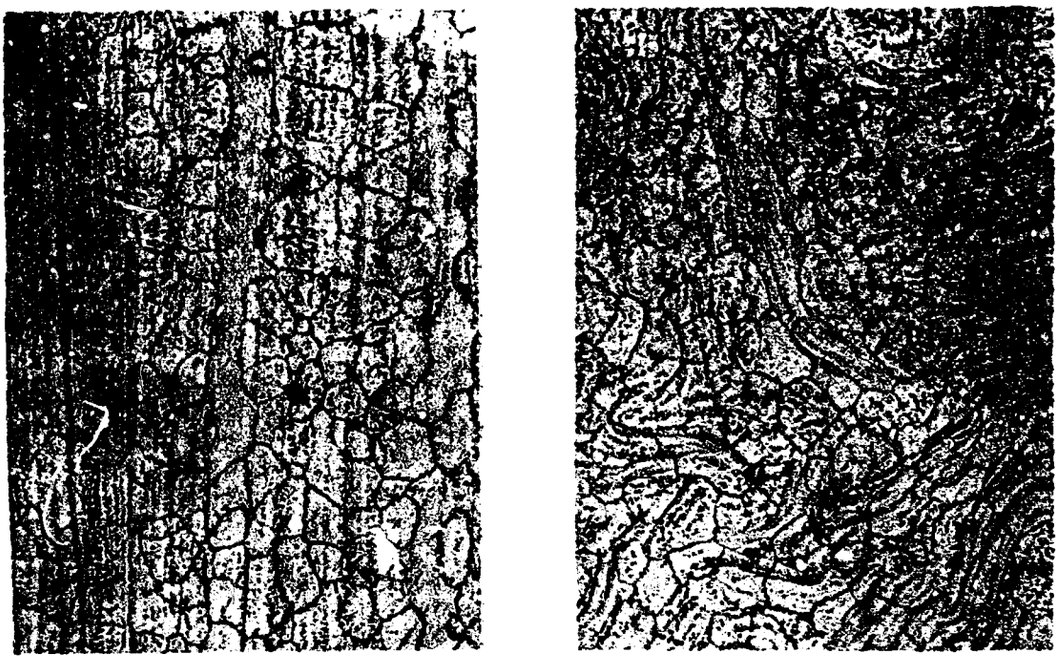

Magnification: 250X

FIGURE 38. TRANSVERSE AND LONGITUDINAL SECTIONS OF AS-RECEIVED Cb132M ALLOY

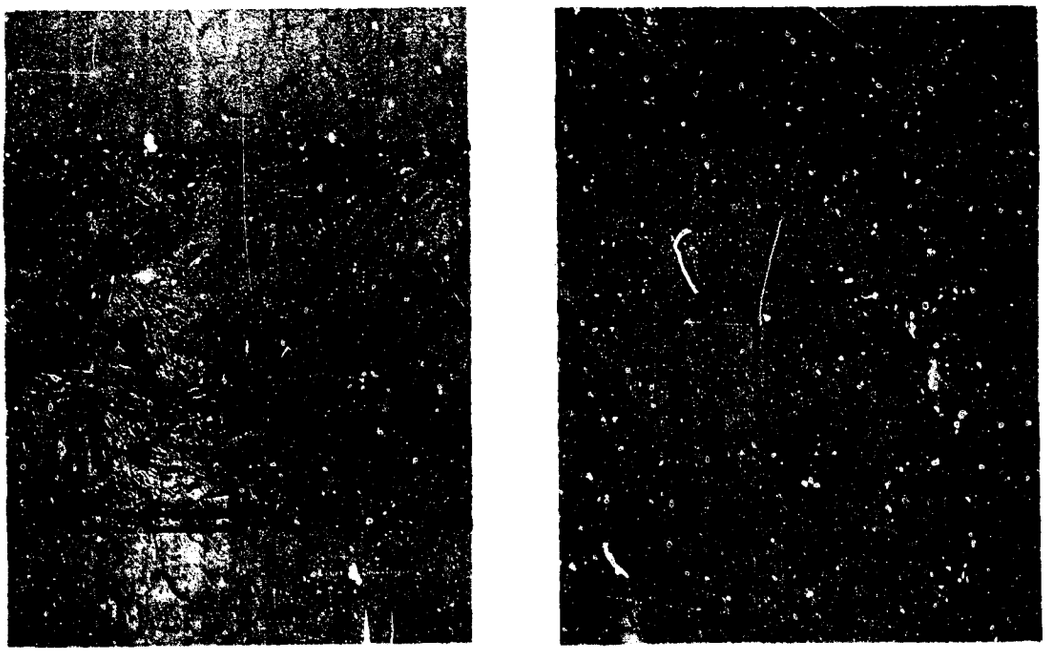

Etched for Titanium Magnification: 250X Etched for Columbium Alloy

FIGURE 39. AS-BONDED Cb132M-TITANIUM DIFFUSION COUPLE

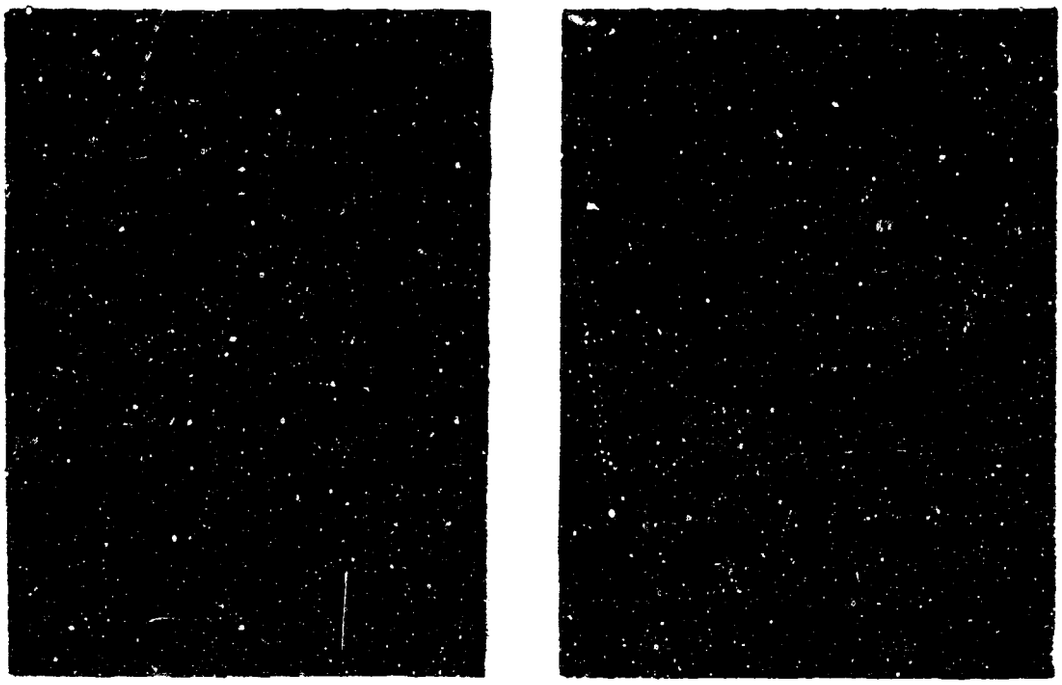

FIGURE 40. Cb132M-TITANIUM ANNEALED 15 HOURS AT 2400 F

3.3 EVALUATION OF PRIMARY OXIDATION BARRIERS

The primary oxidation barriers for use with sublayers are silicides and aluminides. Silicides, and to a lesser extent aluminides, are the most oxidation-resistant intermetallic compounds known so that very long coating lives can be predicted if oxidation alone determines life. Unfortunately, other factors affect the life so that failure generally occurs long before the primary barrier has been completely oxidized. The difference in life between static and cyclic oxidation tests may reach a ratio as high as 10 to 1 (typically 3 to 1), and provides an illustration of the fact that life is controlled by other than the conversion of the primary barrier to oxide. The sublayer concept is designed to avoid failures that result from minor cracks caused by thermal strains. One purpose of the work described in this section was to determine the properties of aluminides and silicides in order to design coatings that will be more resistant to failure.

To assist in the selection of potential coating systems, the oxidation resistance and coefficients of thermal expansion of various silicides and aluminides were determined. In the silicide system, properties were determined on both the M_5Si_3 and MSi_2

silicides and in the aluminide systems on MAl and MAl_3 aluminides. Studies of silicides were concentrated on the (V-Cr), (V-Cr-Cb), (Ti-Mo), (Ti-Mo-Cb), and (Ti-W) and (Ti-W-Cb) systems, with the (Ti-Cr) and (Ti-Cr-Cb) systems being used as controls. The aluminide systems were not as clearly defined at the early stages of the program, but the work tended to support systems containing primarily titanium, and columbium with additives such as chromium and molybdenum and tantalum.

The initial basis for selection of the (V-Cr) modification was to minimize the interstitial sink effect on dispersion strengthened alloys and to minimize Laves phase (MCr_2) formation at the silicide-metal interface. The (Ti-Mo) or (Ti-W) systems were selected based on the elimination of the volatile chromium constituent while introducing a replacement element that had far superior oxidation resistance, as the disilicide, compared with $CrSi_2$.

The aluminide composition primarily grew out of the desire to capitalize on the slight ductility of the tetragonal TiAl (gamma, c/a = 1.02) intermetallic compound.

3.3.1 Oxidation of the MSi_2 and M_5Si_3

The silicide compositions were prepared by mixing together the elemental powders, cold pressing at 10,000 psi, and triple arc melting in a nonconsumable arc furnace using a copper hearth and a tungsten cathode. The melting atmosphere was titanium-gettered argon at a pressure varying from 300 to 700 Torr. After melting, the specimens were annealed in gettered argon at 2200 F for four hours.

The specimens for oxidation testing were cut into rectangular parallelepipeds using a spark-cutting technique (Elox). Size was quite varied, but 0.25 by 0.25 by 0.50 inch was the size objective.

Specimens were tested at 1500 and 2400 F. The lower temperature was chosen to investigate pest-type attack and was based on the thought that although pest attack may be more likely to occur at 1200 to 1400 F for certain silicides, it is more serious if it occurs at the higher temperature of 1500 F because reaction rates are generally much higher. In addition, dwell times at the lower temperatures are generally short for typical Air Force applications such as glide reentry heat shields or blades for gas turbines. It is recognized that selection of another temperature might have changed the pattern of performance. Selection of the upper temperature as 2400 F needs no justification.

In oxidation testing the specimens were supported on Leco Number 528-53 zircon boats. At 1500 F the specimens were tested in a static air environment. Testing at 2400 F was conducted in one-inch diameter mullite tubes in which dry air (-50 F dew point) at a flow rate of four cfh was passed through the tube. Specimens were cycled approximately every 16 hours for 96 to 101 hours or failure. Evaluation of the specimens was by weight change and changes in appearance.

Oxidation of the MSi_2 Silicides

The oxidation results at 1500 and 2400 F on the various MSi_2 silicides are shown in Table XXI. The chemical analyses of the various disilicides are also included in this table. Figures 41 and 42 show the appearance of the specimens after test.

With relatively few exceptions, the disilicides have excellent oxidation resistance at 1500 F. The exceptions were WSi_2 and $CbSi_2$, which failed catastrophically in less than 16 hours. Other more complex disilicides containing high tungsten and columbium (No. 4) or high tungsten only (No. 5) also performed poorly. Most specimens retained a metallic luster throughout the test or developed a very thin, almost interference, oxide film.

Oxidation results at 2400 F showed marked difference between the various disilicides. The $CbSi_2$ disilicide exhibited the poorest oxidation resistance, while $MoSi_2$, WSi_2, $TiSi_2$, and VSi_2 were the outstanding binary disilicides. Disilicides containing appreciable quantities of chromium usually lost weight and spalled on thermal cycling. Alloys of $CrSi_2$ and $TiSi_2$ showed rapid weight gain and rarely lasted 96 hours, even when silicon was in excess of the disilicide ratio. Additions of columbium to the Cr-Ti-Si compositions greatly retarded the oxidation rate. In contrast to the Ti-Cr-Si compositions, disilicides in the V-Cr-Si system had excellent oxidation resistance, although slight weight losses were noted, as is characteristic with chromium-containing disilicides.

Of the disilicides tested containing columbium, the outstanding performers were those containing both titanium and molybdenum, followed on a selective basis by those containing titanium plus tungsten, and vanadium plus chromium. Tolerance for columbium by a disilicide is extremely important in coatings on columbium alloys, because some interdiffusion cannot be avoided in either the application processes or in long-time exposure at elevated temperatures.

TABLE XXI

OXIDATION TEST RESULTS ON SEVERAL MSi_2 COMPOSITIONS

Number	Composition (at. %)(2)	Oxidation at 1500 F		Comments	Oxidation at 2400 F		Comments
		16 hours (mg/cm²)	96 hours (mg/cm²)		16 hours (mg/cm²)	96 hours(1) (mg/cm²)	
1	18.7Ti-14.6Mo-66.7Si (A)	-0.25	-0.18	Very good, metallic.	+6.78	+11.27	Very good, metallic.
2	12.3Ti-6.6Mo-80.1Si (A)	+0.14	+0.52	Very good, metallic.	+0.70	+1.37	Very good, black metallic.
2R	24Ti-6Mo-66Si (N)	---	+0.069	Very good, metallic.	---	5.87	Very good, metallic, no spalling
3	8.7Ti-11.2Mo-10.6Cb-69.2Si (A)	+0.09	+0.12	Very good, metallic.	+0.42	+0.69	Very good, metallic.
4	18.6Ti-8.7Mo-12.7Cb-59.2Si (A)	+4.06	Failed	Poor, failed 48 hours.	+1.25	+2.82	Good, thin black-yellow oxide.
4R	18.5Ti-8.5Mo-10Cb-66Si (N)	---	+0.065	Very good, metallic.	---	+0.35	Excellent, metallic no spall.
5	20.8Ti-15.1W-64.0Si (A)	Failed	---	Poor, failed 24 hours.	+1.02	+2.18	Very good, metallic.
6	11.2Ti-11.3W-77.4Si (A)	+0.01	+0.01	Very good, metallic.	+0.96	+3.19	Good, metallic.
6R	24Ti-9W-66Si (N)	---	-0.36	Very good, metallic.	---	+6.34	Very good, metallic, no spalling.
7	5.6Ti-16.7W-7.4Cb-72.4Si (A)	Failed	---	Poor, failed in 24 hours.	+3.27	+0.51	Very good, dark metallic.
8	16.1Ti-4.7W-14.2Cb-66.1Si (A)	+0.69	+0.96	Fair, yellow porous oxide.	+6.05	+0.34	Fair, yellow porous oxide.
9	13.7Ti-16.7Cr-66.6Si (A)	-0.47	-0.47	Very good, metallic.	+46.7		Poor, failed in 20 hours.
10	11.7Ti-9.6Cr-79.3Si (A)	+0.20	+0.30	Very good, metallic.	+8.90	+8.14	Poor, local melting.
10R	24Ti-9Cr-66Si (N)	---	+0.20	Very good, metallic.	---	+38.2	Poor, heavy oxide, spalling.
11	9.6Ti-23.3Cr-37.2Si (A)	0.00	0.50	Very good, metallic.	+30.19	Failed	Poor, failed 20 hours.
12	14.2Ti-11.1Cr-10.4Cb-64.3Si (A)	+0.22	+0.03	Very good, metallic.	+28.87	+36.16	Fair, green to grey oxide.
13	2.4Ti-6.5Cr-13.7Cb-81.4Si (A)	+0.00	+0.00	Very good, metallic.	+0.61	+1.51	Good, black oxide, some glazing.
13R	16.2Ti-8.5Cr-10Cb-66Si (N)	---	0.12	Very good, metallic.	---	+20.7	Severe spall, poor
14	7.2Ti-14.8Cr-10.9Cb-67.0Si (A)	+0.01	+0.02	Very good, metallic.	-4.15	+9.38	Fair, green to grey oxide.
15	14.4V-17.7Cr-37.9Si (A)	+0.20	+0.30	Very good, metallic.	-0.37	-0.11	Good, black oxide.
16	8.3V-24.7Cr-67.0Si (A)	+0.02	+0.03	Very good, metallic.	+0.32	-0.16	Fair, green to black oxide.
17	25.6V-7.7Cr-67.5Si (A)	+0.05	+0.05	Very good, metallic.	+0.19	+0.23	Good, brown oxide.
18	10.1V-16.9Cr-9.8Cb-63.1Si (A)	+2.28	+2.33	Good, black oxide.	+1.30	+10.11	Fair, green to brown oxide.
19	3.8V-17.4Cr-9.7Cb-67.8Si (A)	+1.19	+2.47	Very good, metallic	+4.15	+19.66	Fair, green to brown oxide.
20	15.3V-6.5Cr-10.9Cb-65.9Si (A)	+0.71	+0.90	Good, black oxide.	+0.48	+1.20	Good, black-brown oxide.
21	14.8V-10.9Cb-60.1Si (A)	+1.81	+4.57	Fair, yellow oxide.	+1.60	+0.77	Good, metallic.
26	31.7Mo-68.3Si (A)	+0.03	+0.03	Fair, porous black oxide.	+0.33	+0.86	Very good, metallic.
26	30.5W-69.5Si (A)	Failed	---	Failed 24 hours - yellow powder	Very low(4)	Very low(4)	Very good, metallic.
27	30.4V-69.6Si (A)	+0.81	+1.21	Excellent, metallic.	+0.34	0.77	Good, black film.
28	33Cb-67Si (A)	Failed	---	Failed 24 hours - grey powder	Failed	---	Poor, failed in 12 hours at 2600 F.
29	33Ti-67Si (N)	>0.23	+0.44	Very good, thin adherent oxide.	+0.3	+0.8(3)	Very good, thin adherent oxide.
29	33Cr-67Si (N)		+1.5	Very good, metallic.	+1.5	+5.5(3)	Fair to good, but oxide spalled continuously.

1. First 12 hours at 2600 F, plus 96 hours at 2400 F. (Weight change is from beginning of 2400 F hour test.)
2. A-analyzed, N-nominal.
3. Tested 2400 F only (no 2600 F testing).
4. Irregular specimen shape did not permit accurate area calculation.

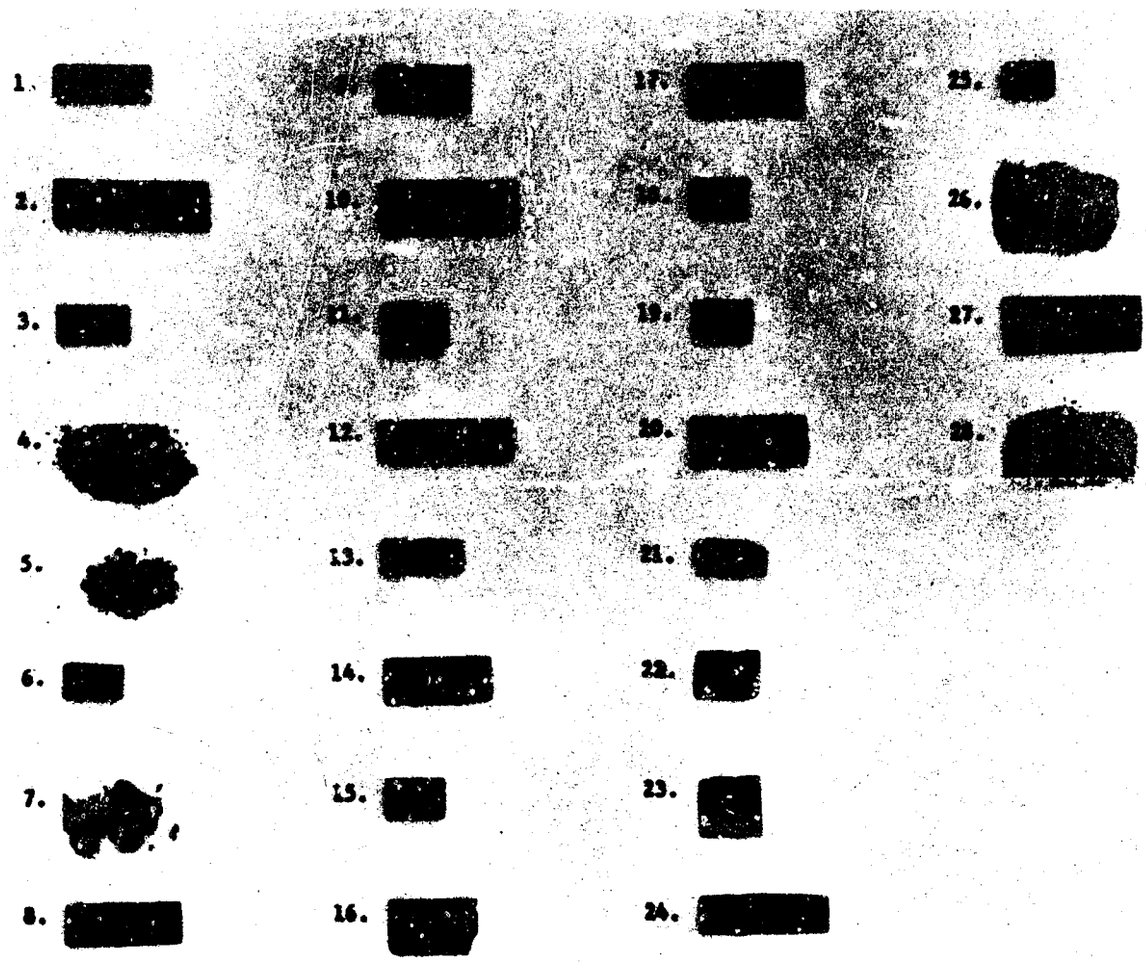

Silicide No. 4 failed after 48 hours
Silicide No. 5, No. 7, No. 26, and No. 28 failed after 24 hours
Duration: 96 Hours at 1500 F in Air

FIGURE 41. 1500 F OXIDATION OF VARIOUS DISILICIDES

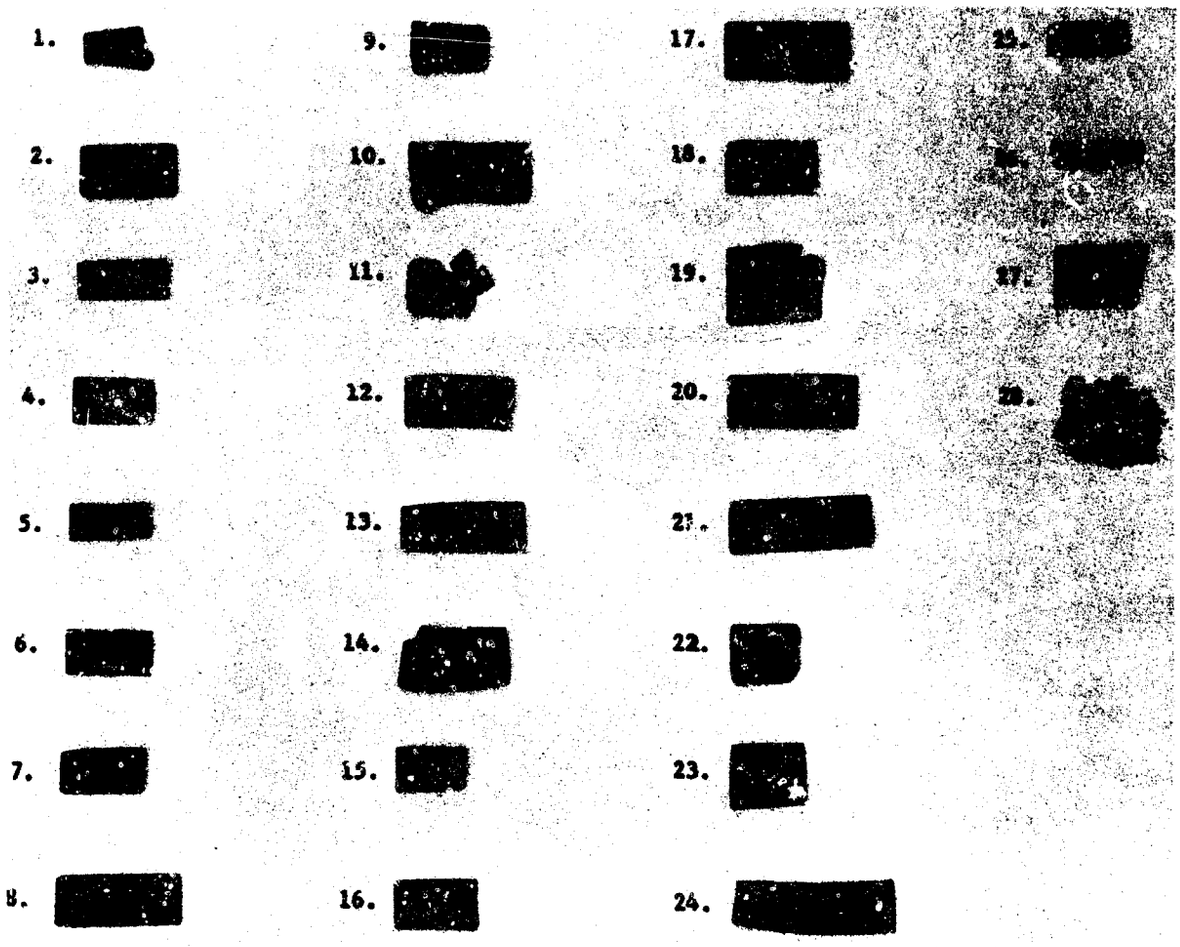

Silicides No. 9 and No. 11 failed after 20 hours
Silicide No. 28 failed after 12 hours
Duration: 96 Hours at 2400 F in Air

FIGURE 42. 2400 F OXIDATION OF VARIOUS DISILICIDES

Oxidation of the M_5Si_3 Silicide

The microstructures of the binary M_5Si_3 silicides (Fig. 43) showed small amounts of secondary phases in all compositions. The Ti_5Si_3, which was silicon deficient, showed the least secondary phase which was in general agreement with the broad composition range for this compound (Ref. 4). The four other silicides, whether silicon excess or silicon deficient, exhibited approximately similar secondary phases at grain boundaries. The secondary phases amounted to less than 10 percent in all specimens.

The ternary M_5Si_3 silicide microstructures (Fig. 44) indicated almost 100 percent single-phase structures for $(Ti\text{-}Cr)_5Si_3$ and $(Ti\text{-}Mo)_5Si_3$, but the $(V\text{-}Cr)_5Si_3$ composition exhibited a secondary phase that constituted 20 to 30 percent of the volume. Since the stoichiometry of this composition was held very closely in preparation, the secondary phase may be due to the restricted substitution of vanadium for chromium in the Cr_5Si_3 structure.

The introduction of columbium into the ternary composition to produce the quaternary M_5Si_3 silicide produced the microstructures shown in Figure 45. The (Ti-Cr-Cb) and (Ti-Mo-Cr) compositions remained essentially single phases; whereas, the vanadium-containing composition (V-Cr-Cb) remained multiple phased.

The oxidation test results for the M_5Si_3 silicide at 1500 and 2400 F are given in Table XXII and the specimens after exposure for 101 hours are shown in Figures 46 and 47.

The binary silicide, Cb_5Si_3, had essentially no oxidation resistance at either test temperature. The binary silicide, Mo_5Si_3, was next poorest in performance, showing relatively severe exfoliation at 1500 F and catastrophic oxidation at 2400 F. At 1500 F, Cr_5Si_3 was the best performer, followed closely by V_5Si_3 and Ti_5Si_3 in that order.

The ternary silicides, $(Ti\text{-}Cr)_5Si_3$, $(Ti\text{-}Mo)_5Si_3$, and $(V\text{-}Cr)_5Si_3$ exhibited good to excellent oxidation resistance at 1500 and 2400 F. The $(Ti\text{-}Cr)_5Si_3$ composition had small positive weight gains at both temperatures and was, therefore, rated best of the group. The $(Ti\text{-}Mo)_5Si_3$ composition broke into a number of large pieces during testing at 1500, but from the appearance, internal stress rather than oxidation was the cause.

Composition No. 31 Ti_5Si_3

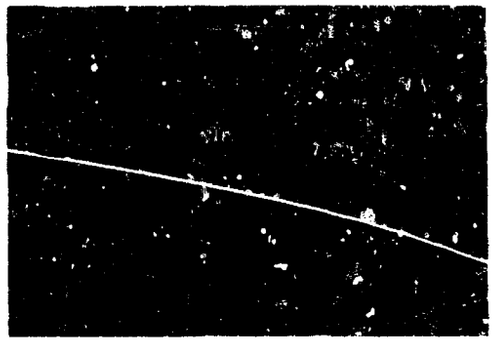

Composition No. 32 Cr_5Si_3

Composition No. 33 Cb_5Si_3

Composition No. 34 V_5Si_3

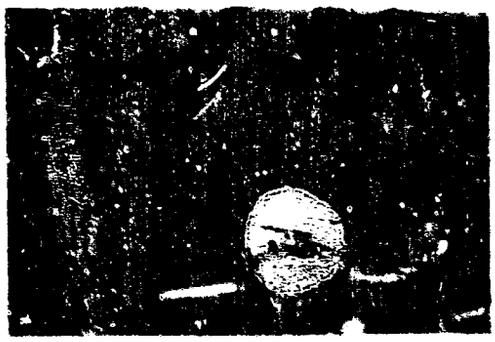

Composition No. 35 Mo_5Si_3

Magnification: 250X

FIGURE 43. THE BINARY M_5Si_3 SILICIDES; Arc Melted and Annealed

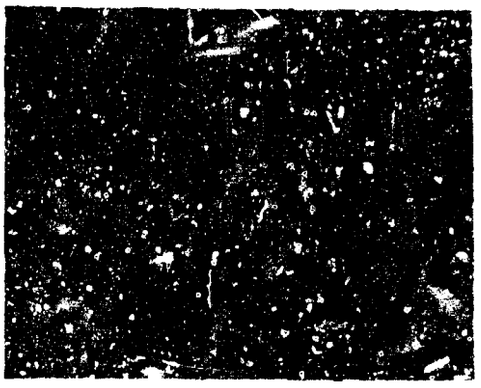

Composition No. 36 $(Ti-Cr)_5Si_3$

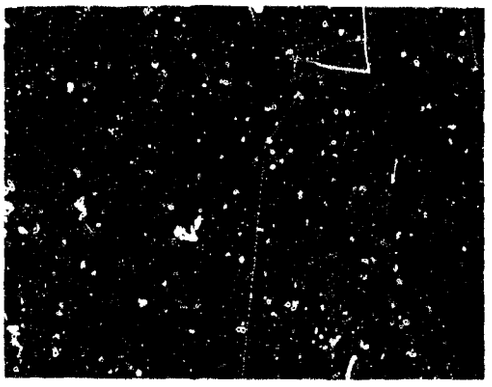

Composition No. 38 $(Ti-Mo)_5Si_3$

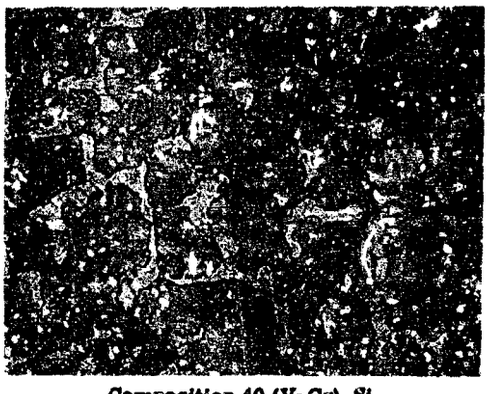

Composition 40 $(V-Cr)_5Si_3$

Magnification: 250X

FIGURE 44. THE TERNARY M_5Si_3 SILICIDES; Arc Melted and Annealed

The three quaternary silicides studied - $(Ti-Cr-Cb)_5Si_3$, $(Ti-Mo-Cb)_5Si_3$, and $(V-Cr-Cb)_5Si_3$ - exhibited some of the more interesting oxidation test data. The oxidation test results for the $(Ti-Cr-Cb)_5Si_3$ composition at 1500 and 2400 F were equal or superior to the disilicide containing these elements. Comparable compositions containing titanium, molybdenum, and columbium or vanadium, chromium and columbium were rapidly oxidized at both temperatures.

A significant point brought out in the oxidation study of the M_5Si_3 silicides was the excellent performance of the $(Ti-Cr)_5Si_3$ and $(Ti-Cr-Cb)_5Si_3$ compositions at the two test temperatures, 1500 and 2400 F. The oxidation resistance of these compositions was superior to similar compositions at the MSi_2 metal-silicon ratio. None of the

Composition No. 37 $(Ti-Cr-Cb)_5Si_3$

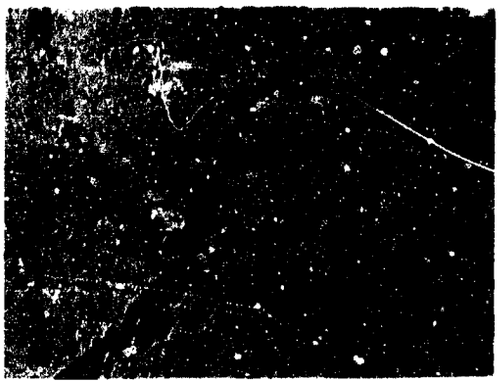

Composition No. 39 $(Ti-Mo-Cb)_5Si_3$

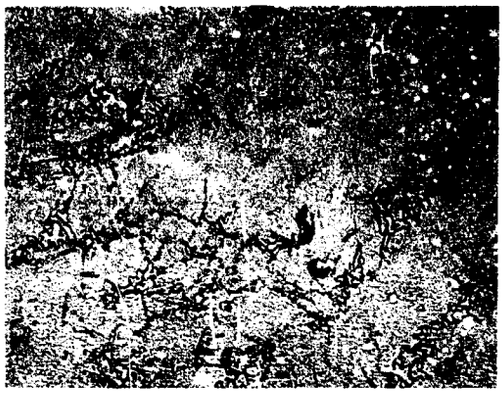

Composition No. 41 $(V-Cr-Cb)_5Si_3$

Magnification: 250X

FIGURE 45. THE QUARTERNARY M_5Si_3 SILICIDES; Arc Melted and Annealed

other M_5Si_3 silicides showed superior oxidation resistance to their MSi_2 counterparts. Also, the tolerance of the other M_5Si_3 silicides for columbium was far less than for the ones containing titanium and chromium.

The past success with the (Ti-Cr)-Si coating on columbium alloys may, in part, be due to the excellent oxidation resistance of the subsilicide layer and the alloy layers formed beneath this silicide; however, the high thermal expansion of the silicides containing substantial amounts of titanium and chromium may play a significant role in lowering the reliable oxidation life of the coating (Ref. 3) by increasing the severity of the craze cracking problem.

TABLE XXII

OXIDATION TEST RESULTS ON SEVERAL M_5Si_3 COMPOSITIONS

Number	Nominal Composition (at. %)	Oxidation at 1500 F		Comments	Oxidation at 2400 F		Comments
		21 hours (mg/cm^2)	101 hours (mg/cm^2)		21 hours (mg/cm^2)	101 hours (mg/cm^2)	
31	62.5Ti-37.5Si	+ 3.98	+ 3.80	Tan, good	+ 30.4	+271.8	Tight oxide, but rapid oxidation.
32	62.5Cr-37.5Si	+ 0.51	0.78	Very thin green-oxide, excellent	3.39	-16.0	Slow exfoliation, corners sharp.
33	62.5Cb-37.5Si	Failed 4 hours	---	Castastrophic oxidation	Failed 4 hours	---	Catastrophic oxidation
34	62.5V-37.5Si	+ 0.82	- 1.96	Glazed, gray to yellow, excellent.	- 8.45	- 9.82	Blue-black, less glazing than at 1500 F.
35	62.5Mo-37.5Si	- 6.24	-10.27	Poor, exfoliation	Failed 4 hours	---	Catastrophic oxide
36	31.3Ti-31.3Cr-37.4Si	+ 1.24	+ 1.89	Blue-green, excellent sharp corners.	+ 1.80	+ 1.66	Gray-brown, excellent
37	20.8Ti-20.8Cr-20.8Cb-37.6Si	+ 0.83	+ 1.05	Light brown, sharp corners, excellent.	+ 1.31	+ 5.90	Not quite as good as No. 36, but excellent.
38	31.3Ti-31.3Mo-37.4Si	-10.49	---	Specimen disintegrated from internal stress not oxidation.	+ 2.37	- 3.05	Slight glaze, sharp edges, good.
39	20.8Ti-20.8Mo-20.8Cb-37.6Si	- 5.75	+75.1 (61 hours)	Very rapid oxidation	+ 36.91 Failed		Rapid oxidation, poor
40	31.3V-31.3Cr-37.4Si	+ 2.01	+ 3.52	Blue-brown, thin oxide good.	- 1.40	- 5.20	Glazed, blue-gray good, sharp edges.
41	20.8V-20.8Cr-20.8Cb-37.6Si	+ 3.87	+20.48	Loose oxide.	+162.35 Failed		Rapid oxidation, poor.

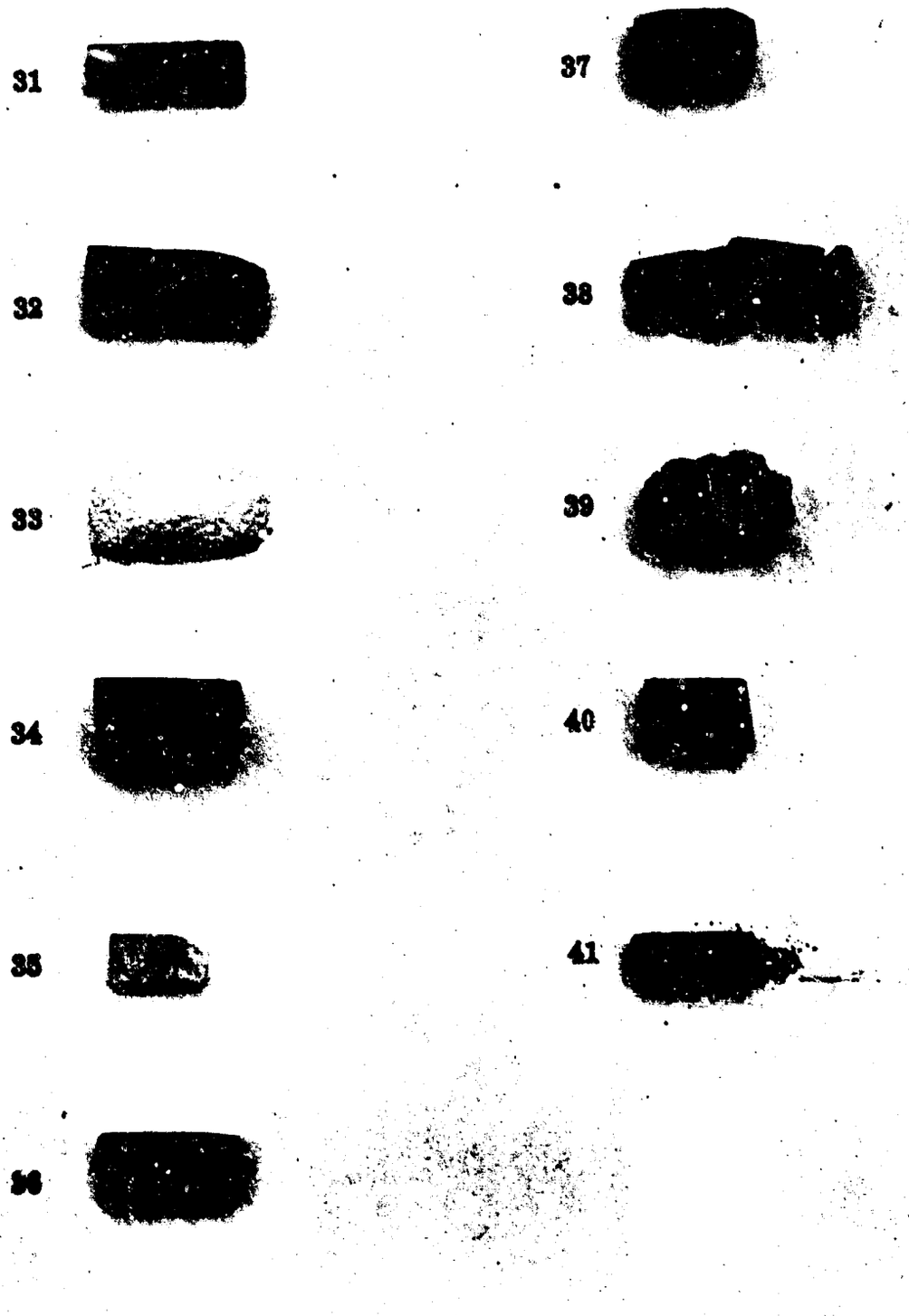

Compositions 33, 38, and 39 failed; see Table XXII

FIGURE 46. M_5Si_3 SILICIDES AFTER 101 HOURS AT 1500 F IN AIR

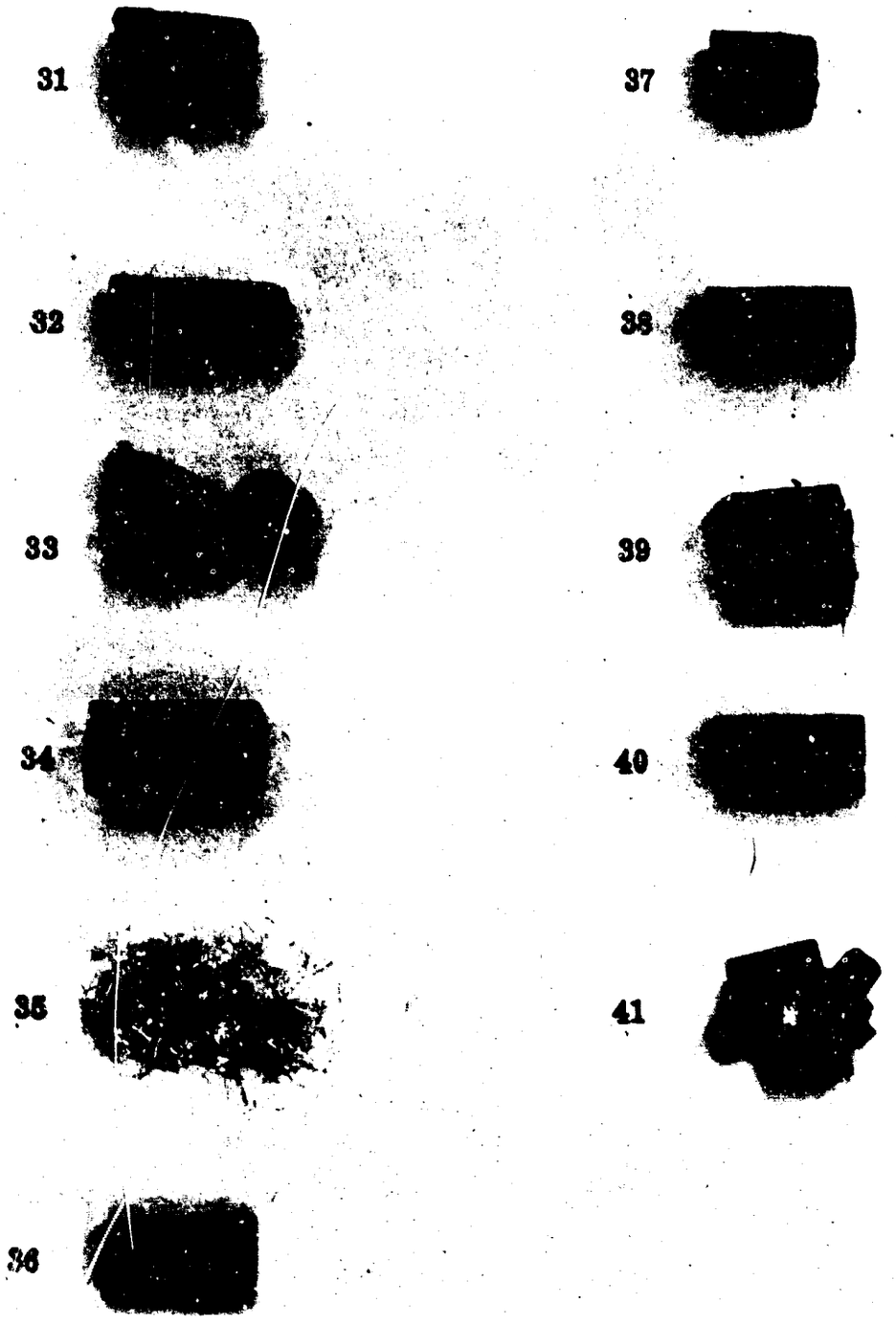

Compositions 33, 38, and 39 failed; see Table XXII

FIGURE 47. M_5Si_3 SILICIDES AFTER 101 HOURS AT 2400 F IN AIR

3.3.2 Oxidation of Aluminides

The objective of the companion program undertaken by IITRI was to perform studies aimed at identifying coating systems for columbium, based on aluminides. Work on the aluminum-containing sublayer is reported here because it was performed as part of an overall study of aluminum-base systems.

Oxidation of Trialuminides

The trialuminide compounds, particularly those based on $CbAl_3$ or $TiAl_3$, were the principal candidates for use as an outer primary oxygen diffusion barrier. Early efforts (Ref. 10-12) showed that $CbAl_3$ was a promising protective coating material for columbium. At temperatures above 2000 F, this compound is moderately oxidation-resistant, forming a scale that is predominantly Al_2O_3. At lower temperatures, or during slow thermal cycling, the compound undergoes rapid catastrophic attack. This effect can be mitigated and high-temperature oxidation further improved through alloying of $CbAl_3$ with titanium, chromium, or silicon (Ref. 12).

A series of compositions was prepared for oxidation testing at 2200 and 2500 F. These included $CbAl_3$, $TiAl_3$, VAl_3, and ternary compositions in which titanium, vanadium, chromium, molybdenum, and tantalum were substituted for columbium. Thirty-gram buttons were prepared by nonconsumable electrode arc melting and subsequently homogenized in vacuum at 2500 F for one hour. Small rectangular test specimens, weighing two to four grams, were oxidized in static air for up to 40 hours, with interrupted weighings at 1/6, 1/2, 1, 4, and 12 hours. The specimens were contained in recrystallized alumina support trays to minimize interaction during oxidation exposure.

Tables XXIII and XXIV present the results for the selected temperatures of 2200 and 2500 F. Preliminary work with VAl_3 showed a weight gain of 29 percent in 40 hours at 2200 F and 21 percent in four hours at 2500 F, and showed further that with more than 10 molecular percent VAl_3 in $CbAl_3$, the oxidation rate remained high. Therefore, only $TiAl_3$ and $CbAl_3$ were continued for study under the more detailed conditions used for the data presented. The titanium aluminide performed better than columbium aluminide which spalled. Ternary columbium-containing compositions showed that this problem could be circumvented by alloying.

TABLE XXIII

OXIDATION DATA FOR TRIALUMINIDE COMPOUNDS EXPOSED AT 2200 F

Nominal Composition		Weight Gain (mg/cm^2)						
(wt %)	(at. %)	1/6 hour	1/2 hour	1 hour	4 hours	12 hours	28 hours	40 hours
Ti-63Al	$TiAl_3$	1.2	1.3	2.0	4.1	(1)	-	-
Cb-46Al	$CbAl_3$	0.7	1.7	0.5(2)	1.0(2)	18(2)	-	-
Cb-6.5Cr-47.5Al	$(Cb_{0.8}Cr_{0.2})Al_3$	1.3	2.0	2.9	4.7	-	8.9	10.9
Cb-6Mo-46Al	$(Cb_{0.9}Mo_{0.1})Al_3$	0.5	0.5	0.5	0.5	-	1.5	1.7
Cb-11Mo-46Al	$(Cb_{0.8}Mo_{0.2})Al_3$	0.6	0.8	1.2	1.6	-	2.9	3.5
Cb-10Ta-44Al	$(Cb_{0.9}Ta_{0.1})Al_3$	0.1	0.4	0.7	1.0	-	2.1	2.6
Cb-19Ta-42Al	$(Cb_{0.8}Ta_{0.2})Al_3$	0.1	0.3	0.7	1.2	-	2.9	3.1

1. Specimen fractured during cooling.
2. Scale spalled.

TABLE XXIV

OXIDATION DATA FOR TRIALUMINIDE COMPOUNDS EXPOSED AT 2500 F

Nominal Composition		Weight Gain (mg/cm^2)					
(wt %)	(at. %)	1/6 hour	1/2 hour	1 hour	4 hours	12 hours	40 hours
Ti-63Al	$TiAl_3$	0.8	1.6	1.7	2.2	7.0	16.3
Cb-46Al	$CbAl_3$	1.4	2.6	2.0	1.8(2)	8.8	(1)
Cb-6.5Cr-47.5Al	$(Cb_{0.8}Cr_{0.2})Al_3$	2.2	5.5	8.0	13.1	18.5	27.6
Cb-6Mo-46Al	$(Cb_{0.9}Mo_{0.1})Al_3$	0.9	1.7	1.8	2.7	3.5(1)	4.8
Cb-11Mo-46Al	$(Cb_{0.8}Mo_{0.2})Al_3$	1.2	1.6	1.9	2.4(2)	3.9	-
Cb-10Ta-44Al	$(Cb_{0.9}Ta_{0.1})Al_3$	0.5	1.2	1.7	3.0	4.7	11.6
Cb-19Ta-42Al	$(Cb_{0.8}Ta_{0.2})Al_3$	0.6	2.0	2.7	5.3	7.3	18.0

1. Specimen fractured during cooling.
2. Scale spalled.

Of the ternary compounds $(Cb_{0.3}Ti_{0.7})Al_3$ and $(Cb_{0.65}Ti_{0.35})Al_3$, the titanium-rich compound showed oxidation resistance comparable to that of the binary trialuminides. The composition $(Cb_{0.65}Ti_{0.35})Al_3$, however, showed markedly improved oxidation resistance at both temperatures. The substitution of chromium for columbium had no marked effect on oxidation behavior at either temperature. The substitution of molybdenum or tantalum for columbium had a pronounced beneficial effect on oxidation behavior at 2200 F (Table XXIII). This effect was also apparent at 2500 F (Table XXIV). At the higher temperature, the oxidation rates for the molybdenum-containing compounds were lower than those in which tantalum was substituted for columbium.

Low-temperature oxidation behavior was studied at 1600 F for selected compositions; specimens were exposed for 24 and 90 hours. Weight gain data are presented in Table XXV. The $CbAl_3$ aluminide and the compositions in which tantalum was substituted for columbium underwent a pest-type attack during the initial 24-hour exposure. The remaining materials showed relatively minor weight gains and developed only a light oxide film during this exposure. During the 90-hour exposure, the titanium-containing ternary compound and $(Cb_{0.8}Mo_{0.2})Al_3$ underwent pest-type attack. The $TiAl_3$ specimen was intact after 90 hours; however, the edges were somewhat cracked. The lower molybdenum- and chromium-containing compounds showed no evidence of pest-type attack.

TABLE XXV

OXIDATION DATA FOR SELECTED TRIALUMINIDE COMPOUNDS EXPOSED AT 1600 F

Nominal Composition		Weight Gain (mg/cm^2)		
(at. %)	(wt. %)	24 hours	90 hours	Remarks
$TiAl_3$	Ti-63Al	0.23	0.93	
$CbAl_3$	Cb-46Al	0.71	-	Powdered
$(Ti_{0.35}Cb_{0.65})Al_3$	Ti-39Cb-51Al	0.40	3.74	Powdered
$(Cb_{0.9}Cr_{0.1})Al_3$	Cb-3Cr-47Al	0.58	1.45	
$(Cb_{0.8}Cr_{0.2})Al_3$	Cb-6.5Cr-48.5Al	0.42	1.14	
$(Cb_{0.9}Mo_{0.1})Al_3$	Cb-6Mo-46Al	0.37	2.01	
$(Cb_{0.8}Mo_{0.2})Al_3$	Cb-11Mo-46Al	0.47	5.43	Powdered
$(Cb_{0.9}Ta_{0.1})Al_3$	Cb-10Ta-44Al	0.79	-	Powdered
$(Cb_{0.8}Ta_{0.2})Al_3$	Cb-19Ta-45Al	3.31	-	Powdered

Further effort was concentrated on the study of compounds in the (Cb, Ti, Mo)Al_3 system. A series of compositions was prepared and oxidation studies were performed at 1600 and 2400 F. The results are summarized in Table XXVI and XXVII.

At 1600 F only $CbAl_3$ was observed to undergo pest-type oxidation during a 24-hour exposure. The other compounds developed thin blue or tan oxide films and showed weight gains of less than 1 mg/cm^2 during the same exposure period. Both $(Ti_{0.35}, Cb_{0.65})Al_3$ and $(Cb_{0.8}, Mo_{0.2})Al_3$ exhibited pest-type attack during a total exposure of 90 hours. At 2400 F, relatively low oxidation rates were observed in all of the complex compounds that were studied. The lowest rates occurred in the (Ti, Mo)Al_3 and (Ti, Cb)Al_3 series. Additions of approximately 0.3 and 1.5 atomic percent silicon were made to the compound $(Ti_{0.9}, Mo_{0.1})Al_3$; however, no significant influence on 2400 F oxidation behavior was observed.

TABLE XXVI

OXIDATION DATA FOR (Cb-Ti-Mo)Al_3 COMPOUNDS EXPOSED AT 1600 F

Nominal Composition		Weight Gain (mg/cm^2)				
(at. %)	(wt %)	1 hour	4 hours	16 hours	24 hours	90 hours
$TiAl_3$	Ti-63Al	-	-	-	0.23	0.[illegible]
$CbAl_3$	Cb-46Al	-	-	-	0.7[illegible](1)	-
$(Ti_{0.35}, Cb_{0.65})Al_3$	Ti-39Cb-51Al	-	-	-	0.40	3.74(1)
$(Ti_{0.9}, Mo_{0.1})Al_3$	Ti-7.2Mo-60.6Al	0.06	0.25	0.54	0.80	-
$(Ti_{0.8}, Mo_{0.2})Al_3$	Ti-13.9Mo-58.5Al	0.09	0.35	0.45	0.55	-
$(Cb_{0.9}, Mo_{0.1})Al_3$	Cb-6Mo-46Al	-	-	-	0.37	2.01
$(Cb_{0.8}, Mo_{0.2})Al_3$	Cb-11Mo-46Al	-	-	-	0.47	5.43(1)

1. Specimens were converted to powder.

TABLE XXVII

OXIDATION DATA FOR (Cb-Ti-Mo)Al_3 COMPOUNDS EXPOSED AT 2400 F

Nominal Composition		Weight Gain (mg/cm^2)		
(at. %)	(wt %)	1 hour	4 hours	16 hours
$TiAl_3$	Ti-63Al	0.35	1.05	2.95
$CbAl_3$	Cb-46Al	0.45	1.45	3.85
$(Ti_{0.35}, Cb_{0.65})Al_3$	Ti-39Cb-51Al	0.21	0.37	0.85
$(Ti_{0.9}, Mo_{0.1})Al_3$	Ti-7.2Mo-60.6Al	0.7[illegible]	0.63	1.[illegible]
$(Ti_{0.8}, Mo_{0.2})Al_3$	Ti-13.9Mo-58.5Al	0.40	0.60	0.77
$(Cb_{0.9}, Mo_{0.1})Al_3$	Cb-6Mo-46Al	0.35	0.65	1.65
$(Cb_{0.9}, Mo_{0.2})Al_3$	Cb-11Mo-46Al	0.60	0.95	1.95

Oxidation of Gamma Titanium Aluminide

The gamma phase, TiAl, is a reasonably oxidation-resistant compound which borders on being ductile. The addition of columbium, which is soluble to the extent of 18 atomic percent when replacing titanium, makes the compound fabricable and has a markedly beneficial effect on toughness and oxidation resistance (Ref. 13). Since many of the Group IV to VI transition metals were expected to be reasonably soluble in the gamma phase, the use of this material as a protective coating system for columbium appeared quite attractive. The gamma phase could be considered a candidate for use either as a ductile sublayer beneath a trialuminide layer or as an outer primary reservoir coating.

Initial effort was concentrated on a study of the oxidation behavior of selected gamma compositions. Experimental materials were prepared in the same way as the trialuminide compounds, and oxidation tests were performed in a similar manner at 2200 and 2500 F.

The gamma alloys that were oxidation tested included the binary compounds TiAl and $Ti_{0.45}Al_{0.55}$ in addition to ternary compositions based on 50 atomic percent aluminum in which zirconium, hafnium, vanadium, columbium, tantalum, chromium, molybdenum, and tungsten substitutions were made for titanium. In general, it was found that zirconium, hafnium, and vanadium had an adverse effect on the oxidation

behavior of gamma alloys at both 2200 and 2500 F. Tungsten additions decreased oxidation rates significantly at both temperatures for short-time exposures. After four hours at 2200 F and less than one hour at 2500 F, the tungsten-containing compounds showed rapid accelerated oxidation. This behavior was associated with segregation of tungsten in the alloys. The remaining substitution elements all decreased the oxidation rate of the gamma alloys. Oxidation data for 2200 and 2500 F exposures are summarized in Tables XXVIII and XXIX, respectively.

The compound TiAl (Ti-36 wt % Al) showed poor oxidation resistance compared to that of the solid-solution compositions Cb-10Al-50Ti and Cb-10Al-60Ti, described in the following sections, at both 2200 and 2500 F. A tan, porous scale developed on the alloys which cracked during growth and spalled upon cooling. Oxygen contamination occurred beneath the scale layers as was evidenced by an increase in hardness and by the development of a two-phase metallic microstructure throughout the specimen. An increase to 55 atomic percent (Ti-41 wt % Al) in the aluminum content of the gamma alloys resulted in a marked improvement in oxidation resistance and the apparent absence of subscale contamination. Similarly, the substitution of columbium, tantalum, chromium, molybdenum, or tungsten for titanium in the γ-TiAl composition produced a marked improvement. The most pronounced effect was at 2200 F; at this temperature, chromium and tantalum additions are the most beneficial. Gamma alloys in which molybdenum substitutions were made showed low oxidation rates after short-exposure time but, as in the case of tungsten, after increased exposure oxidation became more rapid. The scale formed on the chromium and tantalum-containing alloys was adherent, and oxidation appeared to be parabolic for the exposure time investigated. The hardnesses of the molybdenum- and tantalum-containing alloys after exposure were lower than the initial annealed hardness values. The compound $(Ti_{0.8}Cr_{0.2})Al$ showed an increase in hardness from 375 DPN in the annealed condition to 510 DPN after oxidation exposure at 2200 F for 42 hours. Columbium substitutions for titanium decreased the oxidation rate of gamma alloys; however, their influence was not as significant as that noted for the other elements. In general, it was found that increased substitution of columbium, tantalum, chromium, or molybdenum for titanium resulted in increased oxidation resistance of the gamma phase.

At 2500 F the same general trends were noted; the columbium- and tantalum-modified gamma compositions scaled at a considerably more rapid rate than at 2200 F. The chromium- and molybdenum-modified compositions scaled at rates comparable to

TABLE XXVIII

OXIDATION DATA FOR SELECTED GAMMA COMPOSITIONS EXPOSED AT 2200 F

Nominal Composition		Microhardness (DPN)		Weight Gain (mg/cm^2)					
(wt %)	(at. %)	Annealed	Final	1/6 hour	1/2 hour	1 hour	4 hours	12 hours	48 hours
Ti-35.5Al	TiAl	236	335	-1.6	-6.2	-14.6	-36.3	-67.5	-
Ti-41.0Al	$Ti_{0.45}Al_{0.55}$	297	281	9.72	-2.0	- 7.9	-19.7	-	-
Ti-34Al-12Cb	$(Ti_{0.9}Cb_{0.1})Al$	265	220	1.7	2.9	6.6	-14.5	-29.0	-45.0
Ti-32Al-23Cb	$(Ti_{0.8}Cb_{0.2})Al$	545	260	1.0	-2.6	- 4.8	-10.7	-23.5	-72.0
Ti-30Al-37Cb	$(Ti_{0.67}Cb_{0.33})Al$	500	399	1.5	2.1	2.1	1.8	- 1.5	12.3
Ti-30Al-20Ta	$(Ti_{0.9}Ta_{0.1})Al$	230	255	1.3	1.8	- 1.2	- 7.7	-18.1	-40.0
Ti-26Al-35Ta	$(Ti_{0.8}Ta_{0.2})Al$	277	250	0.4	0.8	1.8	1.8	2.2	-
Ti-30Al-12Mo	$(Ti_{0.9}Mo_{0.1})Al$	400	400	-0.5	-0.6	- 0.8	+ 6.3[1]		
Ti-32Al-23Mo	$(Ti_{0.8}Mo_{0.2})Al$	580	506	0.6	1.1	0.9	- 0.2	- 4.5	-15.3
Ti-33Al-7Cr	$(Ti_{0.9}Cr_{0.1})Al$	375	375	0.5	2.1	2.6	3.5	11.5	-
Ti-36Al-13Cr	$(Ti_{0.8}Cr_{0.2})Al$	375	510	0.3	1.6	1.2	1.4	2.3	2.3

1. Evidence of molybdenum segregation.

TABLE XXIX

OXIDATION DATA FOR SELECTED GAMMA COMPOSITIONS EXPOSED AT 2500 F

Nominal Composition		Microhardness (DPN)		Weight Gain (mg/cm^2)				
(wt %)	(at. %)	Annealed	Final	1/6 hour	1/2 hour	1 hour	4 hours	12 hours
Ti-35.5Al	TiAl	226	504	-3.6	-23.0	-55.1	-127.0	
Ti-41.0Al	$Ti_{0.45}Al_{0.55}$	297	350	-3.5	-11.3	-15.1		
Ti-34Al-12Cb	$(Ti_{0.9}Cb_{0.1})Al$	265	410	-6.1	-16.3	-32.0	- 38.0	-107.0
Ti-32Al-23Cb	$(Ti_{0.8}Cb_{0.2})Al$	545	380	-4.9	- 9.9	-25.0	-	
Ti-30Al-37Cb	$(Ti_{0.67}Cb_{0.33})Al$	500	400	3.8	21.0	- 3.1[1]	- 7.1	- 14.7
Ti-30Al-20Ta	$(Ti_{0.9}Ta_{0.1})Al$	230	420	-1.3	- 2.7	-11.9	- 39.8	-122.0
Ti-26Al-35Ta	$(Ti_{0.8}Ta_{0.2})Al$	277	515	-2.2	- 3.5	-10.7	- 35.9	- 71.5
Ti-30Al-12Mo	$(Ti_{0.9}Mo_{0.1})Al$	400	-	0.6	- 3.0	- 7.5		
Ti-32Al-23Mo	$(Ti_{0.8}Mo_{0.2})Al$	580	600	1.2	- 1.1	- 0.7	- 2.6	
Ti-36Al-7Cr	$(Ti_{0.9}Cr_{0.1})Al$	375	670	1.4	-	1.9	6.6[1]	7.7
Ti-36Al-13Cr	$(Ti_{0.8}Cr_{0.2})Al$	375	630	1.3	-	3.9	6.6[2]	

1. Scale spalled.
2. Alloy partially molten

those at the lower temperatures for exposures of four hours or less. The hardness of these materials, however, was considerably higher after the 2500 F oxidation exposure. The composition $(Ti_{0.8}Cr_{0.2})Al$ is partially molten at 2500 F.

The low temperature oxidation behavior of the more promising materials was checked by exposing specimens at 1600 F for 24 and 90 hours. An adherent scale developed, and very low weight gains were measured. The oxidation data appear in Table XXX. All of the specimens had sharp edges and corners after the 90-hour exposure.

TABLE XXX

OXIDATION DATA FOR SELECTED GAMMA ALLOYS EXPOSED AT 1600 F

Nominal Composition		Weight Gain (mg/cm^2)	
(at. %)	(wt %)	24 hours	90 hours
$(Ti_{0.9}, Ta_{0.1})Al$	Ti-20.5Ta-30.6Al	0.21	0.42
$(Ti_{0.8}, Ta_{0.2})Al$	Ti-35.7Ta-26.6Al	0.25	0.98
$(Ti_{0.9}, Mo_{0.1})Al$	Ti-12.0Mo-33.9Al	0.15	0.59
$(Ti_{0.8}, Mo_{0.2})Al$	Ti-22.7Mo-31.9Al	0.16	0.16
$(Ti_{0.9}, Cr_{0.1})Al$	Ti-6.9Cr-35.8Al	0.17	0.67
$(Ti_{0.8}, Cr_{0.2})Al$	Ti-13.7Cr-35.6Al	0.08	0.92

The influence of increased aluminum content on the 2500 F oxidation behavior of selected gamma alloys was investigated. Oxidation data are presented in Table XXXI. The ternary alloys containing 55 atomic percent aluminum, in general, formed adherent scales resulting in a positive weight gain under the test conditions employed. The columbium-modified gamma compositions containing 55 atomic percent aluminum oxidized at a rate comparable to the alloys containing 50 atomic percent aluminum, with the exception that an adherent scale was formed on the higher aluminum materials. The increased aluminum content produced an improvement in the oxidation behavior of the tantalum-, chromium-, and molybdenum-modified gamma alloys.

TABLE XXXI

OXIDATION DATA FOR SELECTED GAMMA ALLOYS EXPOSED AT 2500 F

Nominal Composition		Weight Gain (mg/cm^2)				
(at. %)	(wt %)	1/6 hour	1/2 hour	1 hour	4 hours	12 hours
TiAl	Ti-36Al	-3.6	-23.0	-55.1	-127.0	---
$Ti_{0.45}Al_{0.55}$	Ti-41Al	-3.5	-11.3	-15.1	---	---
$(Ti_{0.9}, Cb_{0.1})Al$	Ti-12Cb-34Al	-6.1	-16.3	-32.0	- 36.0	-107.0
$(Ti_{0.8}, Cb_{0.2})Al$	Ti-23Cb-32Al	-4.0	- 9.9	-25.0	---	---
$(Ti_{0.9}, Cb_{0.1})_{0.45}Al_{0.55}$	Ti-12Cb-43Al	9.6	14.0	18.6	32.8	---
$(Ti_{0.8}, Cb_{0.2})_{0.45}Al_{0.55}$	Ti-37Cb-36Al	7.7	14.3	22.0	44.0	---
$(Ti_{0.9}Ta_{0.1})Al$	Ti-20Ta-30Al	-1.3	- 2.7	-11.9	- 39.8	-122.0
$(Ti_{0.8}Ta_{0.2})Al$	Ti-35Ta-26Al	-2.2	- 3.5	-10.7	- 25.9	- 71.5
$(Ti_{0.8}Ta_{0.2})_{0.45}Al_{0.55}$	Ti-41Ta-34Al	3.5	4.9	6.1	8.5	12.8
$(Ti_{0.9}Mo_{0.1})Al$	Ti-12Mo-34Al	0.6	- 3.0	- 7.5	---	---
$(Ti_{0.8}Mo_{0.2})Al$	Ti-23Mo-32Al	1.2	- 1.1	0.7	- 2.6	---
$(Ti_{0.9}Mo_{0.1})_{0.45}Al_{0.55}$	Ti-12Mo-38Al	1.2	1.8	2.5	4.4	---
$(Ti_{0.8}Mo_{0.2})_{0.45}Al_{0.55}$	Ti-21Mo-36Al	0.64	0.83	1.03	1.30	1.23
$(Ti_{0.9}Cr_{0.1})Al$	Ti-7Cr-36Al	1.4	---	1.9	0.4	7.7
$(Ti_{0.8}Cr_{0.2})Al$	Ti-13Cr-36Al	1.3(1)	---	3.0	6.0	---
$(Ti_{0.9}Cr_{0.1})_{0.45}Al_{0.55}$	Ti-6Cr-41Al	0.86	0.73	1.76	3.2	6.6
$(Ti_{0.8}Cr_{0.2})_{0.45}Al_{0.55}$	Ti-13Cr-40Al	1.9(1)	3.3	5.2	9.2	---

1. Alloy partially molten.

The most oxidation-resistant compositions were those in which molybdenum was substituted for titanium. The microstructure of these alloys after oxidation exposure are shown in Figures 48 and 49. The $(Ti_{0.9}, Mo_{0.1})_{0.45}Al_{0.55}$ alloy (Fig. 48) contained a small quantity of transformation product throughout the microstructure. Small, nodular oxide particles existed near the surface which were the apparent result of internal oxidation. A hardness gradient extended from the surface to a depth of 0.004 inch ranging from 466 DPH to 362 DPH, the hardness of the core. The $(Ti_{0.8}, Mo_{0.2})_{0.45}Al_{0.55}$ alloy was two phase (Fig. 49). Transformation as a result of the oxidation reaction was apparent to a depth of approximately 0.010 inch from the surface. No hardness difference was detectable between this layer and the core.

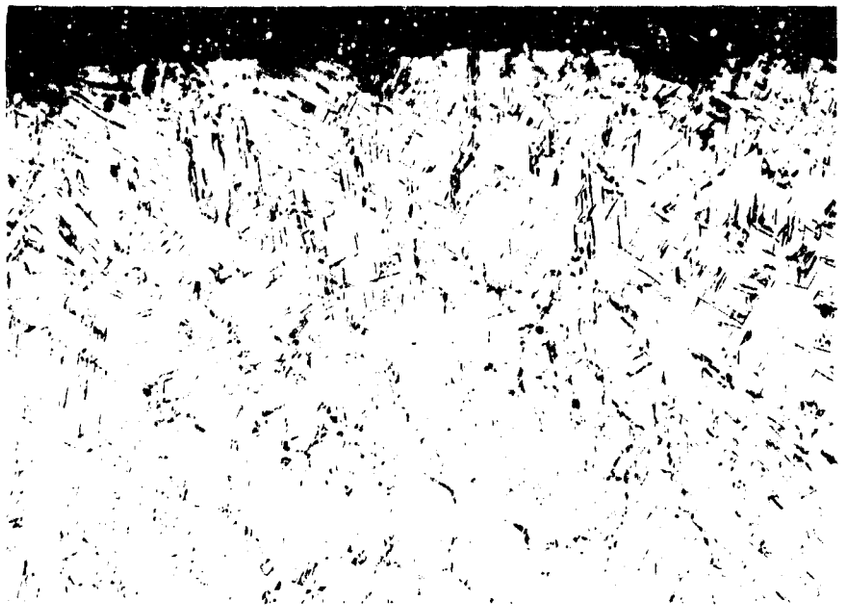

Magnification: 100X

FIGURE 48. MICROSTRUCTURE OF $(Ti_{0.9}, Mo_{0.1})_{0.45}, Al_{0.55}$ ALLOY OXIDIZED 12 HOURS AT 2500 F

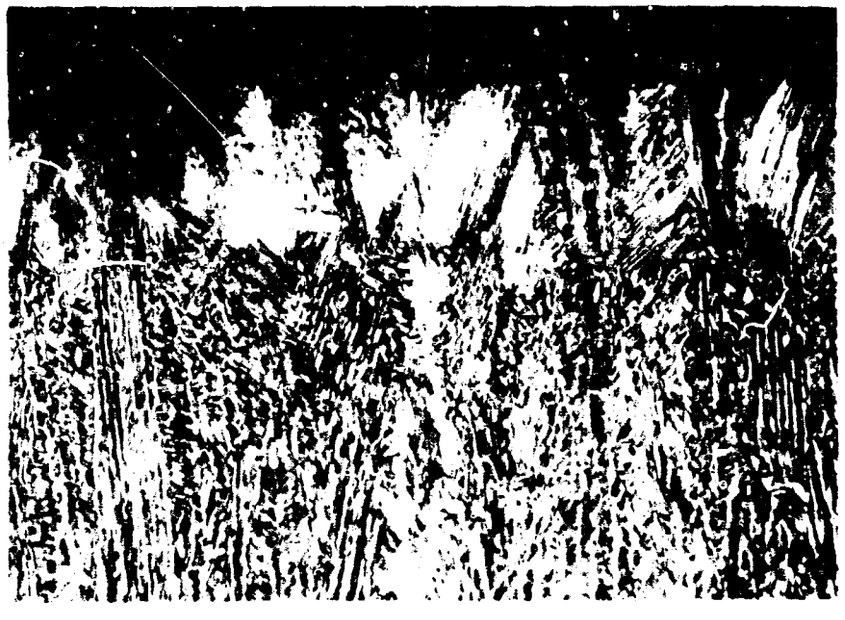

Magnification: 100X

FIGURE 49. MICROSTRUCTURE OF $(Ti_{0.8}, Mo_{0.2})_{0.45}Al_{0.55}$ ALLOY OXIDIZED 12 HOURS AT 2500 F

The low chromium-containing alloy showed microscopic evidence of a grain-boundary melting during oxidation exposure. The quantity of melt was not sufficient to cause the specimen to deform during exposure as was the case with the higher chromium compounds.

In view of the low melting point of the chromium-modified gamma compositions, the molybdenum- or tantalum-modified alloys were of greatest interest to this program. Consequently, the oxidation behavior of these materials was studied in greater detail. As an initial step, the influence of minor additions of silicon to the $(Ti_{0.9}, Mo_{0.1})Al$ alloy was investigated. Additions of approximately 0.3 and 1.5 atomic percent silicon were made as a proportional substitution for each of the elements in the base alloy. At 2500 F the silicon additions decreased the oxidation rate of the alloy, the larger addition being more beneficial.

Alloys of the following compositions were prepared as 100-gram melts by nonconsumable electrode arc melting.

Nominal Composition (at. %)	(wt %)
$(Ti_{0.8}, Cb_{0.1}, Mo_{0.1})Al$	Ti-11Cb-11.4Mo-32Al
$(Ti_{0.7}, Cb_{0.15}, Mo_{0.15})Al$	Ti-15.7Cb-15.2Mo-30.4Al
$(Ti_{0.7}, Cb_{0.2}, Mo_{0.1})Al$	Ti-21Cb-10.8Mo-30.4Al
$(Ti_{0.7}, Cb_{0.1}, Mo_{0.2})Al$	Ti-10.4Cb-20.6Mo-30.3Al
$(Ti_{0.8}, Cb_{0.15}, Mo_{0.05})Al$	Ti-16.1Cb-5.6Mo-31.2Al

These alloys were homogenized for four hours at 2500 F in vacuum at 10^{-5} Torr, and sectioned to produce oxidation test specimens. Specimens were oxidized at 1600 and 2400 F for 1, 4, and 16 hours. The results are summarized in Table XXXII. Individual specimens were used for each exposure. The only specimens in which spalling of the scale occurred were from the compound $(Ti_{0.8}, Cb_{0.15}, Mo_{0.05})Al$ run at 2400 F. All of the loose scale was weighed along with the specimens. Except for the low molybdenum-containing compound, very low weight gains were recorded at both 1600 and 2400 F. The edges of all specimens were sharp at both temperatures, and no evidence of pest attack was observed at the lower temperature.

TABLE XXXII

OXIDATION DATA FOR GAMMA ALLOYS

Nominal Composition		Weight Gain (mg/cm^2)					
		1600 F			2400 F		
(At. %)	(wt %)	1 hour	4 hours	16 hours	1 hour	4 hours	16 hours
$(Ti_{0.8}, Cb_{0.1}, Mo_{0.1})Al$	Ti-11Cb-11.4Mo-32Al	0.31	0.50	3.7	0.90	1.2	1.9
$(Ti_{0.7}, Cb_{0.15}, Mo_{0.15})Al$	Ti-15.7Cb-16.2Mo-30.4Al	1.2	1.1	0.50	0.54	1.2	1.3
$(Ti_{0.7}, Cb_{0.2}, Mo_{0.1})Al$	Ti-21Cb-10.6Mo-30.4Al	0.28	1.0	0.11	0.71	1.0	1.9
$(Ti_{0.7}, Cb_{0.1}, Mo_{0.2})Al$	Ti-10.4Cb-20.6Mo-30.3Al	0.89	0.72	7.6	1.4	1.5	1.4
$(Ti_{0.8}, Cb_{0.15}, Mo_{0.05})Al$	Ti-16.1Cb-5.6Mo-31.2Al	0.07	0.40	2.1	3.3	9.3	14.5

At 1600 F all of the specimens developed a thin blue adherent film. The scale developed at 2400 F was brown for all compositions except $(Ti_{0.8}, Cb_{0.15}, Mo_{0.05})Al$ which developed a tan scale similar to that formed on the (Ti-Cb)Al compounds studied previously. It appeared that concentrations of both columbium and molybdenum in excess of 10 percent, substituted for titanium, were necessary to obtain the greatest oxidation resistance.

Oxidation of Aluminum-Containing Columbium Alloy Sublayers

This work is reported here rather than under the general evaluation of sublayers (par. 3.2), because of the following reasons:

- Work refers to compositions that will be in contact with the gamma phase or trialuminides discussed earlier.
- Work was performed as part of the above investigation by IITRI, whereas all work in Paragraph 3.2 was performed at Solar.
- It was performed as part of a study of the MAl_3-MAl-M system, and not as part of a search for a more oxidation-resistant sublayer.

An outer reservoir layer of gamma or trialuminide would be expected to be in steady-state equilibrium with a columbium-base solid solution in a multilayer coating system. Consequently, the oxidation behavior of ternary columbium-base solid solutions containing aluminum was determined at 2200 and 2500 F. The solubility of aluminum in columbium was initially established to be between four and six weight percent at these temperatures on the basis of annealing and quenching studies. A fixed aluminum

content of four weight percent was selected to represent the near-saturation concentration for most of the ternary alloys studied. Since titanium was a major alloying element to be considered in these coatings, a wide range of Cb-Al-Ti compositions was evaluated. The alloys having higher titanium contents contained increased quantities of aluminum, since titanium increases the solubility of aluminum in columbium.

The alloys were prepared as 30-gram melts by nonconsumable tungsten-electrode arc melting, and were homogenized at 2500 F for one hour in a vacuum of less than 10^{-5} millimeters of mercury before sectioning to produce oxidation test specimens. Metallographic inspection and microhardness measurements were made after this treatment; all of the alloys were found to be single phase. Oxidation studies were performed in the manner previously described. The results of oxidation tests are summarized in Tables XXXIII and XXXIV.

All of the specimens formed a bulky, white or gray porous outer scale that spalled during cooling. Adherent subscale layers were formed on many of the alloys, and a solid-solution oxygen contamination zone was observed that extended throughout the specimens in most cases.

TABLE XXXIII

SUMMARY OF OXIDATION DATA FOR Cb-Al BASE SOLID-SOLUTION ALLOYS EXPOSED AT 2200 F

Nominal Composition	Microhardness (DPN)		Weight Change (mg/cm^2)					
(wt %)	Original	Final	1/6 hour	1/2 hour	1 hour	4 hours	15 hours	40 hours
Cb-4Al	690	---	-12.0	-34.5	-66.5	-279.0	---	---
Cb-4Al-5V	310	850	- 2.2	-18.3	-37.0	-115.0	-260.0	---
Cb-4Al-15V	410	---	-54.6	---	---	---	---	---
Cb-4Al-5Ta	295	---	- 5.2	-23.5	-45.9	-208.0	---	---
Cb-4Al-5Mo	325	630	- 5.4	-14.0	-37.2	-110.0	-267.0	---
Cb-4Al-5W	305	593	- 9.3	-31.0	-57.6	-143.0	-321.0	---
Cb-4Al-5Ti	347	358	- 0.5	- 8.4	-20.3	- 74.0	-178.0	---
Cb-4Al-5Zr	310	695	- 5.5	-25.6	-54.8	-268.0	-630.0	---
Cb-4Al-5Hf	300	330	- 3.2	-25.0	-56.8	-223.0	-603.0	---
Cb-4Al-5Cr	520	480	- 8.3	-17.7	-40.0	-140.0	---	---
Cb-7Al-10Ti	969	956	- 2.9	-16.8	-31.6	- 63.0	-154.0	-344.0
Cb-5Al-20Ti	297	393	- 6.0	-22.3	-39.3	- 86.0	---	---
Cb-8Al-30Ti	297	1097	1.7	- 2.6	-10.5	- 28.0	- 69.0	-256.0
Cb-10Al-50Ti	426	678	- 1.1	0.2	- 4.1	- 4.4	- 19.0	- 44.5
Cb-5Al-40Ti	254	536	- 1.8	- 4.4	- 9.4	- 26.0	- 78.9	-307.0
Cb-10Al-60Ti	466	742	- 0.3	- 2.9	- 5.7	- 12.1	- 21.6	- 45.9

TABLE XXXIV

SUMMARY OF OXIDATION DATA FOR Cb-Al BASE SOLID-SOLUTION ALLOYS EXPOSED AT 2500 F

Nominal Composition	Microhardness (DPN)		Weight Gain (mg/cm^2)				
(wt %)	Original	Final	1/6 hour	1/2 hour	1 hour	4 hours	12 hours
Unalloyed Cb	---	---	-113.0	-284.0			
Cb-4Al	290	---	- 18.8	- 70.3	-144.0	-276.0	---
Cb-4Al-5V	310	900	- 8.88	- 40.6	---	---	---
Cb-4Al-15V	410	---	- 73.7	---	---	---	---
Cb-4Al-5Ta	295	540	- 19.7	- 61.0	-109.0	-347.0	---
Cb-4Al-5Mo	325	---	- 40.2	- 79.7	-185.0	---	---
Cb-4Al-5W	305	700	- 25.7	- 70.2	-116.0	-327.0	---
Cb-4Al-5Ti	347	690	- 8.0	- 34.0	- 58.6	-292.0	---
Cb-4Al-5Zr	310	---	- 57.5	-176.0	-317.0	---	---
Cb-4Al-5Hf	300	575	- 44.2	-116.0	-199.0	-590.0	---
Cb-4Al-5Cr	520	910	0.84	- 20.2	- 55.9	-281.0	---
Cb-7Al-10Ti	969	885	- 9.69	- 27.9	- 44.6	-105.0	---
Cb-5Al-20Ti	297	530	- 5.94	- 11.3	- 31.3	---	---
Cb-8Al-30Ti	297	614	0.33	- 2.49	- 18.9	- 47.3	-141.0
Cb-10Al-50Ti	426	993	- 1.80	- 0.88	- 0.71	- 27.3	- 59.8
Cb-5Al-40Ti	264	780	- 1.55	- 4.69	- 16.9	- 36.3	-100.0
Cb-10Al-60Ti	465	1051	- 2.46	- 10.8	- 19.4	- 36.5	- 74.3

Ternary solid solution alloys based on Cb-4 wt % Al, containing five weight percent additions of titanium, zirconium, hafnium, vanadium, tantalum, chromium, molybdenum, and tungsten were evaluated. At 2200 F the Cb-4Al-5Ti alloy was the most oxidation resistant as determined by weight loss after scale spalling or removal. The alloys containing chromium, molybdenum, tungsten, and vanadium were more oxidation resistant than the binary Cb-4Al composition. However, an increase in vanadium content from 5 to 15 weight percent resulted in catastrophic oxidation, which was associated with the formation of a very fluid scale. The alloys containing tantalum, zirconium, and hafnium showed oxidation behavior comparable to the binary alloy. At 2500 F a similar trend in oxidation behavior was noted, with the exception that chromium appeared to be as beneficial an alloying addition as titanium in decreasing scaling rates at the higher temperature.

Solid solution alloys in the Cb-Al-Ti system, containing up to 60 weight percent titanium and 10 weight percent aluminum were studied. Increases in either the aluminum or titanium content resulted in a decrease in oxidation rate at both 2200 and 2500 F. The alloys, Cb-10Al-50Ti and Cb-10Al-60Ti, were comparable in oxidation resistance. The addition of molybdenum to these alloys was found to further decrease scaling rate. Since this system was of primary interest to the program, supplementary oxidation studies were performed on Cb-Ti-Al and Cb-Ti-Mo-Al alloys.

Individual specimens contained in recrystallized alumina trays were oxidized for 1, 4, and 16 hours at 2400 F in slowly moving air. The specimens and all scale that spalled during exposure or cooling were weighed. The weight gain data are presented in Table XXXV. Oxidation rates were parabolic and decreased with increased aluminum and titanium content. The addition of 10 weight percent molybdenum to selected Cb-Al-Ti compositions caused a further decrease in oxidation rate. The effect was most pronounced in the Cb-5Al-20Ti and Cb-5Al-40Ti alloys.

TABLE XXXV

WEIGHT GAIN DATA FOR Cb-Al BASE SOLID-SOLUTION ALLOYS EXPOSED AT 2400 F

Alloy Composition (wt %)	Weight Gain (mg/cm^2)		
	1 hour	4 hours	16 hours
Cb-4Al-5Ti	22.6	105.0	
Cb-4Al-5Mo	64.0	153.0	
Cb-5Al-20Ti	15.3	38.6	99.4
Cb-5Al-20Ti-10Mo	10.1	21.4	43.1
Cb-5Al-40Ti	4.55	11.2	31.5
Cb-5Al-40Ti-10Mo	2.65	5.60	11.4
Cb-8Al-30Ti	4.60	11.6	37.2
Cb-10Al-50Ti	3.35	6.40	14.2
Cb-10Al-50Ti-10Mo	2.85	5.85	12.1
Cb-10Al-60Ti	3.65	7.70	17.5

It was concluded that sublayers for use with the gamma phase or trialuminides studied earlier will have good intrinsic oxidation resistance, and will have oxidation resistance adequate to complete a mission in the event of failure of the primary oxidation barrier.

3.3.3 Thermal Expansion of Primary Barrier Compositions

On the analysis of the (Ti-Cr)-Si coating (par. 3.1.1), it was shown that the expansion coefficient of a typical disilicide representative of this coating was 60 percent higher than that of columbium alloy substrates. The effect of cooling is to cause thermal strains and cracking. These problems were discussed (par. 3.2) on sublayers where the case was made for an oxidation resistant sublayer, and, further, where a temperature of 1600 F was selected for oxidation studies of sublayers. This selection was based on certain assumptions with regard to cracking of the primary barrier on cooldown as a result of thermal strains.

The tensile stresses that will develop in the primary barrier of a coating on a columbium alloy can be approximated by the following relation:

$$S_c = E_c \epsilon_c = E_c (\alpha_c - \alpha_s) \Delta T$$

where, S_c is stress in primary barrier

E_c is the mean elastic modulus of primary barrier for the temperature range ΔT under consideration

ϵ_c is the strain in the primary barrier assuming the columbium substrate is massive and rigid

α_c and α_s are the coefficients of thermal expansion of the coating and substrate (columbium), respectively

ΔT is the difference of temperature over which primary barrier strains elastically

If E_c is assumed to be 30×10^6 psi and the interval ΔT = 1900 F, the stress in the (Ti-Cr)-Si coating would amount to 147,000 psi at room temperature. It is fully expected, therefore, that the coating will be craze cracked after thermal cycling.

The most important factor in the equation is $(\alpha_c - \alpha_s)$. Reference to Samsonov's Handbook of High-Temperature Materials shows that the elastic modulus term varies by a factor of less than two for several silicides with no data on aluminides. Much greater variation will come from the differential expansion coefficient term. Hence, measurement of expansivity is required to assess the magnitude of this cause

of defects. The work was oriented to lead to primary barrier compositions that would avoid cracking on thermal cycling.

Thermal Expansion of Disilicides

A large number of binary, ternary, and quaternary disilicides were prepared from the pseudo systems such as the pseudo binary $M'Si_2$ - $M''Si_2$. The silicides were prepared by mixing together the elemental materials and melting in a nonconsumable arc melter. The ingot formed was then crushed into powder and reconsolidated by cold pressing at 10,000 psi into a bar 0.25 inch square by 2.0 inches long followed by sintering for seven hours at 2200 F in gettered argon. The expansion of specimens was measured in the same equipment previously described for sublayers. All specimens were measured after dilatation to determine resisidual shrinkage. None was observed.

The test results for the disilicides are shown in Table XXXVI. The data are reported as either constant over the test range of room temperature to 1800 F or as a tangent to the expansion curve at 400 degrees and 1800 degrees F, if it was variable over this range. These data are quite interesting, in that they show that with rare exceptions the coefficients of expansion of disilicides are much higher than columbium alloy substrates. Only the simple binary silicides of molybdenum, tungsten, and columbium are near the expansion of the columbium alloys, with only the molybdenum and tungsten disilicides matching close enough so that stress cracks between the two materials would not be expected to occur. All silicides containing Ti-Cr or V-Cr showed extremely high expansions. Those containing the more refractory elements, molybdenum, tungsten, or columbium showed lower expansions. Ideally then, from an expansion standpoint alone, these elements should be maximized in coating systems.

Thermal Expansion of Trisilicides (M_5Si_3)

The M_5Si_3 silicides form a potential intermediate layer between the disilicides (MSi_2) and the sublayers. The significance of these silicides is that they may provide an intermediate expansion layer between the more protective disilicides and the sublayers. They may also form a crack stoppage layer if the stresses are minimized. The evaluation of the thermal expansion of the trisilicides was much more limited than the disilicides, since the significance of these materials is not well established. Also, as these silicides increase in amount in coatings, the resistance to oxidation usually but not always decreases.

TABLE XXXVI

THERMAL EXPANSION OF VARIOUS DISILICIDES (MSi_2)

Composition Number	Nominal Composition (at. %)	Coefficient of Expansion/ Degree F x 10^6		
		400 F	Constant	1800 F
1	18.7Ti-14.6Mo-66.7Si (A)		5.86	
2	24Ti-8Mo-68Si (N)		6.74	
3	8.7Ti-11.3Mo-10.6Cb-69.3Si (A)		5.68	
4	16.5Ti-6.5M-10Cb-68Si (N)		6.59	
5	20.9Ti-15.1W-64.0Si (A)		5.80	
6	24Ti-8W-68Si (N)		6.80	
7	9.6Ti-10.7W-4Cb-72.4Si (A)		5.74	
8	16.1Ti-4.7W-14.2Cb-65.1Si (A)		6.10	
9	16.7Ti-16.7Cr-66.6Si (A)	6.30		8.86
10	24Ti-8Cr-68Si (N)		8.02	
11	9.6Ti-23.3Cr-67.2Si (A)	6.78		8.84
12	14.2Ti-11.1Cr-10.4Cb-64.3Si (A)		6.95	
13	16.5Ti-5.5Cr-10Cb-68Si		7.14	
14	7.2Ti-14.9Cr-10.9Cb-67.0Si (A)	6.33		7.98
15	14.4V-17.7Cr-67.9Si (A)	6.47		7.75
16	8.3V-24.7Cr-67.0Si (A)	6.56		8.85
17	24.3V-7.7Cr-67.5Si (A)	6.08		7.70
18	10.1V-10.9Cr-9.8Cb-69.1Si (A)		6.83	
19	5.5V-17.0Cr-9.7Cb-67.8Si (A)	6.45		7.76
20	15.5V-9.5Cr-10.0Cb-65.0Si (A)		6.22	
21	14.2V-16.6Cb-69.1Si (A)		6.28	
25	31.7Mo-68.3Si (A)(2)		4.84	
26	30.5W-69.5Si (A)		4.66	
27	30.4V-69.6Si (A)		7.25	
28	33Cb-67Si (A)		5.37	
29	33Ti-67Si (N) (1)		7.72	
30	33Cr-67Si (N)	6.72		9.57

1. N - Nominal
2. A - Analyzed

The specimens for this study were prepared in a similar manner to the disilicides. The thermal expansion coefficients for the M_5Si_3 silicides evaluated are shown in Table XXXVII. Three of these results were unexpected:

- The thermal expansion of Ti_5Si_3 compositions were considerably lower than V_5Si_3 and Cr_5Si_3, which would not be expected from the data on the disilicides (Table XXXVI).
- The thermal expansion of Cb_5Si_3 was lower than Mo_5Si_3, which also indicates divergence from the disilicide data.

TABLE XXXVII

THERMAL EXPANSION OF VARIOUS TRISILICIDES (M_5Si_3)

Composition Number	Nominal Composition (at. %)	Coefficient of Expansion/ Degree F x 10^6		
		400 F	Constant	1800 F
31	62.5Ti-37.5Si	5.38		5.97
32	62.5Cr-37.5Si	7.3		8.97
33	62.5Cb-37.5Si	4.24		5.48
34	62.5V-37.5Si	5.85		7.57
35	62.5Mo-37.5Si	4.54		5.46
36	31.3Ti-31.3Cr-37.4Si	6.03		7.36
37	20.8Ti-20.8C 20.8Cb-37.6Si	5.64		6.92
38	31.3Ti-31.3Mo-37.4Si		5.61	
39	20.8Ti-20.8Mo-20.8Cb-37.6Si		5.22	
40	31.3V-31.3Cr-37.4Si	6.08		7.2
41	20.8V-20.8Cr-20.8Cb-37.6Si	5.75		6.47

The rate of expansion of all of the binary M_5Si_3 silicides showed rapid changes with temperature. With the binary disilicides, a constant expansion rate was noted over a range of 100 to 1800 F with the exception of $CrSi_2$. The thermal expansion data on the ternary and quaternary compositions follow essentially the trend that would be predicted from the rule of mixtures. That is, the composition containing molybdenum or molybdenum and columbium had lower expansion coefficients than compositions containing titanium and chromium or vanadium and chromium. Although no direct comparison of identical ratios of the various metals in the complex M_5Si_3 and MSi_2 silicides was possible, the M_5Si_3 compositions tended to exhibit the lower expansions as can be seen by comparison of the trisilicide and disilicide data.

Thermal Expansion of Aluminides

The thermal expansion behavior of several trialuminide compositions was determined between room temperature and 1800 F. The expansion measurements were made at Solar using previously described techniques. Specimens, approximately 0.25 inch square by 1.0 inch long, were prepared at IITRI by sectioning arc-melted homogenized ingots.

The coefficients of thermal expansion, determined from the slope of the expansion curve between approximately 800 and 1800 F, were:

Compound	Coefficient of Thermal Expansion in./in./degree F x 10^{-6}
$TiAl_3$	8.86
$(Ti_{0.5}, Cb_{0.5})Al_3$	7.74
$CbAl_3$	7.08
$(Cb_{0.9}, Cr_{0.1})Al_3$	7.2

The expansion value for $CbAl_3$, reported above, was obtained from Reference 12. The experimental value for $TiAl_3$ was somewhat high since there was evidence of free aluminum in the sample.

The results show that substitution of both chromium and titanium for columbium in $CbAl_3$ increase the expansivity of the compound. Unfortunately, the influence of molybdenum substitutions, which could be expected to decrease expansivity, was not determined.

The coefficients of thermal expansion for selected gamma alloys, determined from the slope of the expansion curve between approximately 800 and 1800 F are summarized in Table XXXVIII. The data indicated that a severe mismatch would exist between the alloys and a columbium alloy substrate. Thus, the requirement for ductility in the gamma layer becomes even more essential. It was encouraging that the substitution of columbium or tantalum for titanium in gamma alloys decreased the expansivity. Chromium, however, appeared to markedly increase expansion. The expansion coefficients of molybdenum-containing gamma alloys were not determined; however, these would be expected to be lower than the binary compound.

TABLE XXXVIII

COEFFICIENTS OF THERMAL EXPANSION FOR SELECTED GAMMA ALLOYS

Nominal Composition		Coefficient of Thermal Expansion, in./in./degree F x 10^{-6}
(at. %)	(wt %)	
TiAl	Ti-36Al	8.24
$Ti_{0.9}Cb_{0.1}Al$	Ti-34Al-12Cb	8.10
$Ti_{0.8}Cb_{0.2}Al$	Ti-32Al-23Cb	7.52
$Ti_{0.9}Ta_{0.1}Al$	Ti-30Al-20Ta	7.93
$Ti_{0.8}Ta_{0.2}Al$	Ti-26.6Al-35.7Ta	7.85
$Ti_{0.9}Cr_{0.1}Al$	Ti-35.8Al-6.9Cr	9.70
$Ti_{0.45}Al_{0.55}$	Ti-41Al	8.12

Measurements were made on approximately one inch long arc-melted specimens in a Gaertner D1200 fused quartz dilatometer. Heating time to 1800 F was eight hours. All values are corrected for the expansion of fused quartz (0.3 inch x 10^{-6}/degree F).

Discussion of Expansion Effects

A simple relationship for the calculation of coating stress was given in the introduction to this section. Table XXXIX shows some results calculated for $E_c = 30 \times 10^6$ psi and $\Delta T = 1900$ F (assuming no cracking on cooling to room temperature).

A major problem with aluminides is the gross disparity in expansion with a columbium alloy substrate. This problem has plagued aluminum-base alloy coatings for the refractory metals unless the coating was partially molten (e.g., Al-Sn or Ag-Al-Si).

Even with the silicides, expansion matching is not good except for the disilicides of tungsten and molybdenum, and the trisilicide of columbium. As an example, compositions containing Ti-Cr-Cb-Si (comparable to the TRW (Ti-Cr)-Si coating) had average expansions of at least 7.9 x 10^{-6} in./in./ degree F for the appropriate disilicide and 6.3 x 10^{-6} in./in./degree F in the M_5Si_3 composition. Substituting molybdenum or tungsten for chromium in this composition reduced the expansion to below 5.2 x 10^{-6} in./in./degree F, but these values remain considerably above the average expansion of, for example, the Cb752 alloy; that is 4.59 x 10^{-6} in./in./degree F.

TABLE XXXIX

RETAINED STRESS IN HYPOTHETICAL COATINGS ON Cb752 ALLOY

Coating Composition (at. %)	Strain (in./in.)	Calculated Stress in Coating (ksi)
7.2Ti-14.9Cr-10.9Cb-67.0Si	0.0049	147
8.7Ti-11.3Mo-10.6Cb-67.0Si	0.0021	62
9.6Ti-10.7W-7.4Cb-72.4Si	0.0022	66
10.1V-10.9Cr-9.8Cb-69.1Si	0.0042	126
20.8Ti-20.8Cr-20.8Cb-37.6Si	0.0033	98
20.8V-20.8Cr-20.8Cb-37.6Si	0.0029	86
Cb_5Si_3	0.00051	15
$CbSi_2$	0.0014	43
Mo_5Si_3	0.00078	23
$MoSi_2$	0.00049	14
WSi_2	0.00013	4
$TiAl_3$	0.0081	243
$CbAl_3$	0.0049	147
TiAl	0.0069	207

Legend: Coating substrate equilibrated at 2000 F and cooled to 100 F
Coating, E = 30,000 ksi
α for Cb752 = 4.59×10^{-6} in./in./degree F

Reference has been made to the results on expansion of silicides characteristic of the (Ti-Cr)-Si coating (par. 3.1.1). Verification that the results on synthesized disilicides were representative of coatings was provided by measurements on disilicides cracked from the cold ends of tensile and environmental test specimens available from previous Air Force programs at Solar. The coating was removed by hand bending and by passing the specimen through mating gears. The expansion specimen was prepared

by cold pressing and sintering, as previously described for the arc-melted materials. This specimen gave a uniform expansion between room temperature and 1800 F with a coefficient of expansion of 7.37×10^{-6} in./in./degree F. This was approximately the value expected for the typical composition of the disilicides in the (Ti-Cr)-Si coating (e.g., 18 at. % Cr, 10 at. % Ti, 6 at. % Cb and 67 at. % Si) as can be seen by comparison with Figure 8 and Table XXXVI. Hence the validity of the data has been checked indirectly.

A further experiment was tried to confirm that a silicide showing close match to a columbium alloy substrate could actually be developed from a metal and be relatively free of craze cracks. The combination of Cb752 alloy and molybdenum disilicide was chosen for this experiment. To prepare the specimens, 0.5 square inch of pure molybdenum, 0.002 inch thick, was diffusion bonded to 0.012-inch Cb752 alloy using an 0.0003-inch intermediate layer of pure titanium. Diffusion bonding conditions were as follows: pressure - 9,000 psi; temperature - 2200 F; time - 10 seconds; atmosphere - argon. The specimens were siliconized in a pure silicon pack (-20 + 50 mesh) containing 0.04 percent NaF at 2000 F for 15 hours. The specimens and typical Ti-Cr-Si coated specimens are shown in Figure 50. The difference in the frequency of craze cracks is quite apparent. However, it should be noted that the molybdenum disilicide was not completely free of cracks. A quantitative evaluation was made of the number of cracks/inch. The Ti-Cr-Si coating showed 545 cracks/lineal inch; whereas, the molybdenum disilicide coating had only 75 cracks/inch. This comparison is a further indication that improvement can be effected by a close match of expansivity. One factor that has been ignored in this work is anisotropy. Figure 50 shows a distinct columnar growth that is believed to have a preferred orientation. Because the silicides of interest have uniaxial or biaxial crystal symmetries, such anisotropy is to be expected and has been found in the cases where studies have been made (Ref. 14). Hence, the expansion match may not be close in the transverse direction.

Another point that must be considered is the question of failure probability. If failure can begin at the root of any crack, then reduction of the density of cracks will not be of benefit until the last crack is eliminated.

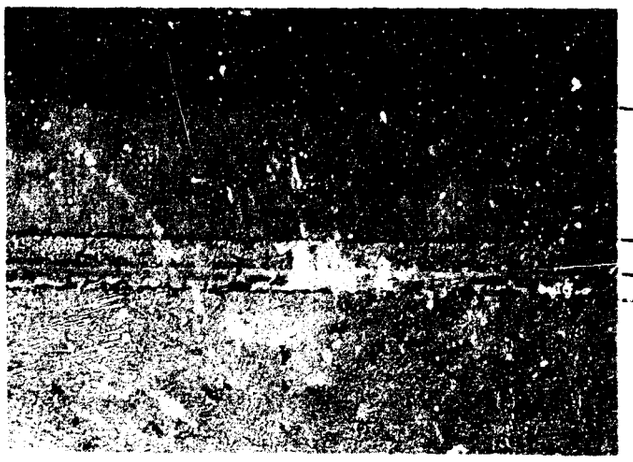

A

B

FIGURE 50. COMPARISON OF CRAZE CRACKING IN $MoSi_2$ AND (Ti-Cr)-Si COATED Cb752 ALLOY

3.4 EVALUATION OF ALL BODY CENTERED CUBIC SYSTEM

This concept was designed to introduce chromium and aluminum into the coating without forming the brittle compounds $CbCr_2$ and Cb_4Al_9. Although the Laves phase, $CbCr_2$, forms in the Cb-Cr system, the Cb-V and V-Cr systems are simple body centered cubic solid solutions. Hence the coating sequence Cb-V-Cr will remain a solid solution until the diffusion of columbium and chromium into the vanadium reach the concentration of the two phase field, $\beta + MCr_2$, in the ternary system. Even at this composition, discontinuous particles of Laves phase will form rather than a continuous layer as would be the case if the chromium were deposited directly on the columbium.

Review of other systems shows that the Cb-Mo-Cr and Cb-W-Cr systems have the same characteristics as the Cb-V-Cr system.

Once a chromium layer is available, other body centered cubic oxidation-resistant alloys can be placed on top. Examples would be Fe-Cr-Al, Fe-Cr-Y, and derived alloys from these. However, the problem again appears to be one of diffusion control to preserve an adequate level of chromium, aluminum, and yttrium at the outer surface and to avoid excessive diffusion of compound-forming elements through the chromium to the vanadium, molybdenum, or tungsten. The experimental approach was to prepare diffusion couples of selected element sequences to establish potential coating lives and determine any adverse effects as a result of interdiffusion. The most promising barrier combinations were also prepared as bonded specimens for oxidation evaluation at 2300 and 2500 F.

3.4.1 Diffusion Barrier Study

Initial effort was directed to study the rates of interdiffusion between the Cb-Fe-25Cr-5Al alloy and the potential diffusion barrier materials. The following diffusion couples were prepared and annealed in vacuum at 2300 F for 1, 15, 20, and 200 hours:

Cb-W	Cb-V-(Fe-25Cr-5Al)
Cb-Mo	Cb-(V-15Cr)-(Fe-25Cr-5Al)
Cb-V	(Fe-25Cr-5Al)-Cr-(V-15Cr)
Cb-(V-15Cr)	(Fe-25Cr-5Al)-Cr-Mo
Cb-Mo-(Fe-25Cr-5Al)	(Fe-25Cr-5Al)-Cr-V
Cb-W-(Fe-25Cr-5Al)	(Fe-25Cr-5Al)-Cr-W

The couples were prepared using specimens approximately 0.375 inch in diameter that varied in thickness from 0.001 to 0.020 inch. The assembled couples were placed in a threaded molybdenum clamping fixture then annealed using a procedure similar to that described by Passmore (Ref. 15). All materials were commercially available for this work except chromium. The chromium was prepared by vacuum evaporation of high-purity iodide chromium onto couples and by the preparation of foil from arc-melted Cr-1Y button ingots. These ingots were initially hot rolled at 2000 F to 0.030-inch sheet. The sheet material was subsequently warm rolled, in a stainless steel pack, to produce foil varying in thickness from 0.003 to 0.005-inch. This material was electrolytically etched in an ethanol-HF-H_2SO_4 solution prior to use in the diffusion couples.

Diffusion results were obtained from microhardness traverses on polished sections of the annealed couples. A diamond pyramid indentor, using a load of 15 to 100 grams, was employed. The load employed was varied, depending on the hardness of the substrate, to produce indentations having a diagonal length of 20 to 30 microns.

Of the three bcc metals - vanadium, molybdenum, and tungsten - considered as barrier materials for columbium, molybdenum, and tungsten were considerably more effective in limiting diffusion than was vanadium. The extent of interdiffusion between columbium and vanadium after 50 hours at 2300 F was approximately 95 microns (3.7 mils). Columbium diffused more rapidly into vanadium resulting in a solution-hardening peak of about 500 DPH at a distance of 0.001 inch from the original interface. After 200 hours the hardness peak was at the same level, but was displaced to approximately 0.002 inch from the original interface. The overall extent of interdiffusion was greater than 0.005 inch after the 200-hour anneal.

In Cb-Mo and Cb-W couples, no appreciable interdiffusion distance could be defined even after 200 hours at 2300 F. Slight hardening was detected in the Cb-Mo couple. An indentation, having a diagonal length of 20 microns, made lightly on the molybdenum side of the Cb-Mo interface showed a hardness of 235 DPH compared to an average value of 186 DPH for the molybdenum. In the 200-hour annealed Cb-W couple, the hardness in this vicinity was 425 DPH. No appreciable hardening of the columbium could be detected in either case; the extent of overall diffusion appeared to be well under 0.5 mil under these annealing conditions.

Chromium and vanadium were selected as barriers between the Fe-Cr-Al alloy and substrate. However, the extent of interdiffusion between the Fe-25Cr-5Al alloy and both of these materials was quite appreciable at 2300 F. Figure 51 shows the hardness traverse obtained for diffusion couples composed of these materials after annealing for 50 and 200 hours. In Figure 51A it may be seen that considerable solution hardening had occurred in the V-(Fe-25Cr-5Al) couple after 50 hours; interdiffusion for a distance greater than 0.010 inch had occurred. The extent of diffusion in the Cr-(Fe-25Cr-5Al) couple was less but still quite appreciable, particularly after 200 hours. High hardness peaks were noted in both couples in the vicinity of the original interface. Vanadium caused pronounced solution hardening of the Fe-25Cr-5Al alloy.

Diffusion couples of V-Cr, (V-15Cr)-Cr, Mo-Cr, and W-Cr were studied to determine their suitability as potential intermediate diffusion barriers. Both the vanadium and V-15Cr alloys appeared to be suitable diffusion barriers for chromium with respect to the extent of hardening resulting from interdiffusion. The highest hardness detected in either V-Cr or (V-15Cr)-Cr couples diffused for 50 hours at

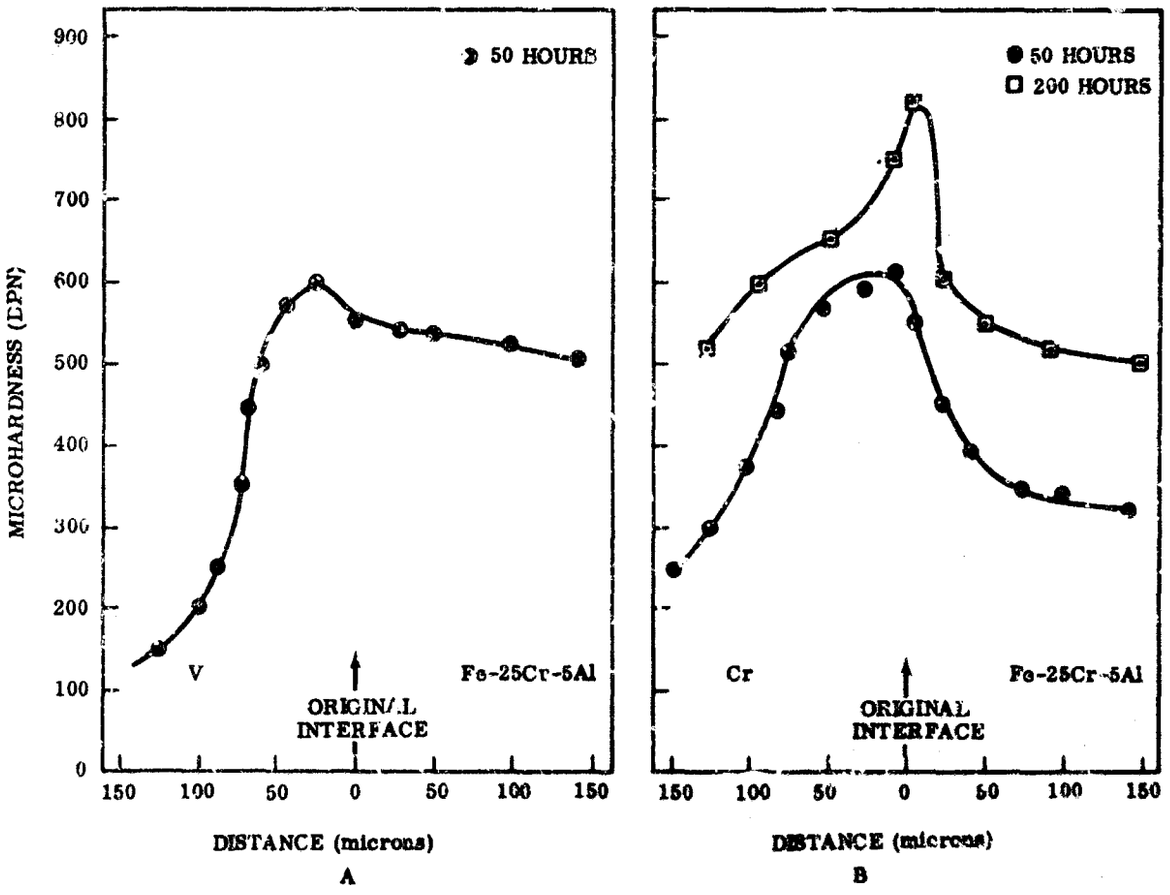

FIGURE 51. MICROHARDNESS TRAVERSE DATA FOR V-(Fe-25Cr-5Al) AND Cr-(Fe-25Cr-5Al) DIFFUSION COUPLES

2300 F was 385 DPN. The width of the diffusion zone formed in the V-Cr couple was 45 microns (1.8 mils) after this exposure. Although relatively slow diffusion rates were apparent in the W-Cr and Mo-Cr systems, significant hardening at the interface of the diffusion couples was observed. In the Mo-Cr couple this hardness was 450 DPN after 50 hours, and in excess of 600 DPN after 200 hours. In W-Cr couples, a hardness of 575 DPN was developed after 50 hours. The width of the diffusion band was narrow in each system and could be defined on the basis of hardness traverse data or metallographic interpretation. On the basis of the diffusion data it appeared that the most compatible systems for the development of a continuous bcc coating system are Cb-Mo-Cr-(Fe-Cr-Al) or Cb-Mo-(Fe-Cr-Al). Tungsten appeared to offer no significant advantage over molybdenum. Vanadium was ineffective as a diffusion barrier for either columbium or the Fe-25Cr-5Al alloy.

Diffusion couples of the above systems were prepared using layer thicknesses approaching those that would exist in a realistic coating system. The results of diffusion annealing couples composed of 0.007 inch of Fe-25Cr-5Al, a 0.003-inch layer of chromium, 0.002-inch of molybdenum, and a 0.030-inch columbium substrate for 50 and 200 hours at 2300 F appear in Figure 52. A pronounced hardening peak occurred at the Cr-Mo interface. A hardness peak was also noted in the Fe-Cr-Al, particularly after the 200-hour exposure. A hardness gradient also existed in the substrate to a depth of nearly 0.010 inch.

3.4.2 Oxidation Results

The behavior of these systems under oxidizing conditions was investigated by preparing diffusion bonded specimens suitable for oxidation testing. Two types of specimen preparations were used. In one method, 1.5-inch wide specimens composed of a columbium core, the appropriate diffusion barrier materials, and Fe-25Cr-5Al cover plates were diffusion bonded between tungsten plates in a bolted fixture at 2000 F in vacuum. These specimens were subsequently clamped in a water-cooled copper fixture which protected the exposed edges. Oxidation was accomplished by heating the center portion of the specimen in an O_2-H_2 torch flame. An alternate method consisted of diffusion bonding 0.5-inch square couples, having 1.5 inch wide cover plates of Fe-25Cr-5Al alloy. The diffusion bonding was carried out in vacuum at Solar. Subsequently, the edges of the couples were sealed using heliarc welding with Fe-25Cr-5Al shims between the cover plates. These specimens were then oxidized in static air in a muffle furnace.

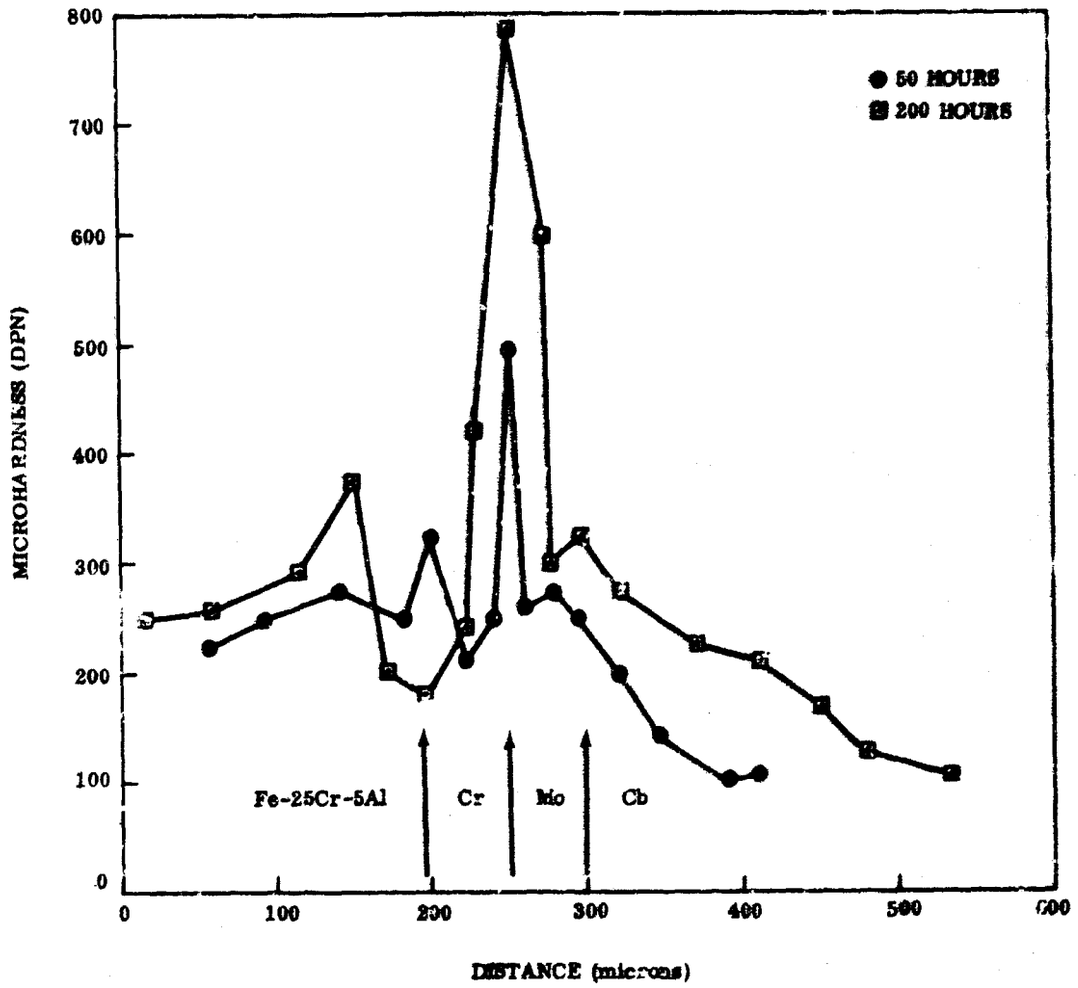

FIGURE 52. HARDNESS TRAVERSE DATA FOR SPECIMENS ANNEALED IN VACUUM AT 2300 F

The bonded specimens were run up to 28 hours at 2300 F, and 10 hours at 2500 F with cycling to room temperature after each one-hour exposure. Figure 53 shows the hardness profile of a specimen oxidized for eight hours in static air at 2300 F. This specimen was composed of the following layers:

Layer		(in.)
Fe-25Cr-5Al	-	0.005
Chromium	-	0.003
Molybdenum	-	0.001
Columbium	-	0.020
Molybdenum	-	0.001
Chromium	-	0.003
Fe-25Cr-5Al	-	0.005

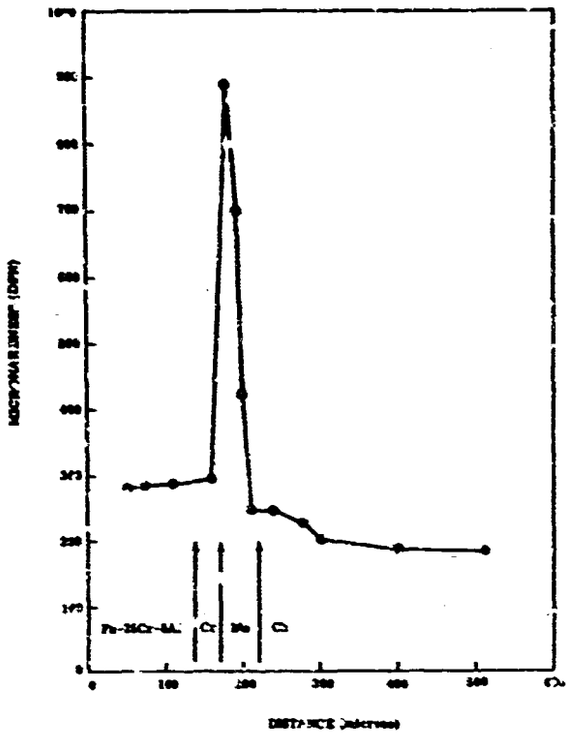

FIGURE 53. HARDNESS TRAVERSE OF DIFFUSION BONDED SPECIMENS OXIDIZED IN STATIC AIR EIGHT HOURS

A photomicrograph of the structure of the oxidized specimen is shown in Figure 54. The Fe-25Cr-5Al layer contained a well defined oxide precipitate; however, the hardness of this material was not significantly altered as may be seen in Figure 53. Considerable interdiffusion occurred between the Cr-(Fe-25Cr-5Al) and the Cr-Mo layers. A high hardness peak at the Cr-Mo interface, similar to that observed in the vacuum annealed couples, was apparent. A hardness gradient existed in the columbium which corresponded to the presence and distribution of a discontinuous precipitate (Fig. 54). The composition of this phase was identified by electron microprobe analysis.

Specimens exposed for shorter times and at higher temperatures did not show the oxide precipitate in the Fe-Cr-Al alloy. This may be seen in Figure 55, which shows the microstructure of a specimen oxidized for one hour at 2450 F. The hardness of the Fe-Cr-Al layer was quite high, showing an average value of 575 DPN. Specimens oxidized at 2500 F for 1 and 10 hours showed similar high hardness values for the Fe-Cr-Al alloy; the hardness increased with longer exposure times. The high hardness peaks at the Cr-Mo interface were not apparent in the specimens oxidized at higher temperatures.

Magnification: 200X

FIGURE 54. DIFFUSION BONDED SPECIMEN OXIDIZED EIGHT HOURS AT 2300 F

Magnification: 200X

FIGURE 55. DIFFUSION BONDED SPECIMEN OXIDIZED 10 HOURS AT 2450 F

Specimens of the continuous bcc coating systems that were oxidation tested at 2300 and 2500 F were examined by electron microprobe analysis in an effort to clarify the cause of hardening reactions occurring at the Mo-(Fe-Cr-Al) or Mo-Cr interfaces and to identify the second phase observed in the columbium substrate. It appeared that hardening at the molybdenum interface was due to the formation of a phase rich in iron, presumably a σ-phase of the Fe(Cr-Mo) type. Iron was also found to be present in large quantities in the precipitated phase occurring in the columbium. The presence of aluminum in these reaction zones was not detected.

Consequently, from these results it was apparent that an iron-free material would be required as the reservoir coating in a system of this type. Chromium-base, Cr-Al solid solutions were considered for this purpose. Alloys of Cr-5 wt % Al and Cr-15 wt % Al were prepared to determine their oxidation behavior and assess their potential. Both alloys were found to be extremely brittle in the as-cast condition. Oxidation studies were run at 2400 and 2500 F. At the lower temperature, the following results were obtained.

Nominal Composition, (wt %)	Weight Gain (mg/cm^2)		
	1 hour	4 hours	16 hours
Cr-5Al	7.10	22.4	--
Cr-15Al	3.19	6.67	21.2

Internal oxidation occurred in both materials, extending to a greater depth in the lower aluminum alloy. An adherent scale was formed on the Cr-15Al but not on the lower aluminum-containing alloy. At 2500 F similar results were obtained, and considerably greater weight gains and depths of internal oxidation were observed. In view of these results, further exploratory studies were abandoned.

3.4.3 Discussion of Results

Although work was stopped on this system because of the problems of interdiffusion and internal oxidation, the approach has definite potential for a short-life coating of high reliability. Short-life coatings were not to be considered within the scope of this work, however.

The diffusion data show a peak hardness of 780 VHN after 200 hours at 2300 F, resulting from iron diffusion through the chromium (Fig. 52). This hardness is not excessive and is much less than typical silicides. Optimization of compositions is no

doubt possible because the typical Fe-Cr-Al alloys with optimum compositions do not oxidize internally as readily as observed here. Higher aluminum contents and lower iron contents might be studied.

3.5 SELECTION OF COATING SYSTEMS

Three systems were considered in this program. These were:

- The all body centered cubic, ductile coating system
- The primary barrier of high oxidation resistance with a mildly oxidation resistance sublayer to resist oxidation at the root of the cracks.
- The primary barrier system with highly oxidation resistant substrate able to resist oxidation for sufficient time to complete a mission in the event of gross primary barrier failure.

The ductile system based on the all body centered cubic solid solution was studied by means of the model system, Cb-Mo-Cr-(Fe, Cr, Al). Although coatings of 0.005 to 0.007 inch were used, the life was limited by interdiffusion and the oxidation rate of the alloy. Because the objectives of the program were not directed to short-life coatings, it was not recommended that this type of coating be scaled up.

The third type of system requires a columbium-rich alloy that can be applied to the substrate and provide a minimum of one hour life at 2400 F. No alloy with adequate oxidation resistance to meet this goal was discovered, so that no further work could be performed with this approach.

All additional work was performed on systems of the second type where a ductile but midly oxidation-resistant layer is applied before the primary barrier. This was called the effective-ductility approach. The sublayer has sufficient ductility to stop cracks that start in the primary barrier and sufficient oxidation resistance to prevent excessive oxidation at the root of these cracks. However, some systems could be selected for coating process development at this point, whereas other systems required examination in more detail preparatory to final selection. The Cb-V-Cr-Si and Cb-Ti-Mo-Si systems were selected for coating process development, but the following systems needed to be examined more extensively:

- Cb-Ti-Mo alloy sublayers with aluminide primary barriers
- Cb-Ti-Cr-Al alloy sublayers with silicide primary barriers
- Standard silicide coating systems with additional ceramic coating to provide better healing of cracks.

The Cb-V-Cr-Si system was selected on the basis of a moderate oxidation-resistant sublayer (if vanadium content were kept less than 10 percent, the absence of Laves phase, the reduction of interstitial sink effect, and good oxidation resistance at 1600 and 2400 F of the disilicide. In addition, the ability of vanadium-containing silicides to be self-healing was a powerful factor in this choice.

Selection of the Cb-Ti-Mo-Si system was based on the moderate oxidation resistance of Cb-Ti-Mo alloys (D31 alloy), the excellent oxidation resistance of molybdenum-containing disilicides, the elimination of volatile chromium that is a problem in low-pressure reentry environments, and the closer expansion match of the disilicide with columbium when the molybdenum content is high. The requirement of high-molybdenum content had a major influence on coating methods used.

The high expansion of aluminides will lead to very high coating stresses (par. 3.3.3). Accordingly, only one system was carried forward for additional study. Preliminary work reported in Paragraph 3.3.2 indicated that the Cb-Ti-Mo-Al system was the best of those examined. It includes the moderately oxidation-resistant substrate Cb-Ti-Mo, and the introduction of molybdenum in the aluminide will reduce expansion, whereas, the titanium will improve oxidation resistance of the aluminides. It was anticipated that an interstitial sink effect would occur in such a system, so that the coating would be expected to be more suitable for solid solution alloys or alloys in the stress-relieved condition.

The only ductile columbium-rich alloys found with oxidation resistance better than Cb-Ti-Cr (sublayer in TRW Cb-Ti-Cr-Si coating) were similar alloys containing titanium, aluminum, and chromium in some instances. Therefore, the effect of adding aluminum to the sublayers prior to siliciding was studied further. Other work had shown that aluminum tends to be rejected from silicides in favor of titanium, chromium, vanadium, and columbium so that the primary barrier of silicide should be little affected by aluminum in the sublayer.

Finally, the third system chosen for additional study was one where an outer ceramic coating was applied over the silicide. It was expected that this would reduce the demands on the sublayer, in the event of coating cracking, by aiding repair.

The three systems that required additional study were selected because data for their component parts indicated some potential when combined into a complete system. At this stage, additional work on the individual components would have provided little aid in evaluation, and the next step required synthesis of the complete coating for evaluation before a decision could be made as to its potential.

IV. EXAMINATION OF SPECIAL NEW COATING SYSTEM

At the conclusion of the basic property measurement program described in Section III, two major systems were selected for development into coatings. These were the (V-Cr)-Si and (Mo-Ti)-Si coatings. In addition to these systems, a number of concepts remained which, although inadequate to justify a full-fledged coating development program, were worthy of additional experimental effort. This section contains data on these experimental systems. Section V describes the development of the two principal coating systems.

The coating systems examined in a preliminary manner and described in this section include:

1. Aluminized alloys containing titanium and columbium with molybdenum or tantalum
2. Titanized and aluminized alloys of Cb-Mo and commercial alloys
3. Fugitive slurry techniques for application of a Ti-Mo-Al coating
4. Coatings containing aluminum in the sublayer to improve low-temperature oxidation resistance and the disilicide as the principal barrier
5. The ceramic overlayed silicided system

The efforts in (1), (2), and (3) above were designed to take advantage of the moderately oxidation-resistant aluminum containing solid solution alloys containing Cb-Ti and molybdenum or tantalum with the trialuminide primary barrier. The work in (4) was designed to use the excellent oxidation resistance (at 1600 F) of the Cb-Ti-Al and Cb-Ti-Cr-Al systems as sublayers and the silicides as the primary barrier. The effort in (5) was not an outgrowth of the basic property studies described in Section III, but rather a special study initiated to show whether refractory silica-base glass coatings (ceramic coatings) could be used over a silicide oxygen barrier to provide protection over typical cracks that develop in columbium disilicide coatings. Ceramic coatings over a disilicide have the advantage that the composition is not dependent on the thermodynamics and kinetics of the oxidation of the disilicide and, consequently,

is constant with temperature. Viscosity and softening point are also more readily controlled than with in situ generated coatings.

4.1 COATING CONTAINING MAJOR ADDITIONS OF ALUMINUM

The oxidation studies conducted at IITRI on arc-melted alloys indicated that the substitution of titanium and molybdenum for columbium in $CbAl_3$ markedly improved oxidation resistance at temperatures in the 2200 to 2500 F range. Similarly, minor columbium and molybdenum substitutions for titanium in $TiAl_3$ resulted in enhanced oxidation behavior in this temperature range. Most of the $(Ti\text{-}Cb\text{-}Mo)Al_3$ compositions that were studied showed no evidence of pest-type attack during exposure for 24 hours at 1600 F; a number of compositions were resistant for at least 90 hours under these conditions. Molybdenum, columbium, tantalum, and chromium enhanced the high-temperature oxidation resistance of γ-TiAl when partially substituted for titanium. An increase in aluminum content is 55 atomic percent, which was within the solubility range for the compositions studied, resulted in a further increase in oxidation resistance for the ternary compounds. No abnormal oxidation was observed at 1600 F in these materials. Both columbium and tantalum substitutions decreased the expansivity of the gamma phase in the 800 to 1800 F range.

The oxidation behavior of aluminum-saturated columbium-base solid solutions was studied. Of the ternary additions made at the 5 atomic percent level, titanium produced the greatest decrease in oxidation rate. Higher titanium additions increased the solubility of aluminum, resulting in ternary alloys with increased oxidation resistance at higher titanium and aluminum levels. Molybdenum additions to the ternary Cb-Ti-Al alloys had a further beneficial effect on oxidation resistance.

Coating system concepts were investigated by performing aluminizing experiments with the intention of developing the coating layers considered to be optimum as a result of the oxidation studies. These specimens were subsequently oxidized to establish a correlation with the oxidation studies on bulk materials and to determine the influence of the coating on the substrate.

Initial experiments involved the aluminizing of Cb-Ti alloys with the intention of developing Cb-Ti-Al solid solution, gamma, and trialuminide layers. Initially, a series of columbium alloys containing 25, 50, 67, and 75 atomic percent titanium were prepared as 0.030-inch sheet, aluminized by dipping into molten aluminum, and subsequently diffused in vacuum at 2000 F for 16 hours. The relative thickness of the

gamma or solid solution alloy layer that formed, as compared to the (Cb-Ti)Al_3 layer, increased with increasing titanium content of the alloy. The specimens were subsequently oxidized at 2300 F for 16 hours. After this exposure, no trialuminide layer remained on the specimens. The most oxidation-resistant coating, on the basis of weight gain and visual appearance, was that formed on the Cb-75 at. % Ti alloy. Metallographic examination of the oxidized specimen indicated, however, that contamination of the substrate occurred (Fig. 56). The hardness of the substrate was uniformly 590 DPN, indicating that interstitial contamination has occurred; however, the visible contamination zone apparent in Figure 56 extends to a depth of only 0.005 inch beneath the surface. The microstructure of a Cb-75 atomic percent titanium alloy, which was not aluminized, after oxidation at 2300 F for one hour may be seen in Figure 57. Visible contamination is apparent throughout the specimen; the hardness is also uniformly 590 DPN. The extent of internal contamination in the coated alloy appears to be related to the presence of cracks in the (Cb-Ti)Al_3 layer that extends partially into the gamma sublayer. It appears that the (Ti-Cb)Al gamma layer is capable of transporting oxygen that is readily absorbed by the titanium alloy substrate; this should be a very effective oxygen sink in the presence of gamma. The true effectiveness of this coating system can only be established by reproducing the columbium, titanium, and aluminum coating layers on a columbium-alloy substrate.

The following additional compositions (at.%) were prepared as substrate materials for aluminizing experiments: Ti-15Cb-10Mo, Ti-15Cb-20Mo, Ti-15Cb-20Ta, Ti-15Cb, Ti-29.2Cb-14.1Mo, and Ti-31.7Cb-6.8Mo. All but the binary Ti-Cb alloy could be cold rolled to a 0.060-inch sheet for the preparation of specimens. The alloys were aluminized by dipping and by pack diffusion, with the objective of establishing compound formation rates and providing specimens for oxidation studies. Specimens that were dip aluminized were subsequently diffused in vacuum at temperatures between 1800 and 2300 F.

Trialuminide layers were not produced on any of the specimens and, based on metallographic and microhardness observations, it appeared that in most cases only a solid-solution layer was formed. The dipping process was not reproducible in terms of applying uniform quantities of aluminum from specimen to specimen. In most cases, a relatively thin aluminum coating, less than 5 mg/cm^2, was obtained. Multiple dipping and diffusion treatments were not successful due to poor wetting; as a consequence, pack aluminizing was adopted.

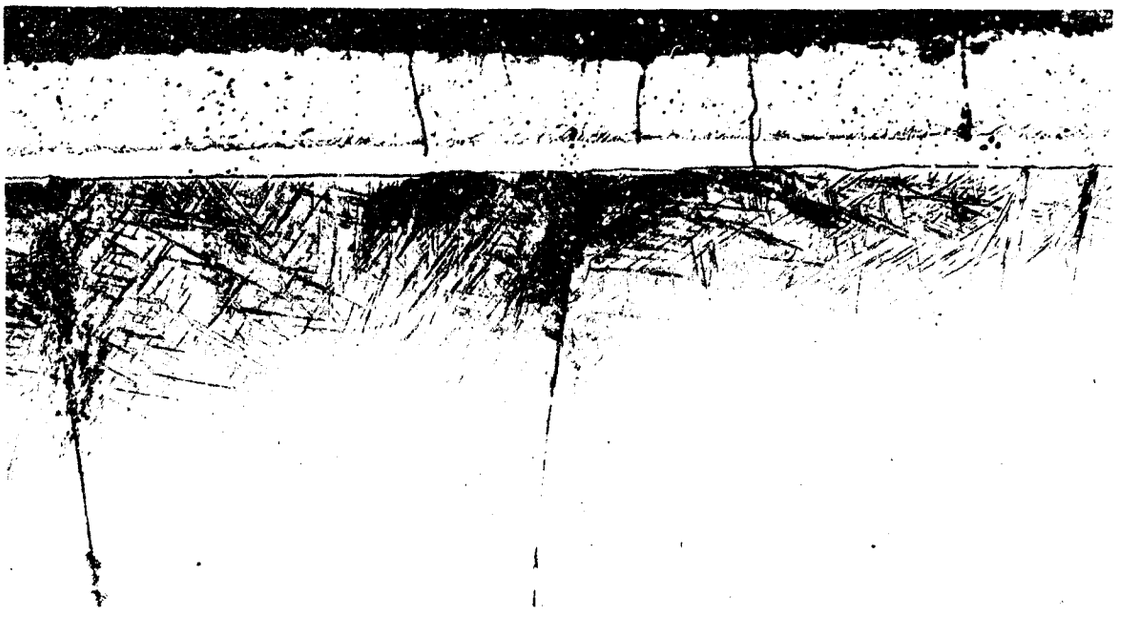

Magnification: 200X

FIGURE 56. ALUMINIZED Cb-75 ATOMIC PERCENT TITANIUM ALLOY OXIDIZED AT 2300 F FOR 16 HOURS

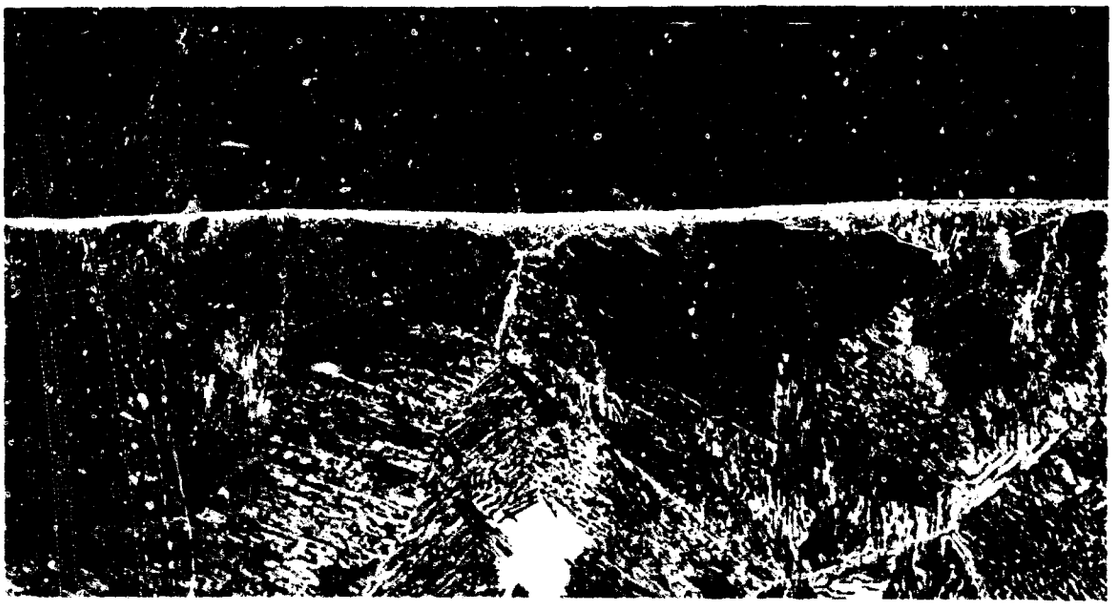

Magnification 200X

FIGURE 57. Cb-75 ATOMIC PERCENT TITANIUM ALLOY OXIDIZED AT 2300 F FOR ONE HOUR

Pack runs were made using a mixture of Al_2O_3, aluminum powder, and NaCl. The pack mixture was contained in graphite within an Inconel retort. The activator concentration was varied between 0.1 and 1.0 weight percent of the total charge. Runs were made at 1600 to 1800 F for 1 to 16 hours. After pack aluminizing, the specimens were vacuum annealed at either 2100 or 2400 F for one hour. The lower vacuum annealing temperature produced a coating approximately 0.004 inch thick that was predominantly trialuminide. Two thin sublayers were also present in these coatings.

Annealing at 2400 F produced a single-layered coating, 0.006 to 0.007 inch thick. The coating was optically inert under polarized light and was assumed to be a solid-solution layer. Specimens of both coating types were oxidized at 2400 F. Weight gain data are reported in Table XL.

TABLE XL

OXIDATION DATA FOR ALUMINIZED ALLOYS EXPOSED AT 2400 F

Substrate Composition (wt %)	Weight Gain (mg/cm^2)					
	Annealed at 2100 F			Annealed at 2400 F		
	1 Hour	4 Hours	16 Hours	1 Hour	4 Hours	16 Hours
Ti-23.4Cb-16.1Mo	10.3	33.2	64.9	25.7	40.1	56.0
Ti-21.7Cb-29.9Mo	0.92	7.28	37.4	1.97	15.1	47.9
Ti-17.1Cb-44.5Ta	1.08	9.52	32	4.65	15.4	47.2
Ti-40Cb-20Mo	0.86	8.12	43.2	1.64	13.2	68.9
Ti-45Cb-10Mo	4.07	14.0	42.7	5.81	22.9	99.1

The weight gain data are influenced by the presence of minor defects in the coating which limit the interpretation of results, particularly for the longer time exposures. More meaningful information was derived from examination of the microstructures of the oxidized specimens. The specimens annealed at 2400 F all show evidence of internal oxygen contamination after oxidation. The least pronounced effect was shown by the two alloys of high-molybdenum content, and was limited to a depth of approximately 0.002 inch after one hour of exposure. After four hours of exposure all of the alloys showed visible evidence of oxygen contamination beneath the aluminum alloy layer. The specimens annealed at 2100 F showed evidence of oxygen contamination that was apparently initiated at the base of cracks in the trialuminide layer. The

amount of contamination was, again, least in the two higher molybdenum alloys. It appears that the (Ti-Mo-Cb)Al gamma layer, as (Ti-Cb)Al, is capable of transporting oxygen that is readily absorbed by the titanium alloy substrate which is a very effective oxygen sink. It must be pointed out again that the true effectiveness of these coating systems can only be established by reproducing the columbium, titanium, molybdenum, and aluminum coating layers on a columbium-alloy substrate.

As a consequence, two alternate experimental methods were initiated. A Cb-15 at. % Mo alloy was prepared for a series of titanizing and aluminizing experiments at Solar. High-pressure pack cementation methods were used to apply titanium and aluminum coatings over the specially prepared Cb-15Mo alloy. Approximately 21 mg/cm^2 of titanium were deposited using an arc-melted 64Ti-36W pack and 0.1 percent NaF activator for a total of 33 hours at 2000 F. An 18 mg/cm^2 coating of aluminum was then applied over the titanized layer using 10 percent Alcoa 201 aluminum powder and 90 percent A14 alumina with 1 percent NaCl for 16 hours at 1600 F. Considerable sintering difficulty was experienced during the titanium deposition. Figures 58 and 59 show the titanium and aluminum coating on the Cb-15Mo alloy.

Specimens oxidation tested at 2400 F had general surface failures recorded at 7, 9, 13, 13, 16, 22, 25, 26, 32, 41, and 43 hours. Coupons at 1600 F were removed from testing after 216 hours. Of the eleven specimens tested at 1600 F there was only one failure, which occurred between 192 and 216 hours.

From Figure 59 it can be seen that the aluminized layer did not completely consume the titanium modified zone. Since the ductile Cb-Mo-Ti-Al alloy at the base of the craze cracks has good oxidation resistance, the 200-hour 1600 F oxidation life of this system is not surprising. However, the poor 2400 F life of the titanized and aluminized Cb-15Mo alloy did not give much support to the Cb-Mo-Ti-Al system. Figure 60 is a weight gain versus time plot, indicating that breakaway (nonparabolic oxide growth) begins as early as nine hours. The system appeared to offer little potential at 2400 F. Work was therefore suspended.

Another method tried for applying Ti-Mo-Al coatings on the Cb752 alloy consisted of using a fugitive vehicle slurry-coating process. The method employed was similar to that concurrently under investigation at IITRI for the deposition of Hf-Ta solid-solution coatings. Slurries were made by blending mixtures of molybdenum, titanium, aluminum, and copper powders and suspending these mixtures in an

Magnification: 3X

FIGURE 58.

Cb-15Mo ALLOY AFTER TITANIZING AND ALUMINIZING

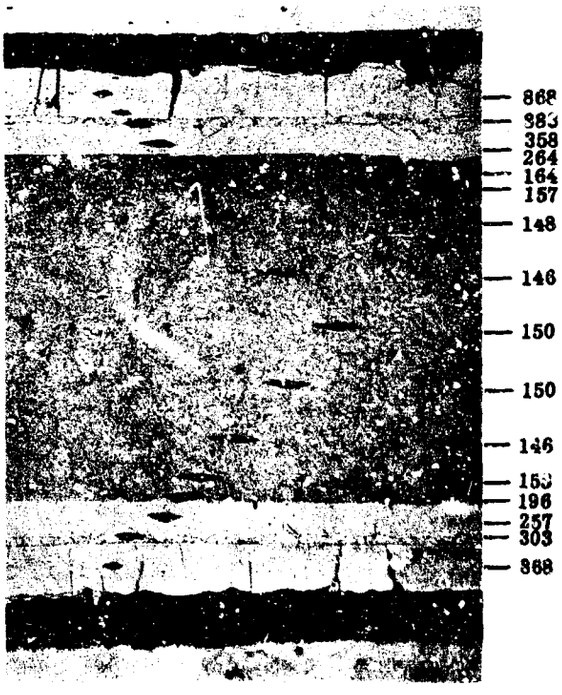

Magnification: 100X

FIGURE 59.

Cb-15Mo ALLOY AFTER TITANIZING AND ALUMINIZING

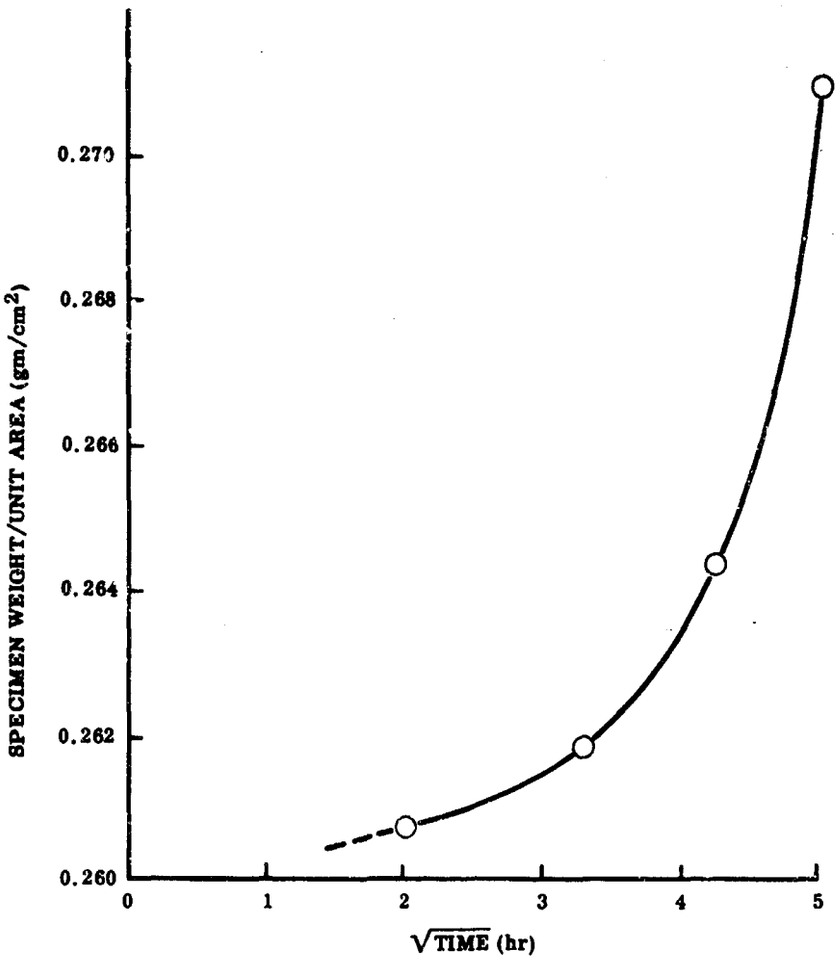

FIGURE 60. SPECIFIC WEIGHT GAIN VERSUS TIME FOR THE (Cb-15Mo)-Ti-Al COATING (2400 F)

organic vehicle. The copper vehicle was added to promote liquid-phase sintering of the coating constituents. The copper was to be removed by subsequent vacuum heat treatment. Slurries of the following compositions were prepared and painted onto Cb752 specimens:

41Cu-44Ti-11Mo-4Al
42Cu-45Ti-9Mo-4Al
40Cu-42Ti-8Mo-10Al
40Cu-40Ti-10Mo-10Al

Coating weights were approximately 15 mg/cm^2. The specimens were vacuum heat treated in sequence at 2010 F for 30 minutes, 2370 F for one hour, and 2730 F for one hour. After this treatment approximately 43 percent of the original coating weight was lost.

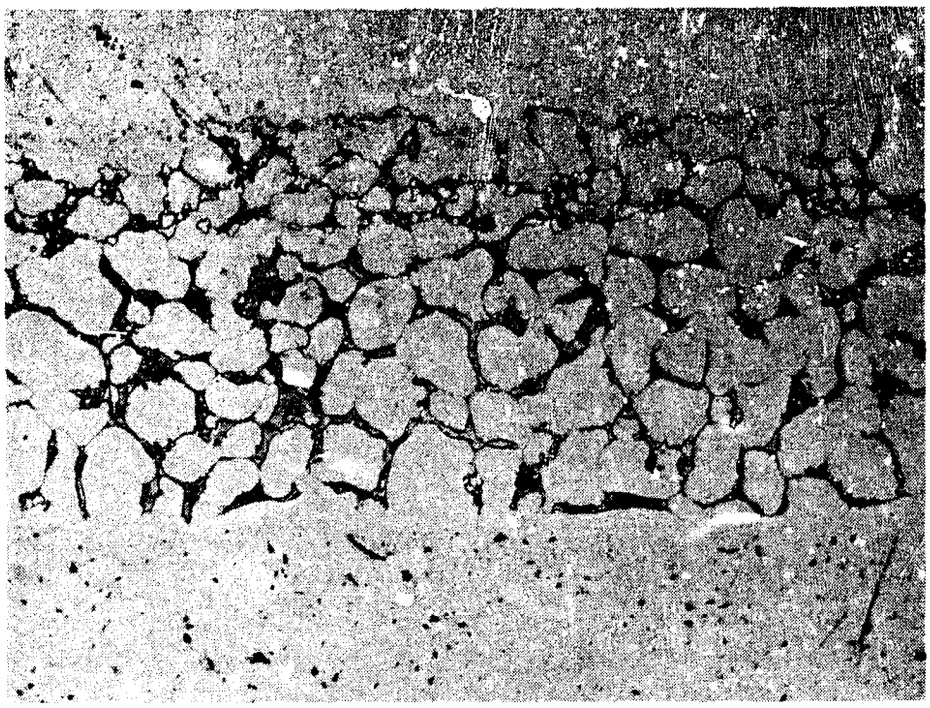

FIGURE 61. COATING FORMED ON Cb-752 USING Cu-40Ti-10Mo-10Al SLURRY

The microstructure of the 40Cu-40Ti-10Mo-10Al coating after this treatment may be seen in Figure 61. It is composed of large Ti-Mo solid-solution grains. The interstices contain what is probably aluminide precipitate and residual vehicle. The microstructure of the 41Cu-44Ti-11Mo-4Al coating (Fig. 62), contains far less interstitial phase. There is apparently some residual copper in this specimen. Oxidation tests were performed at 2200 F on specimens treated in a similar manner. During a 30-minute exposure the specimens oxidized rapidly, forming a loose black powdery scale. This is apparently associated with a residual copper vehicle in the coatings. More recent work at IITRI (Ref. 16), on similar systems, has shown that copper removal can be more effectively accomplished by proper control of the original slurry composition and heat treatment, but this coating system did not show enough promise to warrant further development as a Phase II or III coating.

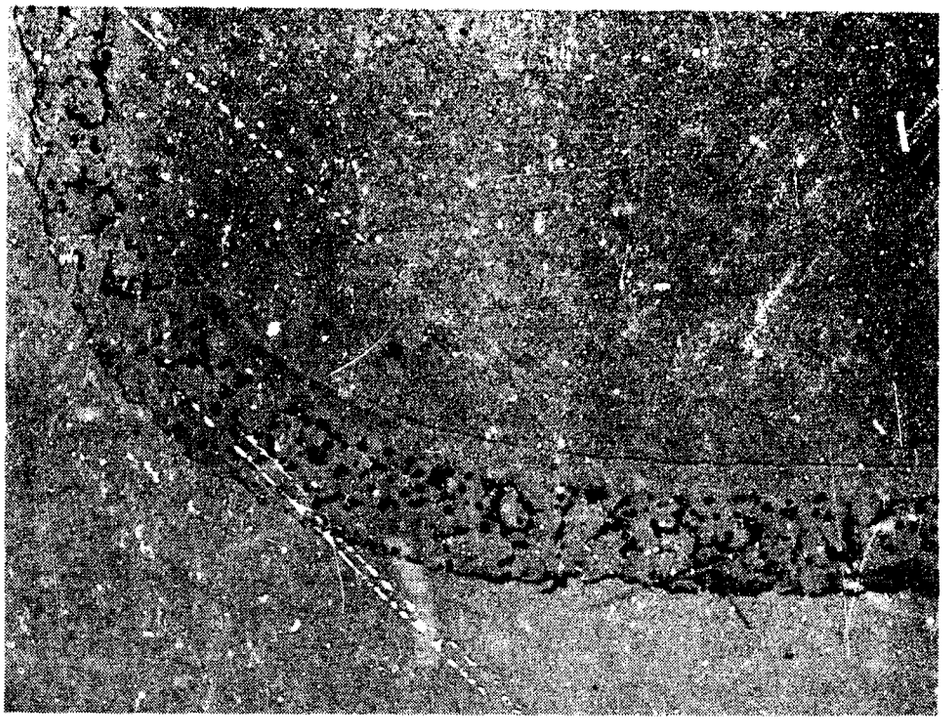

FIGURE 62. COATING FORMED ON Cb-752 USING Cu-44Ti-11Mo-4Al SLURRY

Aluminum-Coated Columbium Alloys

The effect of aluminum and aluminum plus titanium on the mechanical and oxidation properties of columbium alloys was investigated at Solar. Specimens of pure columbium, Cb753, Cb752, D43, and B66 were aluminized or titanized plus aluminized using:

Aluminizing - Pack

89% A14 Al_2O_3

10% Type 201 atomized aluminum

1 % NaCl

Cycle - 3 hours at 1600 F in argon

Titanizing - Pack

99.9% PA8 (64Ti-36W, prealloyed and crushed to -20 + 50 mesh)

0.1% NaF

Cycle - 15 hours at 2000 F

The aluminized and titanized plus aluminized specimens were diffusion treated at 2400 F for 15 hours in argon to alloy the coatings with the substrate. Figure 63 shows some of the specimens from which a solid solution was obtained with Ti-Al coated alloys by restricting the aluminum to the weight increases shown in Table XLI. The alloys coated with aluminum only were not single phased (Fig. 64). (An addition of 2 mg/cm^2 of aluminum on a 0.010-inch columbium specimen is equal to an increase of two percent aluminum when the alloy is completely homogenized.) The annealing treatment led to a change from the original aluminide (probably $CbAl_3$ type) to the lower aluminides, but there was little evidence of solution in the columbium alloy. Examination of the pure columbium specimen (solubility of aluminum in columbium is approximately five percent) showed the same lack of solution, indicating that the diffusion rate of aluminum must be the controlling factor rather than an effect of the alloying elements in the commercial alloys.

The weight gains in oxidation tests are presented in Table XLI, together with data on an arc-melted Cb-Ti-Cr alloy. The latter is representative of the sub-layer in (Ti-Cr)-Si coatings and forms a standard for comparison.

The results for the (Ti-Al) coated specimens are similar to those presented in Table VII for arc-melted alloys containing up to 20 percent titanium. The coarse grain size of these specimens (Fig. 63) is confirmed by those shown in Figure 65 and their excellent appearance after four hours at 1600 F is evident.

TABLE XLI

OXIDATION TEST RESULTS AT 1600 F ON ALUMINIZED AND TITANIZED PLUS ALUMINIZED COLUMBIUM ALLOY

Alloy	Titanium Deposition		Aluminum Deposition		Weight Gain Oxidation Test (mg/cm^2)		Comments
	(wt %)	(mg/cm^2)	(wt %)	(mg/cm^2)	2 hours	4 hours	
Pure Columbium	--	--	1.07	2.14	NT(1)	NT	
Pure Columbium	6.97	15.8	1.68	3.86	+1.29	+1.94	Edges and surface excellent.
Cb753	--	--	1.34	2.87	+1.51	NT	Good edges and surface.
Cb753	7.43	16.9	1.53	3.49	+1.96	+4.04	Edges and surface excellent.
Cb752	--	--	2.49	2.50	+0.76	NT	Some spot oxidation.
Cb752	10.28	13.78	2.51	3.37	+1.32	+2.02	Edges and surface excellent.
B66	--	--	2.28	2.78	+1.73	NT	Good edges and surface.
B66	13.38	16.80	2.67	3.36	+2.53	+6.03	Edges and surface excellent.
B43	--	--	2.66	2.68	+1.21	NT	Spalling at edges.
Cb-27Ti-7.3Cr(2)	--	--	--	--	+1.82	+4.84	

1. Not tested.
2. From Table VII.

A. Cb752

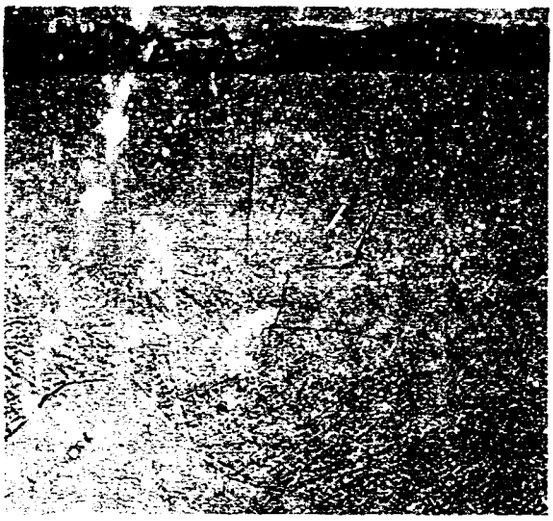

B. Cb753

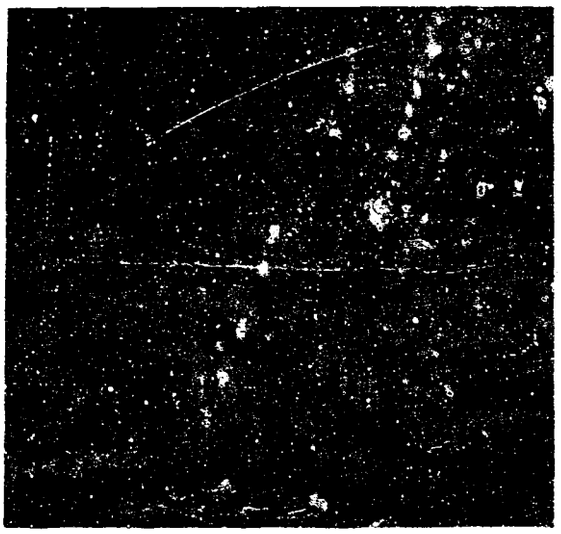

C. B66

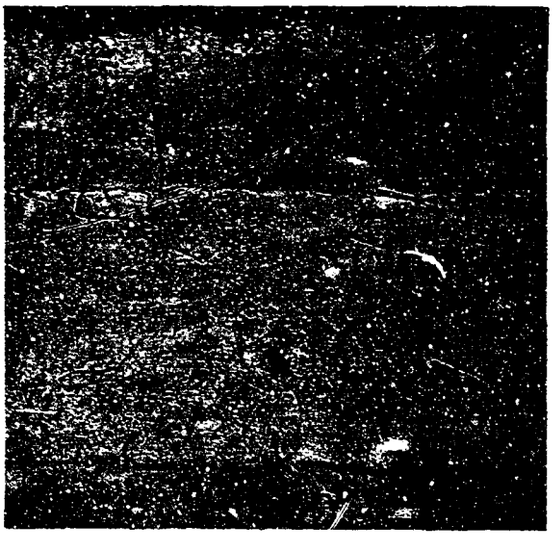

D. D43

Etchant: Lactic HNO_3HF

Magnification: 250X

FIGURE 63. COLUMBIUM ALLOYS COATED WITH TITANIUM AND ALUMINUM AND ANNEALED AT 2400 F FOR 15 HOURS

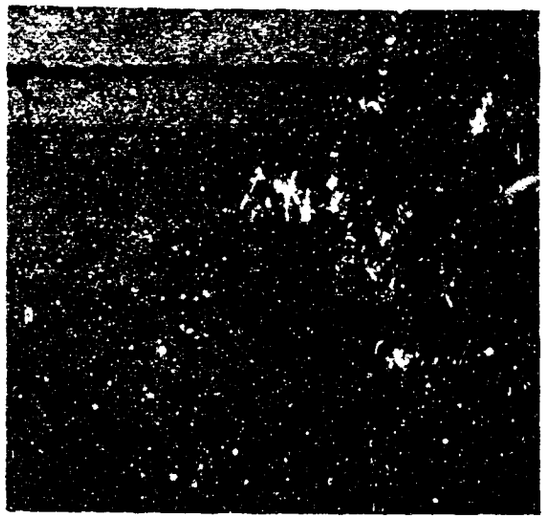

A. Cb753 (2.87/cm^2

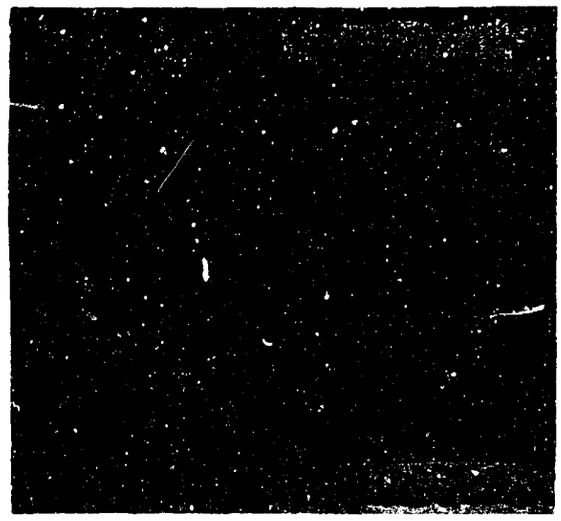

B. Cb752 (2.50 mg/cm^2)

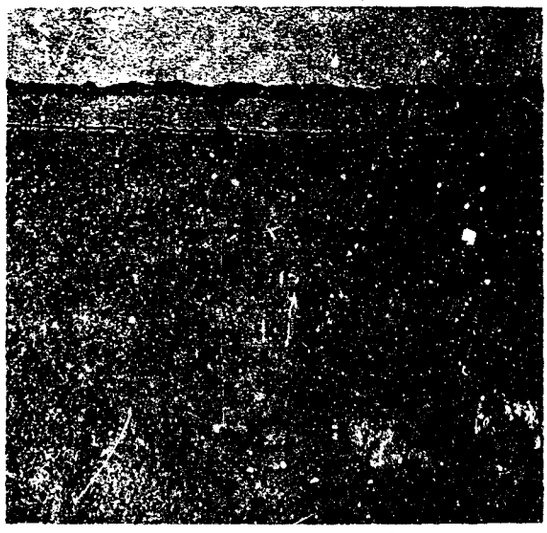

C. B66 (2.78 mg/cm^2)

D. D43 (2.66 mg/cm^2)

Etchant: Lactic HNO_3HF
Magnification: 250X

FIGURE 64. COLUMBIUM ALLOYS COATED WITH ALUMINUM AND ANNEALED AT 2400 F FOR 15 HOURS

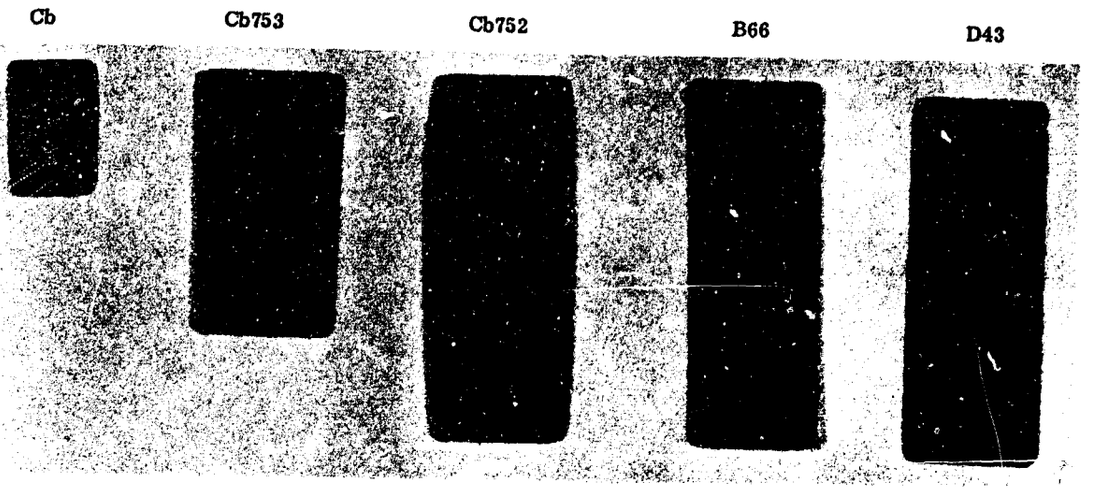

After 15-Hour Anneal at 2400 F

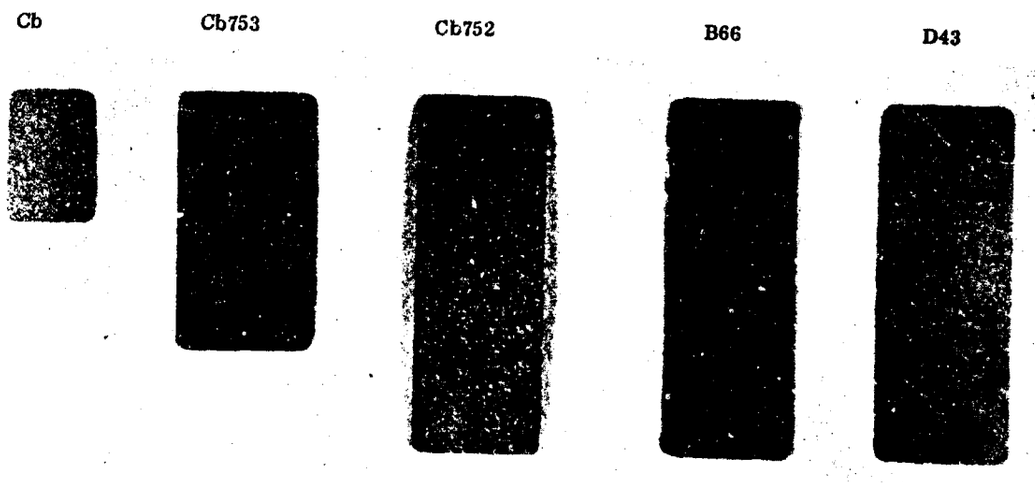

Oxidation Test at 1600 F at 4 Hours

FIGURE 65. TITANIUM + ALUMINUM COATED COLUMBIUM ALLOYS

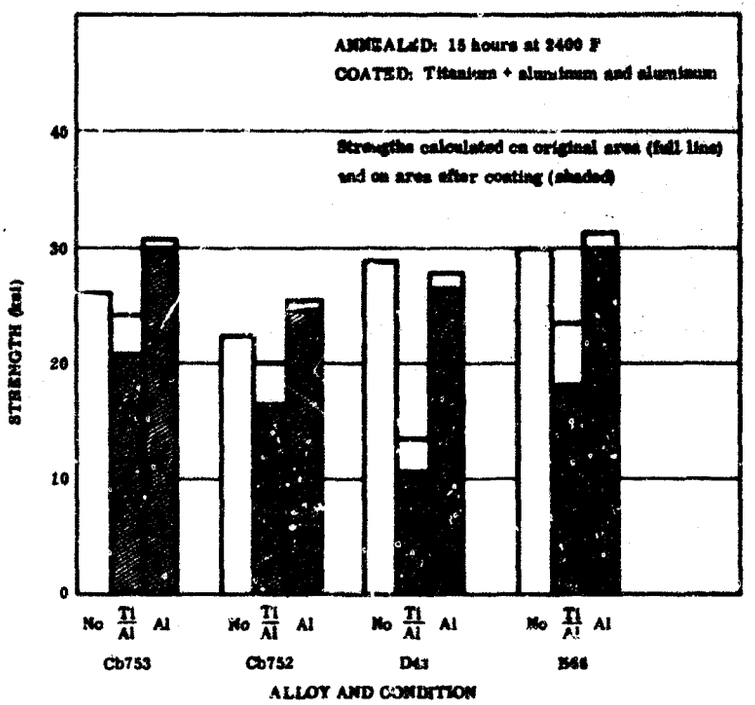

FIGURE 66. YIELD STRENGTH OF COLUMBIUM ALLOYS AT 2000 F

The test results for the aluminum-coated specimens were better than for the (Ti-Al) coated specimens, but metallography (Fig. 63) showed that this resulted from the preservation of an aluminide layer.

In the mechanical property studies, the limited availability of materials caused different thicknesses to be used for the different alloys. Four columbium alloys were studied:

- 0.021-inch Cb753
- 0.012-inch Cb752 (standard processing)
- 0.010-inch D43 (duplex heat treatment)
- 0.011-inch B66

Table XLII gives the mechanical properties of coated alloys after a 15-hour anneal at 2400 F to homogenize the coatings. The uncoated specimens were not given this anneal. The strengths reported in Table XLII are calculated on the original cross-sectional areas, but the thickness change for the 0.500-inch wide specimens are shown. Figure 66 presents the yield strength data calculated for both the original area and the cross-sectional area of the coated specimen.

TABLE XLII

MECHANICAL PROPERTIES AT 2200 F OF ALUMINIZED AND TITANIZED AND ALUMINIZED COLUMBIUM-BASE ALLOYS (1) (2) (3)

Alloy	Thickness (in.)		Type Coating	Yield Strength (psi)	Ultimate Tensile Strength (psi)	Elongation (%)
	Before Coating	After Coating				
Cb753	0.0210	-	None	26,240	29,103	58
Cb753	0.0208	0.0241	Ti + Al	22,420	24,831	56
Cb753	0.0210	0.0245	Ti + Al	25,858	27,194	60
Cb753	0.0215	0.0221	Al	32,242	33,644	39
Cb753	0.0207	0.0212	Al	29,526	30,833	41
Cb752	0.0119	-	None	22,530	27,729	16
Cb752	0.0118	-	None	22,202	28,409	15
Cb752	0.0118	0.0145	Ti + Al	20,724	24,651	39
Cb752	0.0118	0.0145	Ti + Al	19,230	22,202	55
Cb752	0.0119	0.0124	Al	26,042	30,295	28
Cb752	0.0119	0.0124	Al	25,043	26,087	38
D43	0.0100	-	None	28,896	33,024	22
D43	0.0105	0.0135	Ti + Al	13,752	17,181	52
D43	0.0191	0.0130	Ti + Al	13,292	15,848	50
D43	0.0104	0.0110	Al	27,970	30,693	13
D43	0.0102	0.0108	Al	27,770	30,808	16
B66	0.0112	-	None	27,358	28,301	50
B66	0.0112	-	None	32,288	32,887	30
B66	0.0112	0.0147	Ti + Al	23,105	25,323	34
B66	0.0112	0.0145	Ti + Al	24,011	25,188	40
B66	0.0112	0.0117	Al	27,777	28,482	29
B66	0.0110	0.0114	Al	34,539	36,184	25

1. See Table XLI for aluminum + titanium deposit weight and coating cycles. All specimens heat treated in argon for 15 hours at 2400 F before test.
2. One-inch gage length, 0.050 in./in./min.
3. Strength calculation based on cross section prior to coating.

Aluminum had little or no effect on both conventionally processed and duplex-processed columbium alloys. Although the specimens were given 15-hour anneals at 2400 F, the extent of alloying was limited after this treatment. The combination of titanium with aluminum in coatings caused marked loss of strength, particularly for the duplex-processed D43 alloy. Aluminum-titanium containing coatings were therefore not considered as candidates for Phase II and III coating systems.

4.2 ALUMINUM-CONTAINING SILICIDE COATINGS

4.2.1 Basis for the V-(Cr-Ti)-Al-Si system

The work performed at IITRI on this program showed that Cb-Ti-Al and Ti-Cr-Al solid solutions had good oxidation resistance at 1600 F and might, therefore, satisfy the requirements for a ductile, oxidation-resistant sublayer. Aluminum is apparently less deleterious to the strength (in terms of solid-solution effects) of columbium alloys than titanium and microprobe analyses (Ref. 9) have shown that aluminum does not enter the disilicide to any appreciable extent. It was concluded, therefore, that aluminum-containing substrates could be compatible with disilicide coatings and would have no marked adverse effects on columbium alloys.

Studies were initiated to investigate aluminum-containing sublayers and eventually led to the evaluation of the V-(Cr-Ti)-Al-Si coating system. These initial studies included:

1. Oxidation tests at 1600 F of arc-melted solid-solution alloys prepared at IITRI (par. 3.2.1).

2. Siliciding of solid-solution alloys followed by electron microprobe analysis.

3. Oxidation testing of additional compositions at temperatures up to 2400 F (par. 3.2.1)

4. The effect of aluminum and (Ti-Al) coatings on the mechanical properties and oxidation resistance of columbium alloys.

Items 1 and 3 were described previously in Paragraph 3.2.1 to provide continuity to the evaluation of sublayer properties. This section is, therefore, concerned with the evaluation of the silicided solid-solution alloys and aluminum and (Ti-Al) coatings on columbium alloys.

4.2.2 Siliciding of Cb-Ti-Al Solid-Solution Alloys

The purpose of this study wa to determine if aluminum-containing solid-solution alloys could be silicided successfully without side reactions causing interference by the aluminum.

A single specimen of each of the Cb-Ti-Al alloys was siliconized with a standard pack. The run condition, weight gain, and comments on appearance are given in Table XLIII.

TABLE XLIII

SILICIDE FORMATION ON Cb-Ti-Al ALLOY[1]

Specimen Number	Nominal Composition (wt %)	Si Deposition (mg/cm^2)	Comments
IITRI 13	91Cb-4Al-5Ti	19.16	Tendency to spall on sharp corners. General porosity. Fair.
IITRI 33	85Cb-5Al-10Ti	29.78	Even silicide coverage and little porosity. Many inherent cracks in this original specimen. Good.
IITRI 34	75Cb-5Al-20Ti	26.18	Fine smooth silicide coat. Sharp corners. Excellent.
IITRI 35	65Cb-5Al-30Ti	33.10	Smooth even silicide coat. Surface not as good as No. 34; however, it is a good tight coat. Sharp corners.
IITRI 36	40Cb-10Al-50Ti	25.46	Silicide coat looked good but rough. Corners tend to open up. Some deformation of specimens.
IITRI 37	55Cb-5Al-40Ti	21.60	Very good smooth silicide coverage. Corners sharp.
IITRI 38	30Cb-10Al-60Ti	25.46	Very irregular, heavy preferential buildup.

1. Evaluation of silicide pack cementation over Cb-Al-Ti coating compositions. 100 percent silicon, 1 percent NaF activator at 2150 F for 4.5 hours.

The specimens were introduced into the pack with sharply ground corners, i.e., with less than an 0.002-inch radius. The appearance after the very heavy silicide deposit was remarkable. The majority of the compositions exhibited perfect edge coverage except at porosity within the specimen. This excellent edge coverage may be the result of the low strength of the alloys which permits considerable creep of the alloy during growth of the silicide and during cooling.

Figures 67 through 72 show the appearance of silicided alloys.

Electron microprobe analysis of the silicided Cb-Ti-Al alloys were performed at IITRI. Line scans for the four elements, silicon, aluminum, titanium, and columbium were made.

Figures 73 through 76 show the superimposed traces for the four elements. The full-scale values varied from 100 cps (for aluminum) to as high as 3000 cps (for titanium). Table XLIV summarizes the results. No corrections have been applied to any of the data. However, by comparing the ratio of counts/second from the alloys and assuming nominal compositions, it was possible to gain a semi-quantitative value for the Cb:Ti ratios in the other layers. In addition, assuming the outer layer is the disilicide, the silicon content of other layers could be estimated using the appropriate disilicide. The aluminum content was estimated by comparison with an alloy containing the appropriate Cb:Ti ratio.

The probable identification of each layer is given in the last column of Table XLIV. The following conclusions were reached:

- The second layer has a different silicon content and has been identified tentatively as M_5Si_3 for alloys from Cb-10Ti-5Al to Cb-30Ti-5Al. At higher titanium contents, increasing amounts of aluminum and higher silicon contents make the interpretation less certain. A second disilicide with a different metal atom ratio has been observed in Ti-Cr-Si coatings. This may be the case for the 40 and 50 percent titanium alloys.

- The low and uncertain counts for aluminum in the alloy make calculations uncertain, but based on known aluminides the M_2Al or M_3Al phases are present in Cb-5Ti-4Al and Cb-10Ti-5Al. The 20 and 30 percent titanium alloys appear to contain MAl (gamma phase TiAl), although the variation of titanium across this phase (Fig. 76) may correspond to Cb_2Al at the inner face.

- No aluminide was present in the Cb-40Ti-5Al and Cb-50Ti-10Al composition, but there was a silicide phase containing some aluminum which was tentatively identified as M_5Si_3.

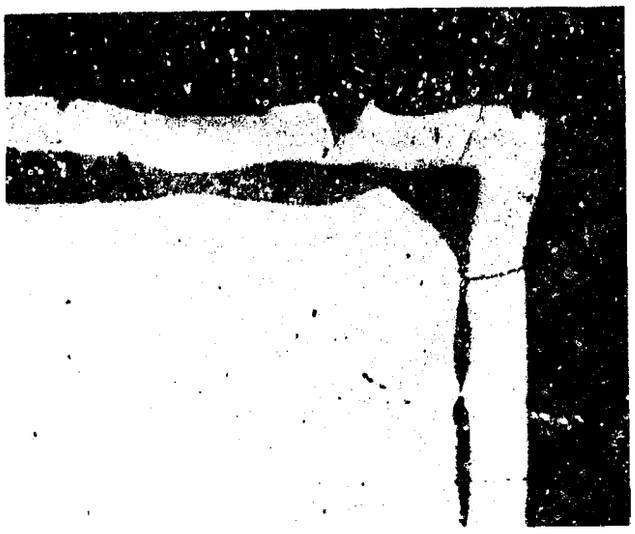

Solid-solution alloy; three layers in coating; freedom from cracks, especially at corner.

Etchant: Kellers
Magnification: 100X

FIGURE 67.
SILICIDED Cb-5Ti-4Al; IITRI13

Two-phase alloy showing segregation and porosity typical of arc-melt button; multiple layers in coating; freedom from cracks.

Etchant: Kellers
Magnification: 100X

FIGURE 68.
SILICIDED Cb-10Ti-5Al; IITRI33

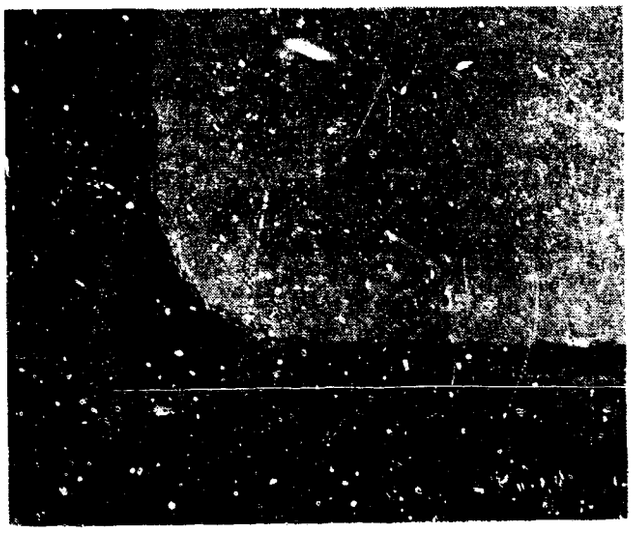

Unusual freedom from cracks and edge separation; solid-solution alloy; multiple layer coating.

Etchant: Kellers
Magnification: 100X

FIGURE 69.
SILICIDED Cb-30Ti-5Al; IITRI35

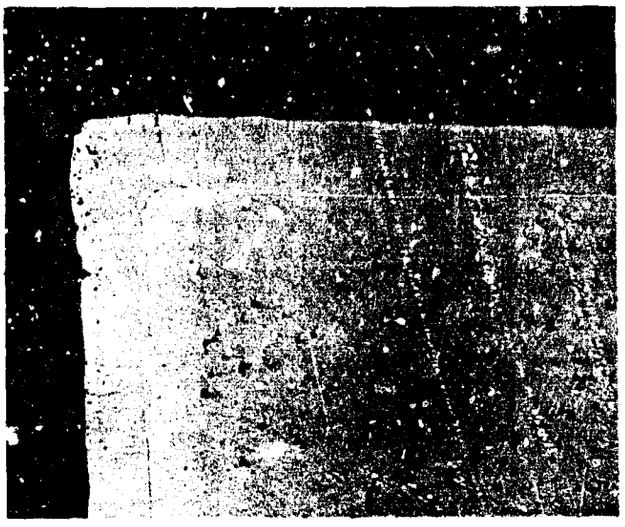

Excellent coating in spite of sharp corners.

Etchant: Kellers
Magnification: 100X

FIGURE 70.
SILICIDED Cb-40Ti-5Al; IITRI37

Excellent coating.

Etchant: Kellers
Magnification: 100X

FIGURE 71.
SILICIDED Cb-60Ti-10Al; IITRI38

Porosity in subsilicide layer; distinct aluminide (inner) layer, and excellent corner (crack formed in metallographic preparation).

Etchant: Kellers
Magnification: 100X

FIGURE 72.
SILICIDED Cb-20Ti-5Al; IITRI34

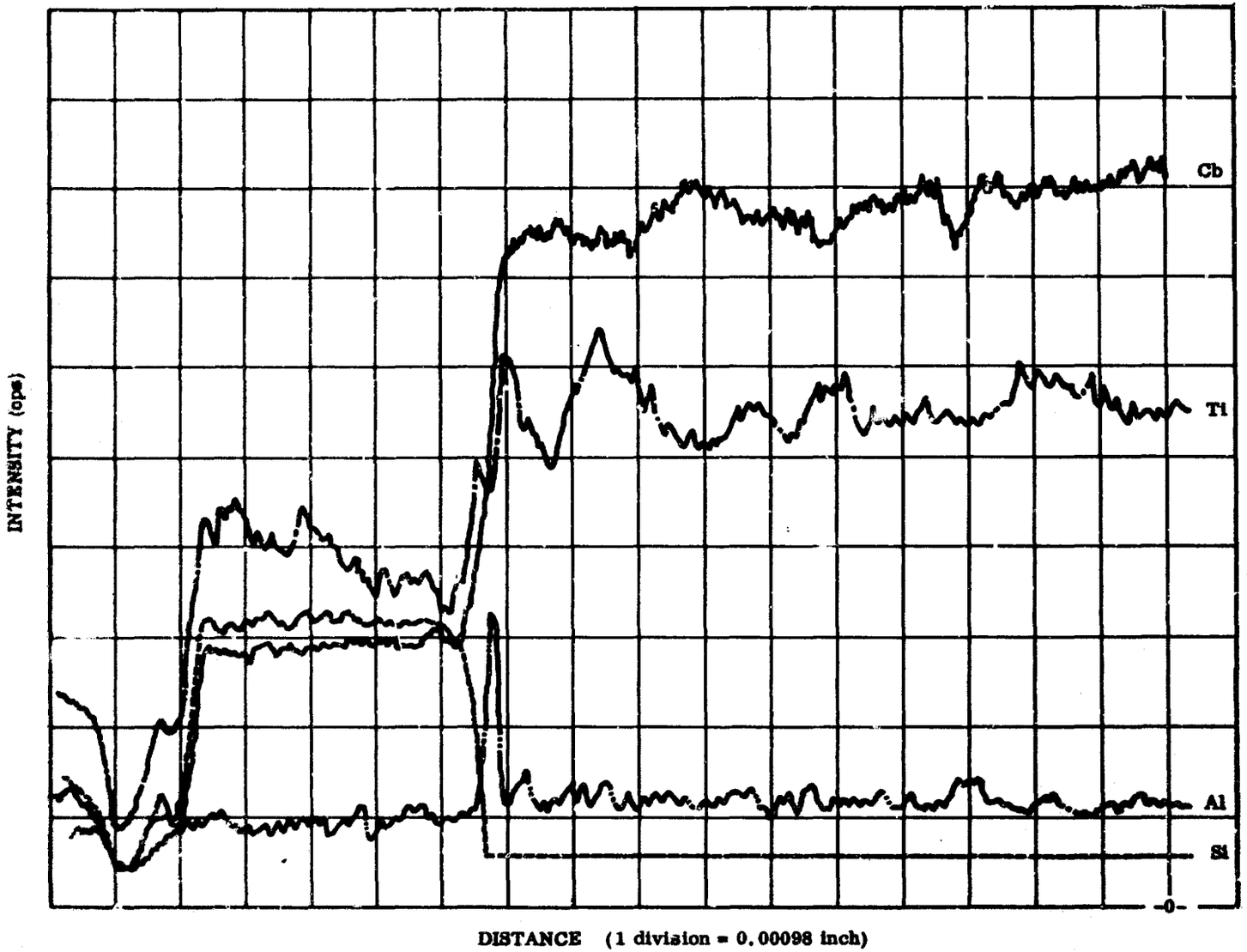

FIGURE 73. ELECTRON MICROPROBE SCAN OF Cb-4Al-5Ti ALLOY

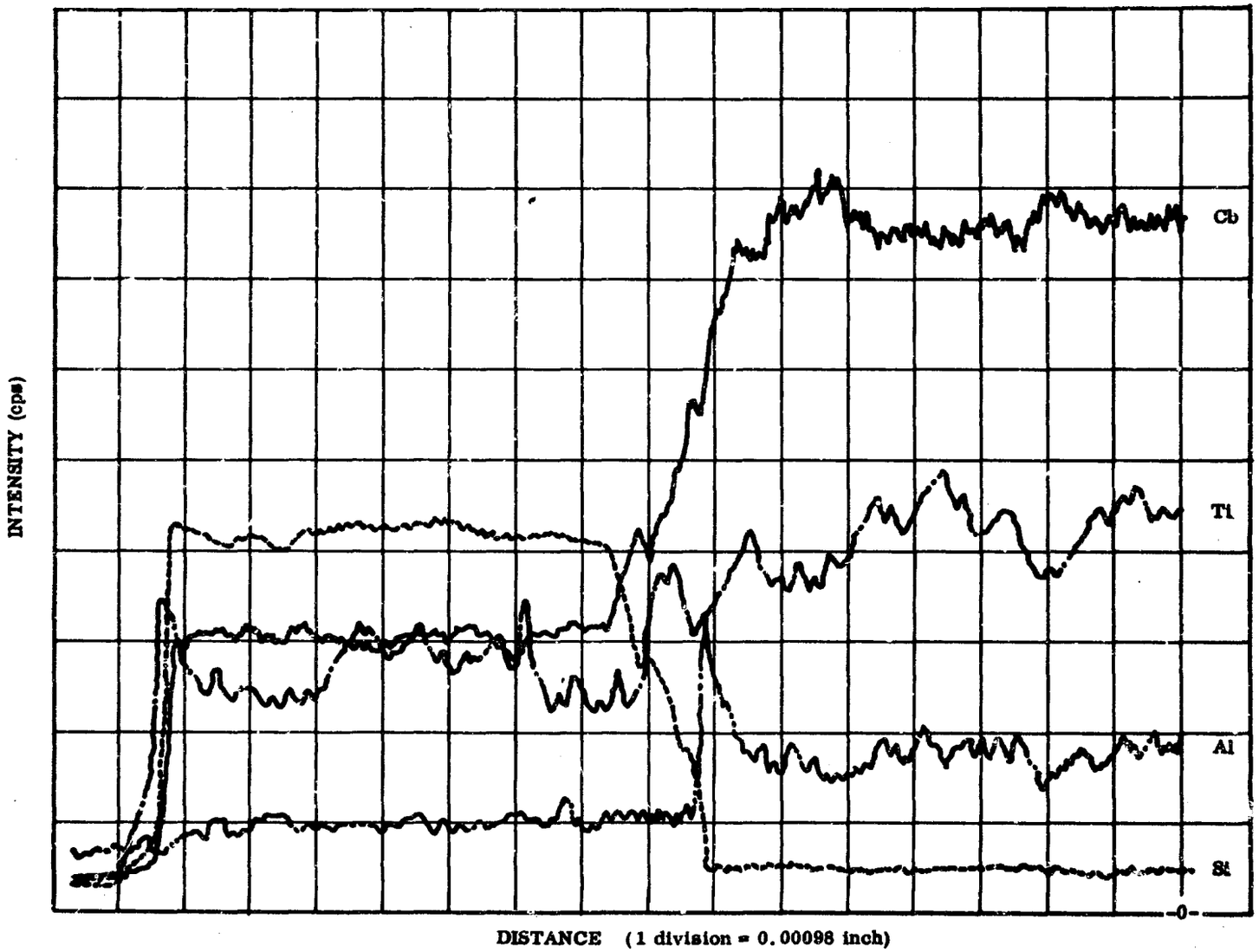

FIGURE 74. ELECTRON MICROPROBE SCAN OF Cb-5Al-10Ti ALLOY

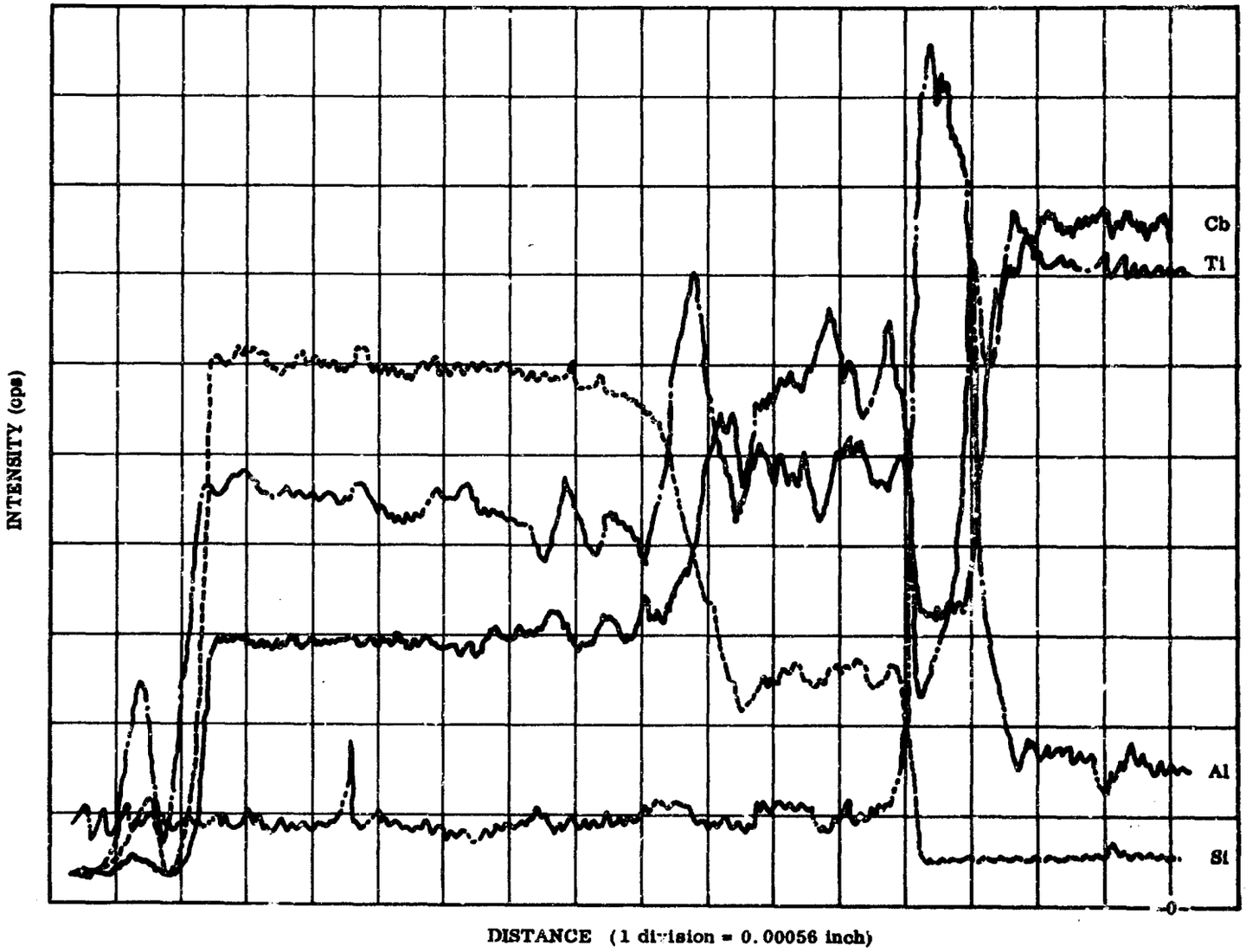

FIGURE 75. ELECTRON MICROPROBE SCAN OF Cb-5Al-20Ti ALLOY

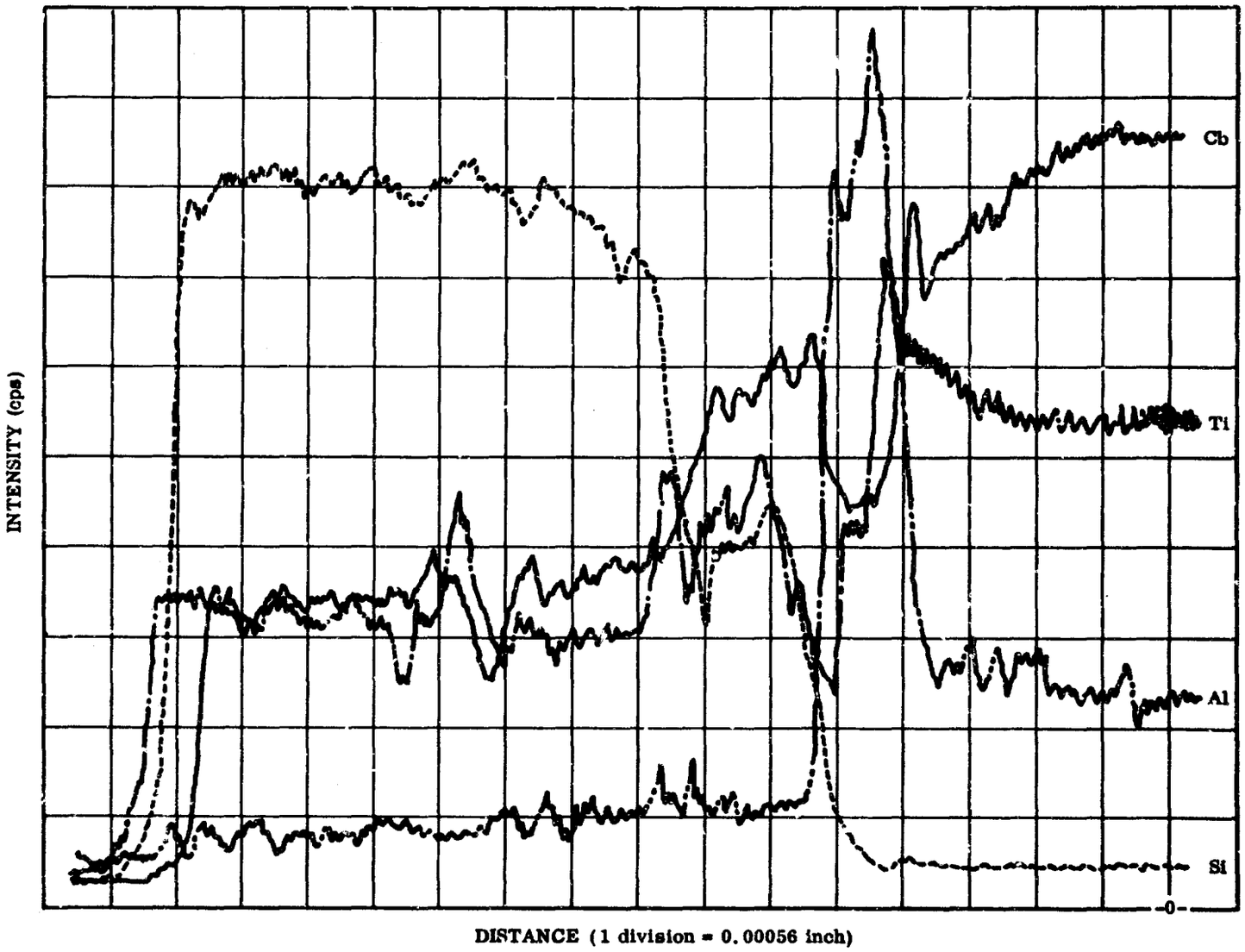

FIGURE 76. ELECTRON MICROPROBE SCAN OF Cb-5Al-30Ti ALLOY

TABLE XLIV

ELECTRON MICROPROBE RESULTS

Alloy	Composition (counts/second)				Identification
	Si	Al	Ti	Cb	
	(i) Outer layer - assumed to be disilicide.				
Cb-5Ti-4Al	260	4	90	240	Assumed to be disilicide
Cb-10Ti-5Al	390	3	230	270	Assumed to be disilicide
Cb-20Ti-5Al	580	0	410	370	Assumed to be disilicide
Cb-30Ti-5Al	750	3	840	310	Assumed to be disilicide
Cb-40Ti-5Al	700	13	1395	220	Assumed to be disilicide
Cb-50Ti-10Al	700	37	1180	205	Assumed to be disilicide
	(ii) Second layer				
Cb-5Ti-4Al	None	None	None	None	None
Cb-10Ti-5Al	(200)	4	220	400	Subsilicide (M_5Si_3)
Cb-20Ti-5Al	220	1	560	460	Subsilicide (M_5Si_3)
Cb-30Ti-5Al	360	6	1170	550	Subsilicide (M_5Si_3)
Cb-40Ti-5Al	715	19	1530	200	Disilicide with different Cb/Ti ratio
Cb-50Ti-10Al	600	40	1320	240	Disilicide with different Cb/Ti ratio
	(iii) Third layer				
Cb-5Ti-4Al	None	28	(160)	(800)	Cb_2Al
Cb-10Ti-5Al	1	23	(300)	(550)	Cb_2Al or Cb_3Al
Cb-20Ti-5Al	20	80	300	300	MAl (?)
Cb-30Ti-5Al	10	80	2100-600	420	Cb_2Al-MAl (?)
Cb-40Ti-5Al	265	19	2190	350	M_5Si_3
Cb-50Ti-10Al	360	45	1680	390	M_5Si_3
	(iv) Fourth layer - Base alloy				
Cb-5Ti-4Al	None	7	160	730	
Cb-10Ti-5Al	1	10	380	720	
Cb-20Ti-5Al	20	7	670	730	
Cb-30Ti-5Al	10	20	1500	820	
Cb-40Ti-5Al	None	40	2040	650	
Cb-50Ti-10Al	20	70	1850	590	

4.2.3 The Ti-Al-Si and Cr-Al-Si Coating Systems Containing Aluminum

Two additional coating systems containing aluminum were initially selected for oxidation testing. These were the Ti-Al-Si and (Cr-Ti)-Al-Si systems. Although mechanical property tests showed that titanium + aluminum layers were detrimental to the strength of columbium alloys, siliciding experiments on Cb-Ti-Al alloys showed that an excellent disilicide coating was formed over these alloys which was relatively crack-free. It was also anticipated that the order of deposition of titanium and aluminum layers might have some effect on the extent of interstitial migration from the substrate alloy into the coating sublayers.

Application of Titanium, Aluminum, and Cr-Ti Modifier Layers

Development and improvements of application techniques proceeded throughout the experimental program and, particularly in the early coating experiments, limitations on coating chemistry (layer thickness) and quality were imposed by application technology. For instance, it was found to be very difficult to deposit (80Cr-20Ti) uniformly onto a columbium alloy substrate; whereas, this alloy layer would deposit more readily if an intermediate vanadium layer was first deposited.

All modifier layers were deposited by halide pack processes from closed retorts. Coupon samples of D43, Cb752, or B66 alloys, after normal edge preparation and cleaning, were placed directly into the pack medium and fired in either high-purity argon or a sealed vacuum environment. Chloride or fluoride salts were used as the halide activator to effect vapor phase transport. The details of typical deposition processes are given in Section V. Deposition of the (Cr-Ti) layer was initially conducted from a prealloyed 60Cr-40Ti mixture, but later in the program an 80Cr-20Ti pack mixture was generally adopted since this composition appeared to provide a coating with longer life at 2400 F (Section V).

Typical deposition parameters for (Cr-Ti), titanium, aluminum, and silicon are shown in Table XLV. Deposition of (Cr-Ti) over aluminum resulted in the formation of a low melting point phase as evidenced by the growth of metallic whiskers on the surface, during diffusion annealing, and upheaval of the silicide layer in the final coating operation. However, it was found possible to siliconize the same system when the diffusion anneal (2400 F) stage was eliminated so that this melting was avoided. Specimens prepared in this manner were subsequently tested for oxidation resistance. Evidently, a low melting point phase was formed between some combinations of

TABLE XLV

DEPOSITION PARAMETERS FOR THE (80Cr-20Ti)-Al-Si AND Ti-Al-Si COATING SYSTEMS.

System Number	Alloy	Coating	Deposition Parameters											
			80Cr-20Ti			Titanium			Aluminum			Silicon		
			Temperature (F)	Time (hr)	Deposition (mg/cm^2)	Temperature (F)	Time (hr)	Deposition (mg/cm^2)	Temperature (F)	Time (hr)	Deposition (mg/cm^2)	Temperature (F)	Time (hr)	Deposition (mg/cm^2)
1	B66	(Cr-Ti)-Al-Si[1]-Si	2300	10	6.8 to 8.2	--	--	--	1600	2.5	1.6 to 2.7	1900	2.5	11.2 to 11.8
	D43	(Cr-Ti)-Al-D-Si	2300	10	6.8 to 9.1	--	--	--	1600	2.5	1.3 to 1.6	1900	2.5	11.5 to 12.9
2	B66	Al-(Cr-Ti)-Si	2300	10	5.4 to 7.0	--	--	--	1600	2.5	1.3 to 1.6	1850	2.5	12.2 to 12.9
	D43	Al-(Cr-Ti)-D-Si	2300	10	5.1 to 6.2	--	--	--	1600	2.5	1.3 to 1.4	1850	2.5	12.6 to 12.9
3	B66	Al-(Cr-Ti)-Si	2300	10	6.8 to 7.1	--	--	--	1600	2.5	1.3 to 1.4	1900	2.5	12.2 to 12.7
	D43	Al-(Cr-Ti)-Si	2300	10	5.3 to 6.19	--	--	--	1600	2.5	1.3 to 1.6	1900	2.5	12.7 to 12.3
4	B66	Ti-Al-D-Si	--	--	--	2000	6	13.9 to 16.9	1600	1.5	1.6 to 1.7	1850	4.0	9.1 to 9.3
	D43	Ti-Al-D-Si	--	--	--	2000	6	14.9 to 12.9	1600	1.5	1.6 to 1.7	1900	4.0	10.1 to 10.4
5	B66	Al-Ti-D-Si	--	--	--	2000	6	11.0 to 12.0	1600	2.5	1.3 to 1.6	1900	2.5	9.6 to 10.1
	D43	Al-Ti-D-Si	--	--	--	2000	6	9.0 to 10.2	1600	2.5	1.5 to 3.2	1900	2.5	10.6 to 10.9
6	B66	Al-Ti-Si	--	--	--	2000	6	7.2 to 11.6	1600	2.5	1.7 to 3.0	1850	4.0	10.7 to 11.2
	D43	Al-Ti-Si	--	--	--	2000	6	8.3 to 11.0	1600	2.5	1.6 to 3.2	1900	4.00	11.1 to 11.4

1. Diffusion anneal: 2400 F for 15 hours.

Pack Compositions - wt %

Ti:	90.9(67.0Ti-32.2W)	0.1NaF
Al:	10.0Al	89.0Al_2O_3 0.0%Cl
Ti-Cr:	99(20.0Ti-69.0Cr)	1.0NaF
Si:	99.0Si (-200 mesh)	1.0NaF

columbium, aluminum, chromium, and titanium. When specimens were siliconized without an intervening diffusion anneal, it is probable that most of the chromium and titanium were consumed to form the disilicide, before extensive diffusion had occurred, thereby eliminating the low melting point alloy composition.

The deposition rates of (Cr-Ti) from this 80-20 pack were less than anticipated, and a single 10-hour run gave what was considered to be the minimum acceptable thickness (based on a 10 to 12-mg/cm^2 deposit of silicon with no pure columbium disilicide). These specimens were then silicided and put into oxidation testing. However, it was shown in subsequent metallographic studies that the Cr-Ti alloy cover was not of uniform thickness, and it was likely, therefore, that the relatively poor oxidation resistant $CbSi_2$ was formed in certain areas. Systems 4 through 6 coated extremely well with excellent control over thickness and uniformity of deposit.

Oxidation tests were run on both systems, (Cr-Ti)-Al-Si and Ti-Al-Si, although it was recognized that the effectiveness of (Cr-Ti)-Al as a coating system could not be fully assessed because of the less than optimum coating quality.

Oxidation data for tests conducted at 1600 and 2400 F are summarized in Tables XLVI and XLVII. Total recorded weight gains with corresponding times are presented in the final columns. The weight measurements can only be regarded as an indication of the severity of oxidation since the weight changes were the result of a number of reactions. For instance, high weight gains (up to 0.1 mg/cm^2/hr) were noted at both 1600 and 2400 F for the first one- or two-hour exposure as a thin oxide layer was formed over the silicide; weight increases then fell off rapidly to <0.1 mg/cm^2/hr and in the case of coatings high in chromium content, negative weight changes were recorded after about 10 hours. For these columbium alloy coating systems, visual observation could usually predict the beginning of failures before weight changes.

TABLE XLVI

OXIDATION TESTS OF THE (80Cr-20Ti)-Al-Si AND Ti-Al-Si COATINGS AT 1600 F

System Number	Substrate	Coating	Appearance[1]	Oxidation Behavior	Total Weight Gain	
					(mg/cm^2)	(hr)
1	B66	Cr-Ti-Al-D[2]-Si	Purple-brown surface	Stopped test 26 hours. Disilicide chipped from surface - no signs of failure.	0.088	26
	D43	Cr-Ti-Al-D-Si	Purple-brown surface	Very thin outer silicide layer. Edge failures 9 and 26 hours.	0.022	5
2	B66	Al-Cr-Ti-D-Si	Upheaval of coating during siliciding	Good oxidation resistance despite pronounced chipping or flaking. Stopped test 26 hours.	0.041	26
	D43	Al-Cr-Ti-D-Si	Gray-brown	Good oxidation resistance despite pronounced chipping or flaking. Stopped test 26 hours.	<0.100	26
3	B66	Al-Cr-Ti-Si	Gray-brown	Silicide bursting, but no catastrophic failures, stopped test 26 hours, edge failures 10 and 22 hours.	0.550	26
	D43	Al-Cr-Ti-Si	Light brown	Silicide bursting, but no catastrophic failures, stopped test 26 hours, edge failures 10 and 22 hours.	<0.100	6
4	B66	Ti-Al-D-Si	Blue-gray, satiny	Stopped test 26 hours. Excellent.	0.170	26
	D43	Ti-Al-D-Si	Blue-gray	Stopped test 26 hours. Excellent.	0.290	26
5	B66	Al-Ti-D-Si	Gray-satiny	Stopped test 26 hours. Excellent.	0.100	26
	D43	Al-Ti-D-Si	Blue-gray	Stopped test 26 hours. Excellent.	0.250	26
6	B66	Al-Ti-Si	Gray, smooth	Beginning edge failures 26 hours.	0.670	26
	D43	Al-Ti-Si	Gray-brown	Edge failures 9 and 15 hours.	--	--

1. After first 5 hours exposure.
2. Diffusion anneal: 2400 F for 15 hours.

TABLE XLVII

CYCLIC OXIDATION TESTS OF THE (80Cr-20Ti)-Al-Si AND Ti-Al-Si COATINGS AT 2400 F

System Number	Substrate	Coating	Appearance[1]	Oxidation Behavior	Total Weight Gain	
					(mg/cm^2)	(hr)
1	B66	(Cr-Ti)-Al-D[2]-Si	Green-glazed surface	Stopped test 57 hours. Very low weight gains.	0.0057	57
	D43	(Cr-Ti)-Al-D-Si	Green-glazed surface	Failures. 15, 37 hours. Failed at thin areas in coating.	3.0000	34
2	B66	Al-(Cr-Ti)-D-Si	Formed low melting point phase. Upheaval of coating during oxidizing.	Completely oxidized. 7 hours.	---	---
	D43	Al-(Cr-Ti)-D-Si	Formed low melting point phase. Upheaval of coating during oxidizing.	No test.	---	---
3	B66	Al-(Cr-Ti)-Si	Brown. Not as glazed as shown in system 1	Stopped test 57 hours. Sign of failure.	1.6700	50
	D43	Al-(Cr-Ti)-Si	Brown. Not as glazed as System 1.	Failures 45, 50 hours. Edge failures.	1.5040	44
4	B66	Ti-Al-D-Si	Light-brown matte	Stopped test 57 hours. Fairly good.	0.0000	50
	D43	Ti-Al-D-Si	Gray-brown matte	Failures 36 hours. Bad surface.	2.4300	31
5	B66	Al-Ti-D-Si	Brown matte	Stopped test 57 hours, still good, considerable crazing.	1.5200	56
	D43	Al-Ti-D-Si	Brown matte	Stopped test 57 hours, fairly good, rougher surface.	3.0200	50
6	B66	Al-Ti-Si	Brown - slight glaze	Stopped test 57 hours, fairly good, considerable crazing.	2.3200	50
	D43	Al-Ti-Si	Brown - slight glaze	Both failed 37 hours, edge failures, surface good.	1.0000	33

1. After first five hours exposure.
2. Diffusion anneal: 2400 F for 15 hours.

At 1600 F the Ti-Al Systems 4 and 5 had the best surface appearance after 26 hours (first six hours in one-hour cycles, followed by eight-hour cycles). The (Cr-Ti)-Al coating generally had longer life on B[illegible] specimens, which was in accord with the observation on coating quality.

At 2400 F, the most promising system in terms of surface appearance and weight gains was System No. 1 (Cr-Ti)-Al-D-Si; however, the D43 samples had early failures at thin areas in the coating. These failures were on the flat surfaces and not at the edges, indicating that the coating would have longer potential life if a uniformly thick alloy layer is deposited. On the basis of these and earlier tests, it was decided that the Ti-Al systems did not have sufficient potential to warrant further studies.

These studies also showed that it was impractical to deposit (Cr-Ti) over aluminum and that satisfactorily uniform deposits of (80Cr-20Ti) directly on columbium alloy substrates was difficult to achieve because this alloyed layer apparently developed the very stable $CbCr_2$ Laves phase under these conditions.

4.2.4 V-(Cr-Ti)-Al-Si System

To finally establish if the presence of aluminum in the alloy sublayer was desirable, it was decided to modify the (Cr-Ti)-Al system by first applying a vanadium layer. Prior deposition of vanadium would allow deposition of a uniformily thick chromium-titanium layer while minimizing the formation of $CbCr_2$.

Close control over thickness and quality of deposited metallic layers was considered imperative for this series of experiments since many failures have been shown to originate at localized inhomogeneities caused by lack of control in the coating application techniques. Accordingly, preparation of the coating system V-(Cr-Ti)-Al-Si on D43 and Cb752 specimens was initiated.

Vanadium was applied in a closed, evacuated retort using a pack of 0.25-inch coarse granules of 99.8 percent purity and a 0.25 percent activator consisting of equal parts K_2VF_5 and NaF. Two 15-hour runs at 2150 F were required to deposit an average of 15.0 mg/cm^2 of vanadium. Aluminum and (80Cr-20Ti) were deposited by the previously described techniques to give an average of 1.5 and 16.0 mg/cm^2, respectively.

The specimens were silicided in the usual high-pressure pack to give three silicide thicknesses corresponding to weight increases of 7, 14, and 17 mg/cm^2, (i.e., 1.0, 2.0, and 2.5 mils).

The appearance of a typical sample in the as-coated condition is shown in Figure 77. The large open cracks which are evident in the coating on this D43 specimen are a result of pullout during metallographic preparation. It is virtually impossible, however, to identify the cause of fine cracks as being due to metallographic preparation or to differential stresses that arise in cooling from the coating temperature. It was not possible, with current metallographic techniques, to satisfactorily etch coated samples to reveal the structure of the substrate metal. It appears that the chemically active silicide has some inhibitory effect on the normal etching reaction.

Samples with the three silicide thicknesses were oxidation tested at 2400 F, but only the heaviest silicide coating was tested at 1600 F. These oxidation data are presented in Tables XLVIII and XLVIX.

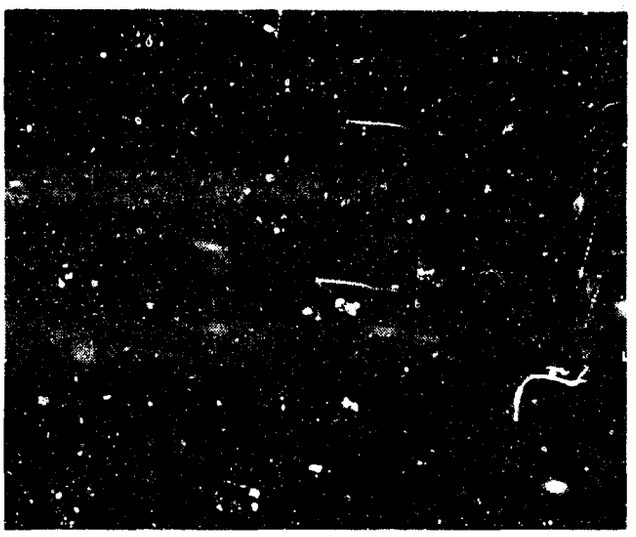

Magnification: 100X

As coated

Magnification: 500X

FIGURE 77. V-(Cr-Ti)-Al-Si COATING ON D43 ALLOY

TABLE XLVIII

2400 F OXIDATION TEST DATA OF THE V-(Cr-Ti)-Al-Si COATING

Substrate	Number of Samples	Coating Layer (mg/cm^2)				Time to Failure in Hours (1-hour cycle)	Total Weight Gain (mg/cm^2)	Remarks
		V	Cr-Ti	Al	Si			
Cb752	2	17	16.0	1.6	7.0	2, 3	3.87, 1.89	Good glaze.
D43	2	14	15.5	1.3	7.0	6, 15	1.50, 0.87	Weighed after six hours only
Cb752	3	17	16.0	1.6	14.0	57, 83, 86	4.06, 3.91 5.24	Very slow oxidation rate after initial failure site observed. Edge failure. Good glaze.
D43	3	14	15.5	1.5	14.8	35, 104, 106	2.52, 2.70 5.06	Very slow oxidation rate after first pinhole (corners). Two specimens further exposed 120 and 133 hours without much additional loss of substrate.
Cb752	2	17	16.0	1.6	17.0	111, 128	6.22, 6.61	Edge failures - very slow substrate decay after first signs of failure.
D43	2	14	15.5	1.3	18.4	100, 100	6.22, 5.85	Test stopped. Edge failures developing at 93 hours. No increase in weight-gain rate.

TABLE XLIX

1600 F OXIDATION TEST DATA ON THE V-(Cr-Ti)-Al-Si COATING

Substrate	Number of Samples	Coating Layer (mg/cm^2)				Time to Failure in Hours (16-hour cycle)	Total Weight Gain (mg/cm^2)
		V	Cr-Ti	Al	Si		
Cb752	1	17	16.0	1.6	17.0	509+	0.47
D43	1	14	15.5	1.3	18.4	509+	0.39

At 2400 F, the thinnest silicide coating resulted in predictable early failures since metallography showed an uneven silicide layer with regions having essentially no silicide protection.

The standard 0.002-inch thick silicide produced better results with 86 and 106 hours of life, respectively, for Cb752 and D43 specimens. One specimen from each batch (three specimens) failed at edge sinter sites considerably earlier than the

remaining two. This coating appeared to have exceptional self-healing properties since after the initial failure site had been observed (usually edge or corner) extremely slow oxidation of the substrate took place, and in the case of one D43 sample, even after an additional 30 cycles, the defect did not propagate very far and slow weight gains were recorded. A good, glazed surface was preserved over the remainder of the specimen surfaces.

The coating with the heaviest silicide layer showed higher weight gains than normally observed, but a high density, slightly glazed surface was obtained which appeared to be very stable. Both D43 samples were removed from testing at 100 hours with small edge failures, while the Cb752 samples were removed after 111 and 128 hours with the development of edge failures.

The appearance of these four samples after 93 hours at 2400 F is shown in Figure 78. One D43 sample was placed back into test after it had failed in order to observe the decay rate. The appearance of this specimen after a total of 133 hours is shown in Figure 79. It was apparent that the oxidation rate of the substrate was considerably retarded - probably due to the presence of a low melting point glass which had formed between V_2O_5, Al_2O_3, and SiO_2. The formation of an oxide glaze is particularly evident in Figure 80 which shows a Cb752 sample with 14.0 mg/cm^2 of silicon after 83 hours at 2400 F. Figure 81 shows a D43 sample with the thicker silicide coat after 100 hours at 2400 F. Only one sample of each alloy (with 17.0 mg/cm^2 of silicon was tested at 1600 F due to a shortage of specimens. The excellent stability of this coating at 1600 F is shown by the low weight gains in Table XLIX, and the appearance of the coating after 500 hours exposure (Fig. 82 and 83).

Owing to the complexity of the application processes, it is doubtful if this coating composition is of practical significance unless a simpler application technique such as a spray or paint slurry can be developed.

These experiments do indicate, however, that the combined presence of aluminum, vanadium, and silicon can result in the formation of a relatively stable and fluid glass which imparts excellent self-healing properties to the coating.

D43

Magnification: Approximately 1.5X

Cb752

FIGURE 78.

D43 AND Cb752 SPECIMENS AFTER 93 HOURS AT 2400 F

Magnification: Approximately 2X

FIGURE 79.

D43 SPECIMEN AFTER ADDITIONAL 40 HOURS (133 TOTAL) AT 2400 F

Magnification: 100X

Magnification: 500X

FIGURE 80. Cb752 COATED WITH V-(Cr-Ti)-Al-Si (14.0 mg/cm^2 Si) OXIDATION TESTED 83 HOURS AT 2400 F

Magnification: 100X

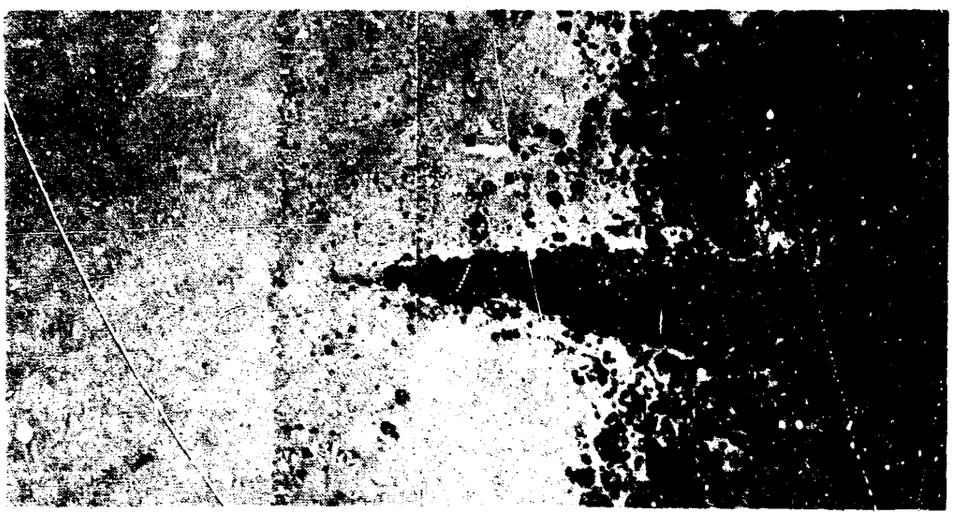

Magnification: 500X

FIGURE 81. D43 COATED WITH V-(Cr-Ti)-Al-Si (180 mg/cm^2 Si); 100 hrs at 2400 F

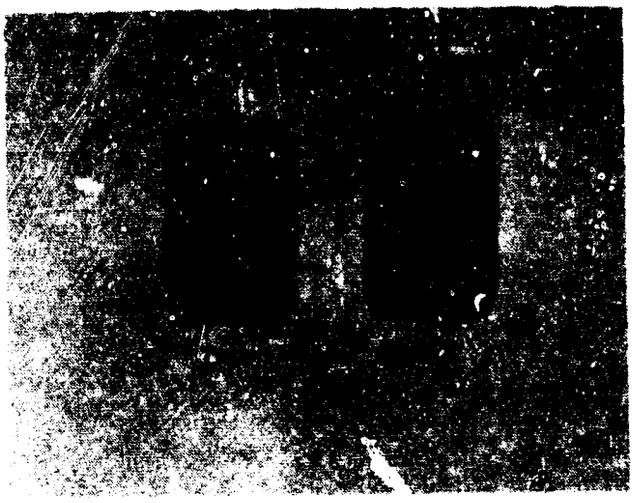

Magnification: Approximately 1.5X

FIGURE 82.

D43 AND Cb752 SAMPLES AFTER 500 HOURS AT 1600 F; 16-Hour Cycles

4.3 THE SILICIDE-CERAMIC SYSTEM

4.3.1 Basis For The System

Very little effort has been concentrated on the development of ceramic coatings for use on the columbium-base alloys. This apparent omission is understandable in light of the fact that silicate-base ceramic coatings cannot be applied directly without severe embrittlement of the alloy by oxygen. To be used effectively, ceramic coatings require an oxygen barrier making the application of two coats imperative.

In the early work on refractory metal coatings, when single-cycle coatings were the rule and the major activities were concentrated in the simple or modified silicide, the use of ceramic coatings would have added another processing step after the silicide process. Now, however, when the duplex (metal-silicon) coating requiring a minimum of two cycles is the rule rather than the exception, a process incorporating a ceramic coating as one of the steps is certainly feasible.

Ceramic coatings have definite potential advantages and disadvantages as coatings for the columbium alloy. The advantages are:

- A low softening temperature that minimizes stress crack formation because of differential thermal expansion.
- Controlled composition - the coating is not generated from the metal and consequently its composition is, in general, not affected by it.
- Low cost of application - the coating is applied by spraying or dipping and then air fired for periods usually less than 15 minutes.

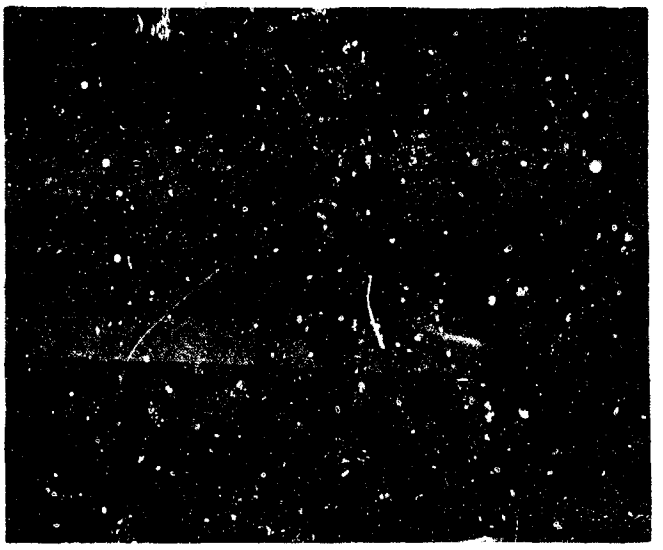

Magnification: 100X

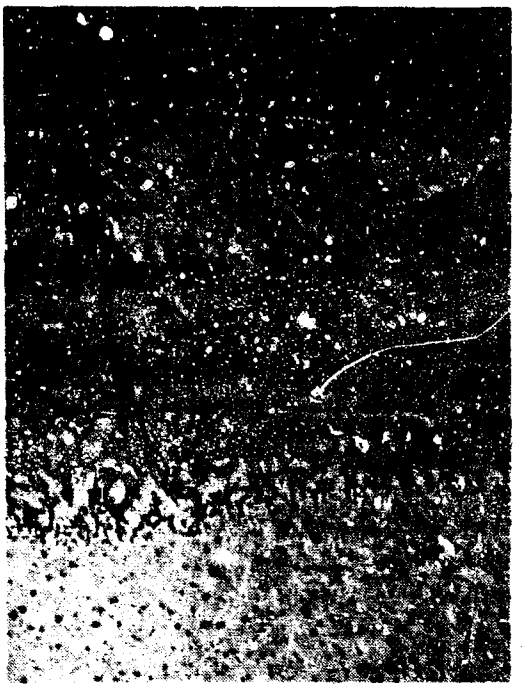

Magnification: 500X

FIGURE 83. V-(Cr-Ti)-Al-Si COATING ON Cb752 ALLOY: Oxidation Tested 509 Hours at 1600 F, 16-Hour Cycles

- **The part size that can be coated is almost unlimited.**
- **Part distortion in firing is minimized because heating can be uniform.**

The disadvantages are:

- **Cannot be applied directly to the substrate.**
- **The low softening point and viscous properties do not permit application to parts that are subject to severe erosion, aerodynamic shear, or centrifugal forces.**

The disadvantages of ceramic coatings restrict their potential usage, in gas turbines, primarily to parts where ceramic coatings have been used successfully in the modern gas turbine engine, i.e., in combustion chambers, transition liners, afterburner liners, and tail cones. Application to blade and vanes is not feasible. In manned reentry applications, there does not appear to be any restriction to the use of ceramic coatings. The aerodynamic shear is not believed to be high enough to produce any significant amount of viscous flow.

Because of the potential of ceramic coating in protecting columbium-base alloys, a small screening program was set up to determine, with a minimum of laboratory effort, whether or not ceramic coatings justified a more detailed study. Coatings were prepared for the screening effort using commercially available frits[1] and refractory mill additions. A straight, simple silicide coating applied by pack cementation was used as an oxygen diffusion barrier. The material and procedure are described in subsequent paragraphs.

4.3.2 Deposition of The Coating

Two alloys were used in the study - Cb752 (0.012 inch) and D43 (0.006 inch). The standard specimen size was 0.5 inch by 0.75 inch. The specimens were hand finished to remove all burrs and sharp edges and then silicide coated using the following pack and cycle:

- Composition: 100 parts silicon (-100 +200 mesh)
  1 part NaF (Reagent)
- Cycle: Graphite lined Inconel retort - 15 hours at 1900 F
  Deposit weight was 12 mg/cm^2

1. Frit - a thermally fractured glass.

Four relatively refractory frits were selected for use in the program. All of the frits have been used successfully in coatings designed for use at high temperature in jet and reciprocating engines or in nuclear reactors. Basically, all of the frits are barium silicate glasses with other additives. The distinguishing feature of each frit is given below.

Frit	Characteristics
NBS 332[1]	Alkali oxide free, barium borosilicate glass. Low SiO_2 and high BaO percentages.
Solar S5210[1]	Low alkali oxide, barium borosilicate glass. High SiO_2 and moderate BaO percentages.
Solar S35[1]	Low alkali oxide, boron-free, barium silicate glass. High SiO_2 and moderate BaO percentages.
Solar S355[1]	Very low alkali oxide, boron-free, barium silicate. High SiO_2 and moderate BaO percentages.

Ceramic slips[2] were prepared by ball milling various refractory oxides with the frits, a clay suspending agent, and water until 0 to 1 gram from 50 milliliters of slip was retained on a 325 mesh standard sieve. The slip was adjusted to a specific gravity of 1.70. The compositions of the slips are shown in Table L.

The slips were applied to the silicide-coated specimens by spraying. Two coats were applied (0.001 inch ± 0.0005 inch thick) with firing between each coat. Firing was performed in a gas-fired furnace at temperatures between 1900 and 2300 F for seven minutes. The best firing temperatures for each of the coatings is shown in Table LI. Typical as-fired specimens are shown in Figure 34.

Oxidation testing of ceramic-coated specimens was performed in air at 2400 F in Burrell tube furnaces. Four-hour cycles were standard. Support boats were primary Leco boats (modified zircon).

---

1. These frits are all commercially available. The NBS 332 frit can be obtained from any of the major suppliers of porcelain enamel frit. The Solar frits are produced under license by the Ferro Corp., Cleveland, Ohio.

2. The finely milled paint-like slurry-containing frit, other refractory mill additions, electrolytes, water, and suspending agents.

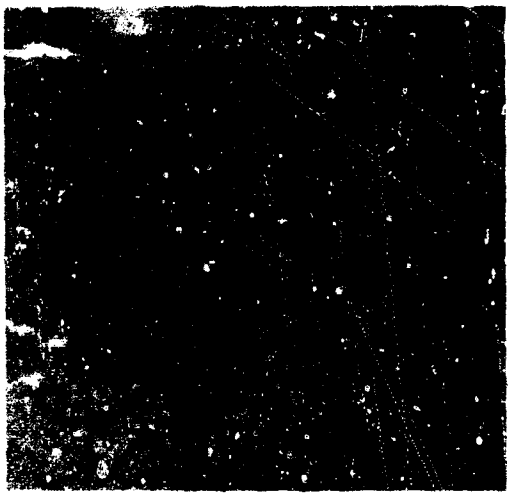

Coating: Simple Silicide Base
Double Coat of A-418-2

Coating: Simple Silicide Base
Double Coat of SOLARAMIC S61-2

FIGURE 84. TYPICAL AS-COATED APPEARANCE OF CERAMIC-COATED Cb752 ALLOY

TABLE L

COATING COMPOSITIONS - PARTS BY WEIGHTS

Coating Number	NBS332	Green Label Clay	TiO_2, TG	Cr_2O_3	SiO_2	Treopax	Solaramic S5210	Solaramic S35	Solaramic S355
A418	70	5		30					
A418-1	70	5	80	30					
A418-2	70	5	40	30	40				
A418-3	70	5	40	30		40			
S61		6	40	5			100		
S61-1		6	80	5			100		
S61-2		6	40	5	40		100		
S61-3		6	40	5		40	100		
S35A		6	40	5				100	
S35A-1		6	80	5				100	
S35A-2		6	40	5	40			100	
S35A-4		6	80	5	80			100	
S35A-5		6	40		40			100	
S35A-6		6	80		80			100	
S355A		6	40	5					100
S355A-1		6	80	5					100
S355A-2		6	40	5	40				100
S355A-5		6	160	5					100
S355A-7		6		5	100				100
S355A-8		6	80	5	80				100

TABLE LI

COATING PROPERTIES

Coating Number	Firing Temperature (7 minutes)						Remarks
	1950 F	2000 F	2050 F	2150 F	2200 F	2300 F	
A418	Good(1)						Glassy
A418-1		Spall		Spall		Spall	
A418-2		Good(1)		Spall		Spall	Matte
A418-3		Spall		Spall		Spall	
S61			Good(1)				Semi-matte
S61-1		Good		Good	Good(1)	Good	Matte
S61-2		Good		Good	Good(1)	Good	Semi-matte
S61-3		Spall		Spall		Spall	
S35A		Good(1)					Semi-matte
S35A-1		Good		Good	Good(1)	Good	Semi-matte
S35A-2		Good		Good	Good(1)	Good	Semi-matte
S35A-4					Good(1)		Matte
S35A-5					Good(1)		Mottled
S35A-6					Good(1)		Matte
S355A		Good(1)					Matte
S355A-1		Good		Good	Good(1)	Good	Semi-matte
S355A-2		Good		Good	Good(1)	Good	Matte
S355A-5					Good(1)		Mottled
S355A-7					Good(1)		Semi-matte
S355A-8					Good(1)		Matte

1. Recommended firing temperature.

4.3.3 Oxidation Test Results

The coatings that could be successfully fired on silicide-coated Cb752 or D43 alloys (Table LI) were oxidation tested at 2400 F. The test results are contained in Table LII and typical specimens after test are shown in Figure 85 and Figure 86.

The A418 series of coatings was completely unsatisfactory due to inadequate refractoriness and to the rapid loss of chromium sesquioxide from the coatings. As an example of the rate of loss of chromium oxide, the color was observed to change from a brilliant green in the A418 coating (30 percent Cr_2O_3) before test to gray in four hours at 2400 F. Removal of the Cr_2O_3 mill addition and replacement with TiO_2 and/or SiO_2 may be a means of improving the coating performance.

Of the SOLARAMIC series coatings, S61, S35, S355, composition S61-2, S35A-2, and S355A-5 were the best in each series. All of these coatings could withstand at least three 4-hour cycles at 2400 F without catastrophic failure. The specimens appeared to be in excellent condition (Fig. 85) except at the support holes and contact points.

Reaction of the ceramic coatings with the support boat continually plagued the oxidation phase of the program. Coating the boats with the ceramic slip and prefiring decreased the reaction slightly, but offered no permanent solution. Figure 86 shows typical reaction sites on several typical specimens. Reaction of specimens with a support boat precluded any evaluation of the actual cycle life of the coatings.

Weight change measurements on two coatings, exhibiting a minimum of boat reaction, are plotted in Figure 87 and are compared to the Cb752 alloy with the straight silicide only. Considerable improvement in surface stability is effected with the ceramic coatings.

Photomicrographs are shown in Figures 88 and 89 of a typical ceramic coating before and after oxidation testing. The underlying silicides, as-coated specimen, can be seen to exhibit a typical uniform crack pattern which is probably the result of differential thermal expansion. The cracks do not, in general, propagate through the ceramic coating.

The large bubble structure in the as-coated specimens is probably the result of outgasing the silicide coating or columbium alloy rather than reaction with the substrate. This conclusion is based on the fact that the porosity does not appear in the tested coating (Fig. 89).

TABLE LII

CERAMIC COATING CYCLIC OXIDATION IN AIR

Coating	Substrate	First Cycle	Second Cycle	Third Cycle
A418	0.012-in. Cb752	Glassy, chrome volatilizing	Failed, contact failures	
A418-2	0.012-in. Cb752	Attack at hole	Attack at edges	Failure at hole, oxide on surface
S61	0.012-in. Cb752	Glassy, smooth	Contact failures	
S61-1	0.012-in. Cb752	Attack at hole and contact	Continued attack at hole and contact	Some oxidation
S61-2	0.012-in. Cb752	Good, no change	Slight attack at hole and contact	Good, except for hole and contact
S35A	0.012-in. Cb752	Good, smooth surface	Contact failure surface good	
S35A-1	0.012-in. Cb752	Good, glassy	Attack at contact area	Continued attack at contact area
S35A-2	0.012-in. Cb752	Good	Slight attack at contact area	Continued attack at contact area,
S35A-4	0.012-in. Cb752	Pinhole failures, hole and edge failures	Continued pinhole failure	
S35A-5	0.012-in. Cb752	Hole failure on one specimen	No attack on one specimen	One specimen good
S35A-6	0.012-in. Cb752	Good	Edge failure on one specimen	Start of edge failure on one specimen
S355A	0.012-in. Cb752	Good, glassy	Contact failure	
S355A-1	0.012-in. Cb752	Good edges, attack at contact area	Continued attack at contact area	Glassy
S355A-2	0.012-in. Cb752	Attack at contact	Continued attack at contact	Severe attack at contact. Glassy
S355A-5	0.006-in. D43	Good	Good	Darker, some oxide
S355A-7	0.006-in. D43	Pinholes	Failure complete	
S355A-8	0.006-in. D43	Pinhole and hole attack	Continued attack, darker	

Two specimens tested for each coating cycle - four hours at 2400 F

The microstructure of the tested specimens (Fig. 89) shows severe oxidation and enlargement of the cracks in the silicide coating; although the ceramic coatings appear to be affording excellent protection to the substrate, severe oxidation of the silicide coating is occurring. The ceramic coatings in the thicknesses applied appear to be inadequate as oxygen barriers to prevent the very rapid oxidation that is characteristic of fissures in straight silicide coatings. Some of the oxidation at fissure can be ascribed to pores in the ceramic coating, but others appear to occur underneath a continuous ceramic coating (Fig. 89).

Alloy: 0.012-inch Cb752

Magnification: 2X

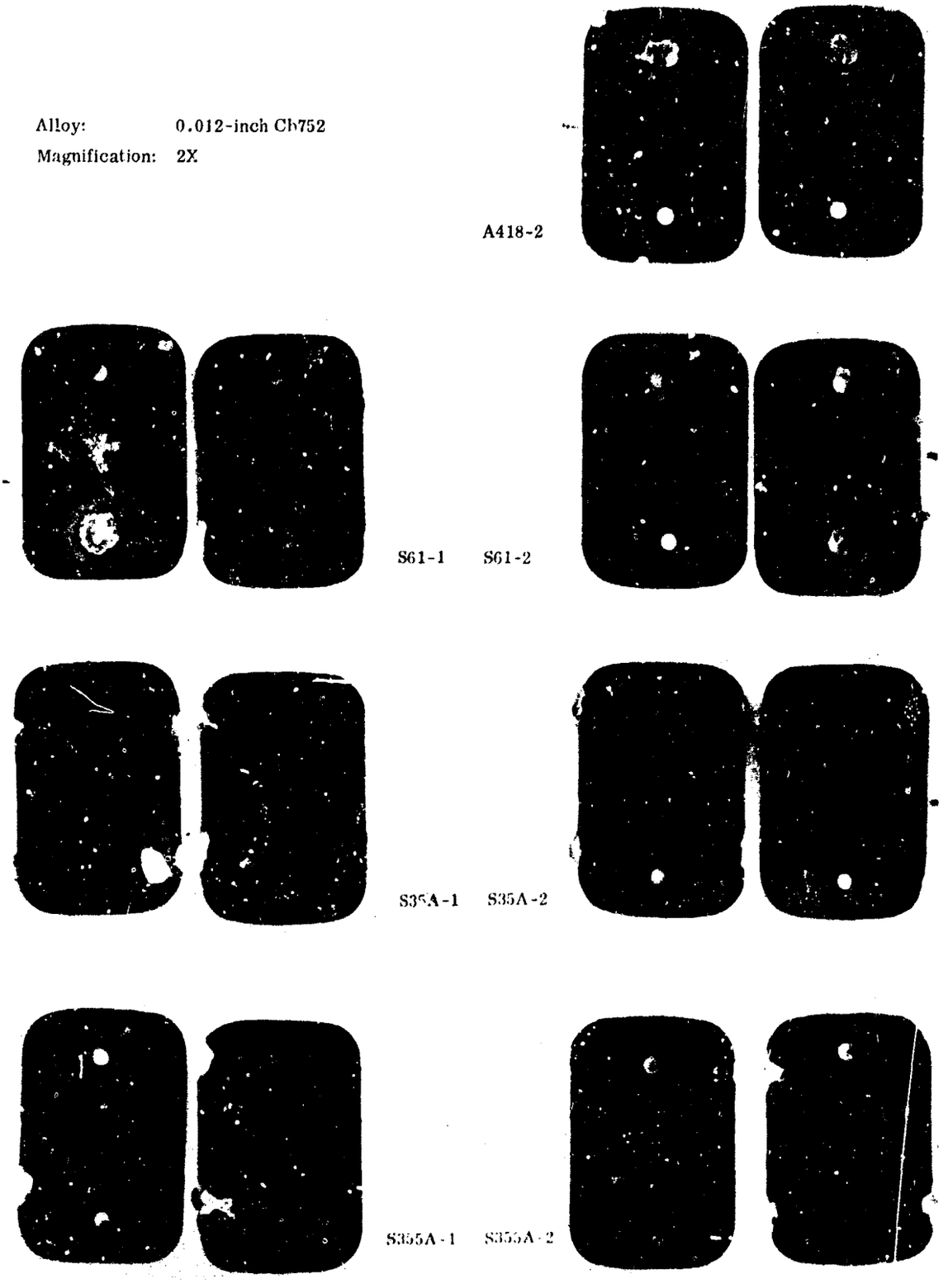

FIGURE 85. TYPICAL CERAMIC-COATED SPECIMEN AFTER THREE FOUR-HOUR CYCLES AT 2400 F

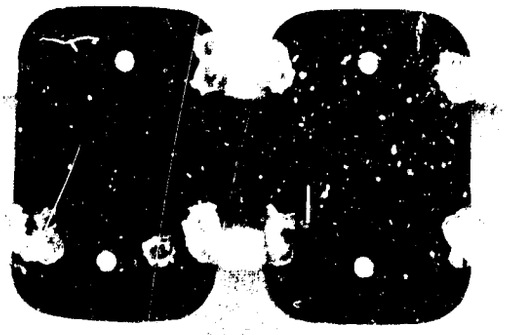

Coating: S35A-1
Alloy: 0.012-inch Cb752
Magnification: 2X

Coating: S35A-2
Alloy: 0.012-inch Cb752
Magnification: 2X

FIGURE 86. TYPICAL CONTACT AREA FAILURES OF CERAMIC COATINGS AFTER THREE FOUR-HOUR CYCLES AT 2400 F

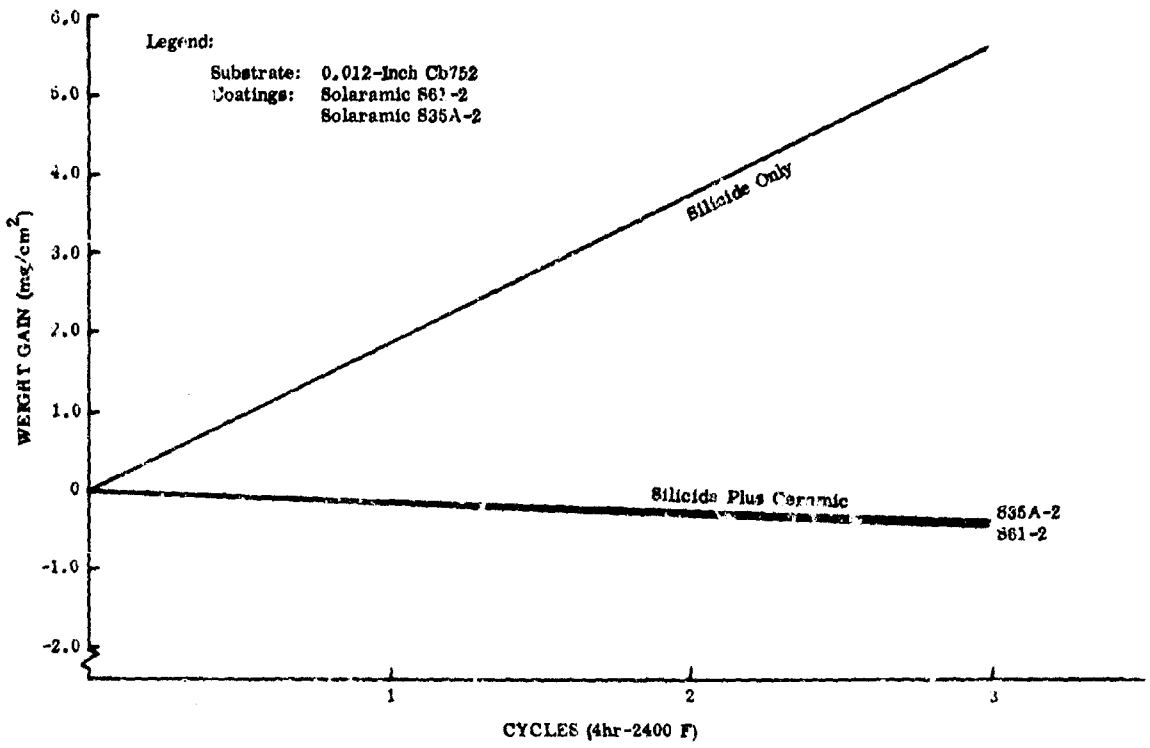

FIGURE 87. WEIGHT CHANGE AFTER CYCLIC OXIDATION

Magnification: 100X Coating: Solaramic 535A-2 Magnification: 500X

Cycles: As coated

FIGURE 88. TYPICAL MICROSTRUCTURE OF CERAMIC-COATED 0.012-INCH Cb752 ALLOY

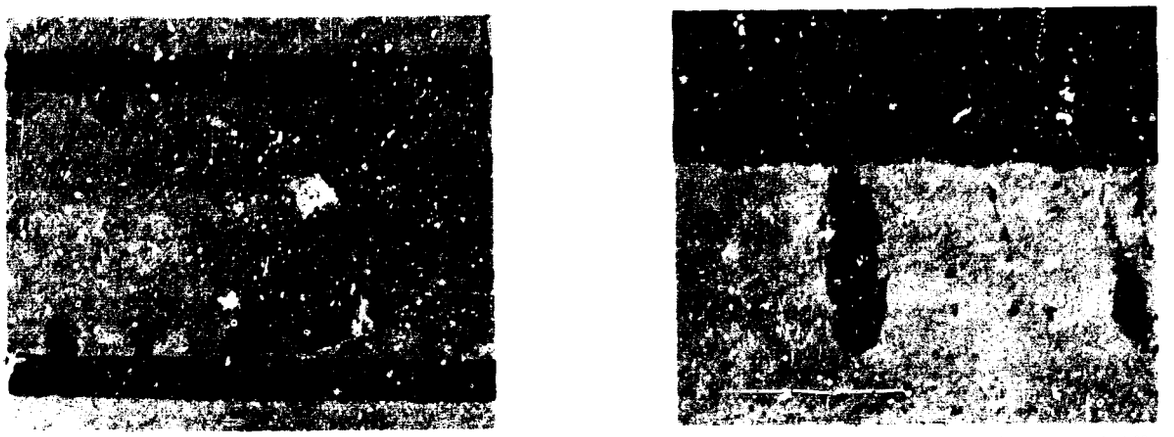

Magnification: 500X Coating: Solaramic 535A-2 Magnification: 100X

Cycles: Three 4-hour cycles at 2400 F

FIGURE 89. TYPICAL CERAMIC-COATED Cb752 ALLOY AFTER THE 2400 F TEST

4.3.4 Discussion of the Ceramic Coating System

Silicate-base ceramic coatings can be readily applied to columbium-base alloys that are silicide coated. Considerable improvement in oxidation resistance is afforded by the coatings as evidenced by weight change measurements at 2400 F; however, the coatings in their present form are not sufficiently impermeable to prevent continued oxidation at fissures in the silicide coating. In effect, deterioration at fissure appears to be accelerated by the presence of the coating, although gross oxidation is retarded. This effect may be galvanic.

Developing ceramic coatings into a full-fledged protective coating system for the refractory metals does not appear warranted by the results of this very brief study. The principal basis on which this decision is made is the inability of the coatings to protect the cracks in the silicide coating. The theoretical advantages in using a ceramic coating are the low softening temperature (approximately 1200 F) and the ability to flow over defects and effectively heal them. Since the latter effect was not realized, it appears that the reservoir-type coatings, offer more potential for development.

4.4 DISCUSSION OF SPECIAL NEW COATING SYSTEMS

Three different types of systems were evaluated in the category of special new coating systems:

- Coating using aluminum to form the principal oxygen barrier
- Coating using aluminum-modified sublayers with silicides to form the outer barriers
- The simple silicide overlayed with a ceramic coating

The work on these systems was concurrent with the development of the V-(Cr-Ti)-Si and (Mo-Ti)-Si to be described in Section V and, consequently, any interpretation of performance must be between these special and primary systems.

4.4.1 Aluminum primary barrier coatings

When considering only oxidation of a ductile layer, the aluminum coatings, e.g., Cb-Ti-Al, Cb-Ti-Cr-Al, Cb-Ti-Mo-Al, and Cb-Ti-Ta-Al, are in a class by themselves. Unfortunately, the ductile alloys have inadequate oxidation resistance to be used above perhaps 1600 to 1800 F without some additional protection if 100-hour life is used as the criterion. When a coating is applied which uses the excellent low-temperature oxidation resistance of the ductile sublayer, e.g., Cb-Mo-Ti-Al, and is aluminized to form the MAl and MAl_3 intermetallic compounds for high-temperature oxidation resistance, performance is not comparable in cyclic performance with the duplex silicide coatings. The maximum one-hour cyclic life at 2400 F of any specimen tested was only 43 hours compared to multiple hundred hours for the (Mo-Ti)-Si and V-(Cr-Ti)-Si coatings at this temperature. At 1600 F, as would be expected, the cyclic life is comparable to these coatings.

The inability of the aluminide coating to protect columbium alloys in cyclic exposures is probably related to the characteristic of the oxide formed. Alumina is a non-vitreous, refractory, high modulus oxide that severely cracks as a consequence of differential expansion with the substrate. The oxide also forms within craze cracks of the aluminide on cooldown and heatup, preventing crack sealing. The oxide is too refractory to be extruded from the cracks and thus produces a continual compressive deformation of the aluminide with every cycle.

With the current knowledge of the high expansion of the aluminides (Section III) and the extensive background in coating development, it appears safe to conclude that without a major advance in surface alloying to change the characteristics of the oxide

formed, aluminum-base primary barrier coatings will not be used in applications requiring extensive thermal cycling. The liquid phase coatings (i.e., Al-Sn-Mo or Ag-Al-Si) were an approach to preserving a continuous Al_2O_3 surface layer, but liquation of the reservoir seriously limits the applications to which this type of coating can be subjected. This approach is not recommended for aerospace and gas turbine applications.

4.4.2 Aluminum Modified Sublayer with Disilicide Outer Layer

Combining the low-temperature oxidation resistance of the Ti-Al and Ti-Cr-Al alloys with the disilicide oxidation resistance at elevated temperatures was investigated. The order of deposition of aluminum was also included as a variable, e.g., aluminum before or after titanium and (Cr-Ti) followed in all cases by silicon. The results showed that oxidation resistance at 1600 F was more consistent for the Al-Ti-Si and Ti-Al-Si than for the comparable (Cr-Ti)-Al-Si coating; however, at 2400 F the reverse was the case, except that the order of deposition of aluminum was very critical. The most satisfactory order was (Cr-Ti)-Al-diffusion-Si. The (80Cr-20Ti)-Al-diffusion-Si is not a practical coating system due to the difficulty of application of (80Cr-20Ti). To overcome this difficulty, vanadium was deposited to decrease the formation of the $CbCr_2$ Laves phase The coating then consisted of V-(Cr-Ti)-Al-diffusion-Si and except for the aluminum and diffusion step, was comparable to the V-(Cr-Ti)-Si coating (Sec. V). The performance of this coating was excellent, exhibiting no failure on the Cb752 and D43 alloys after testing for 509 hours at 1600 F and consistently tested for more than 100 hours at 2400 F. The coating, essentially, never underwent catastrophic oxidation at defect sites due apparently to mobility of a surface oxide; however, the coating did not out-perform the V-(Cr-Ti)-Si coating which has fewer processing steps.

The work with the aluminum-containing sublayers can apparently eliminate low-temperature failures common to silicide coatings, but significant contribution to high-temperature protection could not be demonstrated. Since the system already under study, (Mo-Ti)-Si-Glass and V-(Cr-Ti)-Si, did not have a low-temperature problem, the use of the aluminum-containing sublayer coatings was not carried into Phase II and III.

4.4.3 Silicide-Ceramic Coatings

The silicide-ceramic coatings were formed by siliciding Cb752 or D43 alloys and then applying a thin 0.002-inch ceramic coating (fused silica-base composition used to protect superalloys) to the surface. The silicide acted to minimize reaction between the ceramic coating and the columbium alloy to minimize the effect of minor oxygen diffusion. The ceramic coating was added to improve the oxidation resistance of the $CbSi_2$ and, particularly, to improve cyclic performance by covering the craze cracks in the silicide. No new ceramic coatings were developed, but rather barium borosilicate and barium silicate glasses of various complexities and refractoriness were used in the study.

The coatings appeared to be capable of protecting the alloys up to 12 hours at 2400 F, but because of the mobility of the ceramic coatings, incompatibility with the supporting material was a serious problem. Cyclic testing evaluated compatibility more than it did protection. Bonding to the support media occurred in every cycle, and shear of the bond occurred after each cycle.

Evaluation in great depth was not possible within the scope of the program. It was apparent, however, that the coatings used in the study had a compatibility problem with the silicide layer in the area of cracks in the silicide. The cracks showed extreme enlargement indicating chemical attack. Since elimination of attack at the cracks was a goal of the program, and was not attained, work with the system was abandoned. The system does, however, deserve additional study, particularly due to the simplicity of application. A future study should investigate chemical compatibility between silicide and glass constituents and should include glasses of much greater refractoriness than included in this study, or perhaps glasses that are nucleated and 80 to 90 percent crystallized to maximize the effective viscosity and minimize compatibility problems with support media. Viscosity control by crystallization would probably permit use of this type of coating in high-shear environments, currently not possible with existing ceramic coatings on superalloys.

V. DEVELOPMENT OF SILICIDE COATING PROCESS

The basic approach investigated in silicide coating development required surface alloying the substrate and development of the silicide from the surface alloy. This duplex approach offers greater potential transport of all of the elements, whereas codeposition of silicon and modifiers does not. Also, prealloying is desirable for modification of the substrate to eliminate or reduce the Laves phase formation, improve low-temperature oxidation resistance (below 2000 F), improve the expansion match between silicide and substrate, and increase oxidation resistance of the disilicide formed therefrom.

The duplex approach requires development of surface alloys a minimum of 0.002 to 0.005 inch thick to prevent penetration of the layer when siliciding to a thickness of at least 0.002 inch. The principal area of development thus becomes one of determining the process conditions necessary to effect the required modifier coating.

From the basic studies presented in Section III, two systems and five compositions were initially selected for application studies. The selected systems were (Mo-Ti)-Si and (Cr-V)-Si, and the modifier compositions selected within these systems in weight percent were:

- Molybdenum/Titanium
  - 25Mo-75Ti
  - 50Mo-50Ti
  - 75Mo-25Ti
- Vanadium/Chromium
  - 80Cr-20V
  - 50Cr-50V

Other systems including 95Mo-5Ti, modifications thereof and the addition of titanium to the V-Cr system to effect better control of the interstitial transport and to increase the rate of deposition of chromium were also studied. This latter change also increased the number of deposition cycles, requiring the initial deposition of vanadium followed by (Cr-Ti) and silicon.

The principal deposition technique investigated in the program was transport in packs; however, very late in the program, slurry sintering techniques were used to apply the Mo-Ti coatings because of the success achieved with this system on a NASA program (Ref. 17). Short experimental programs were also conducted to test the merits of development of a substitutional reaction for the deposition of molybdenum and tungsten, and nondiffusion-controlled deposition of molybdenum from molten metals.

5.1 THE (Ti-Mo)-Si SYSTEM

At the outset of the coating development effort, the investigation concentrated on the applications of three modifier alloys, 75Mo-25Ti, 50Mo-50Ti, and 25Mo-75Ti by the pack deposition technique using conventional halide transfer techniques. As the program developed the transport of molybdenum was found to be extremely slow and other transport techniques were studied as was exchange reaction with a silicide alloy. In the final stages of the development program, vacuum sintering of slurry-applied coatings provided the only positive control over the alloy composition.

5.1.1 Pack Deposition of Titanium-Molybdenum Modifiers

Three basic arc-melted compositions within this system were evaluated:

- 75Mo-25Ti
- 50Mo-50Ti
- 25Mo-75Ti

Preparation of Pack Alloys

The three pack alloys used in this study were prepared using the following technique:

- Cold pressing the elemental powder into compacts
- Double arc melting the compact in an atmosphere of argon at a pressure varying from 300 to 700 Torr.
- Hydriding if required
- Crushing the arc-melted ingots to the required particle size
- Acid washing of the sized particles to remove any iron contamination from the crushing operation.

Commercially available materials were used throughout the investigation. Typical materials, sources, and oxygen content are shown in Table LIII. The arc-melted molybdenum and coarse grade of titanium provide the better starting materials based on analysis, but performance in arc melting was otherwise similar.

TABLE LIII

CHEMICAL ANALYSIS OF Ti AND Mo MATERIAL FOR PACK PREPARATION

Metal	Sieve Analysis	Vendor	Grade	Lot No.	Oxygen Content (%)
Molybdenum	-20 + 50	Wah Chang	Hydrogen reduced	Mo-238	0.20(V)[1] 0.25(S)[2]
Molybdenum	-20 + 50	Oremet	Arc melted	Mo-66412	0.01(V)
Titanium	-10 + 50	Oremet	Sponge	1t-3650	0.17(S)
Titanium	-20 + 50	Oremet	Sponge	1t-3925	0.344(S)

1. V - vendor
2. S - Solar

Approximately 10 pounds of each of the three alloys were melted in 100-gram ingots. The 75Mo-25Ti could be directly crushed. The 50Mo-50Ti and 25Mo-75Ti were hydrided and crushed. The oxygen content of the Ti-25Mo and Ti-75Mo packs at two stages of preparation are shown in Table LIV. While arc melting appears to decrease the oxygen content, the hydriding operation markedly increases the oxygen content. Crushing appears to have only a minor effect on the oxygen content based on the result with the Ti-75Mo alloy. The difference in the oxygen content for the hydrided 75Ti-25Mo and the 25Ti-75Mo compositions may also have been due to the difference in solubility of oxygen in the alloy rather than processing conditions.

TABLE LIV

ANALYSIS OF ARC-MELTED Ti-Mo ALLOYS

Alloy	Oxygen Content (%)		
	Starting Powder	Arc-Melted Ingot	Crushed Alloy
Ti-25Mo	0.129	0.098	0.250 (hydrided -20 + 50 mesh)
Ti-75Mo	0.050	---	0.059 (-20 + 50 mesh) 0.081 (-50 mesh)

Specimen Preparation

Three substrate alloys were included in the deposition studies - Cb752(Cb-10W-2.5Zr), B66(Cb-5Mo-5V-1Zr), and D43(Cb-10W-1Zr-0.1C). Gage of the alloys was 0.006 inch because of the availability of this alloy from previous programs at Solar under Contracts AF33(657)-9442, AF33(657)-9443, and AF33(657)-2049). The test programs in Phases II and III were conducted on heavier gage alloys.

Specimens were sheared to 0.5 inch by 0.75 inch and the corners were uniformly hand radiused to approximately 0.125 inch. Edges were deburred by milling in a mixture of A14 alumina and acetone in a ball mill for approximately 48 hours. A few 0.75-inch alumina balls were used in the mill to prevent packing. The specimens were then cleaned in hot alkaline cleaner and etched in the following solution for 10 to 15 seconds, water rinsed, and acetone dried.

	Parts by Volume
Hydrofluoric acid	1
Nitric acid	2
Sulfuric acid	1
Water	4

All specimens were weighed prior to coating.

Preparation of the Pack

The standard technique used in the deposition studies were identical to those developed under Contract AF33(657)-11259 (Ref. 18). In brief, the pack-media active metal and activator were poured into a graphite retort liner (CS grade, National Carbon), and the specimens were placed vertically in the media. The liner was then placed in an Inconel retort (0.125-inch walls), covered with a 0.5-inch thick graphite plate, and a 0.050-inch Inconel cover was heliarc welded in place. The retort was tested for leaks and then evacuated to less than one Torr and backfilled with argon for

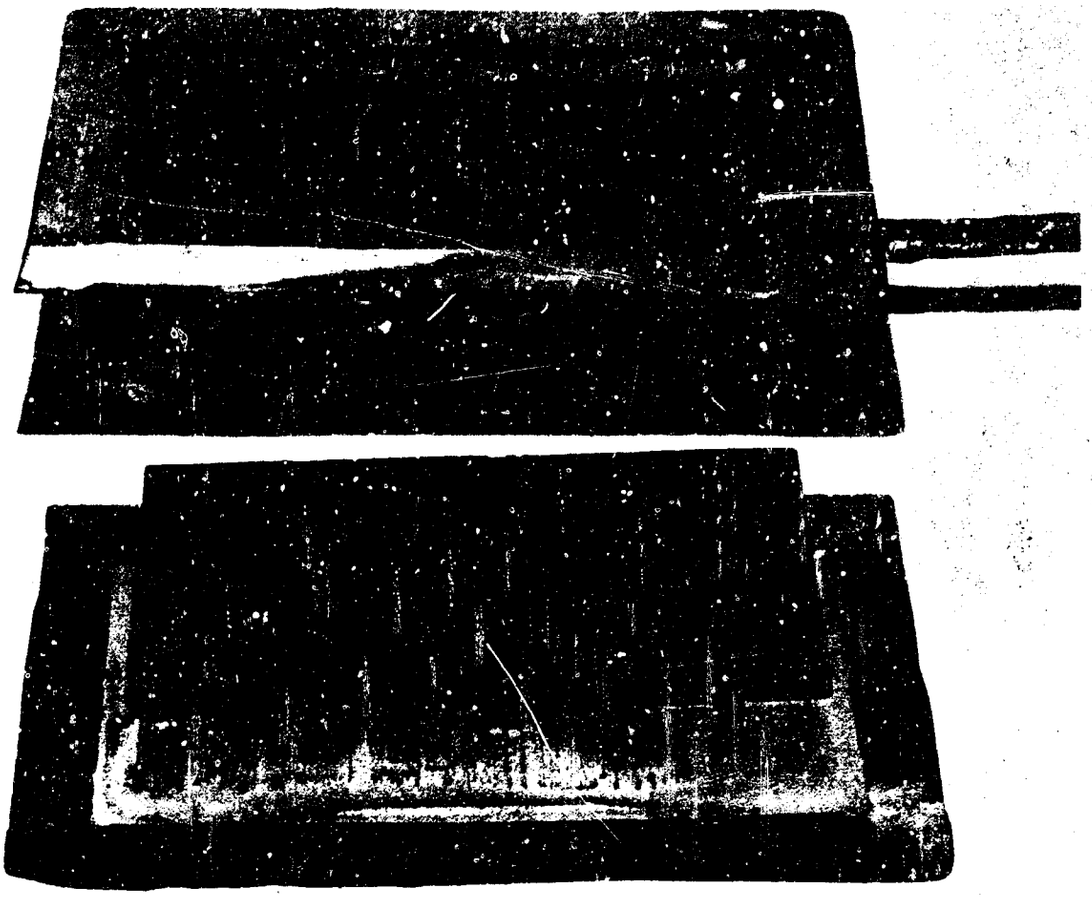

FIGURE 90. TYPICAL GRAPHITE-LINED INCONEL RETORT

a minimum of five times. Figure 90 shows a typical retort and liner, and Figure 91 and 92 show, respectively, the purging control console and a schematic of the purging system.

Pressure was maintained in the retorts at approximately 770 Torr by a mercury seal and argon gas pressure. No gas flow into the retort was used.

The retorts were charged into a furnace heated to the selected temperature for the scheduled time interval, and then removed and allowed to air cool. The lids were then ground or roller cut and the specimens removed, brushed, and weighed. Appearance was noted and the room temperature bend ductility was determined by bending around a 0.0625-inch radius to 90 degrees.

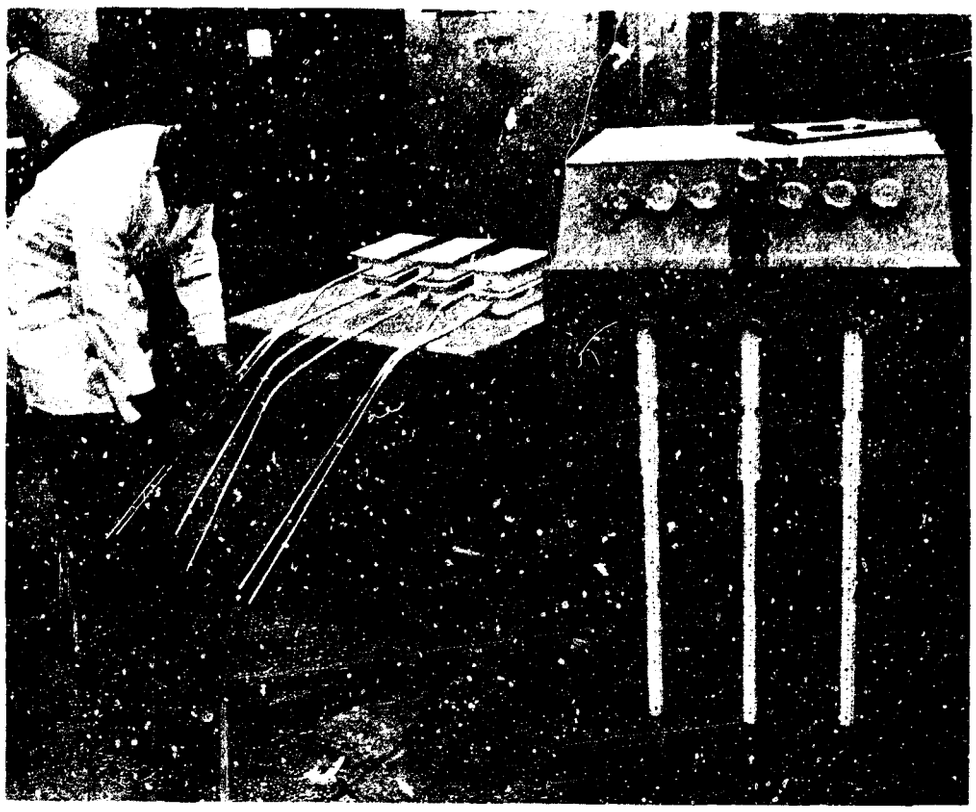

FIGURE 91. CYCLE PURGING AND PRESSURE CONTROI FIXTURES

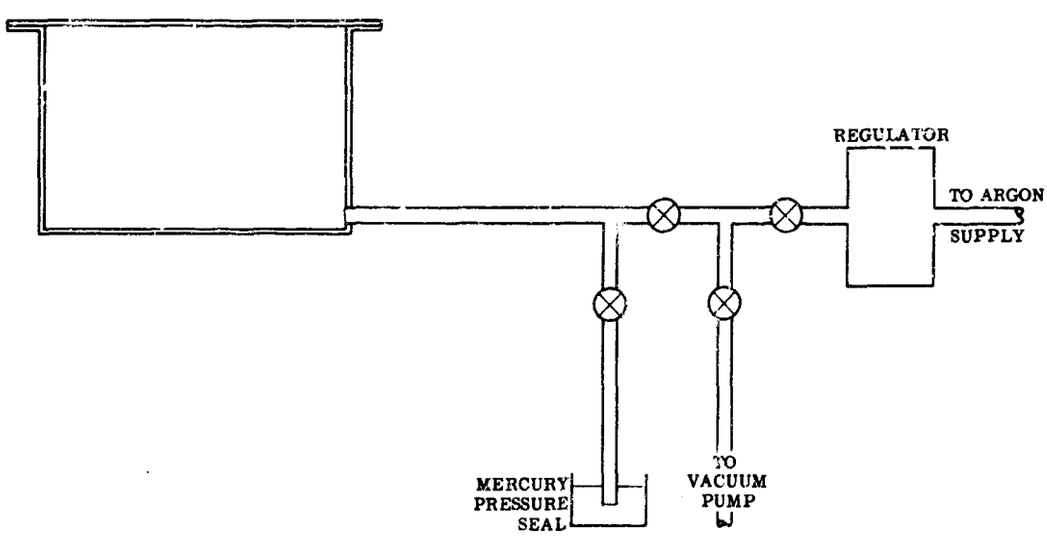

FIGURE 92. RETORT PRESSURE CONTROL SYSTEM

The Ti-75Mo Alloy Deposition

Sodium chloride was selected as the activator in the deposition studies using the 75Mo-25Ti pack alloy based on test results with molybdenum deposition on tantalum (Ref. 18). The following process variables were studied:

- Activator concentration - 0.04 and 0.4 weight percent
- Pack grit size - -20 + 50M and -50 + 200M
- Temperature - 2000 and 2200 F
- Time - 6 and 15 hours
- Alloys - Cb752, D43, B66

The deposition results are shown graphically in Figure 93. Also included are results for arc-melted and crushed molybdenum as the pack medium.

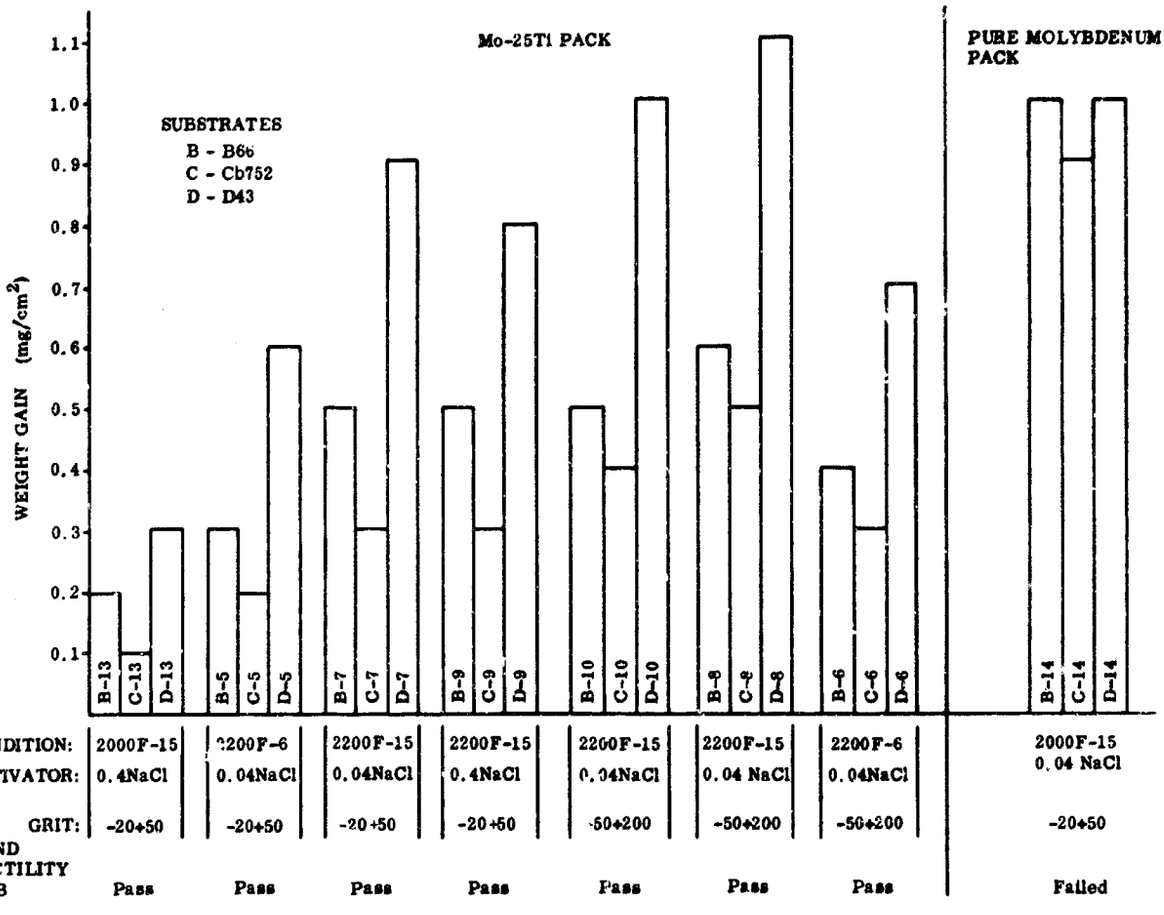

FIGURE 93. DEPOSITION FROM Mo-25Ti AND PURE MOLYBDENUM PACKS OF TWO GRIT SIZES USING NaCl ACTIVATOR

The following are the general conclusions that can be made of the effect of the various process variables:

- **Activator** — Increasing the percentage of activator decreased the deposition rate or had no effect.
- **Temperature** — Increasing the temperature increased the deposition rate.
- **Grit size** — Decreasing the grit size increased the deposition rate.
- **Alloy** — Deposition rate was highest on D43 followed by B66, and then by Cb752.

The coated specimens, excepting those coated in pure molybdenum, retained bend ductility at room temperature. Appearance of the specimens after coating was bright metallic except for the D43 alloy which had a metallic but dull appearance. This dull appearance is probably the result of surface carbide formation from reaction of the carbon in the substrate alloy with titanium pack vapors. The reaction of carbon with the pack vapor is probably also responsible for the higher deposition rates observed on the D43 alloy.

Deposition rates on alloys were too slow to effect the major modification required in the duplex coating system. As an estimate of the temperature that would be necessary to effect the required deposit (20 mg/cm^2) in 15 hours, the effective deposition rate coefficient (EDRC) was determined at 2000 and 2200 F for a 15-hour coating cycle using the following expression:

$$W^2 = Kt$$

where W is weight deposited in mg/cm^2, K is the effective deposition rate coefficient and t is the pack cycle time in hours. The values for K are given in Table LV for the B66 alloy coated with the -20 + 50M and -50 + 200M pack media.

The change in rate of a diffusion-controlled process with temperature should obey the general Arrhenius rate equation:

$$K = K_o \exp(-\Delta H/RT).$$

Thus, using the two temperature points, 2000 and 2200 F, and the EDRC values, it is possible to estimate the temperature required to obtain the desired EDRC value for a practical process, i.e., $K \cong 26.7\ mg^2/cm^4$ hr. Figure 94 shows a graph of the data.

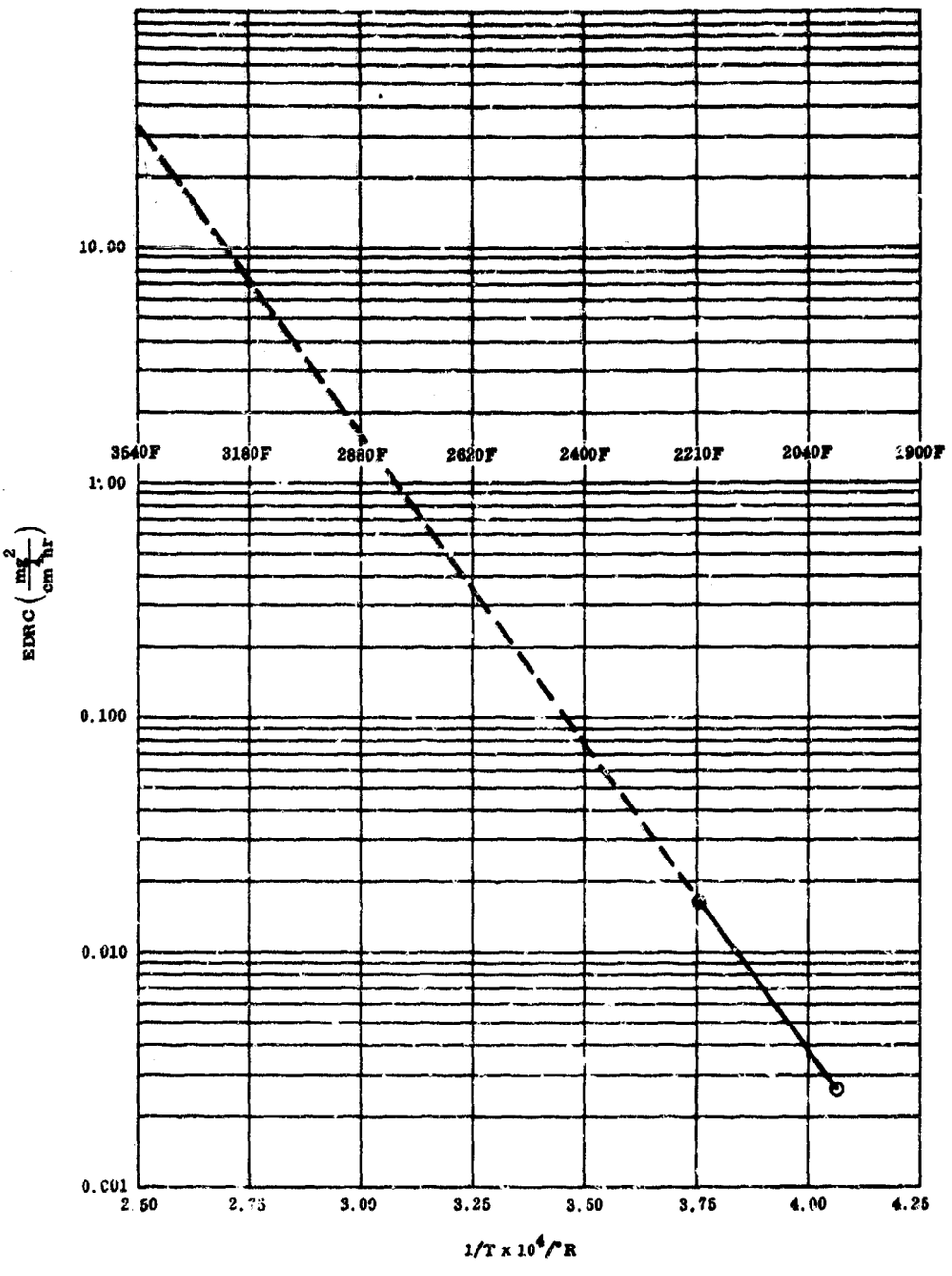

FIGURE 94. PLOT OF EFFECTIVE DEPOSITION RATE COEFFICIENTS FOR THE Mo-25Ti PACK WITH NaCl ACTIVATOR

TABLE LV

EFFECTIVE DEPOSITION RATE COEFFICIENT FOR THE 75Mo-25Ti PACK ON B66 ALLOY

Run No.	Pack Composition	Pack Cycle		Deposit Weight (mg/cm^2)	Coefficient K (mg^2/cm^4 hr)
		Temperature (F)	Time (hr)		
B13	-20 + 50M, 0.4 wt % NaCl	2000	15	0.2	0.00267
B9	-20 + 50M, 0.4 wt % NaCl	2200	15	0.5	0.0167
B7	-20 + 50M, 0.04 wt % NaCl	2200	15	0.5	0.0167
B5	-20 + 50M, 0.04 wt % NaCl	2200	6	0.3	0.0150
B10	-50 + 200M, 0.4 wt % NaCl	2200	15	0.5	0.0167
B8	-50 + 200M, 0.04 wt % NaCl	2200	15	0.6	0.0240
B6	-50 + 200M, 0.04 wt % NaCl	2200	6	0.4	0.0267

The extrapolated temperature for an EDRC of 26.7 is 3480 F. Essentially, the data show that the deposition of a 75Mo-25Ti alloy is impractical by a diffusion-controlled process, such as pack cementation, within the capabilities of existing facilities.

In a second series of deposition runs with the 75Mo-25Ti pack, temperatures of 2000, 2200, and 2600 F were investigated. Activators included were primarily NaF and NaCl at weight percentages of 0.04 and 0.4, but several runs were made with silver halides and sulfur to evaluate the effect of activators that thermodynamically were more reactive toward molybdenum than NaF and NaCl.

The results of the second series are shown in Table LVI. Influence of activator concentration or type was relatively slight. NaF and NaCl produced essentially identical deposition rates at all temperatures. Increasing the concentration of activator by an order of magnitude (0.04 to 0.4 percent) had no effect on deposition rate. The deposition rate increased slightly with the silver halides (AgCl, AgBr, and AgI), but silver was retained in the deposit.

Decreasing the pressure to 5×10^{-6} Torr during deposition considerably reduced the deposition rate (Run 46B) over a conventional high-pressure run (770 Torr). Complete loss of activator is probably responsible for the lower rate. Comparable runs (No. 26B and 42B) were made at 2600 F and 5×10^{-6} Torr with 0.04 percent

TABLE LVI

PACK DEPOSITION RESULTS - 75MO-25Ti ALLOY

Run No.	Pack Composition	Grit Size (mesh)	Activator (weight percent)	Temperature and Time (F)	Time (hr)	Weight Gain (mg/cm²)	Bend Test	Qualitative Chemical Analysis	EDRC (mg²/cm⁴/Hr)
1B	75Mo-25Ti	-20 + 50	0.04 NaF	2000	15	0.4	P		0.008
C						0.3	P		0.005
D						0.6	P		0.019
2B	75Mo-25Ti	-50 + 200	0.04 NaF	2000	15	0.4	P		0.008
C						0.3	P		0.005
D						0.7	P		0.026
3B	75Mo-25Ti	-20 + 50	0.04 NaF	2000	15	0.4	P		0.011
C						0.3	P		0.006
D						0.8	P		0.024
4B	75Mo-25Ti	-50 + 200	0.04 NaF	2000	15	0.4	P		0.011
C						0.3	P		0.006
D						0.8	P		0.024
5B	75Mo-25Ti	-20 + 150	0.04 NaCl	2000	6	0.3	P		0.015
C						0.2	P		0.007
D						0.6	P		0.020
6B	75Mo-25Ti	-50 + 100	0.04 NaCl	2200	6	0.4	P		0.027
C						0.3	P		0.015
D						0.7	P		0.061
7B	75Mo-25Ti	-20 + 50	0.04 NaCl	2200	15	0.5	P		0.016
C						0.4	P		0.010
D						0.9	P		0.054
8B	75Mo-25Ti	-50 + 200	0.04 NaCl	2200	15	0.6	P		0.024
C						0.5	P		0.017
D						1.1	P		0.081
9B	75Mo-25Ti	-20 + 50	0.4 NaCl	2200	15	0.5	P		0.016
C						0.3	P		0.006
D						0.8	P		0.043
10B	75Mo-25Ti	-50 + 200	0.4 NaCl	2200	15	0.5	P		0.016
C						0.4	P		0.010
D						1.0	P		0.067
11B	75Mo-25Ti	-20 + 50	0.4 NaCl	2000	15	0.2	P		0.003
C						0.1	P		0.001
D						0.3	P		0.006
26B	75Mo-25Ti	-20 + 50	None	2800	5(1)	0.7	P		0.068
C						0.8	P		0.128
D						0.8	P		0.128
40D	Graphite	-325	None	2200	15	0.8	F		0.533
D_1	75Mo-25Ti	-20 + 50	0.04 NaCl	2200	15	2.2	P		0.322
43B	75Mo-25Ti	-20 + 50	0.04 NaCl	2800	5(1)	1.0	P		0.280
C						1.2	P		0.288
D						1.1	P		0.242
46B	75Mo-25Ti	-20 + 50	0.04 NaCl	2100	5(1)	0.04	P		0.0003
C						0.04	P		0.0003
D						0.08	P		0.017
47B	75Mo-25Ti	-20 + 50	0.04 NaCl	2200	15	0.5	P		0.017
C						0.4	P		0.011
D						0.8	P		0.043
50B	75Mo-25Ti	-20 + 50	0.04 S	2200	15	0.8	P	Trace Mo	0.043
C						0.7	P	Trace Mo	0.033
51B	75Mo-25Ti	-20 + 50	0.04 AgCl	2200	15	1.4	P	Ag present - no Mo	0.131
C						0.5	P	Ag present - no Mo	0.006
D						0.6	P	Ag present - no Mo	0.024
52B	75Mo-25Ti	-20 + 50	0.04 AgI	2200	15	1.7	P	Ag present - no Mo	0.193
C						-	P	Ag present - no Mo	-
D						0.7	P	Ag present - no Mo	0.033
53B	75Mo-25Ti	-20 + 50	0.04 AgBr	2200	15	0.9	P	Ag present - no Mo	0.054
C						1.5	P	Ag present - no Mo	0.150
D						1.1	P	Ag present - no Mo	0.081
68C	75Mo-25Ti	-20 + 50	0.1 AgBr	2200	15	0.5	P	No Mo present	-
D						0.9	P	No Mo present	-
69C	75Mo-25Ti	-20 + 50	1.0 AgBr	2200	15	1.4(5)	P_f	No Mo present	0.131
D						1.2(5)	P	No Mo present	0.096
70C	75Mo-25Ti	-20 + 50	1.0 $AgBr^{(5)}$	2200	15	0.7	F	Ag present - no Mo	0.033
D						0.8	P	Ag present - no Mo	0.054
8[illegible]	75Mo-25Ti	-20 + 50	1.0 Cryolite(2)	2[illegible]	15	0.5	F		0.016
D						1.2	P		0.088

LEGEND

1 Low pressure run (5×10^{-6} Torr)

2 Activator aggregated from area of specimens

B B66 alloy

C C67S3 alloy

D D43 alloy

S Peak stressed to destruction

P Passed 90 degree RT bend test

P_f Cracks at completion of bend test

F Failed 90 degree RT bend test

EDRC Effective deposition rate coefficient = $\frac{K^2}{4} = \frac{[illegible]}{4t}$

NaCl and without an activator. The activator run had the higher deposition rate indicating that a high concentration of activator is not required but that the rate is definitely enhanced by the presence of the activator.

The D43 alloy consistently had a higher deposit weight than the Cb752 and D66 alloy. This weight difference was hypothesized to be the result of the presence of carbon in the D43 alloy which acted as a compound former providing a greater driving potential for the deposition reaction. An experiment was performed (Run 40) in which the D43 alloy was carburized in pure graphite and subsequently coated with the 75Mo-25Ti pack to determine if the deposition rate could be significantly increased by this technique. The results showed that:

- The carburizing completely embrittled the substrate
- The ductility was restored by the deposition cycle.

The rate was twice as high for the carburized base as for the uncarburized alloy. Compound formation thus appears as a significant driving mechanism.

The rate of deposition from the 75Mo-25Ti pack was extremely slow under all conditions and with all activators. Surface X-ray fluorescence analyses also showed that no molybdenum was transferred in any alkali halide run.

To determine if an oxidation-reduction type reaction could be used to effect deposition of molybdenum from the 75Mo-25Ti pack, two approaches were tried:

- Segregation of a silver halide in the pack to effect the following series of reaction:

$$3AgBr + Mo \longrightarrow 3Ag + MoCl_3$$

$$MoCl_3 + Cb \longrightarrow CbCl_3 + Mo$$

- Use of sulfur as the molybdenum transport media to force the following series of reaction:

$$Mo + S_2 \longrightarrow MoS_2$$

$$5/2\ MoS_2 + 2Cb \longrightarrow 5/2\ Mo + Cb_2S_5$$

The results of the oxidation-reduction experiment are listed under Runs 70 and 50. Neither reaction gave a high deposition rate, but the use of sulfur produced the only indication of molybdenum in the deposit.

Activities were suspended with the 75Mo-25Ti system because of low deposition rate and the difficulty of transferring molybdenum.

50Mo-50Ti Composition

Deposition results for the 50Mo-50Ti alloyed pack are shown in Table LVII. Specimen weight gains from coating runs were from 5 to 10 times greater than those obtained from the 75Mo-25Ti composition. Appearance of the coated specimens were generally bright and clean, but with a slightly rough texture. All specimens passed the 90-degree room-temperature bend test. Sintering occurred at 2200 F in the high-pressure pack and resulted in the particles of the pack being welded by contact diffusion to the surface of the specimens. At 2600 F for 5 hours at 5×10^{-5} Torr, however, very little sintering was noted.

TABLE LVII

PACK DEPOSITION RESULTS - 50Mo-50Ti ALLOY

Run No.	Pack Composition	Grit Size (mesh)	Activator (weight percent)	Temperature and Time		Weight Gain (mg/cm^2)	Bend Test	EDRC ($mg^2/cm^4/hr$)
				(F)	(hr)			
27B	50Mo-50Ti[1]	-20 +50	0.04 NaCl	2000	15	- (2)	P	-
C						- (2)	P	-
D						2.3	P	0.451
28B	50Mo-50Ti	-50 +200	0.04 NaCl	2000	15	3.3	P	0.726
C						- (2)	P	-
D						3.1	P	0.641
31B	50Mo-50Ti	-20 +50	0.04 NaCl	2200	15	4.9 (S)	P	1.500
C						3.7 (S)	P	0.913
D						4.4 (S)	P	1.291
39B	50Mo-50Ti	-20 +50	0.04 NaCl	2000	15	1.6	P	0.171
C						1.4	P	0.131
D						1.8	P	0.216
42B	50Mo-50Ti	-20 +50	0.04 NaCl	2600	5[3]	4.2	P	3.528
C						4.1	P	3.362
D						3.6	P	2.592
67C	50Mo-50Ti	-20 +50	2.0 NaCl	2000	15	1.5	P	0.150
D						1.8	P	0.215

LEGEND

1	Hydride condition
2	Specimens cracked from using a hydrided pack not previously out gassed
3	Low pressure run (5×10^{-6} Torr) (columbium alloy open retort)
B	B66 alloy
C	Cb752 alloy
D	D43 alloy
S	Pack sintered to specimens
P	Passed 90 degree RT bend test
F	Failed 90 degree RT bend test
EDRC	Effective deposition rate coefficient $= \frac{w^2}{t} = \frac{(mg/cm^2)^2}{hr}$

D39 (Modifier Only)

Substrate:	D43
Coating:	50Mo-50
Condition:	15 Hours at 2000 F
Activator:	0.04 NaCl
Deposition:	1.8 mg/cm^2
Bend Test:	Passed
Magnification:	250X

FIGURE 95. DEPOSIT FROM 50Mo-50Ti PACK

Only NaCl was used as the pack activator. The deposition rate was insensitive to the amount of activator between the limits investigated (0.04 to 2.0 weight percent).

Two runs were made with packs in the hydrided condition (No. 27 and 28). The specimens were severely cracked but not brittle. The end-point ductility indicates that the specimens were embrittled and damaged in heatup by the hydrogen evolution of the pack. To outgas the hydrided packs heating to 2000 F before use is required.

A typical photomicrograph of a deposit from the 50Mo-50Ti pack is shown in Figure 95. The deposit is uniform and single phased and exhibits the characteristic tendency of titanium to diffuse intergranularly. Chemical analysis of the deposits showed them to be molybdenum-free indicating, as in the 75Mo-25Ti pack runs, that titanium only is transported.

25Mo-75Ti Modifier Pack

Deposition results with the 25Mo-75Ti alloyed pack are given in Table LVIII and typical photomicrographs are shown in Figure 96. Deposition rates were higher than for packs with higher molybdenum contents, but otherwise the pack performed similarly. The maximum temperature at which this pack can be used with the high-pressure deposition techniques is 2000 F without severe sintering. This high temperature does not severely limit the use of the pack however, because 10 mg/cm^2 can be deposited at this temperature in 15 hours.

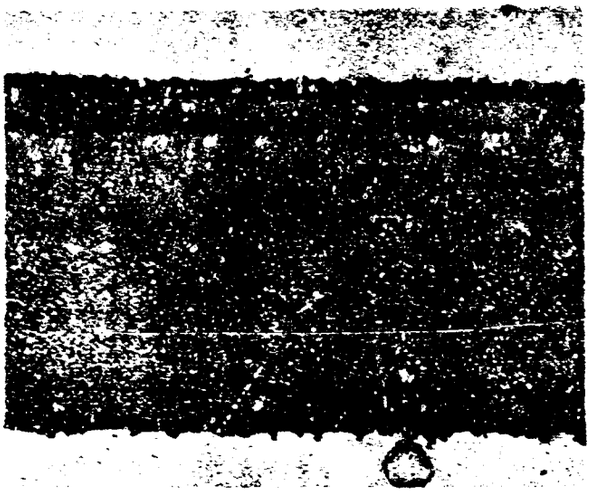

C24 (Modifier Only)

Substrate: Cb752
Coating: 25Mo-75Ti
Condition: 15 Hours at 1900 F
Activator: 0.04 NaCl
Deposition: 6.2 mg/cm^2
Bend Test: Passed

Over etched to show titanium grain boundary penetration

Substrate: D43
Coating: 25Mo-75Ti
Condition: 15 Hours at 1900 F
Activator: 0.04 NaCl
Deposition: 6.2 mg/cm^2
Bend Test: Passed

Magnification: 250X

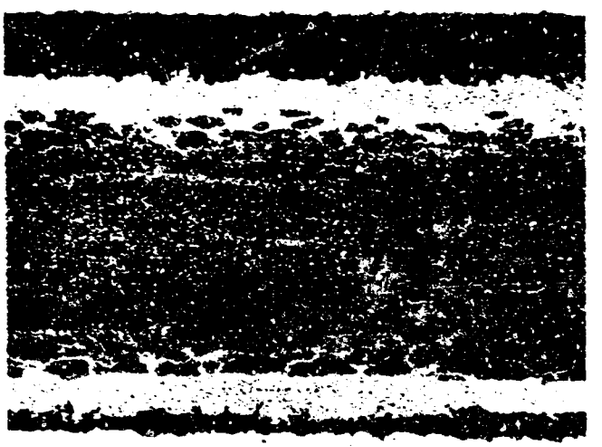

FIGURE 96. DEPOSIT FROM 25Mo-75Ti PACK

TABLE LVIII

PACK DEPOSITION RESULTS - 25Mo-75Ti ALLOY

Run No.	Pack Composition	Grit Size (mesh)	Activator (weight percent)	Temperature and Time (F)	Temperature and Time (hr)	Weight Gain (mg/cm^2)	Bend Test	EDRC ($mg^2/cm^4/hr$)
19C[1]	25Mo-75Ti	-20 +50	0.1 CaF_2	2200	15	S	P	-
C			0.1 NaF			S	P	-
C			0.1 NaCl			S	P	-
C			0.1 NaBr			S	P	-
C			0.1 NaI			S	P	-
C			0.1 K_2TiF_6			S	P	-
C			0.1 $CaCl_2$			S	P	-
C			None			S	P	-
22B	25Mo-75Ti	-20 +50	0.04 NaCl	2000	15	11.3	P	8.513
C						9.7	P	6.273
D						10.2	P	6.936
23B	25Mo-75Ti	-50 +200	0.04 NaCl	2000	15	11.6	P	8.971
C						9.9	P	6.534
D						10.7	P	7.633
24B	25Mo-75Ti	-20 +50	0.04 NaCl	1900	15	6.4	P	3.731
C						-	-	-
D						6.2	P	2.563
25B	25Mo-75Ti	-200[2] -20 +50	0.04 NaCl	1900	15	S	P	-
C						S	P	-
D						S	P	-
57B	25Mo-75Ti	-20 +50	0.04 NaCl	2200	6[3]	0.4	P	0.027
C						0.3	P	0.015
D						0.7	P	0.062

LEGEND

1	Activator analysis series
2	Occluding experiment. Fine pack around specimen, surrounded by coarser particles
3	Low pressure run (5×10^{-6} Torr) (columbium alloy open retort)
B	B66 alloy
C	C752 alloy
D	D43 alloy
P	Passed 90 degree RT bend test
S	Pack sintered to specimens
EDRC	Effective deposition rate coefficient = $\frac{w^2}{t} = \frac{(mg/cm^2)^2}{hr}$

The deposit contains titanium only as with the other titanium-molybdenum pack alloys. The very severe intergramular penetration of titanium at only 1900 F is shown in the photomicrograph (Fig. 96) of an over-etched, coated specimen.

Discussion of the Deposition of Titanium-Molybdenum from Packs

Codeposition of titanium and molybdenum by pack deposition has been shown to be essentially impossible. Both thermodynamic and kinetic factors inhibit deposition of molybdenum. In the presence of metallic titanium the possibility of generating a halide of molybdenum is remote based on the free energies of formation of halides of titanium and molybdenum, e.g., -80kcal for $MoCl_{2(1000K)}$ per gm atom chlorine compared to -44 kcal for $TiCl_{2(1000K)}$. Also, when the reaction of NaCl ($\Delta F = -76.5_{(1000K)}$ kcal) with molybdenum to form $MoCl_2$ is considered, the thermodynamics become even more unfavorable. Although data are not readily available on the interdiffusion rate of molybdenum in columbium relative to titanium in columbium, the difference in rates should be marked based on melting temperatures alone. It, therefore, appears safe to assume that codeposition of titanium and molybdenum by simple pack technique cannot be effected.

5.1.2 Molten Metal Deposition of Molybdenum

A brief investigation was undertaken to study coating systems for molybdenum which were not diffusion controlled, as opposed to those diffusion-controlled processes previously described. In pack cementation, the reactions for depositing molybdenum on the columbium alloy substrate are driven largely by the molybdenum concentration gradient in the substrate. Therefore, the dissolution and diffusion of molybdenum into the substrate govern the rate at which molybdenum coatings can develop. Inasmuch as the rate of molybdenum diffusion in columbium is quite slow at process temperatures (2000 to 2600 F), the diffusion-controlled coating processes would at best be time consuming, requiring many hours at temperature.

To obtain a molybdenum coating process which may be rapid and capable of depositing relatively pure molybdenum, binary systems were studied in which pure molybdenum precipitates from liquid solutions. These potential coating systems are driven by phase equilibria forces, and, theoretically, should be insensitive to the surface concentration of molybdenum or diffusion-controlled concentration gradients in the substrate.

The silver-molybdenum and lead-molybdenum systems were selected for this study based upon a survey of available phase equilibrium diagrams and related information (Ref. 4, 19, and 20).

Results with the silver-molybdenum system were not encouraging. Although Hansen (Ref. 4) states that "at 2912 F, at least five weight percent molybdenum is soluble in silver," work at Solar with arc-melted heats of 95Ag-5Mo and 98Ag-2Mo failed to show any tendency for the molybdenum component to dissolve in, or precipitate from, the liquid-silver phase. Hansen refers to the work of Driebholz (Ref. 4) which concludes "The microstructure of five percent molybdenum alloy consisted of primary molybdenum crystals in a matrix of pure silver."

The lead-molybdenum system exhibited greater promise. A study of three arc-melted alloys (90Pb-10Mo, 95Pb-5Mo, and 98Pb-2Mo) indicated that the lead-molybdenum system is probably a limiting case of a eutectic or peritectic (Fig. 97). Based upon the evidence generated, the eutectic or peritectic very likely occurs quite close to the lead axis, so close that only one liquidus curve is evident.

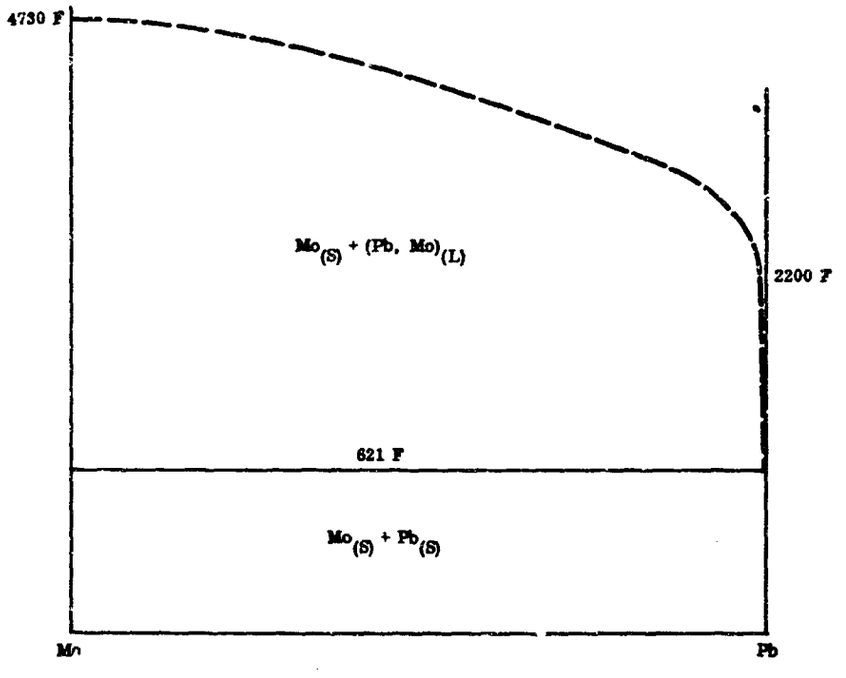

FIGURE 97. PROBABLE FORM OF THE Pb-Mo EQUILIBRIUM PHASE DIAGRAM

Apparently the liquidus curve rises very steeply from near the melting point of lead to about 2200 F, inasmuch as no sign of molybdenum dissolution in, or precipitation from, the liquid-lead phase was manifest in this temperature range. However, on cooling from temperatures of 2300 F and above, progressively more molybdenum was observed to precipitate within the lead-rich phase, indicating a more negative slope to the liquidus curve above 2300 F (Fig. 98). This information matches the results of Guertler (Ref. 4) who reported that "The primary phase (in lead-molybdenum alloys with up to 20 percent molybdenum) is elemental molybdenum, which precipitates from the melt at very high temperatures." It was found impossible to dissolve all of the molybdenum in the three test alloys even though process temperatures up to 3000 F were applied, indicating solubility of less than two percent at this temperature.

By immersing a specimen of pure columbium in a bath of 95Pb-5Mo at 2500 F, (argon atmosphere) then slowly super-cooling the bath to 2000 F (100 degrees F/min), a thin (0.00003 inch), but continuous coating of molybdenum can be deposited on the columbium (Fig. 99A). This procedure requires eight minutes. By increasing the initial temperature of the bath to 2750 F, a molybdenum coating 0.0001 inch thick can be deposited in a single run similar to the preceding run. Conducting five (2750 F $\rightleftharpoons$ 2000 F) runs in sequence on the same columbium specimen builds up a molybdenum surface layer approximately 0.0002 inch thick (Fig. 99B). Coatings 0.0002 to 0.0005 inch thick conceivably could be applied in an hour or less of process time, using sequential deposition.

Massive white phase is undissolved Mo; White filigree in grey etching matrix is Mo precipitated in the Pb-rich phase.

Etchant: Murakami's

Magnification: 250X

FIGURE 98.

MICROSTRUCTURE OF Pb-10Mo ALLOY; Quenched From 3000 F

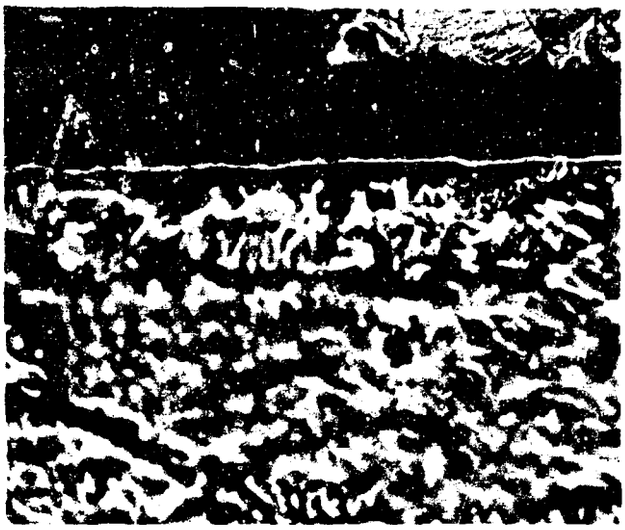

A

Cycle: 2500 F —2000 F (100 degrees F/min)

Coating
Thickness: 0.00003 inch

B

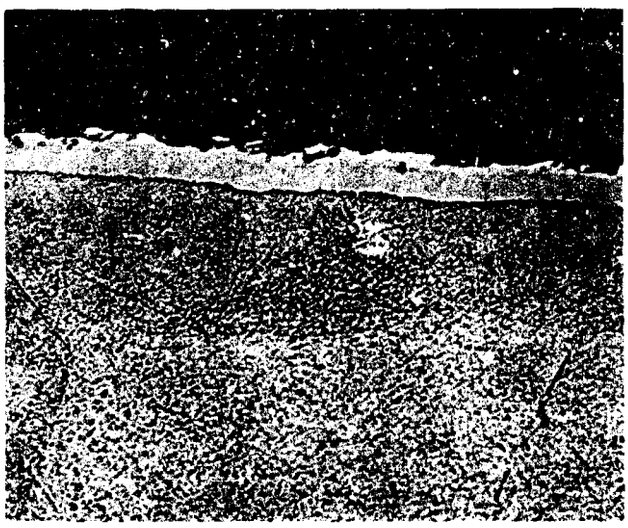

Etchant: Hf-HNO_3 + Murakami's

Magnification: 1000X

Cycle: Five sequential runs 2750 F—2000 F (100 degrees F/min)

Coating
Thickness: 0.0002 inch

FIGURE 99. MOLYBDENUM COATING DEPOSITED ON PURE COLUMBIUM SUBSTRATE FROM Pb-5Mo LIQUID BATh

Although the coatings appeared metallographically to be single-phase molybdenum, X-ray fluorescent analysis revealed heavy lead concentrations together with molybdenum. This condition was also true following high-vacuum heat treatment to boil off residual lead at 2000 F. The Mo-Pb coating was abnormally hard (KHN 815) indicating significant contamination. The most probable source of contamination is dissolved oxygen and nitrogen in commercially pure lead, inasmuch as a columbium wetting problem was not solved until a trace of titanium was added to the Pb-Mo baths. Vacuum annealing the coatings (one hour at 1850 F) helped reduce the coating hardness to 530 KHN, but this hardness level was still appreciably higher than that of the columbium substrate (KHN 100) or the molybdenum melting stock (KHN 175). The process was set aside due to other program requirements, but additional work in this area may yield some interesting nondiffusion-controlled coating processes.

5.1.3 Displacement Diffusion From the Disilicide

The slow diffusion rate of molybdenum or tungsten in columbium precluded any possibility of driving a significant amount of these elements into columbium using activity difference as the driving mechanism. The high mobility of silicon in the silicides as indicated by the rapid diffusion of silicon in the formation of the disilicide offered another possible approach to the deposition of these elements. By considering a displacement diffusion reaction between a halide of tungsten or molybdenum and silicon in the disilicide, a reaction potential can be postulated, e.g.,

$$2WF_6 + 3Si \longrightarrow 2W + 3SiF_4.$$

Assuming a silicon activity of one in the disilicide, the free energy of the above reaction at 1400 K (2060 F) is -564 kcal indicating a very strong potential for reaction of WF_6 with silicon.

To test this method of depositing tungsten or molybdenum, WF_6 was passed over crushed molybdenum to effect some reduction of the compound prior to coming in contact with the silicide. The following reaction would be predicted by reacting WF_6 with molybdenum.

$$aWF_6 + bMo \longrightarrow cWF_5 + dMoF_5 + eW$$

Thermodynamics favor the formation of the MoF_5 over WF_5. The gases from this reaction in an argon carrier gas were then passed over silicide-coated specimens for 16 hours at 2000 F.

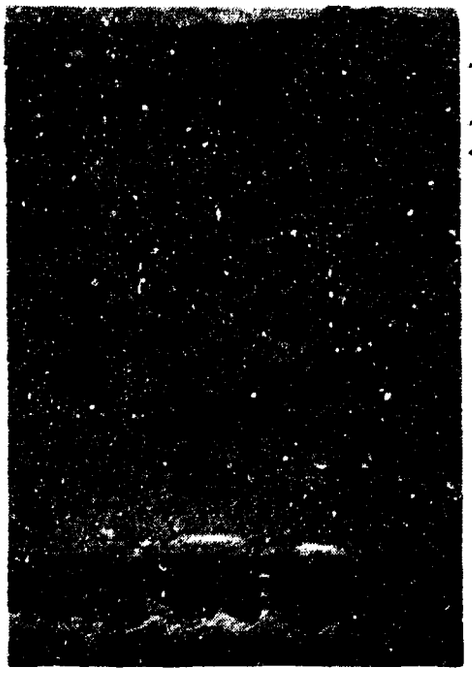

W, Mo and Si coated residual silicide

Magnification: 250 X

FIGURE 100.

TUNGSTEN AND MOLYBDENUM COATED B66

In one experiment, 19 mg/cm^2 of tungsten and molybdenum were deposited on a silicided B66 substrate. In another 28 mg/cm^2 of tungsten and molybdenum were deposited on silicided TZM. Figure 100 shows a deposit of tungsten and molybdenum on silicided B66. X-ray fluorescence analysis of the B66 specimen having the 19 mg/cm^2 deposit is given in Table LIX.

TABLE LIX

X-RAY COUNTS OF A COATED B66 SPECIMEN

Specimen	Molybdenum	Tungsten
Molybdenum Standard	26,650	750
Tungsten Standard	134	11,850
Coated B66 Specimen	14,550	4,780

Although the X-ray fluorescent analysis indicates transfer of molybdenum and tungsten the specimens were severely embrittled, and since a major study would be required, the technique was not pursued.

5.1.4 Slurry Deposition of Titanium-Molybdenum Modifiers

A successful slurry technique for introducing molybdenum into coatings for columbium alloys was evolved very late in the program. It was an adaptation of a technique developed on a concurrently funded program at Solar for tantalum alloy coatings. (Ref. 17). The slurry materials used throughout the study are listed in Table LX.

TABLE LX

MATERIALS USED FOR SLURRY COATING Cb752

Material	Particle Size	Purity	Source
Titanium	-325 mesh	99.5	Metals Disintegrating
Molybdenum	-325 mesh	99.95	Dill Industrial
Iron	Plast - Iron	-	Glidden
Manganese	Plast - Manganese	-	Glidden
Boron	Amorphous	94-97	American Potash
Ethyl cellulose		N-200	Hercules Powder
Xylene		-	Shell
Secondary butyl alcohol		-	Mefford Chemical Co.

Commercial spray guns were used exclusively apply the metal modifiers which were suspended in an organic vehicle. Siliciding of the sprayed and sintered modifier layer was accomplished by pack cementation in retorts shown schematically in Figure 101.

The retort was evacuated and cycle purged approximately five times with argon, prior to system seal-off with a mercury bubbler.

The modifier systems initially studied were 95Mo-5Ti, 90Mo-10Ti, 80Mo-20Ti, and 70Mo-30Ti (all weight percent). Slurries of each system were prepared by suspending the metal powders in a vehicle of ethyl cellulose, xylene, secondary butyl alcohol, and Stoddard solvent. The slurries were applied to 1.0 by 2.0 by 0.03-inch Cb752 coupons by spraying. A cycle of 15 hours at 2400 F and 10^{-4} Torr vacuum was employed for sintering the 70Mo-30Ti and 80Mo-20Ti compositions, and a cycle of 15 hours at 2700 F and 10^{-4} Torr vacuum was used for the sintering of the 90Mo-10Ti and 95Mo-5Ti compositions. Pack siliciding of all specimens was accomplished in a

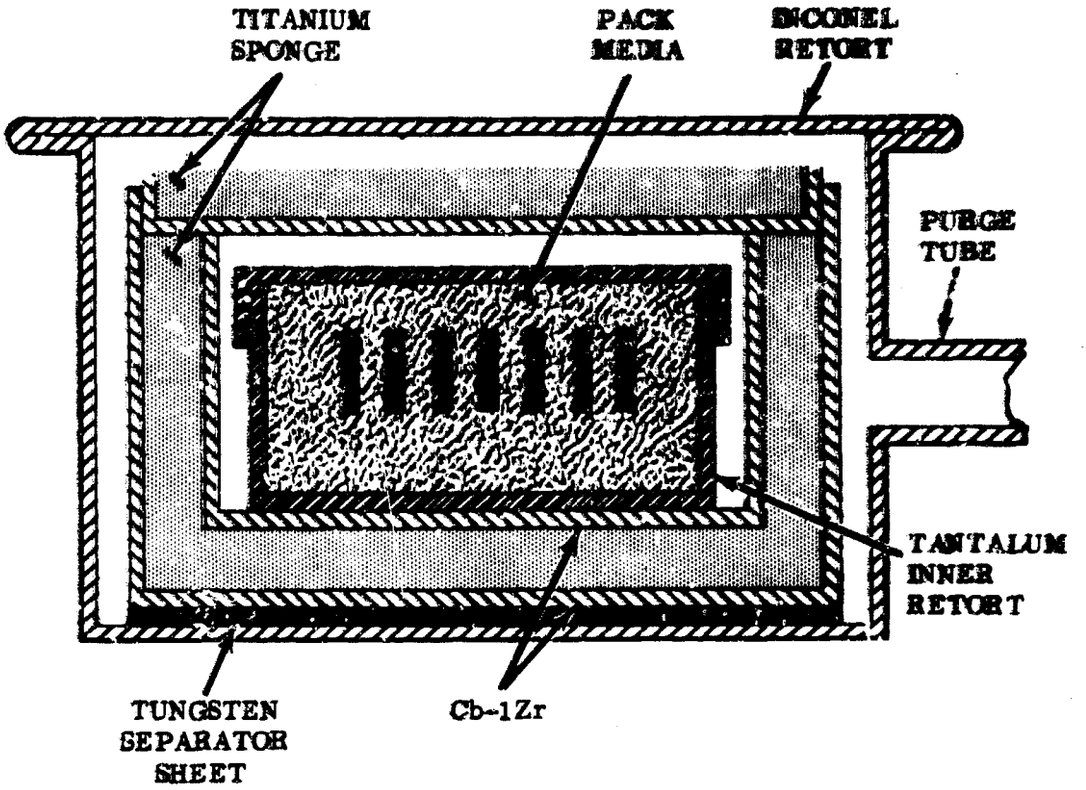

FIGURE 101. SCHEMATIC DRAWING OF A HIGH-PRESSURE RETORT

seven hour, 2150 F cycle. The resultant modifier and silicon depositions are summarized in Table LXI. Figures 102 and 103 show, respectively, the coating microstructures before and after siliciding. The 80Mo-20Ti coating spalled on siliciding and is not shown. A comparison of the as-modified and silicided microstructures indicated a considerable decrease in coating porosity as a result of the volume expansion during siliciding.

TABLE LXI

DEPOSITION OF THE Mo-Ti MODIFIERS AND SILICON

Slurry Modifier Composition (wt %)	Modifier Cycle	Deposition (mg/cm^2)	Silicon Cycle	Deposition (mg/cm^2)
70Mo-30Ti	15 hours at 2400 F	59	7 hours at 2150 F	38
80Mo-20Ti	15 hours at 2400 F	71	7 hours at 2150 F	43
90Mo-10Ti	15 hours at 2700 F	67	7 hours at 2150 F	34
95Mo-5Ti	15 hours at 2700 F	68	7 hours at 2150 F	32

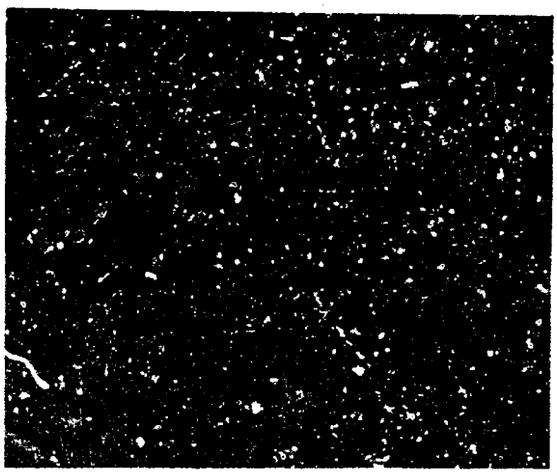

70Mo-30Ti Composition

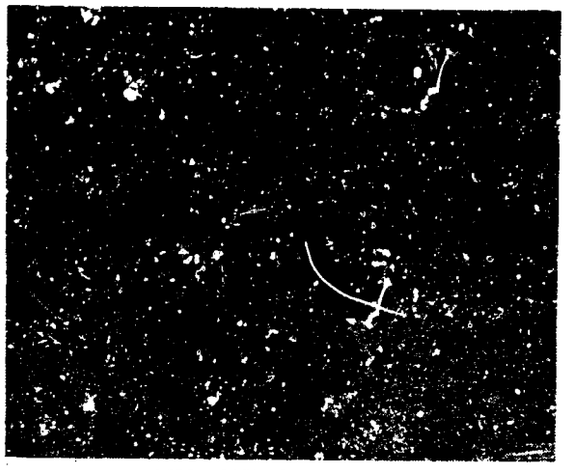

80Mo-20Ti Composition

Magnification: 250X

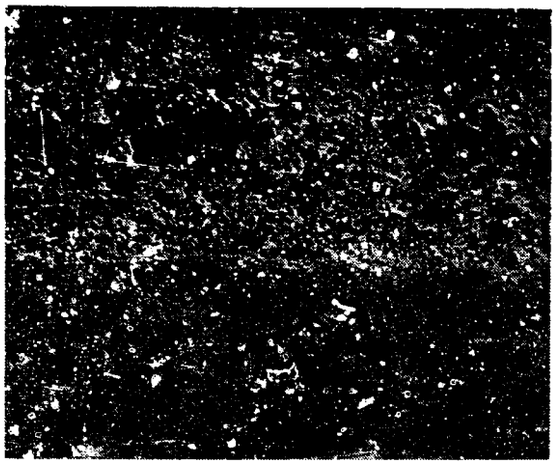

90Mo-10Ti Composition

95Mo-5Ti Composition

FIGURE 102. MICROSTRUCTURE OF SEVERAL MOLYBDENUM-TITANIUM MODIFIER COATINGS

Triplicate specimens of each coating were oxidation tested at 1600 and 2400 F. The results, summarized in Table LXII indicated that the 95Mo-5Ti modifier composition performed best at 2400 F, although 1600 F protection was poor.

To improve the oxidation resistance at 1600 F by a self-healing mechanism, the addition of glass network modifiers such as iron, manganese, and boron was investigated. The following compositions were spray slurry applied on Cb752 coupons and vacuum sintered for 15 hours at 2700 F: 89Mo-5Ti-6B, 86Mo-4Ti-10Fe, and 86Mo-4Ti-10Mn. The sintered microstructure of these modifiers is shown in

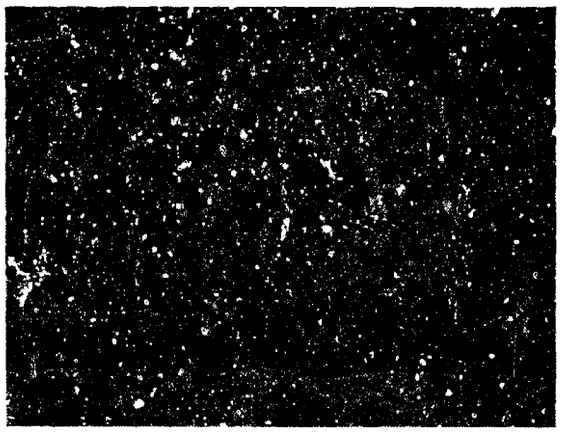

Silicided 70Mo-30Ti Composition

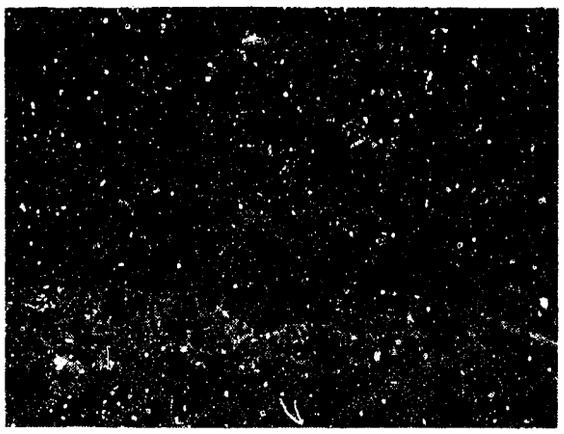

Silicided 90Mo-10Ti Composition

Magnification: 250X

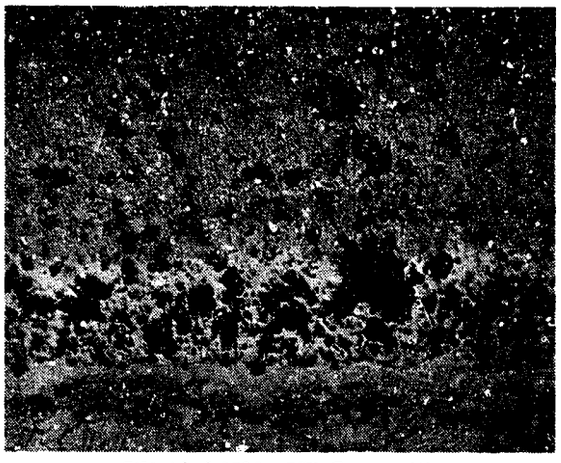

Silicided 95Mo-5Ti Composition

FIGURE 103. MICROSTRUCTURE OF THE SILICIDED MOLYBDENUM-TITANIUM COATINGS

Figure 104. All siliciding of these modifiers was done in -200 mesh unactivated pure silicon high-pressure pack, using a seven-hour, 2150 F cycle. A summary of the modifier and silicon deposition is presented in Table LXIII.

Triplicate specimens of each coating were oxidation tested at 1600 and 2400 F. The test results are summarized in Table LXII and the systems are discussed in Paragraph 5.1.5.

One series of specimens coated with the silicided 95Mo-5Ti composition was impregnated with a barium borosilicate glass (Solar S5210 frit) to improve the 1600 F oxidation resistance.

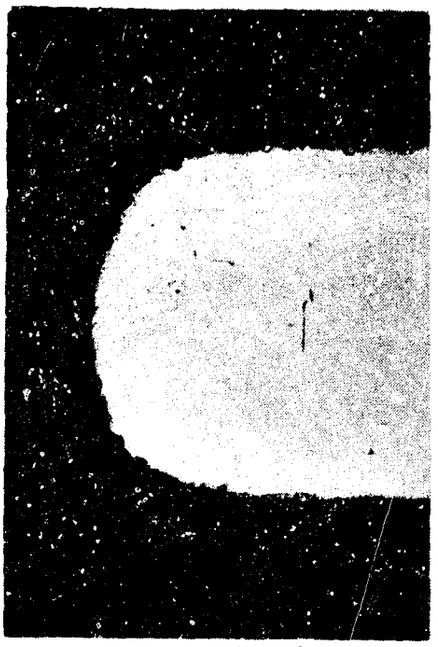

Magnification: 75X

89Mo-5Ti-6B Composition

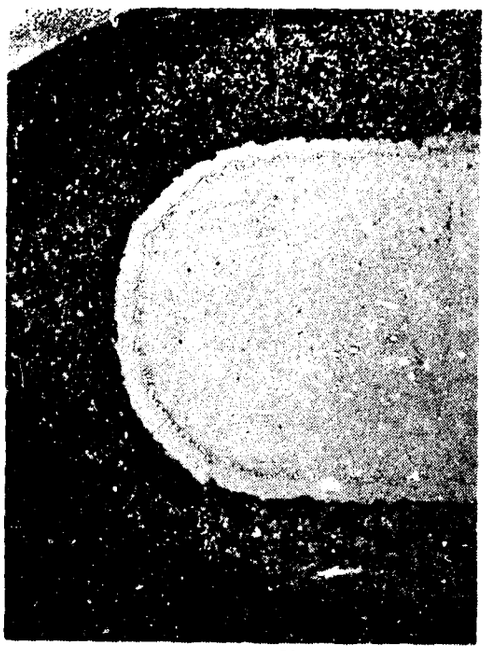

Magnification: 75X

Silicided 89Mo-5Ti-6B Composition

Magnification: 100X

86Mo-4Ti-10Fe Composition

Magnification: 75X

Silicided 86Mo-4Ti-10Fe Composition

FIGURE 104. MICROSTRUCTURE OF THE MODIFIED MOLYBDENUM-TITANIUM COATINGS BEFORE AND AFTER SILICIDING (Sheet 1 of 2)

Magnification: 100X

86Mo-4Ti-10Mn Composition

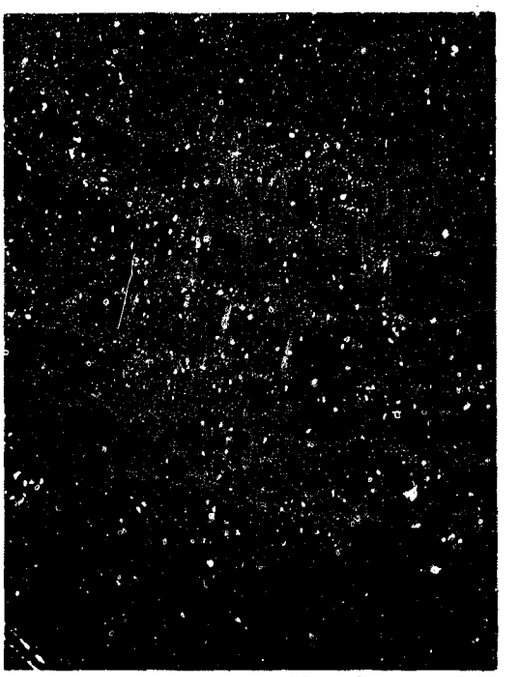

Magnification: 75X

Silicided 86Mo-4Ti-10Mn Composition

FIGURE 104. MICROSTRUCTURE OF THE MODIFIED MOLYBDENUM-TITANIUM COATINGS BEFORE AND AFTER SILICIDING (Sheet 2 of 2)

TABLE LXII

OXIDATION PERFORMANCE OF THE (Mo-Ti)-Si AND (Mo-Ti-X)-Si COATING SYSTEMS ON 0.030-INCH Cb752 ALLOY

Coating Composition	Oxidation Performance Hours to Failure for Each Specimen	
	1600 F	2400 F
(70Mo-30Ti)-Si	<96, <144, <264	11, 14, 35
(90Mo-10Ti)-Si	<24, <24, <24	104, 166, 166
(95Mo-5Ti)-Si	<24, <24, <24	130, 171(1), 281
(80Mo-5Ti-6B)-Si	>576, >576, >576	24, 31, 36
(86Mo-4Ti-10Fe)-Si	<24, >576, >576	202, 210, 220
(86Mo-4Ti-10Mn)-Si	<24, <24, <24	166, 166, 166
(95Mo-5Ti)-Si-impregnated	<240, >552, >552	222, 229, 255

1. Specimen dropped and damaged.

TABLE LXIII

DEPOSITION OF THE IRON-, MANGANESE-, BORON-CONTAINING MODIFIERS AND SILICON

Slurry Modifier Composition (wt %)	Modifier Cycle	Deposition (mg/cm^2)	Silicon Cycle	Deposition (mg/cm^2)
89Mo-5Ti-6B	15 hours at 2700 F	71	7 hours at 2150 F	42
86Mo-4Ti-10Fe	15 hours at 2700 F	67	7 hours at 2150 F	38
86Mo-4Ti-10Mn	15 hours at 2700 F	66	7 hours at 2150 F	39

The finely milled glass slurry was sprayed over the coating, allowed to penetrate into the coating by capillary action, and then removed from the specimen surface by wiping. The specimens were subsequently fired at 1800 F, resulting in an average coating weight gain of 0.5 mg/cm^2. Again, triplicate specimens of the impregnated coatings were oxidation tested at 1600 and 2400 F.

5.1.5 Oxidation Testing of the (Mo-Ti)-Si and (Mo-Ti-X)-Si Systems

Cyclic oxidation test results on the slurry-coated specimens are summarized in Table LXII. The microstructure of the (95Mo-5Ti)-Si and (90Mo-10Ti)-Si coatings after failure at 2400 F are shown in Figure 105. Each view shows considerable oxidation undercutting of the unsilicided zone of the coating. Failure generally occurs by a gradual increase in the width and depth of cracks which permits oxygen ingress to the substrate.

An impregnated (95Mo-5Ti)-Si and a (86Mo-4Ti-10Fe)-Si coated Cb752 specimen, both of which survived more than 200 hours of MAB-201M cyclic oxidation testing at 2400 F, were examined by microhardness traverses to determine the extent of oxygen contamination (Fig. 106). The iron-bearing coating appeared to be most contaminated but bend tests performed on the specimens revealed that room temperature ductility was lost in both specimens.

5.1.6 Discussion of the Systems Titanium-Molybdenum Slurry System

On the basis of oxidation resistance at 1600 F and 2400 F and substrate deterioration, the glass impregnated (95Mo-5Ti)-Si coating exhibited the most outstanding performance. The iron-modified 95Mo-5Ti composition gave some problems at

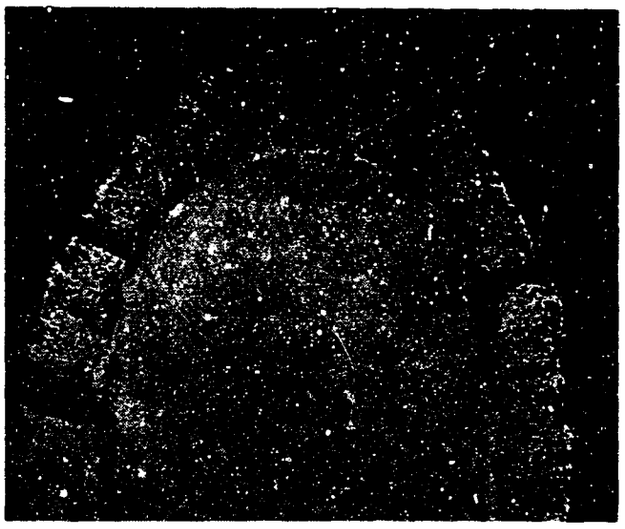

Silicided 95Mo-5Ti Composition
Failure after 104 hours at 2400 F

Magnification: 75X

Silicided 90Mo-10Ti Composition
Failure after 130 hours at 2400 F

Magnification: 75X

FIGURE 105. MICROSTRUCTURE OF FAILED (Mo-Ti)-Si COATINGS

1600 F and was slightly inferior at 2400 F to the glass impregnated (95Mo-5Ti)-Si composition. Oxidation resistance at 1600 F was considered poor for the manganese modified coating. Its performance at 2400 F was also inferior.

Slurries sintered at 2400 F (the 70Mo-30Ti and 80Mo-20Ti compositions) either spalled on siliciding or performed poorly at 2400 F. The 70Mo-30Ti composition, however, gave fair performance at 1600 F, whereas, the 95Mo-5Ti and 90Mo-10Ti coatings sintered at 2700 F had most of their trouble at 1600 F.

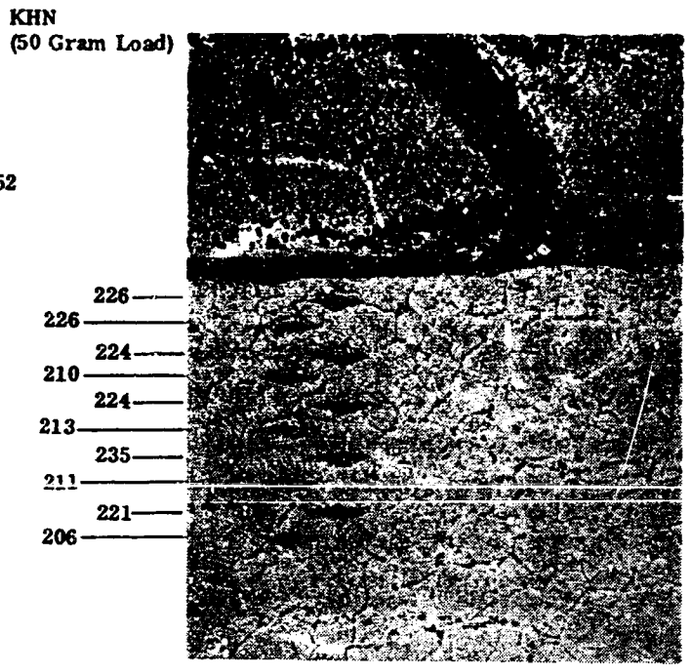

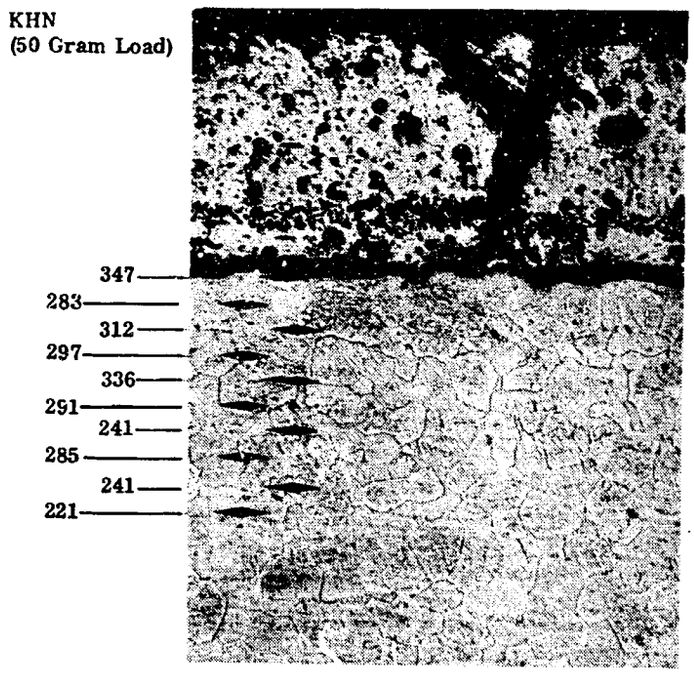

FIGURE 106. MICROHARDNESS OF SELECTED SLURRY COATINGS AFTER 2400 F OXIDATION

Because of the small effort that was expended on slurries little more can be concluded about them. They do appear promising and more effort should be devoted to them to compliment the current studies being performed at Solar on the protection of tantalum with slurry coatings (Ref. 17). Lives of 600 hours or more at 2400 F have been obtained with slurry coatings on tantalum in that program with retained bend ductility.

Specimen of the (95Mo-5Ti)-Si glass impregnated coating were erosion rig tested in Phase III of this program and in a concurrent program (Ref. 1) at Pratt & Whitney. Results appeared quite satisfactory relative to any other coating investigated, but the number of specimens tested was small leaving considerable future work to prove these slurry sintered coatings.

5.2 THE V-(Cr-Ti)-Si SYSTEM

In the initiation of the development activities on the (V-Cr)-Si coating, numerous methods were investigated in an effort to deposit uniform V-Cr modified layers on D43 and Cb752 alloys (0.012 inch). Alloy purification studies were also included to minimize oxygen transport from the V-Cr modifier alloys to the specimens. The activities covered:

- Coating deposition
  - V-Cr codeposition
    - High-pressure pack
    - Vacuum pack
  - Vanadium deposition
    - High-pressure pack
    - Low-pressure pack
    - Fused salt electrodeposition
  - Chromium deposition
    - Fused salt
  - (Cr-Ti) deposition
    - High-pressure pack
    - Low-pressure pack
- Pack alloy purification
  - V-Cr - Arc melting alloys with additions of rare earths, titanium, and carbon

This section will not include the presentation of all of these data, but rather will present the most satisfactory approaches to the development of a surface layer containing vanadium and chromium, i.e., the multicycle V-(Cr-Ti)-Si coating applied by pack deposition techniques. Pack alloy purification studies and the other deposition approaches are summarized in the Appendix. In brief, codeposition of V-Cr was not possible in the amounts desired (15 to 20 mg/cm^2) at temperatures up to 2600 F. Fused salt deposition of chromium severely embrittled the alloys, although deposits of adequate thickness could easily be plated; and addition of rare earths to V-Cr minimized oxygen transport when the alloys were used in packs, but deposition rates were low and there was indication of specimen staining as a result of rare earth metal transport. The use of titanium in the chromium packs was essential to increase the deposition rate and to control the oxygen transport, although, as will be noted later, titanium could not completely prevent the embrittlement of the high zirconium Cb752 alloy.

For comparison with the V-(Cr-Ti)-Si coating system, a brief presentation of data on the (Cr-Ti)-Si, (Cr-Ti)-V-Si, and V-Si coatings is included to show the differences in oxidation performance.

Preliminary work on the V-(Cr-Ti)-Si coating was largely distributed among three series of specimens. The initial series was a small number of Cb752 coupons designed to determine whether or not the system was promising, and also to contrast the performance of titanium-chrome deposited from 60Cr-40Ti and 80Cr-20Ti packs.

In addition to verifying by Weibull analysis the conclusions of the first series, the second series specimens were (Cr-Ti) coated in a sealed vacuum container to help eliminate the embrittlement of the Cb752 alloy. The post (Cr-Ti) diffusion anneals were also carried out in a vacuum. The D43 as well as the Cb752 alloy was included in the second series.

The purpose of the third series was to resolve whether or not the diffusion annealing cycles contributed anything to the performance of the coating. The deposition of vanadium and (Cr-Ti) from vacuum containers was a second goal for that series, but difficulties with welding the Cb752 container postponed accomplishment. Like the second series, both the D43 and Cb752 alloys were tested.

Prior to work on the third series specimens, a small side effort was given to developing the low-pressure vanadium pack on a number of Cb132M specimens. As a result of that study, a decision was made to use this pack for further vanadizing.

The final activity in Phase I of the program was the application of the selected coating, V-(Cr-Ti)-Si, to the specimens to be evaluated in Phase II (Reentry application, Part II) and Phase III (Turbomachinery application, Part III).

5.2.1 Deposition of Vanadium

Four approaches were investigated in an effort to deposit vanadium onto Cb752 and D43 alloys - high pressure pack deposition, low pressure pack deposition, non-electrolytic and electrolytic deposition from fused salt. Fused salt deposition is presented in the Appendix since it was not the selected technique. Pack techniques were emphasized, since they required the minimum development to effect the program goals of 3 to 7 mg/cm^2 vanadium without severe substrate embrittlement.

Pack Deposition

Materials. All vanadium pack media used on the program was of the purity designated by Union Carbide as 99.8 percent. The oxygen content was guaranteed to be less than 1000 ppm and the iron was less than 1200 ppm.

Early in the program, reagent grade NaF was used as the pack activator, but K_2VF_5 was found to be much more effective. The latter chemical was produced at Solar by the following procedure:

Potassium Vanadium Pentafluoride (K_2VF_5) Preparation

- 100 grams of 99.8 percent vanadium were slowly dissolved in concentrated hydrofluoric acid to produce the dark green vanadium trifluoride solution.
- 450 grams of reagent grade potassium bifluoride (KF.HF) were dissolved in hot water and added to the vanadium trifluoride solution. The mixture was allowed to stand overnight to ensure complete precipitation of the green $K_2VF_5 . nH_2O$ product.
- The clear supernatant liquid was decanted.
- The filtered green precipitate was water and acetone rinsed vacuum dried for 16 hours at 250 F.
- The precipitate was further dried at 500 F for 16 hours in a protective atmosphere of hydrogen fluoride gas and was cooled in an argon atmosphere. This treatment is required to prevent oxyfluoride formation and ensure complete removal of water.
- The light green K_2VF_5 product (approximately 250 grams) was stored in a desiccator until needed

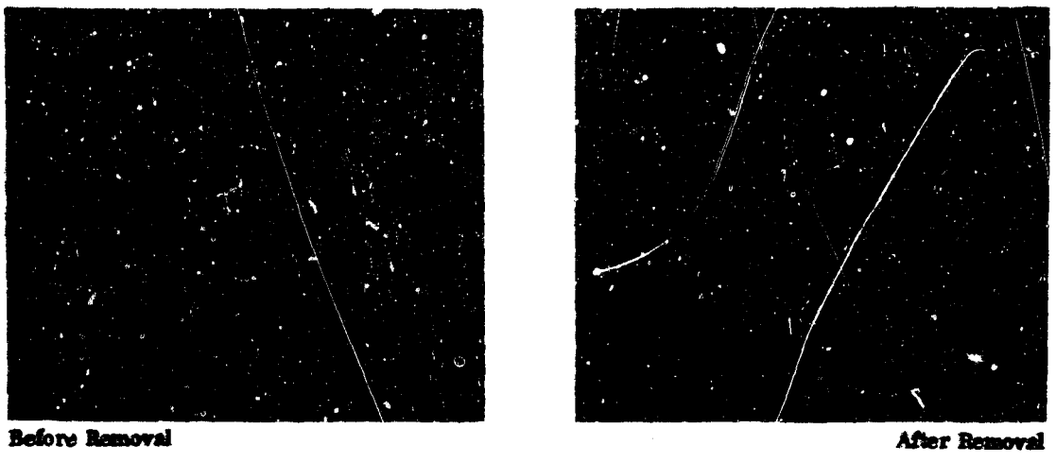

Before Removal

After Removal

Deposition Cycles: 2250 F, 15 hours in a 99% vanadium pack (-8 + 20) with 1 percent NaF

Magnification: 3X

FIGURE 107. SINTERING DURING VANADIUM DEPOSITION

High-Pressure Pack Deposition

Series I. In Series I, 70 specimens (0.012 by 1/2 by 3/4-inch Cb752 alloy) were vanadized in a 99 percent vanadium (99.8% V, -8 + 20 mesh size) -1 percent NaF high-pressure pack using a 2250 F, 15-hour cycle. Weight gains average 9.1 mg/cm^2, but this was not a uniform deposit since considerable sintering of particles to the specimens was in evidence. Sintering was so acute after the 15-hour run that the pack had to be broken by chiseling, and the removal of vanadium particles bonded to the specimens often damaged the coating.

The macrophotographs in Figure 107 show the specimens before and after the vanadium particles were removed.

To decrease the concentration of vanadium on the surface to approach the range of greater oxidation resistance in the Cb-V field, the Series I specimens were given a 2500 F, six-hour anneal in a 10^{-5} Torr vacuum. A comparative X-ray fluorescent analysis before and after annealing is given below.

Element	Before Annealing	After Annealing
Columbium	26,900	32,600
Vanadium	7900	2910
Iron	2239	247

A Cb752 specimen used as a standard gave the following rates: Cb18,300; V30.7; Fe275.

The microstructure and KHN (50-gram load) microhardness traverses are shown in Figure 108. The hardness results show very little hardening of the Cb752 substrate and a relatively soft coating, particularly as deposited. The specimen exhibited bend ductility before and after diffusion annealing.

The principal limitation of the Series I process for vanadium deposition was in the excessive sintering of particles to the specimen and in particle-to-particle sintering in the pack that made it extremely difficult to extricate the specimens.

Series II. In the Series II vanadizing runs, several approaches were undertaken to lessen the sintering problem noted in Series I. These were use of K_2VF_5 as an activator hopefully to increase the deposition rate by increasing the vanadium ion concentration in the vapor phase, and a reduction in deposition time to minimize solid-state bonding. Both 0.012- by 0.5- by 0.75-inch D43 and Cb752 alloy specimens were included in Series II runs. The same high-pressure deposition technique used in Series I was used in Series II runs. Activators were added at the one percent level.

To determine the effect of time on the deposition weight, a group of D43 and Cb752 specimens were coated for three hours at 2250 F in a NaF-activated pack similar to Series I. Sintering was negligible in this time, but deposition was only 1 mg/cm^2. The run was repeated on the same specimens with the anticipation that all of the retort materials would have become coated with vanadium and the rate would increase. A slight increase was noted to 1.5 mg/cm^2, but the time and expense to attain the objective of 7 mg/cm^2 would be prohibitive by this multiple cycling technique. Multiple cycling did, however decrease sintering.

In an attempt to increase the deposition rate, the same specimens that had been cycled twice were cycled again, but this time one percent K_2VF_5 was used as the activator. A three-hour, 2250 F cycle was used. The deposition rate, even though there was already considerable vanadium on the specimens, was markedly increased (Table LXIV). Sintering was also greatly reduced relative to the Series I runs (Fig. 108).

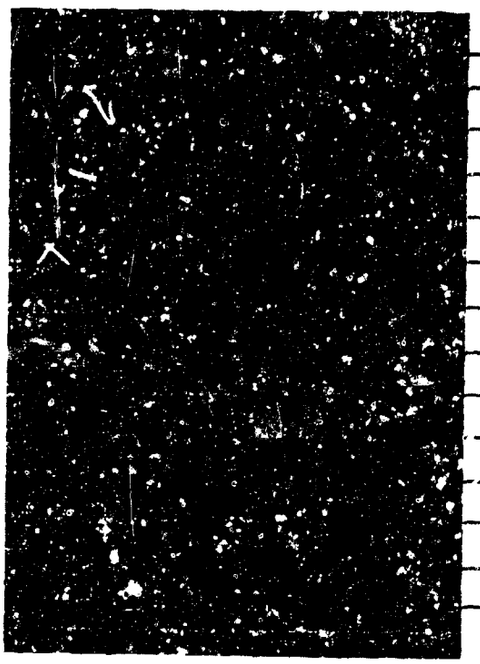

A. As Coated

Initial specimen hardness equals 213

Magnification 250X

B. Annealed for 6 hours at 2500 F in 10^{-5} Torr vacuum

FIGURE 108. VANADIUM COATED Cb752 ALLOY; Series I Specimens

TABLE LXIV

SERIES II VANADIUM DEPOSITION

Cycle	Activator	Deposition (mg/cm^2)	Time (min)	Temperature (F)	Pack Type	X-ray Counting (cycles/sec)			
						Cb	V	Fe	Ni
Cb752 Alloy									
I	NaF	1.1	180	2250	HPP	--	--	--	--
II	NaF	1.5	180	2250	HPP	--	--	--	--
III	K_2VF_5	4.8	180	2250	HPP	15,100	1470	232	103
Total	--	7.4	--	--	--	--	--	--	--
IV (anneal)	none	--	360	2500	Vacuum	17,900	410	227	127
D43									
I	NaF	1.0	180	2250	HPP	--	--	--	--
II	NaF	1.4	180	2250	HPP	--	--	--	--
III	K_2VF_5	4.3	180	2250	HPP	16,300	1360	217	85
Total	--	6.7	--	--	--	--	--	--	--
IV (anneal)	--	--	360	2500	Vacuum	17,900	423	229	101

*High pressure pack (slightly above atmospheric pressure with argon).

The microstructure and hardness of vanadized Series II Cb752 and D43 specimens are shown in Figures 109 and 110. Ductility was retained in the as-deposited and annealed conditions, and the microhardness of the substrate was only slightly increased. The diffused coating was markedly harder than the as-deposited vanadium indicating major solid-solution hardening, interstitial contamination, or the formation of the CbV_2 intermetallic analogous to the $CbCr_2$ Laves phases. The low-vanadium content, as indicated from the fluorescent analysis Table LXV, after annealing would not support the Laves phase hypothesis; consequently the first two reasons given are probably responsible for the high hardness.

TABLE LXV

X-RAY FLUORESCENT ANALYSES OF THE Cr-Ti COATED SPECIMENS

Finish	Counts/Second			
	Cb	Cr	V	Ti
60Cr-40Ti deposited	39,600	1415	550	480
80Cr-20Ti deposited	39,900	4560	495	340
60Cr-40Ti annealed	41,400	1188	716	243
80Cr-20Ti annealed	43,800	3520	598	156

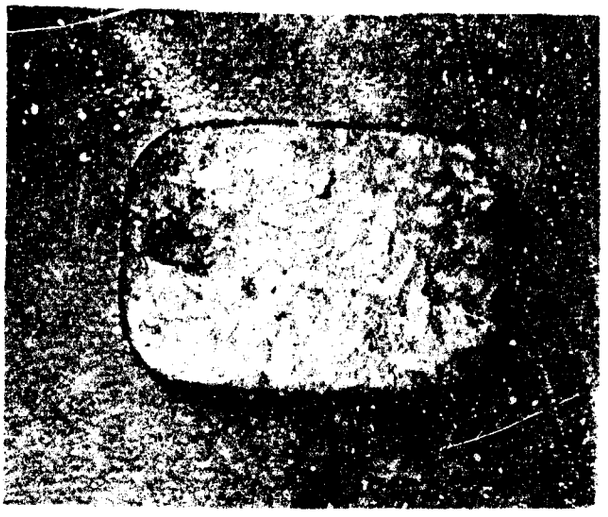

Cb752 alloy; K_2VF_5 activator - 7.4 mg/cm^{2}V

Magnification: 3X

D43 alloy; K_2VF_5 activator - 6.7 mg/cm^{2}V

Magnification: 3X

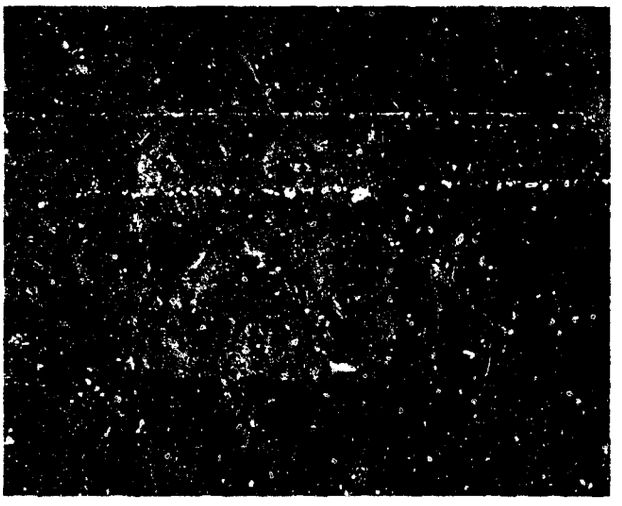

FIGURE 109. AS-VANADIZED Cb752 AND D43 ALLOYS; Series II Specimens

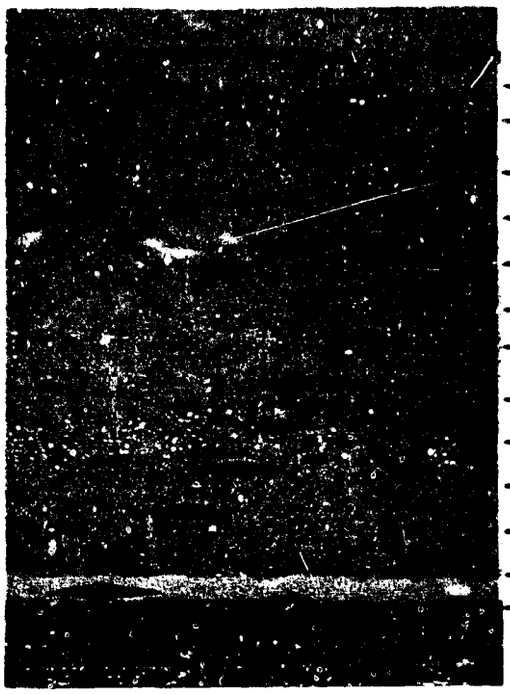

As Vanadized Cb752 Alloy
Magnification: 250 X

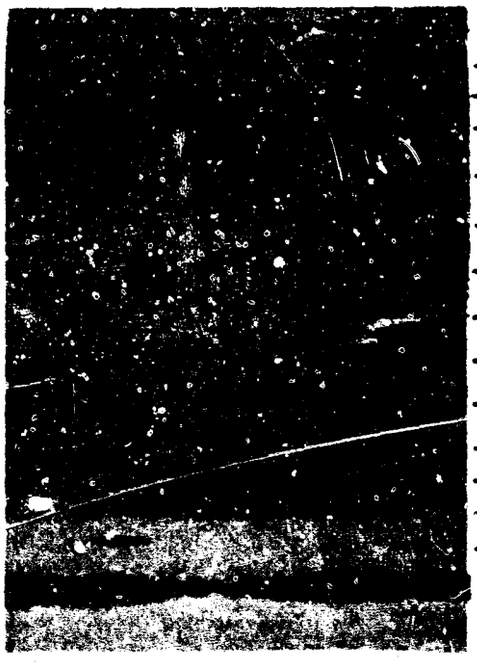

Vanadized and Annealed Cb752 Alloy
Magnification: 250 X

FIGURE 110. VANADIZED AND ANNEALED Cb752 AND D43 ALLOYS;
Series II Specimens (Sheet 1 of 2)

KHN
(50 Gram Load)

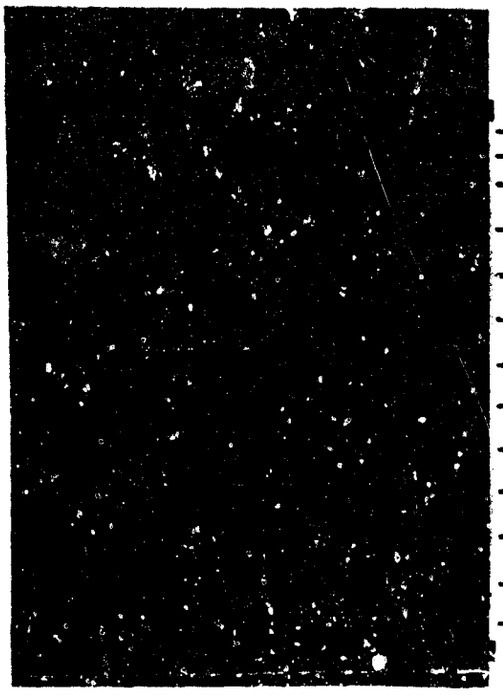

— 288
— 219
— 208
— 237
— 217
— 226
— 208
— 221
— 226
— 211
— 215
— 230
— 185

As Vanadized D43 Alloy
Magnification: 250 X

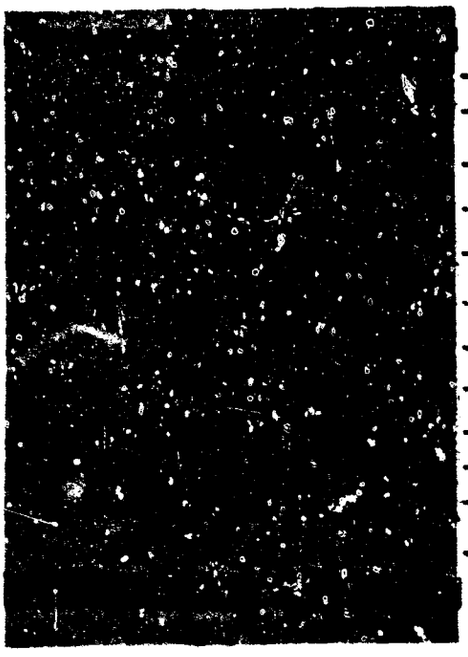

— 521
— 206
— 208
— 196
— 217
— 194
— 211
— 211
— 224
— 199
— 202
— 499

Vanadized and Annealed D43 Alloy
Magnification: 250 X

FIGURE 110. VANADIZED AND ANNEALED Cb752 AND D43 ALLOYS, Series II Specimens (Sheet 2 of 2)

Series III. The Series III vanadized specimens were prepared primarily to determine, for the oxidized V-(Cr-Ti)-Si coating, if the diffusion cycle after vanadizing was essential to long oxidation life. The vanadizing was performed using the high-pressure pack system, 1 percent K_2VF_5, 99 percent vanadium (-8 + 20 mesh) and a cycle of 300 minutes at 2250 F.

Separated activator was used in this series. The activator was added by first laying down a 0.25-inch layer of vanadium, then the activator followed by another 0.25-inch of vanadium. All of the specimens were then immersed in vanadium granules above this activator reservoir. Elimination of the liquid-phase activator contact with the specimen was designed to eliminate any nonelectrolytic fused salt transfer of vanadium that would occur at the contact site, perhaps contributing to sintering.

Deposition weights were 7.3 and 5.0 on Cb752 and D43 alloys, respectively. Sintering was similar to the Series II specimens, but this was considered an improvement because the deposition weight in the group of specimens in a single cycle was greater than for the Series II specimens. All other characteristics were similar to the Series II deposit. Bend ductility was retained.

Vacuum Pack Deposition

Two vanadizing runs were made in vacuum packs. The runs used the separated activator (one percent) of the Series III runs and the -8 + 20 mesh vanadium granules. A pure vanadium retort was used. Sealing of the retort was by a TIG and EB welding procedure as shown in Figure 111. Overnight pumpdown in the EB welder was used to outgas the retort prior to final sealing.

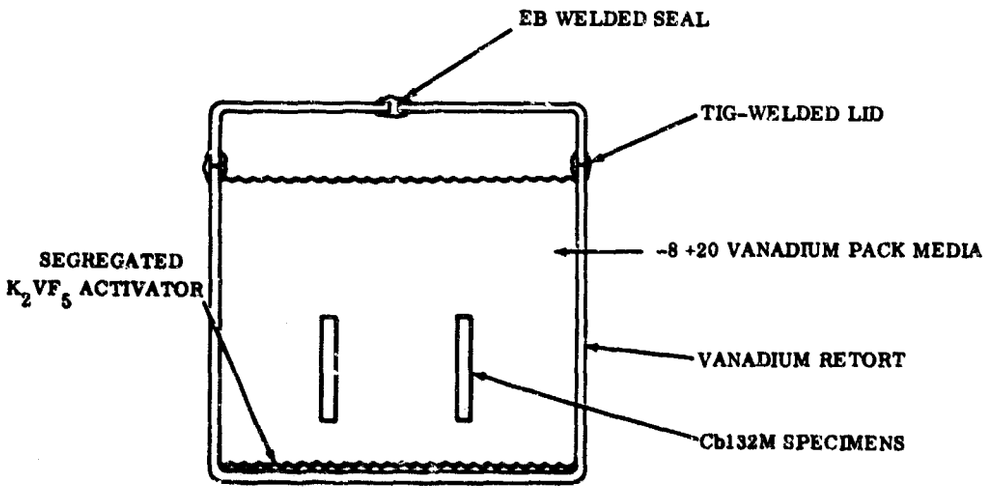

FIGURE 111. SCHEMATIC ARRANGEMENT OF A LOW-PRESSURE RETORT

Two runs were made with 300-minute cycles at 2300 F and yielded 4.8 and 7.7 mg/cm^2 of vanadium with slightly less sintering than the Series III runs. Cause of variation in deposition weight is not known, but this technique was very sensitive to loss of activator from the retort. Since the retort is heated in a 10^{-5} vacuum, activator losses can be quite high even from undectable weld fissures.

5.2.2 Deposition of Chromium-Titanium

Two pack materials, 60Cr-40Ti and 80Cr-20Ti, were investigated to determine the one which would provide the most oxidation-resistant coating over vanadized Cb752 and D43 alloys. The goal was the highest chromium content possible to minimize the effect of the titanium in the coating as an interstitial sink for carbon and oxygen from the substrate.

Material

Chromium-titanium pack media in weight percent were either of arc-melted 60Cr-40Ti powder or an 80Cr-20Ti mixture. The latter was produced by blending 50 weight percent (60Cr-40Ti) alloy with 50 weight percent hydrogen-reduced electrolytic chromium. Table LXVI lists the pack powders used, the manufacturer, their mesh size, and iron and oxygen analyses.

TABLE LXVI

CHROME-TITANIUM PACK MEDIA

Material	Mesh Size	Chemical Analysis (wt %) Oxygen (%)	Iron (%)	Manufacturer
60 wt % - 40 wt % Ti	-50 + 100	0.083	0.21	Oremet
Hydrogen reduced electrolytic chromium	-50 + 100	0.119	0.24	Union Carbide

Preliminary Deposition Studies

Initial deposition studies were designed to determine the most effective pack activator and (Cr-Ti) pack composition for coating the vanadized columbium alloys. High-pressure runs made with both 60Cr-40Ti and 80Cr-20Ti materials and NaF and K_2VF_5 activators at 2300 F showed that there were no advantages in the use of K_2VF_5 over the NaF activator. Sodium fluoride was, therefore, selected at the one percent

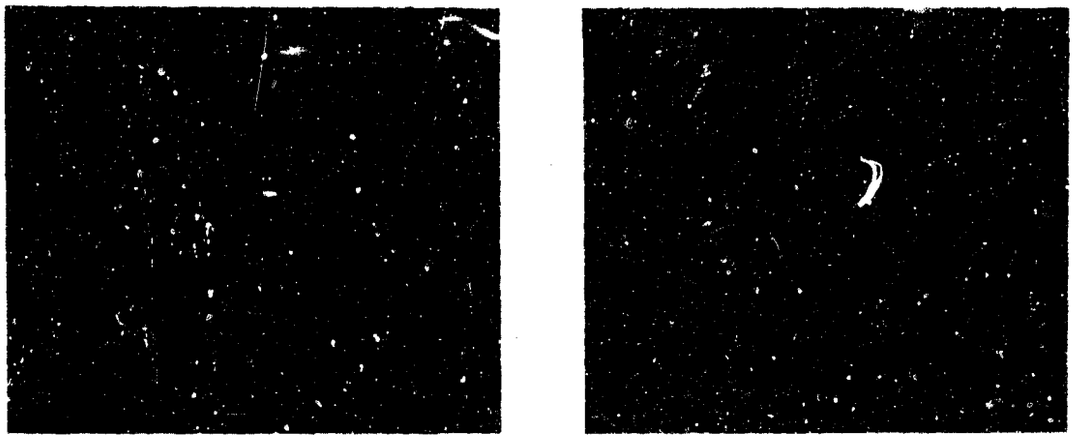

80Cr-40Ti 60Cr-40Ti

Magnification: 3X

FIGURE 112. AS-COATED SURFACE FINISH OF CHROMIUM-TITANIUM VANADIZED Cb752 ALLOY

level for all subsequent studies. These preliminary studies also showed that it required approximately 1.5 hours to deposit 8 to 11 mg/cm^2 from the 60Cr-40Ti pack at 2300 F, and 5.0 hours to deposit a similar quantity from the 80Cr-20Ti pack.

Neither the 60Cr-40Ti nor the 80-20 specimens would pass the 90-degree bend test after the Cr-Ti deposition. However, after the 15-hour, 2200 F anneal, the 60Cr-40Ti specimens regained enough ductility to resist fracturing on bending.

Some sintering of the fine (-100) 60Cr-40Ti pack particles to the specimens occurred at the relatively high deposition temperature used. Figure 112 shows the surface finish as coated.

Microstructure and microhardness traverses of both Ti-Cr coatings before annealing are shown in Figure 113. There appears to be very little correlation between substrate bend ductility and microhardness. Both coatings exhibited brittle bend behavior, but substrate hardening was almost negligible. Coating hardness was high, however.

Microstructures and hardness traverses after annealing the Cr-Ti coatings are shown in Figure 113. The 60Cr-40Ti coating is uniform, single phased, and exhibits a slightly lower hardness than the as-deposited coating. The 80Cr-20Ti is also uniform, but exhibits a minor second phase on the surface which may be indicative of the start of the Laves (MCr_2) phase formation. The surface hardness is slightly increased over the 60Cr-40Ti composition. Neither of the processes exhibit appreciable substrate hardening after the 2200 F anneal.

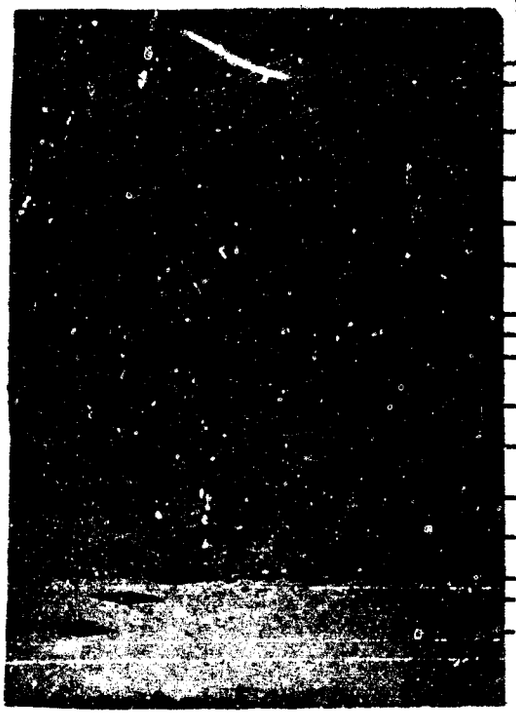

As Coated

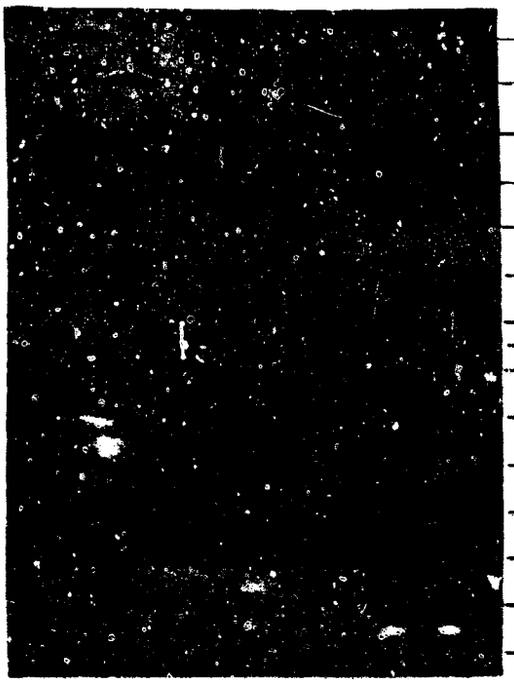

60Cr-40Ti
Magnification: 250X

Annealed at 2200 F for 15 hours

FIGURE 113. CHROMIUM-TITANIUM COATED VANADIZED Cb752 ALLOY: Series I Specimens (Sheet 1 of 2)

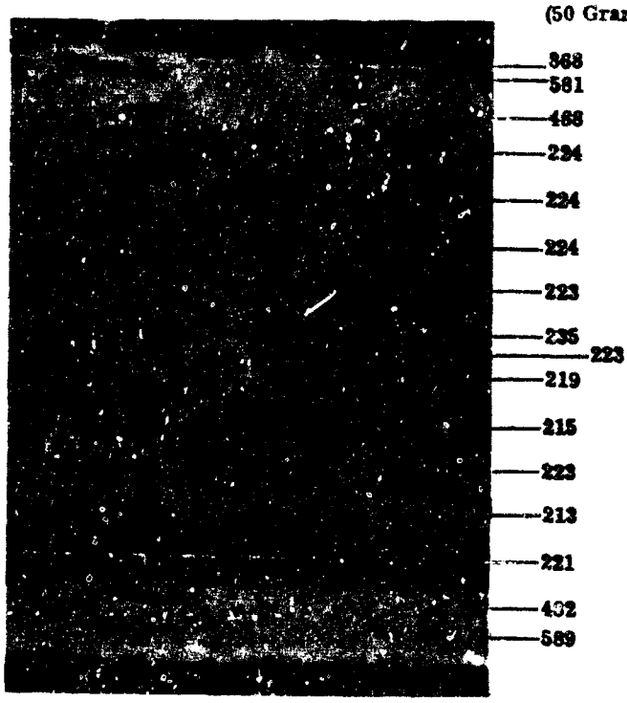

FIGURE 113. CHROMIUM-TITANIUM COATED VANADIZED Cb752 ALLOY; Series I Specimens (Sheet 2 of 2)

The apparent substrate embrittlement as indicated by bend testing may be due either to the precipitation of zirconium oxide at the grain boundaries leaving the substrate at a constant hardness value, or to the inability of the thin substrate (0.010 inch) to absorb the strain energy released in fracture of the very hard coating.

Surface fluorescent analysis is at best a semi-quantitative analytical technique because of the variable depth of penetration of the beam, but the data (Table LXVI) clearly show a marked increase in chromium content of the coating in going from the 60Cr-40Ti to the 80Cr-20Ti composition. Vanadium and titanium content do not appear to vary in the same percentage as the chromium, indicating that there is probably a notable decrease in mobility of columbium in the high-chromium coating as a consequence of the increased stability of the $CbCr_2$ Laves phase.

The specimens were silicided at 1950 F in a 99Si-1NaF high-pressure pack to a thickness that would not completely penetrate the modified zone. (Details of the siliciding process will be provided in Section 5.2.3.) A cycle of 2.5 hours at 1950 F was used and it deposited 10.9 mg/cm^2 on the 60Cr-40Ti, and 12.2 mg/cm^2 on the 80Cr-20Ti modified specimens. A comparison of the two coatings as silicided is shown in Figure 114.

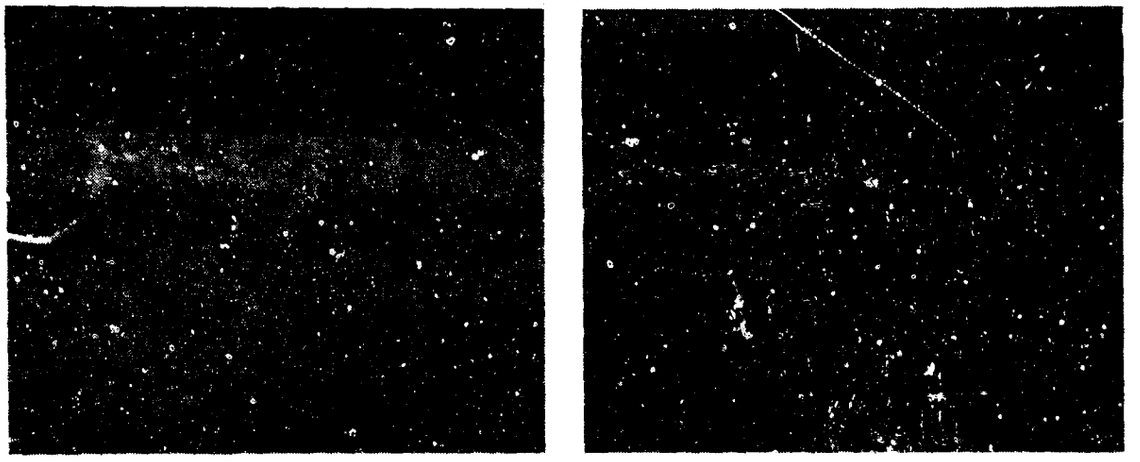

V-(60Cr-40Ti)-Si Coated Cb752 Specimen of Series I V-(80Cr-20Ti)-Si Coated Cb752 Specimen of Series I

Magnification: 250X

FIGURE 114. MICROSTRUCTURE COMPARISON OF V-(60Cr-40Ti)-Si AND V-(80Cr-40Ti)-Si COATINGS

A summary of the oxidation and deposition data are given in Table LXVII. Although there was a 12 percent difference in the amount of silicon deposited on the 60Cr-40Ti and 80Cr-20Ti alloys, this appeared inadequate to account for the outstandingly superior oxidation performance of the V-(80Cr-20Ti)-Si coating at 2400 F. At this point in the program, the 60Cr-40Ti composition was dropped in preference to the 80Cr-20Ti composition.

TABLE LXVII

PRELIMINARY SUMMARY OF OXIDATION DATA ON THE V-(60Cr-40Ti-Si AND V-(80Cr-20Ti)-Si COATINGS

Coating Weight				
V[1] (mg/cm^2)	60Cr-40Ti[2] (mg/cm^2)	80Cr-20Ti[3] (mg/cm^2)	Si[4]	Oxidation Life (1-hour cycles, 2400 F)
9.1	11	--	10.9	9, 9, 31
9.1	--	8	12.2	26, 120, 120

1. Series I vanadium
2. Deposited 2300 F in 1.5 hours.
3. Deposited 2300 F in 5.0 hours.
4. Deposited 1950 F in 2.5 hours.

High-Pressure Pack Deposition of the 80Cr-20Ti Composition

Series I and III vanadized specimens were coated with 80Cr-20Ti using the high-pressure pack technique; whereas, Series II specimens were coated using the low-pressure technique described in the next section. Because of severe particle sintering during vanadizing of the Series I specimens, they were not considered of adequate quality to be used for screening purposes, but were carried through all of the coating steps to obtain a feeling for the effect that the heavier vanadium coating plus sintering would have on the life of the coating after Cr-Si and silicon coatings.

High-pressure pack techniques using the retort type shown in Figure 101, -50 + 100 grit 80Cr-20Ti pack media, a temperature of 2300 F and one percent NaF activator were used in all deposition cycles. Time was varied to effect a minimum of 10 mg/cm^2 on Series III specimens. Series I specimens received an 8 mg/cm^2 deposit in five hours as previously noted. Either of these deposits when combined with the vanadium was believed adequate to retain some unsiliciced surface alloy after the deposition of 12 mg/cm^2 of silicon.

Based on the preliminary deposition results with Series I specimens, it was believed that 10 mg/cm^2 of Cr-Ti could easily be achieved with a 10-hour cycle at 2300 F; however, it was found necessary to recycle the specimens in the pack for an additional five hours to achieve the deposition weight on the Series III specimens. The deposition rate appears to be a strong function of the amount of vanadium present. Destabilization of the Laves phase with vanadium is imperative to obtain a moderately rapid deposit rate from the 80Cr-20Ti pack. For example, 30 hours are required to deposit 11 mg/cm^2 of 80Cr-20Ti directly onto the Cb752 alloy; whereas, this same amount can be deposited on a vanadized substrate in 10 to 15 hours.

The deposition results for the Series I and III are given in Table LXVIII, and the microstructure and microhardness of the Series III specimens are shown in Figures 115 and 116 for the Cb752 and D43 alloys, respectively. As previously noted in the preliminary screening studies for 60Cr-40Ti and 80Cr-20Ti, the application of the 80Cr-20Ti coating has essentially no effect on substrate hardness, but bend ductility is not retained. The D43 alloy with the lower zirconium content exhibits considerably more bend ductility than the Cb752 alloy.

TABLE LXVIII

DEPOSITION HISTORY OF SERIES I AND III SPECIMENS THROUGH THE 80Cr-20Ti CYCLES(1)

Series	Alloy	Cycle Activator	Deposition (mg/cm^2)	Time (min)	Temperature (F)	Pack Type
I	Cb752	Vanadium-NaF	9.1	900	2250	HPP
		80Cr-20Ti-NaF	8.0	300	2300	HPP
III	Cb752	Vanadium-K_2VF_5	7.3	300	2250	HPP
		80Cr-20Ti-NaF				
		First cycle	8.6	600	2300	HPP
		Second cycle	2.0	300	2300	HPP
			10.6			
	D43	Vanadium-K_2VF_5	5.0	300	2250	HPP
		80Cr-20Ti-NaF				
		First cycle	9.1	600	2300	HPP
		Second cycle	1.9	300	2300	HPP
			11.0			

1. Specimen 0.12 by 0.5 by 0.75 inch.

Magnification: 200X

FIGURE 115.

Cb752 ALLOY AFTER COATING WITH VANADIUM AND (Cr-Ti); Series III Specimens

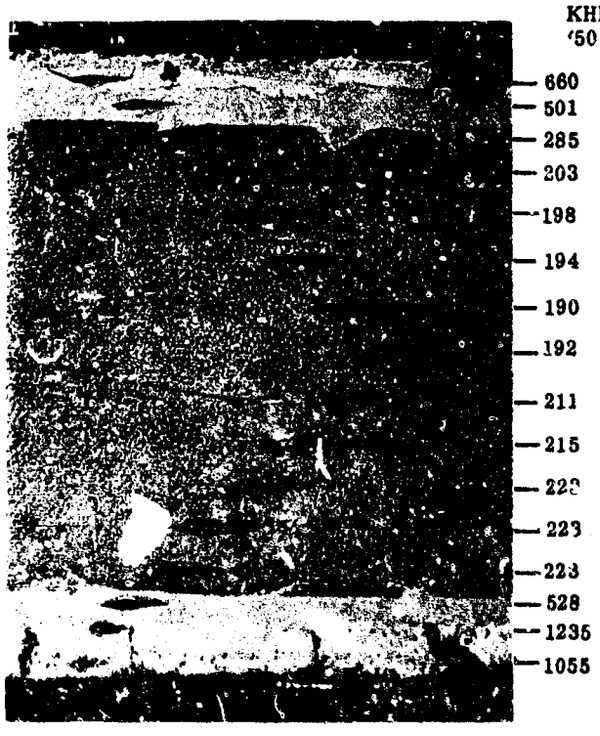

Magnification: 200X

FIGURE 116.

D43 ALLOY AFTER COATING WI VANADIUM AND (Cr-Ti); Series Specimens

Low-Pressure Pack Deposition of 80Cr-20Ti Composition

Loss of bend ductility in the Cb752 alloy during application of the 80Cr-20Ti by high-pressure pack techniques was the primary basis for experimenting with the low-pressure technique for deposition of this surface modifier. The low-pressure technique, which used Cb752 retorts and the sealing techniques described for low-pressure deposition of vanadium (Fig. 111), essentially eliminates gaseous environmental contamination, but not transfer from the pack media.

The pack materials used were 80Cr-20Ti (-50 + 100 mesh) and one percent NaF as the activator. Deposition conditions were the same as in the first cycle high-pressure pack, i.e., 2300 F for 10 hours.

Table LXIX shows the deposition results on D43 and Cb752 alloys, and the effect of a 2200 F, 16-hour vacuum diffusion cycle. Figure 117 shows the specimens both before and after annealing.

Under a comparable temperature-time cycle condition, the low-pressure pack technique deposits a more uniform coating with a greater weight of the 80Cr-20Ti modifier than the high-pressure pack technique. For example, on vanadized Cb752 alloy, a 10-hour cycle at 2300 F in the low-pressure pack deposited 12.8 mg/cm^2 compared to only 8.6 mg/cm^2 in the high-pressure pack technique. Deposition on the D43 was slightly more rapid than on the Cb752 alloy.

The V-(Cr-Ti) coated specimens were vacuum annealed at 2200 F for 16 hours to increase the chromium and titanium in the Cb-V modified zone. This annealing cycle had the unfortunate effect of vaporizing 4 mg/cm^2 of the coating (Table LXIX). This loss is probably all chromium due to the relatively high vapor pressure of this element as compared to columbium, vanadium and titanium. The surface X-ray emission data (Table LXV) do not necessarily support this selective loss of chromium.

The microstructure and microhardness of the coatings (Fig. 118 and 119) are similar to the Series I and III Cr-Ti modified alloys. Although a clearly defined two-phase structure is not apparent in the photomicrographs, visual examination supports a definite two-phase coating. The inner layer is probably the solid-solution region in the Cb-V-Cr-Ti region; whereas, the outer high-chromium layer is probably Laves phase (Cb-Ti) $(V-Cr)_2$. The high hardness of outer surface is indicative of compound formation.

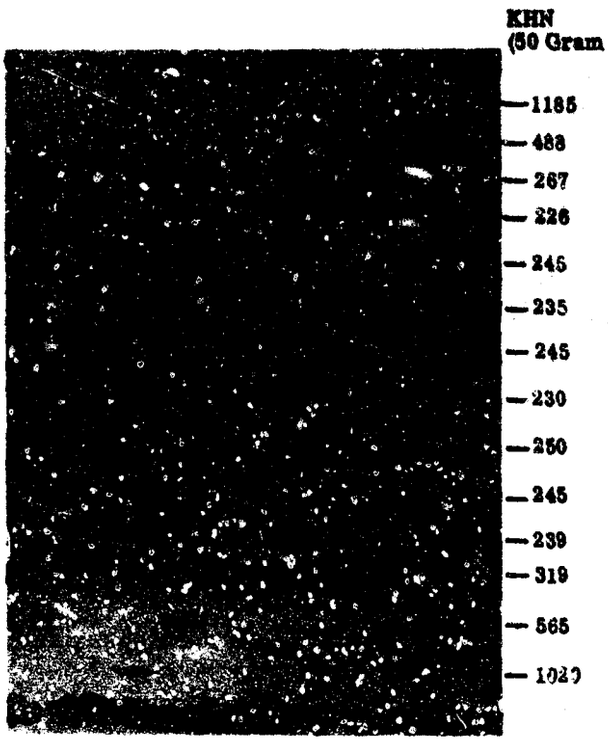

As-Coated Cb752 Alloy
Magnification: 250X

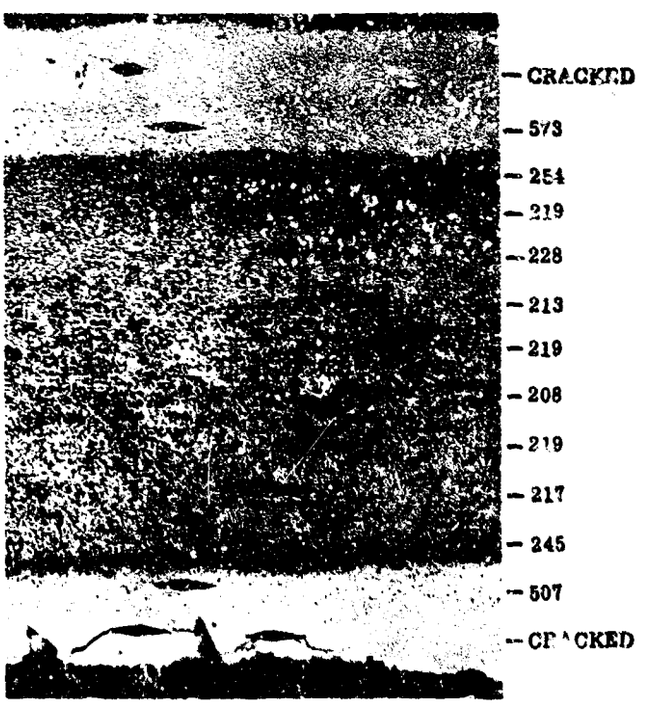

Annealed in vaccum for 16 hours at 2200 F
Magnification: 250X

FIGURE 117. VANADIZED SPECIMENS COATED WITH 80Cr-20Ti USING LOW-PRESSURE TECHNIQUES; Series II (Sheet 1 of 2)

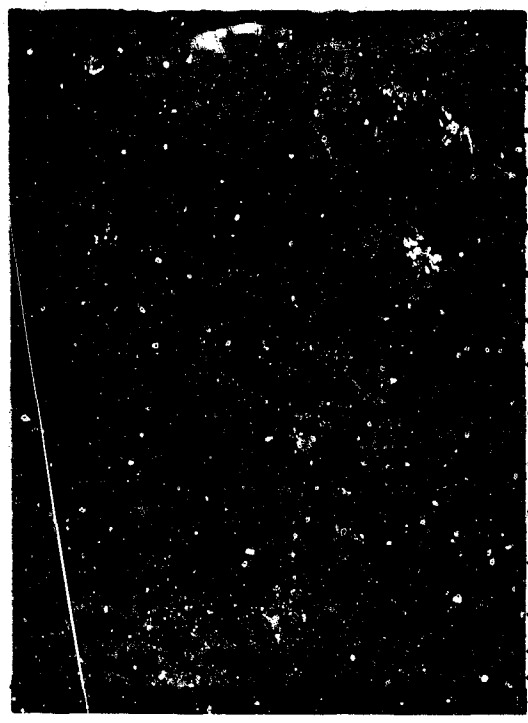

As-Coated D43 Alloy

Magnification: 250X

Cb752

Annealed in vacuum for 16 hours at 2300 F

Magnification: 250X

FIGURE 117. VANADIZED SPECIMENS COATED WITH 80Cr-20Ti USING LOW-PRESSURE TECHNIQUES; Series II (Sheet 2 of 2)

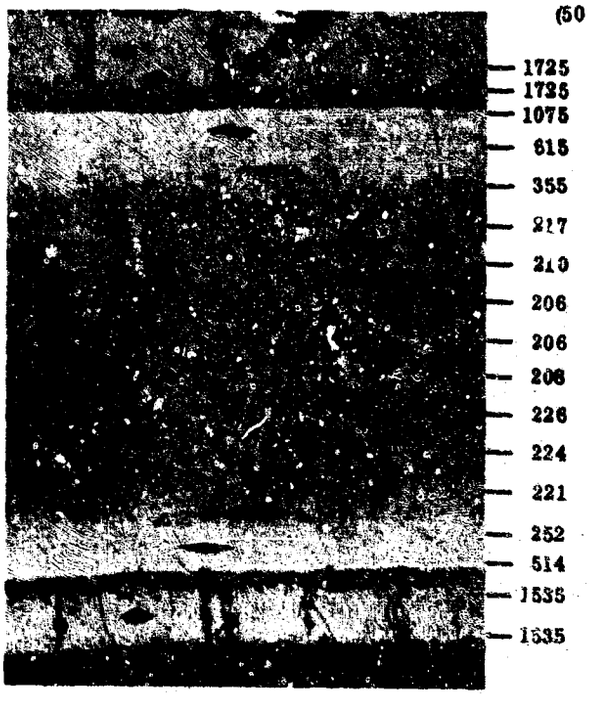

Magnification: 200X

FIGURE 118.

V-(Cr-Ti)-Si COATED Cb752 SPECIMEN; Series II

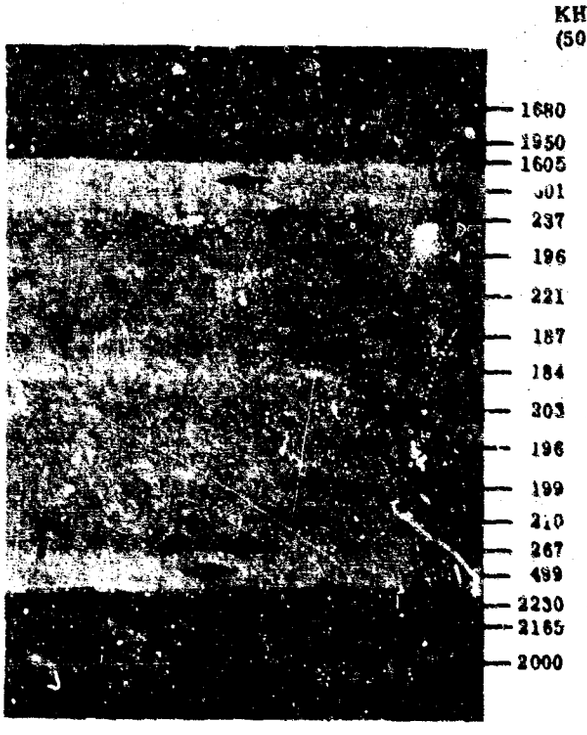

FIGURE 119.

V-(Cr-Ti)-Si COATED D43 SPECIMEN Series II

TABLE LXIX

DEPOSITION AND CHEMICAL ANALYSES FOR THE LOW-PRESSURE PACK DEPOSITION ON SERIES II VANADIZED SPECIMENS

Series	Alloy	Cycle Activator	Deposition (mg/cm^2)	Time (min)	Temperature (F)	Pack Type	X-ray Counting Rate (cps)					
							Cb	V	Cr	Ti	Fe	Ni
II	Cb752	Vanadium										
		NaF	1.1	180	2250	HPP[1]	---	---	---	---	---	---
		NaF	1.5	180	2250	HPP	---	---	---	---	---	---
		K_2VF_5	4.8	180	2250	HPP	15100	1470	---	---	232	103
		Total	7.4									
		Diffusion annealed		360	2500	Vacuum	17900	410	---	---	227	127
		CrTi										
		NaF	14.8	600	2300	LPP[2]	12720	3073	3831	230	---	---
		Diffusion	~4	960	2200	Vacuum	11570	3173	3371	159	---	---
II	D43	Vanadium										
		NaF	1.0	180	2250	HPP	---	---	---	---	---	---
		NaF	1.4	180	2250	HPP	---	---	---	---	---	---
		K_2VF_5	4.3	180	2250	HPP	16300	1360	---	---	217	85
		Total	6.7									
		Diffusion annealed	---	360	2500	Vacuum	17900	433	---	---	229	101
		CrTi										
		NaF	14.1	600	2300	LPP	9870	2323	3936	221	---	---
		Diffusion annealed	~4	960	2200	Vacuum	11700	3253	2961	231	---	---

1. HPP - High-pressure pack.
2. LPP - Low pressure pack process

Specimens coated with the low-pressure pack technique showed only modest improvement in bend ductility. The Cb752 specimens all fractured in bending 90 degrees; whereas, the D43 alloy did not fracture.

5.2.3 Deposition of Silicon

Specimens from Series I, II, and III were silicided using a cycle of 1950 F for 2.5 hours. The retorts used were of two types - one was Inconel with a graphite liner similar to Figure 90 and the other was Inconel with the refractory metal titanium gettered inner liner similar to Figure 101. Pack media was -200 mesh silicon with one percent NaF.

TABLE LXX

DEPOSITION WEIGHT GAINS AND OXIDATION PERFORMANCE OF THE PRELIMINARY V-(Cr-Ti)-Si COATED SPECIMENS (1)

Series	Alloy	Deposition Weight Gains						Hours to Failure of Specimen	
		V	Pack Type	CrTi	Pack Type	Si	Pack Type	1600 F	2400 F
I	Cb752	9.1	HPP	11.0	60Cr-40Ti HPP	10.9	HPP		9 9 31
I	Cb752	9.1	HPP	8.0	80Cr-20Ti HPP	12.2	HPP	>200 >200 >200	26 138 145
II	Cb752	7.4	HPP	9(net)	80Cr-20Ti LPP	12.6	HPP		114 136 170
II	Cb752	7.4	HPP	9	80Cr-20Ti LPP	14.2	HPP		1 59 78 78 80 86 86 86 93 96
II	D43	6.7	HPP	10	80Cr-20Ti LPP	12.9	HPP		24 78 88
III	Cb752	7.3	HPP	10.6	80Cr-20Ti HPP	11.2	HPP		108 137 143 161 175 240
III	D43	5.0	HPP	11.0	80Cr-20Ti HPP	9.9	HPP	>288 >288 >288	58 64 64 77 83 98
	Cb132M	4.8	LPP	11.0	LPP	12.6	HPP	>240 >240 >240 >240	61 102 112 116 143

1. 0.012 by 0.5 by 0.75-inch specimen

The summary of the V(Cr-Ti), and silicon deposits on Series I, II, and III specimens are shown in Table LXX. The silicon deposits ranged between 10 and 14 mg/cm^2, and exhibited excellent appearance on the edges and the flat areas.

Microstructures of the V-(Cr-Ti)-Si Series II and III coatings on Cb752 and D43 alloys are shown in Figures 118 through 121. One difference that is particularly noticeable between the Cb752 and D43 coated alloys is a second phase in the outer Cr-Ti rich zone on the D43 alloy (Fig. 122). This zone is of extreme hardness and may be titanium carbide which could form as a result of the migration of carbon from the substrate.

5.2.4 Oxidation Testing of the V-(Cr-Ti)-Si Coated Alloys - Phase I Screening Tests

Oxidation tests were performed at 1600 and 2400 F (16 hours and 1-hour cycles, respectively) on the Series I, II, and III specimens. Series I specimens were supported on high-purity alumina boats, but after a number of contact failures at 2400 F Dyna Quartz (a high-purity silica fiber matte by Johns Manville) was used. Contact failures were completely eliminated with this support media.

Oxidation data is presented in Table LXX as is the average deposition of vanadium, Cr-Ti, and silicon on the specimens. There is a marked difference between the performance of the V-(60Cr-40Ti)-Si and V-(80Cr-20Ti)-Si coatings.

Differences between Series II and III specimens with the 80Cr-20Ti coating applied by low-or high-pressure pack techniques are less marked. In both series the protection afforded the Cb752 alloy is superior to that afforded the D43 alloy. This difference is particularly noticeable in the Series III coating where the first failure at 2400 F occurred in 108 hours on the Cb752 and in 58 hours on the D43 alloy. The maximum lives of Series II and III coatings on these alloys displayed similar differences, i.e., 240 hours against 98 hours, respectively. This difference in performance between the two alloys may be the result of the extremely hard phase within the coating on the D43 alloy (Fig. 123) which could possibly initiate shear failure within the coating.

A Weibull cumulative failure plot of the Series II, Cb752 specimens oxidized at 2400 F shows a narrow failure distribution and a rather steep slope. The data indicate that only 0.5 percent of the coated specimens should fail in 60 hours.

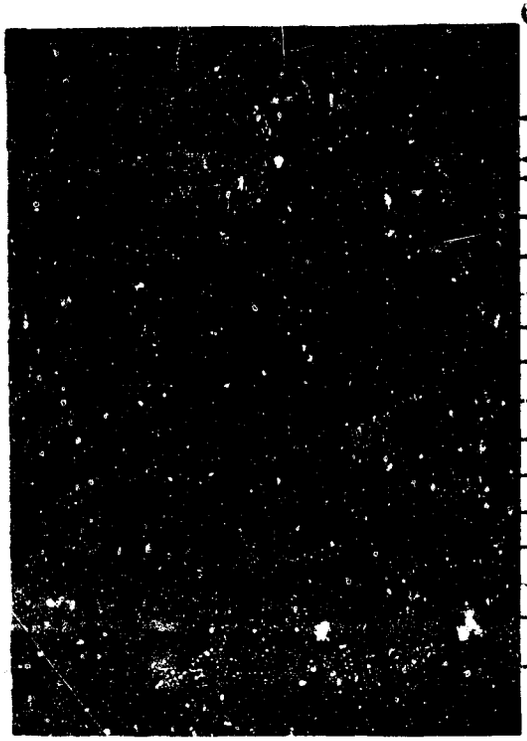

Magnification: 200X

FIGURE 120.

V-(Cr-Ti)-Si COATED Cb752 SPECIMEN; Series III

Magnification: 200X

FIGURE 121.

V-(Cr-Ti)-Si COATED D43 SPECIMEN, Series III

FIGURE 122.
UNIDENTIFIED PHASE IN V-(Cr-Ti)-Si COATED D43 ALLOY

A typical weight change versus time for the V-(80Cr-20Ti)-Si coating at 2400 F is shown in Figure 124. The shape is nonparabolic. There is an initial weight gain followed by a continual weight loss. This change of the oxidation curve is probably due to the buildup of a critical thickness of SiO_2 and other nonvolatile oxides. Vaporization of chromium oxides and other volatile oxides are responsible for the weight losses.

The microstructure of the coating and surface finish after extended 2400 F thermal cycling is shown in Figure 125 and 126. The coating exhibits the extensive craze cracking characteristic of coatings having a coefficient of thermal expansion considerably higher than the substrate. These craze cracks, however, do not appear to be the prime contributors to coating failure, but since edge failures predominate, the differential expansion between coating and substrate is undoubtedly a major factor in determining the life of the coating.

The coating does not appear to have a low-temperature problem. In 1600 F testing no specimens failed within the 288-hour test limit on Cb752, D43, or Cb132M alloys.

The performance of the Series III V-(Cr-Ti)-Si coated D43 alloy was somewhat inferior to that of the identically processed Cb752 alloy. To determine if the observed difference in oxidation resistance could be attributed to differences in coating composition and/or element distribution, electron microprobe analyses were performed on the coated alloys after each cycle in the coating process.

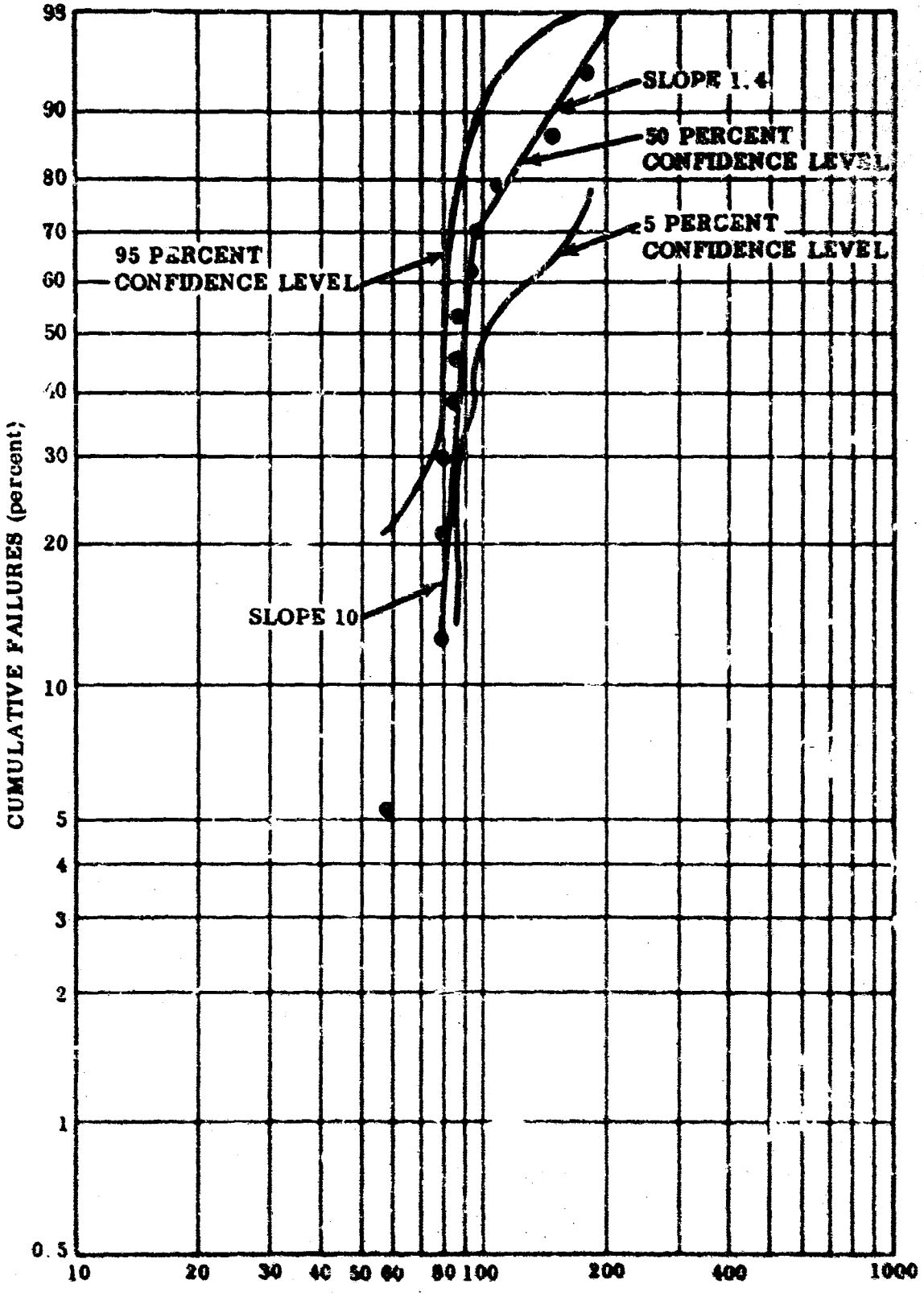

FIGURE 113. WEIBULL CUMULATIVE FAILURE PLOT OF V-(Cr-Ti)-Si COATED Cb752 SPECIMENS AFTER OXIDATION TESTING AT 2400 F; Series II One-Hour Cycles

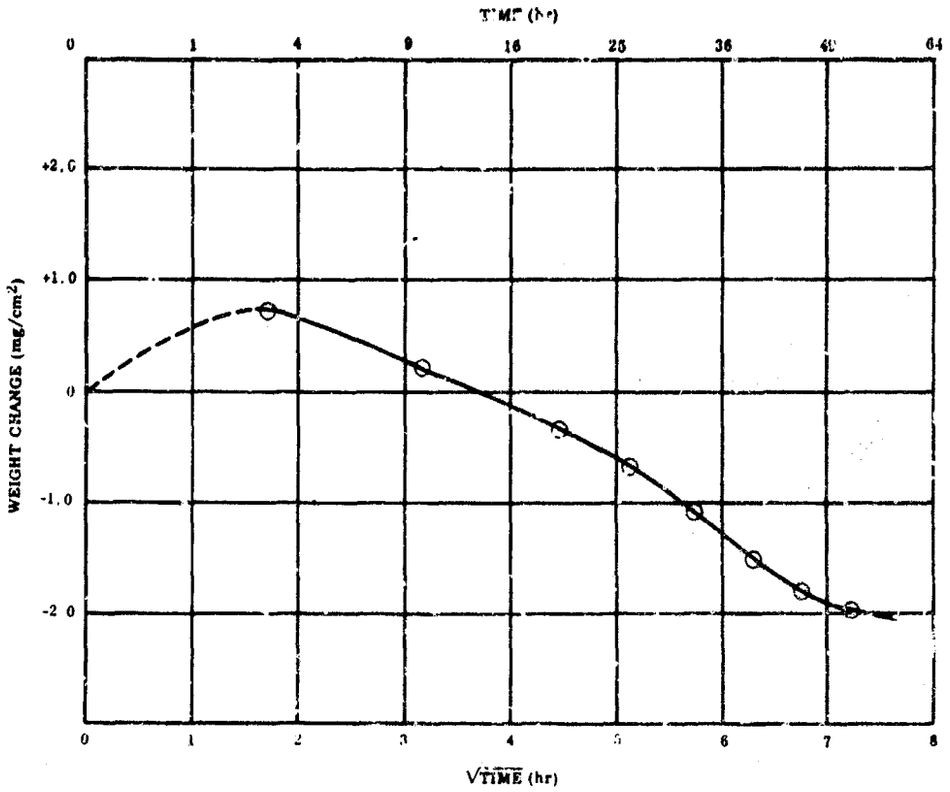

FIGURE 124. WEIGHT CHANGE VERSUS TIME FOR V-(Cr-Ti)-Si COATING ON Cb752 ALLOY AT 2400 F IN AIR

The analyses were performed on a Norelco-Phillips electron microprobe analyzer, Model AMR/3. The instrument is capable of continuous scanning and two elements can be simultaneously analyzed over a given traverse length.

The coated specimens, together with appropriate element standards, were mounted in red bakelite and polished in a conventional manner. The specimens were grouped in three mounts:

Mount 1 - Vanadized Cb752, vanadized D43, and a 99.8 wt% vanadium standard. The unaffected Cb752 and D43 substrates served as columbium standards.

Mount 2 - (Cr-Ti)-V coated Cb752, (Cr-Ti)-V coated D43, and 65Cb-7.12V-13.4Ti-14.5Cr alloy as a standard for columbium, vanadium, titanium, and chromium. This alloy was designated Q5 in the sublayer property study (Table VII).

Mount 3 - Si-(Cr-Ti)-V coated Cb752, Si-(Cr-Ti)-V coated D43 and 24Cb-6.4V-3.8Ti-21.3Cr-44.4Si alloy as a standard for columbium, vanadium, titanium, chromium, and silicon. This alloy was designated No. 24 in the basic silicide studies (Table XXXVI).

Magnification: 200X

FIGURE 125.

V-(Cr-Ti)-Si COATED Cb752 ALLOY; Series I Edge Failure at 150 Hours

Magnification: 1[illegible]

FIGURE 126.

V-(Cr-Ti)-Si COATED Cb752 ALLOY SURFACE AFTER 106 ONE-HOUR CYCLES AT 2400 F; Series III

The use of alloy standards which approximated the actual coating composition permitted analyses and reduction of the recorded intensity data without the use of correction factors.

Figures 127 and 128 indicate, respectively, the distribution of vanadium and columbium in the Cb752 and D43 alloys after the initial vanadizing cycle. Vanadium has diffused slightly further into the Cb752 alloy and the vanadium concentration at the outer edge of the coating is 53 wt % in the Cb752 alloy and 73 wt % in the D43 alloy.

The distributions of chromium, titanium, vanadium, and columbium in the Cb752 and D43 alloys after the chrome-titanium coating cycle are shown in Figures 129 and 130. Here again, the coating elements have diffused further into the Cb752 substrate than into the D43 substrate. A major difference between the coated alloys involves the distribution of chromium and titanium near the outer coating edge. The Cb752 alloy is characterized by a high-chromium content (49 wt %) and medium titanium content (28 wt %) whereas the opposite is evident on the D43 alloy (26 wt % Cr-55 wt % Ti).

Figures 131 and 132 indicate, respectively, the distribution of silicon, chromium, titanium, vanadium, and columbium in the Cb752 and D43 alloys after the siliciding cycle. The resultant overall diffusion zone is slightly thicker in the Cb752 alloy, and the major difference between the two coated alloys appears to be the titanium distribution. In the Cb752 alloy, the highest titanium concentration coincides with maxima exhibited for chromium and vandium, and is related microstructurally to the light phase evident in the silicide coating - Cb752 substrate interface region. In contrast, the titanium maximum in the coated D43 alloy does not coincide with the chromium and vanadium maxima, but occurs within the silicide coating where a darker phase is evident. This darker phase which exists from approximately midway in the silicide coating to the outer edge of the silicide coating on the D43 alloy does not appear in the coated Cb752 alloy in the etched or unetched conditions.

In summary, the microprobe analyses indicate that the observed difference in oxidation resistance between V-(Cr-Ti)-Si coated Cb752 and D43 alloys may be due to the presence of a titanium-rich second phase in the outer half of the silicide coating on the D43 alloy. Since the presence of titanium is high, a buildup of titanium oxide in the protective silicate layer at the air-coating interface would be a logical explanation for the poorer oxidation resistance of the coated D43 alloy.

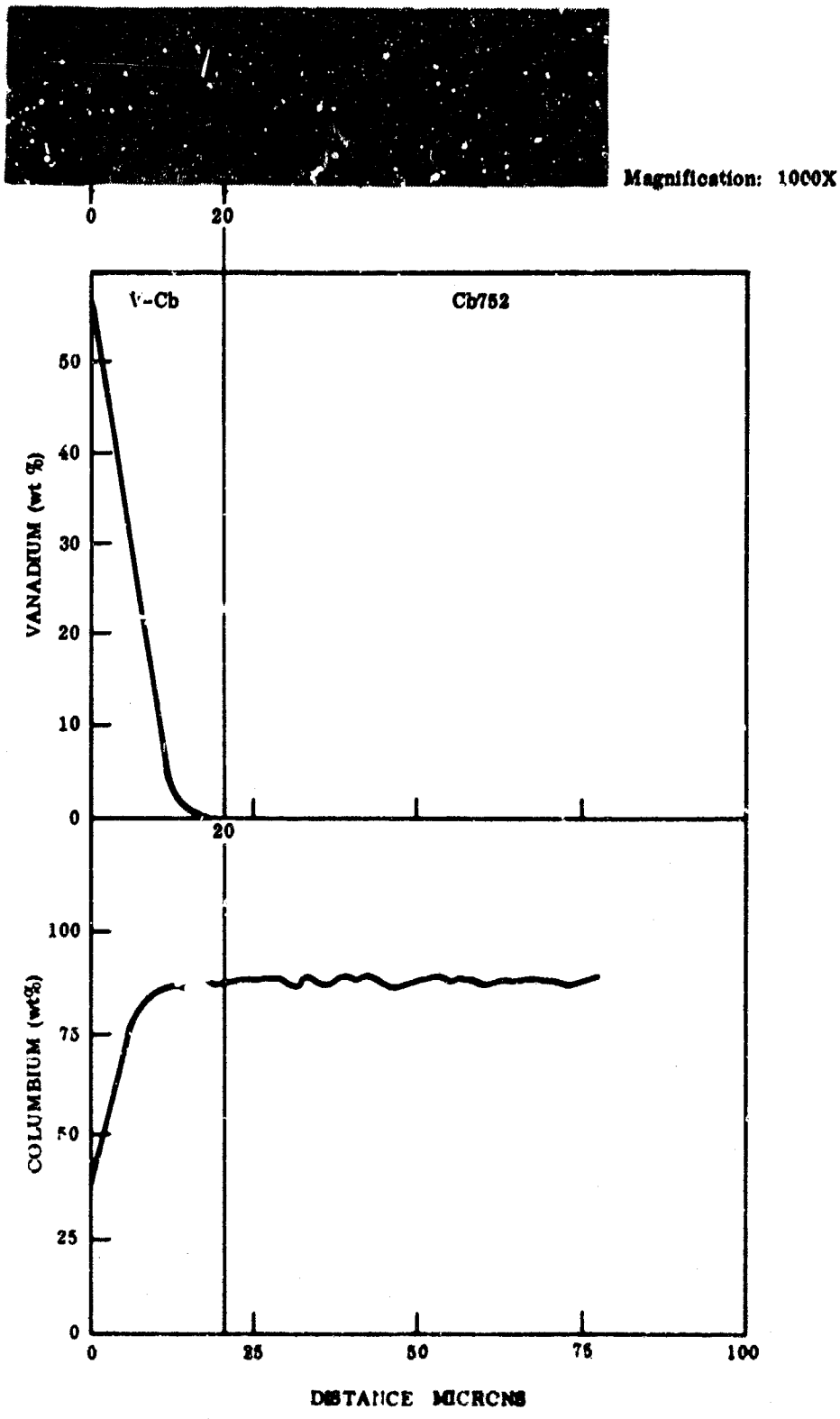

FIGURE 127. ELECTRON MICROPROBE ANALYSIS OF VANADIUM AND COLUMBIUM IN VANADIZED Cb752 ALLOY

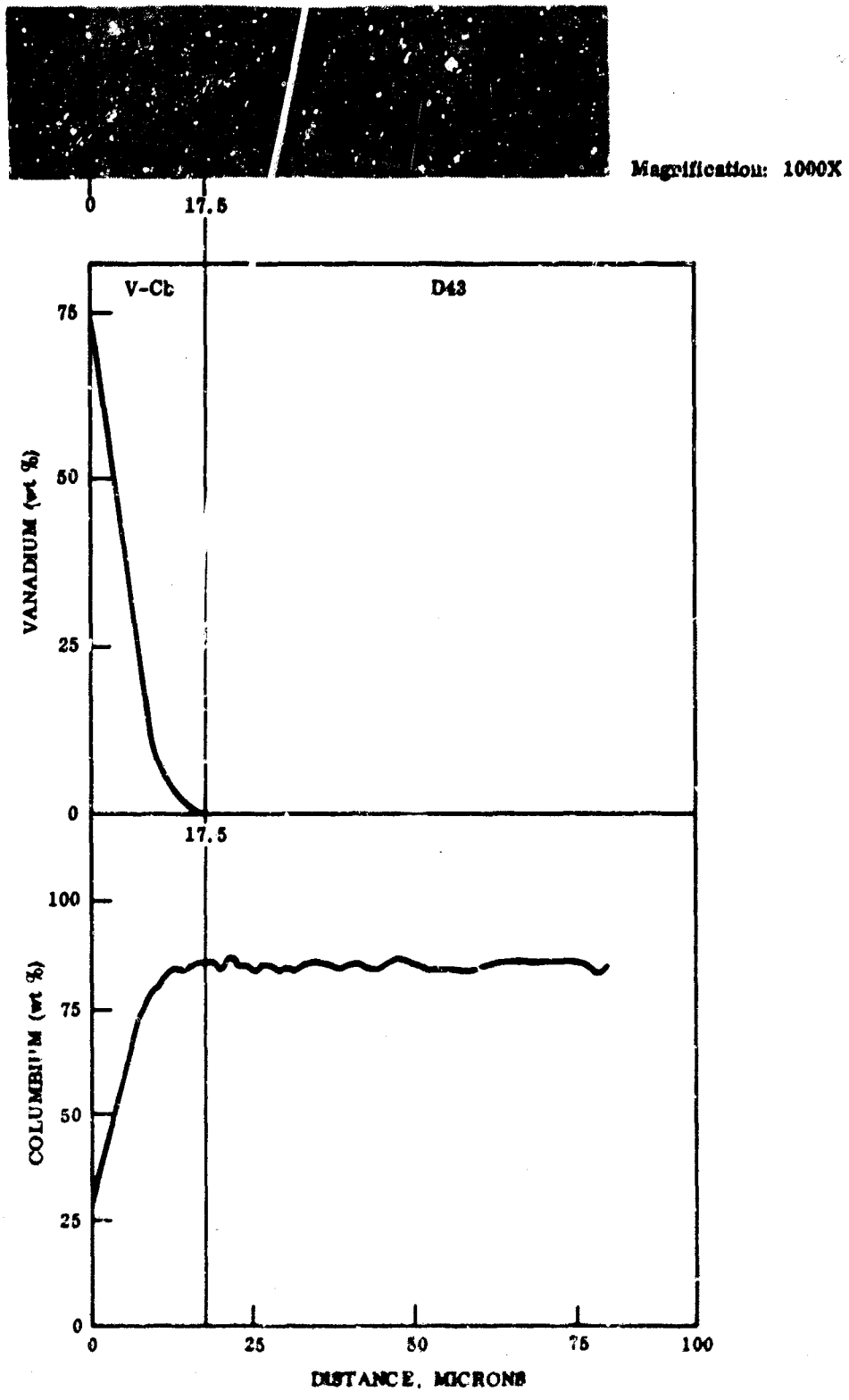

FIGURE 128. ELECTRON MICROPROBE ANALYSIS OF VANADIUM AND COLUMBIUM IN VANADIZED D43 ALLOY

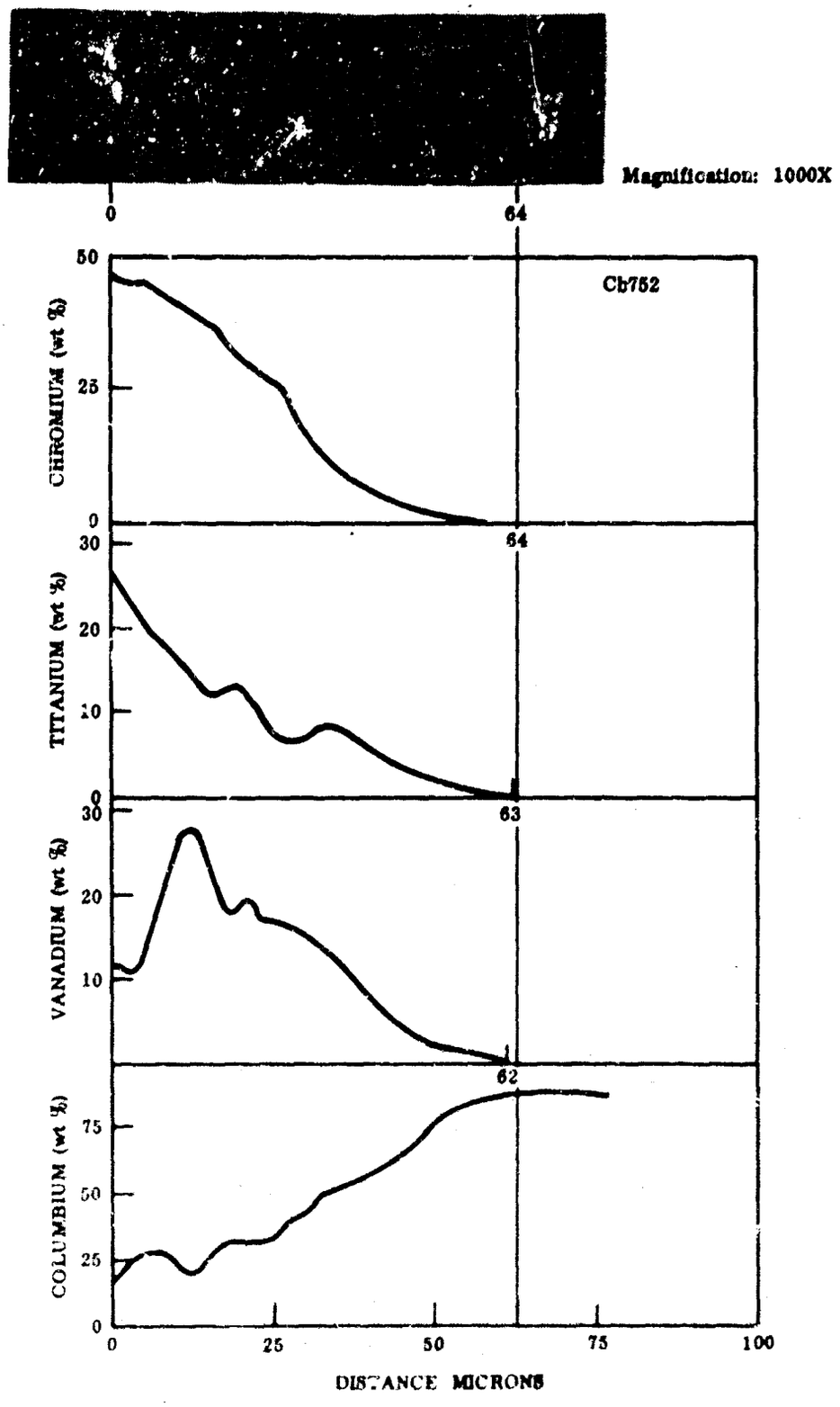

FIGURE 129. ELECTRON MICROPROBE ANALYSIS OF CHROMIUM, TITANIUM, VANADIUM, AND COLUMBIUM IN (Cr-Ti)-V COATED Cb752 ALLOY

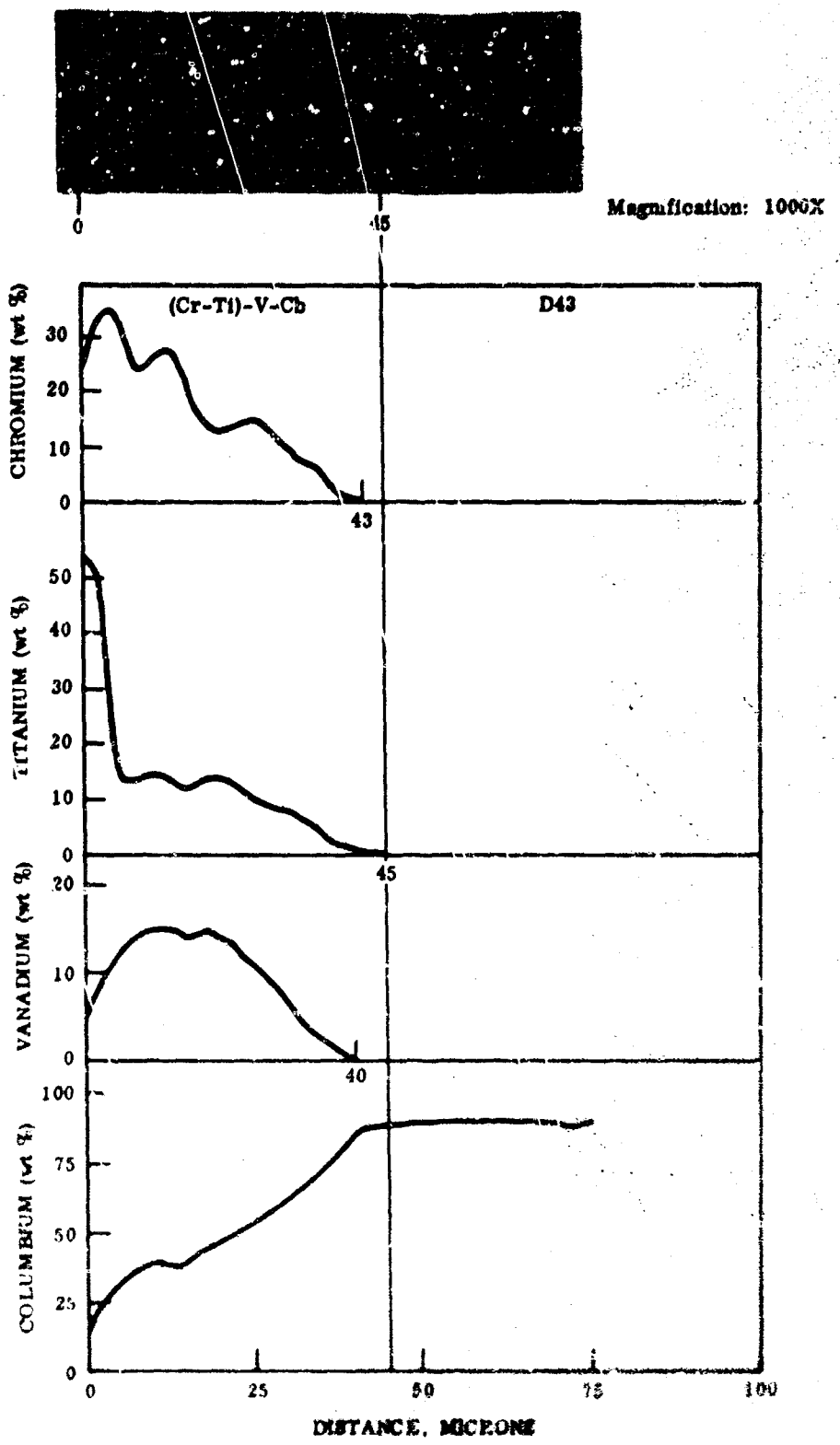

FIGURE 130. ELECTRON MICROPROBE ANALYSIS OF CHROMIUM, TITANIUM, VANADIUM, AND COLUMBIUM IN (Cr-Ti)-V COATED D43 ALLOY

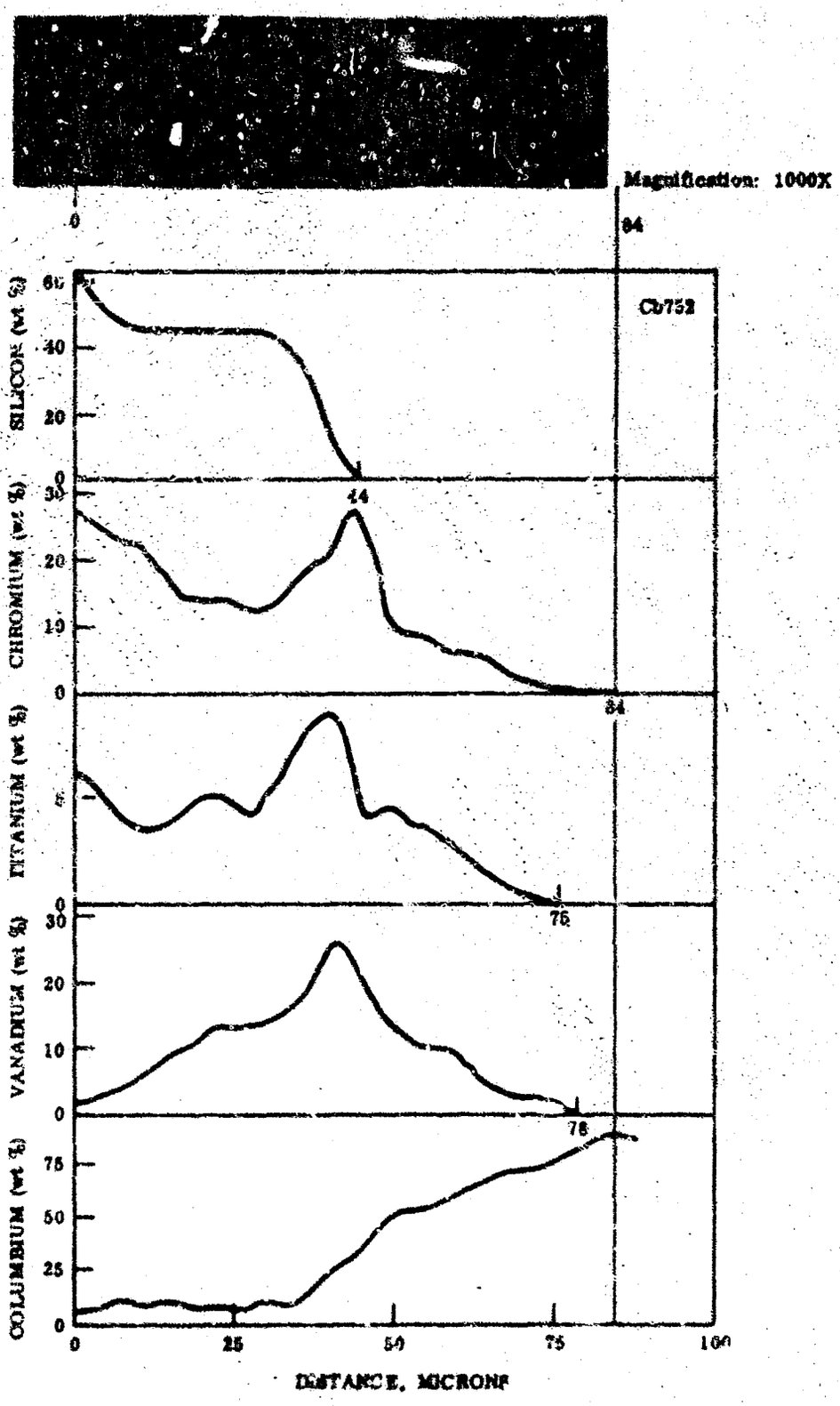

FIGURE 131. ELECTRON MICROPROBE ANALYSIS OF SILICON, CHROMIUM, TITANIUM, VANADIUM, AND COLUMBIUM IN Si-(Cr-Ti)-V COATED Cb752 ALLOY

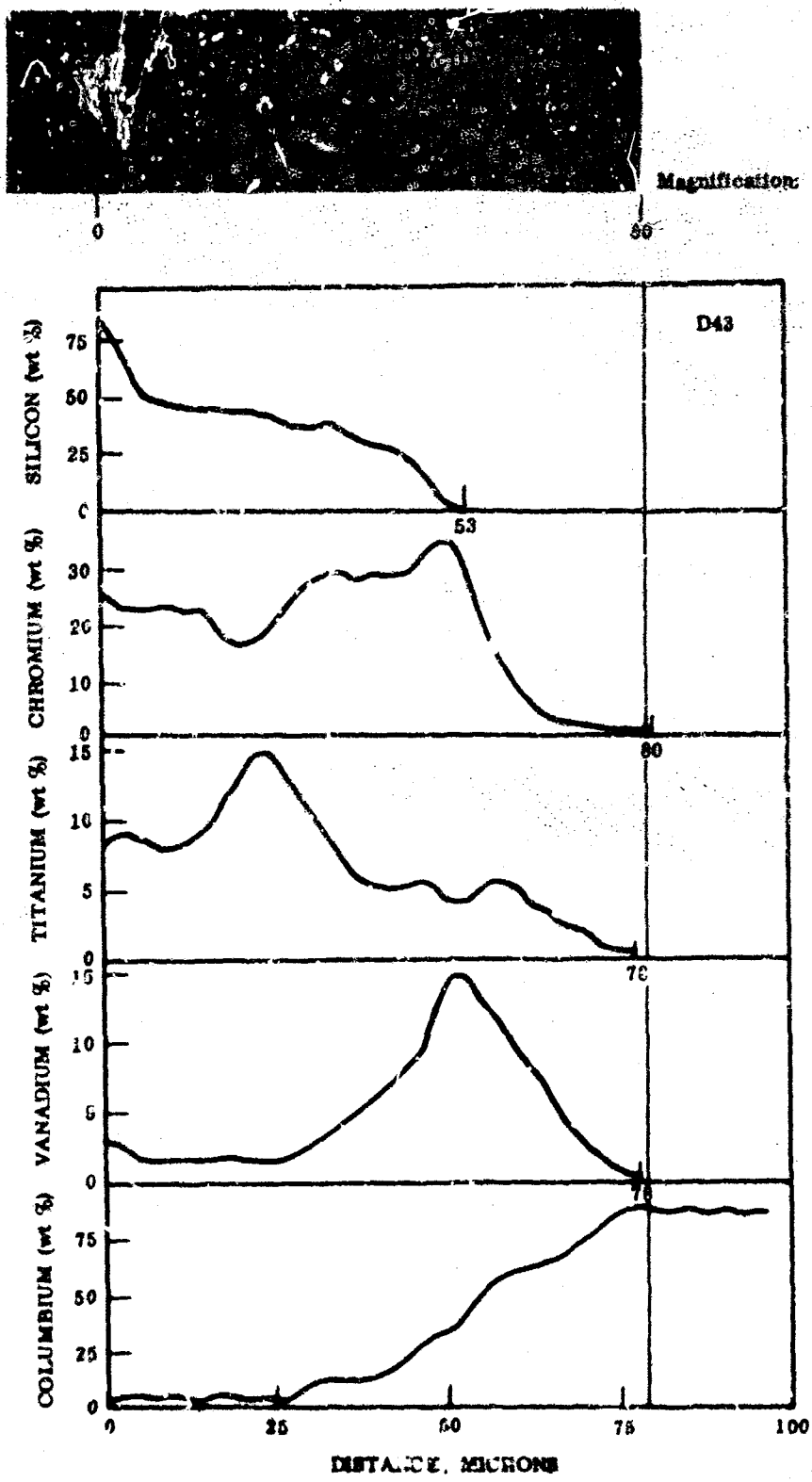

FIGURE 132. ELECTRON MICROPROBE ANALYSIS OF SILICON, CHROMIUM, TITANIUM, VANADIUM, AND COLUMBIUM IN Si-(Cr-Ti)-V COATED D43 ALLOY

5.2.5 Additional Silicide Coating Systems

Three other coating syrtems were studied and compared with the V-(Cr-Ti)-Si coating for ease of deposition and oxidation life with similar silicon deposition weights. The systems were (Cr-Ti)-Si, (Cr-Ti)-V-Si, and V-Si. The (Cr-Ti) layer was deposited from an 80Cr-20Ti pack.

(Cr-Ti)-Si Coating System

Approximately 10.3 mg/cm^2 of (80Cr-20Ti) were deposited with much difficulty on 10 Cb752 coupons. Six 5-hour cycles at 2300 F, using a 1.0 percent NaF activated pack and -50 + 100 mesh 80Cr-20Ti pack media, were required to effect the deposition. Over the (Cr-Ti), 11.0 to 11.8 mg/cm^2 of silicon were deposited from a -200 mesh pack. The microstructure of this coating is shown in Figure 133. Unusually wide craze cracking can be seen. Edge cracking of the specimens could be seen with the unaided eye. Nearly every specimen of this system failed at an edge during oxidation.

Both of the (Cr-Ti)-Si coated specimens tested at 1600 F failed between 192 and 216 hours. Of the five cycled at 2400 F, there were failures at 45, 62, 64, 72, and 76 hours.

The oxidation test results for all three coating systems are shown in Table LXXI.

(Cr-Ti)-V-Si Coating System

Again with tedious recycling, 7.4 mg/cm^2 of 80Cr-20Ti and 10.3 mg/cm^2 of vanadium were deposited on Cb752 substrates. The specimens were then coated with 12.8 mg/cm^2 of silicon and oxidation tested. All four coupons at 2400 F failed within nine hours. Localized melting seemed to be the cause for failure. It was ever noticed on the specimens tested at 1600 F; these, however, ran more than 200 hours.

V-Si Coating System

An average deposit of 12.6 mg/cm^2 of vanadium was applied to several Cb752 specimens by two 5-hour cycles at 2300 F. Subsequently, 12.8 mg/cm^2 of silicon, from a -200 mesh pack, were deposited on seven of the vanadized Cb752 specimens. The resultant coating microstructure is shown in Figure 134.

The silicided specimens were oxidized at 1600 F and 2400 F. The two coupons tested at 1600 F failed between 24 and 48 hours, failure occurring at the specimen

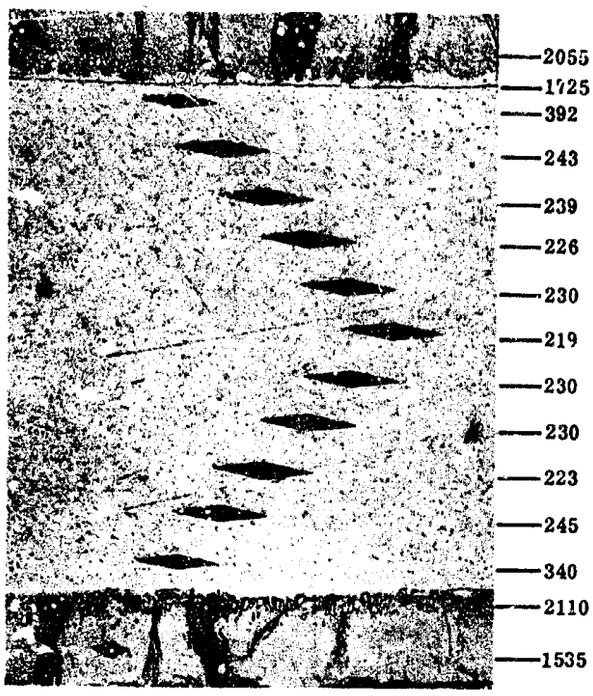

Magnification: 250X

FIGURE 133.

Cb752 ALLOY COATED WITH 80Cr-20Ti AND SILICON

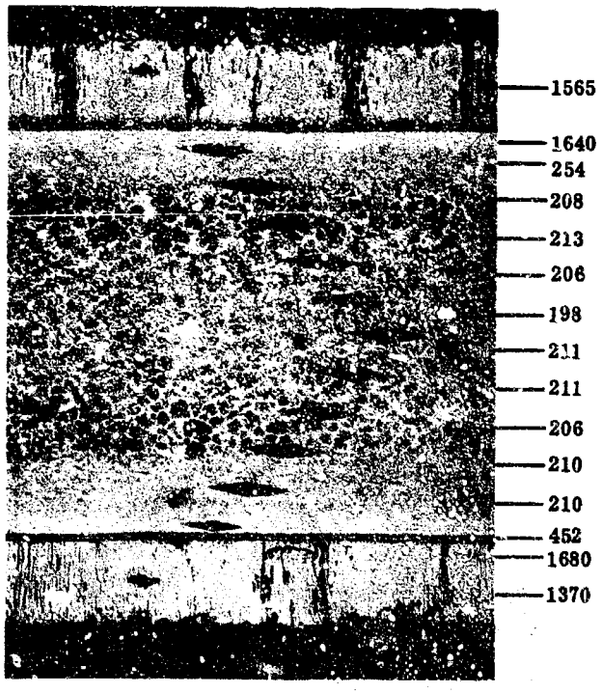

Magnification: 200X

FIGURE 134.

VANADIZED AND SILICIDED Cb752 ALLOY

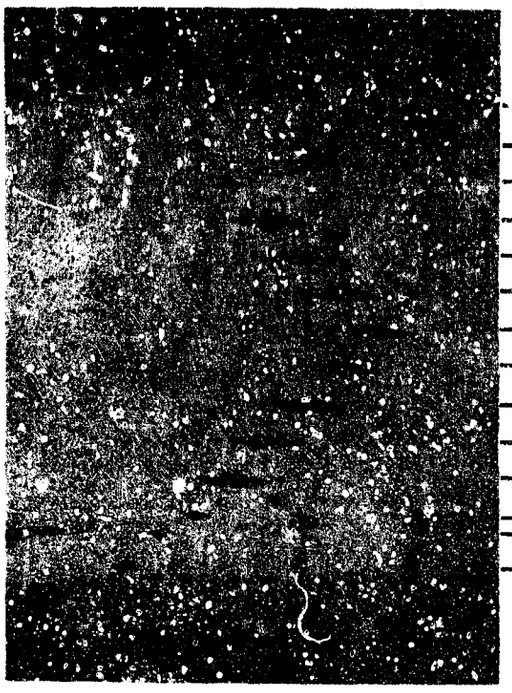

Magnification: 200X

FIGURE 135.

VANADIZED AND SILICONIZED Cb752 ALLOY; Oxidation Tested 131 Hours at 2400 F

edges. At 2400 F, one failure occurred at 74 hours while the remaining two specimens failed at 131 hours. One of the 131-hour failures was sectioned and the microstructure is shown in Figure 135.

The weight change versus time curve for the V-Si coating system at 2400 F is shown in Figure 136. The oxide growth is essentially parabolic, exhibiting none of the gain-loss curve characteristics of the V-(Cr-Ti)-Si system, which is also shown in Figure 136.

TABLE LXXI

DEPOSITION RESULTS AND OXIDATION PERFORMANCE OF ADDITIONAL SILICIDE COATING SYSTEMS

System	Deposition Results (mg/cm^2)		Oxidation Performance (hr) Each Specimen	
			1600 F	2400 F
(80Cr-20Ti)-Si	Cr-Ti Silicon	10.3 11.5	<216, <216	45, 62, 64, 72, 76
(80Cr-20Ti)-V-Si	Cr-Ti Vanadium Silicon	7.4 10.2	>200, >200, >200	All three failed in <9
V-Si	Vanadium Silicon	12.6 12.8	<48, <48	74, 131, 131

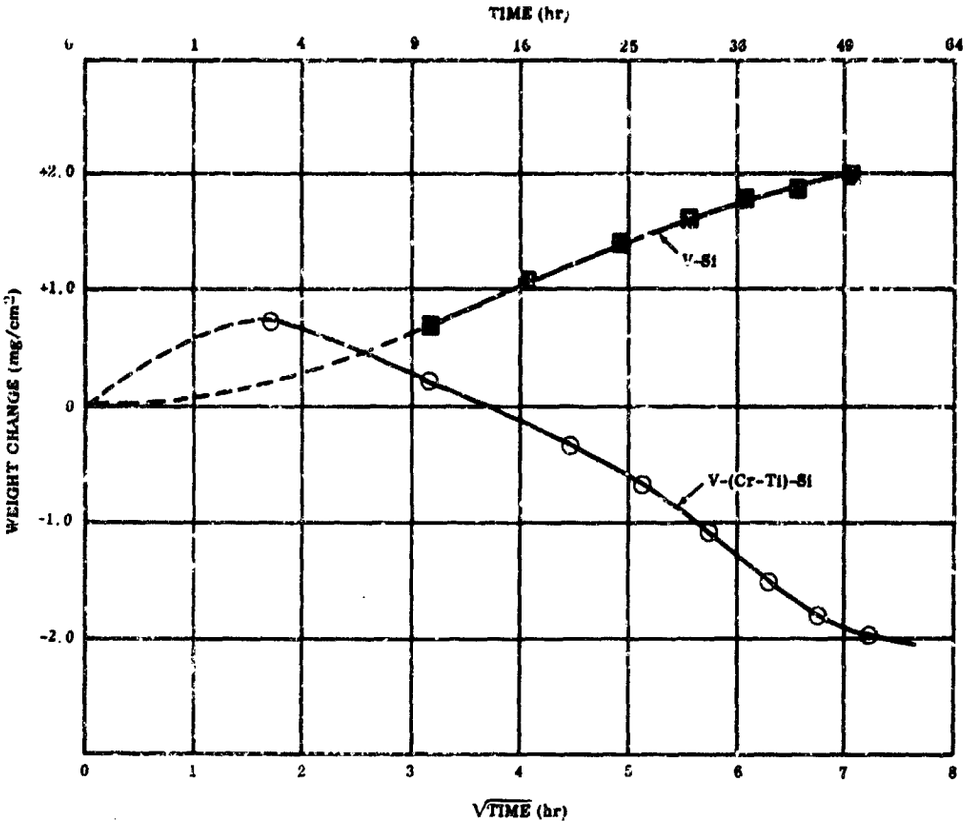

FIGURE 136. WEIGHT CHANGE VERSUS TIME FOR V-(Cr-Ti)-Si AND V-Si COATINGS ON Cb752 ALLOY AT 2400 F IN AIR

5.2.6 Discussion of the Coating Systems

The V-(Cr-Ti)-Si coating has considerable potential, but exhibits several deficiencies which are characteristic of pack-deposited coatings. Severe vanadium sintering is definitely the most critical problem. This problem was somewhat alleviated by replacing NaF with K_2VF_5, but vanadium sinter sites continue to initiate oxidation failures in a large number of instances.

The V-(Cr-Ti)-Si coating did not protect the D43 alloy as well as the Cb752 alloy, but this is believed to be a minor problem capable of improvement by optimization of the vanadium, chrome-titanium, and silicon weight ratios. In all instances, the D43 specimen had a lighter vanadium coating than the Cb752 specimens.

Embrittlement of the Cb752 alloy by the V-(Cr-Ti)-Si process has continually been a problem. However, loss of ductility in that alloy has not been accompanied by a noticeable increase in the Knopp hardness of the substrate. Embrittlement, therefore, is probably occurring only in the grain boundaries. Because this embrittlement

indicates a marginal oxygen transfer during the coating operation, it is felt that the problem could be eliminated by the selection of higher quality pack materials, particularly chromium.

The (Cr-Ti)-Si, (Cr-Ti)-V-Si, and V-Si coating systems did not perform as well in oxidation at 1600 F and 2400 F as the V-(Cr-Ti)-Si coating and were not carried into Phase II and III.

The prime coating selected for application to the Phase II and III specimens was V-(80Cr-20Ti)-Si, because of its satisfactory performance in Phase I cyclic testing at 1600 and 2400 F. The deposition goals set for each of the layers were:

Vanadium	7 to 9 mg/cm^2
80Cr-20Ti	10 to 14 mg/cm^2
Silicon	11 to 14 mg/cm^2

By establishing equivalent deposition goals for each of the alloys to be included in Phases II (Cb752, D43) and Phase III (Cb752, D43, and Cb132M) it was anticipated that the difference in performance observed between the Cb752 and D43 alloys in Phase I testing could be avoided. Solving the bend ductility problem with the V-(Cr-Ti)-Si coated Cb752 alloy was not considered imperative in this program. Solution of the problem represents a process optimization step which can be readily accomplished in the future by using chromium and titanium starting material of higher purity, or by developing a chromium-titanium alloy additive that will minimize oxygen transport. Prealloying the chromium and titanium (current packs use a 50-50 mixture of hydrogen reduced electrolytic chromium and 60 Cr-40Ti arc-melted alloy) may be all that is necessary. Additions of one of the rare earth elements, or yttrium in small quantities, to the alloy should also control oxygen transport (Appendix).

Application techniques for the deposition of the V-(80Cr-20Ti)-Si coating were not considered critical. Both the low-and high-pressure packs used in application of vanadium and 80Cr-20Ti produced essentially comparable protection at the same deposition weight when silicided. Interdiffusion of the vanadium deposit and Cr-Ti deposit after deposition was not considered essential based on oxidation data for the Series I, II, and III specimens.

5.3 APPLICATION OF THE V-(Cr-Ti)-Si COATING TO PHASE II AND III SPECIMENS

The final activity in Phase I was the coating of the specimens required for evaluation in Phase II and III with the V-(Cr-Ti)-Si. A limited number of erosion bars were coated with the (95Mo-5Ti)-Si glass-impregnated coating, but no deviation from the procedure described in Paragraph 3.1.4 was used. The data on the latter coating are not, therefore, included in this section.

5.3.1 Substrate Alloys

Three substrate alloys were included in the program - D43, Cb752, and Cb132M. The D43 alloy was used in two conditions, i.e., 0.012-inch and 0.030-inch sheet in the duplex heat treat condition (solution at 2900 to 3000 F followed by 25 percent cold reduction and aging at 2650 F) and 0.5-inch bar in recrystallized condition. The Cb752 alloy (0.012-inch and 0.030-inch) was also used in the duplex heat treated condition (solution at 2800 F followed by 40 percent cold reduction and aging at 2450 F). The Cb132M (0.5-inch bar only) was used in the as-extruded condition. Chemical analyses of all of the alloys are shown in Table LXXII.

TABLE LXXII

COMPOSITIONS PHASE II AND III ALLOYS

Alloy and Heat Number		Thickness (in.)	ELEMENT (wt %)					
			W	Zr	O	H	N	C
D43	387-23	0.030	9.4	1.0	136	3	40	1070
D43	387-32	0.030	10.2	0.96	188	2	34	1020
D43	43-488	0.030	9.8	1.0	366	1	38	994
D43	389-22	0.013	9.9	0.89	293	12	50	1025
D43	43-372	0.50 dia	10.0	1.1	50	2	30	828
D43	43-409	0.50 dia	11.0	0.97	116	8	31	863
D43	43-423	0.50 dia	9.6	0.91	56	9	33	945
Cb752	UMC-1	0.030	9.97	2.5	52	6	42	10
Cb752	52 342	0.013	10.0	2.5	65		78	60
Cb132M	(Nominal)	0.50 dia	13.5 to 16.5	0.75 to 1.25	400 max	20 max	100 max	800 to 1200 Ta18 to 20 Mo4.5 to 5.5

Prior to coating the Phase II and III specimens, close examination of the D43 alloy revealed numerous localized surface defects of the type shown in Figure 137. Due to the late discovery of the defect, replacement material could not be obtained. The specimens were, therefore, made from the material; however, by careful and selective shearing the surface defects were at a minimum in the coated specimens.

5.3.2 The Application of Coating

Initially, Phase II and III specimens were vanadium and chrome-titanium coated in low-pressure Cb-1Zr retorts (Fig. 138 through 140).

The retorts used were fabricated from 0.050-inch thick Cb-1Zr sheet stock. To coat the many sizes and shapes of the program test specimens, two retort sizes were used. The inside dimensions were 4-inches wide by 8-inches long by 3-inches high, and 3-inches wide by 12-inches long by 3-inches high. The retorts were fabricated by shearing the sheet stock to the appropriate size, bending to give the correct inside dimensions, and then TIG welding the seams in a high-purity argon (dry box) weld chamber. Initially, a 0.5-inch diameter by 3.0-inch long columbium tube was welded into each retort to provide a means of evacuating the retort after loading with specimens and pack material and welding on the lid. However, this method of sealing proved to be unreliable and the tube was eliminated in favor of an overnight pump-down to 10^{-4} Torr in an EB welding chamber followed by sealing (beam welding) a small hole drilled in the retort lid.

Vanadizing

Undoubtedly, the low-pressure vanadium pack was the cleanest system investigated for the deposition of the metal, but problems of dendritic deposition shown in Figure 141 and poor oxidation performance of V-(Cr-Ti)-Si coated specimens processed in low-pressure vanadium packs forced a return to high-pressure packs.

High-pressure retorts were used to vanadize the Phase II and III specimens (Fig. 142). A pack containing (-80+20) mesh vanadium powder and 1 wt % K_2VF_5 activator was used. The activator was segregated to prevent it from touching the specimens before complete reduction had occurred. A total of two 8-hour cycles at 2250 F were used to deposit the vanadium since a single 16-hour run produced severe sintering of vanadium particles onto the specimens.

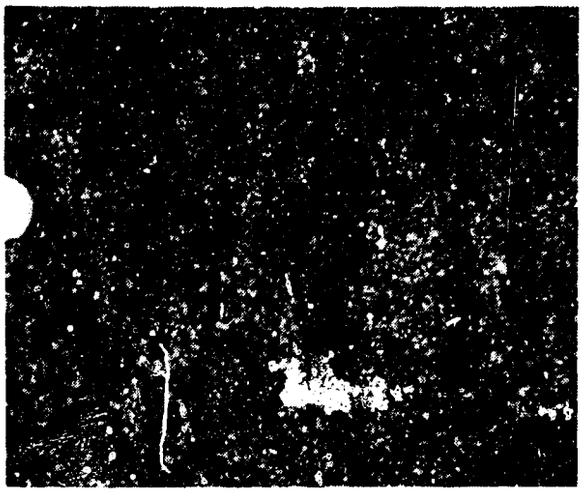

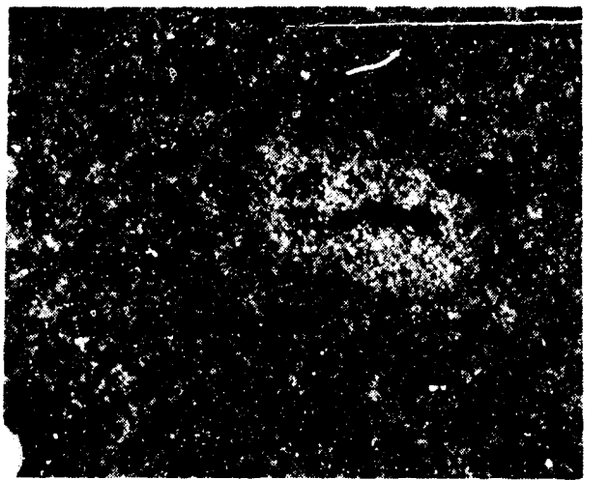

Magnification: 35X

FIGURE 137. SURFACE DEFECTS IN D43 COLUMBIUM ALLOY SHEET (Sheet 1 of 2)

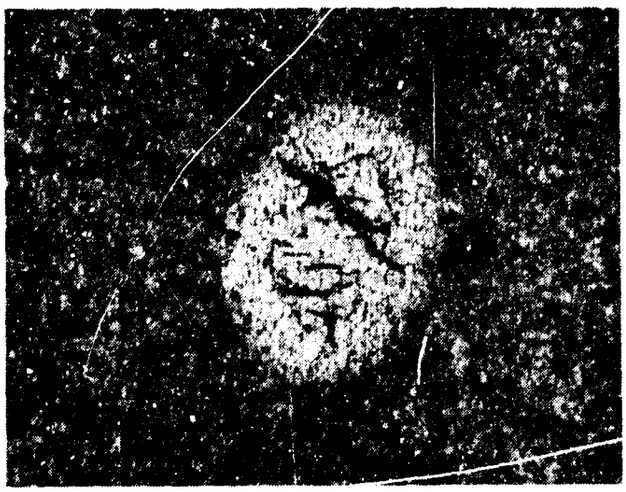

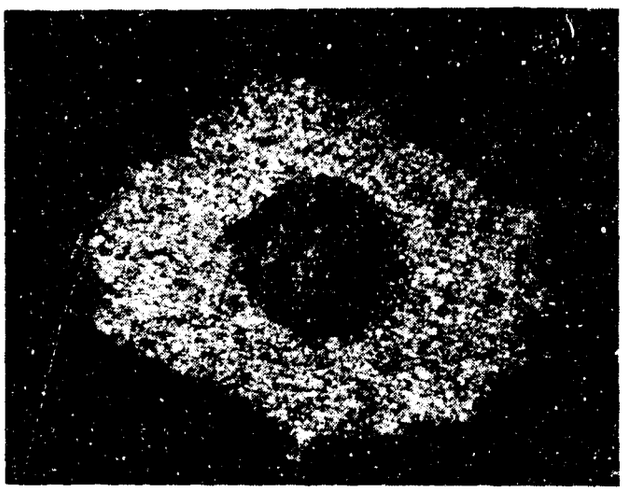

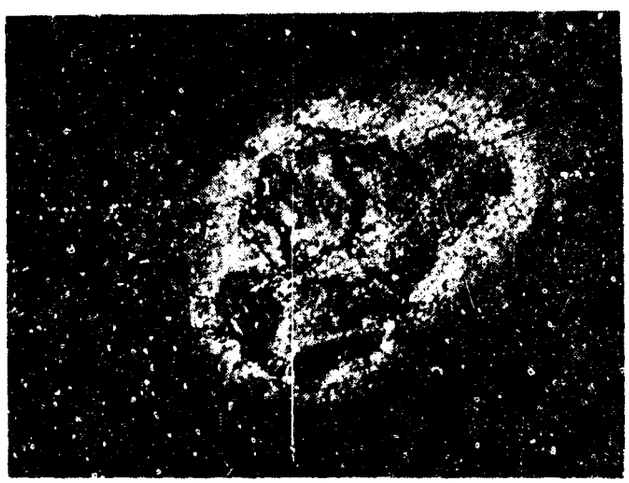

Magnification: 35X

FIGURE 137. SURFACE DEFECTS IN D43 COLUMBIUM ALLOY SHEET (Sheet 2 of 2)

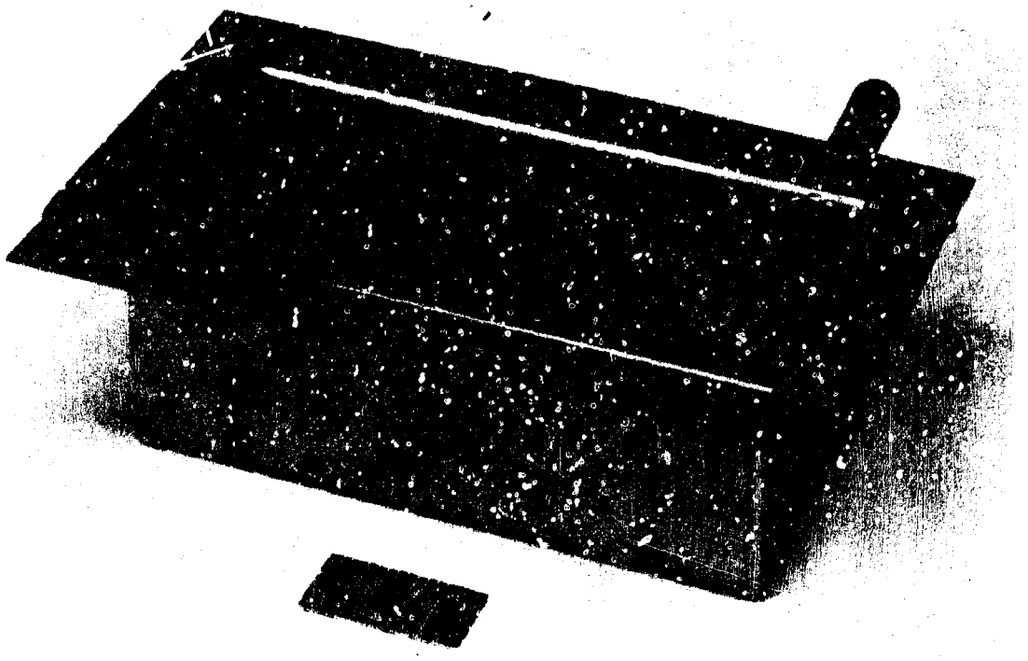

FIGURE 138. VACUUM COATING RETORT; Cb-1Zr Material

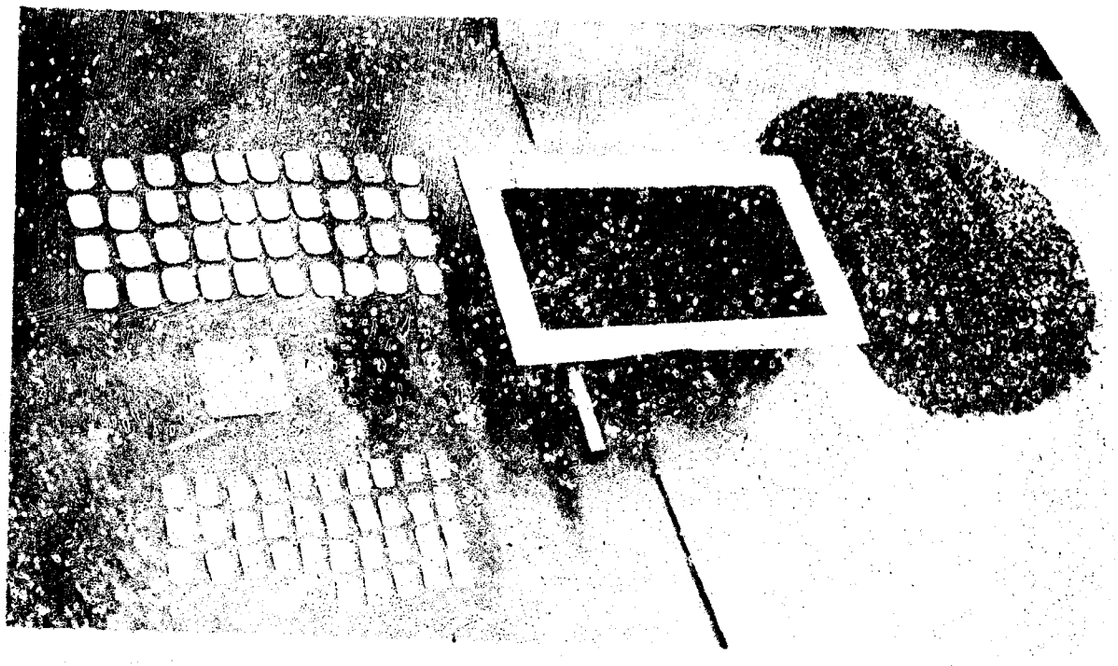

FIGURE 139. VACUUM VANADIUM COATING RETORT SPECIMENS AND PACK MATERIAL

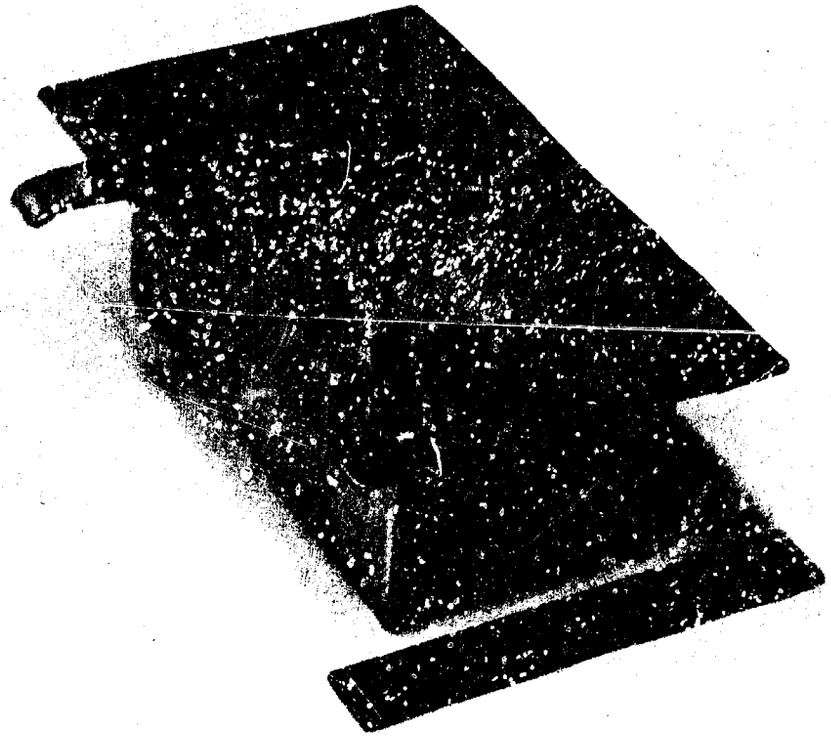

FIGURE 140. EVACUATED AND SEALED RETORT READY FOR VACUUM FURNACE

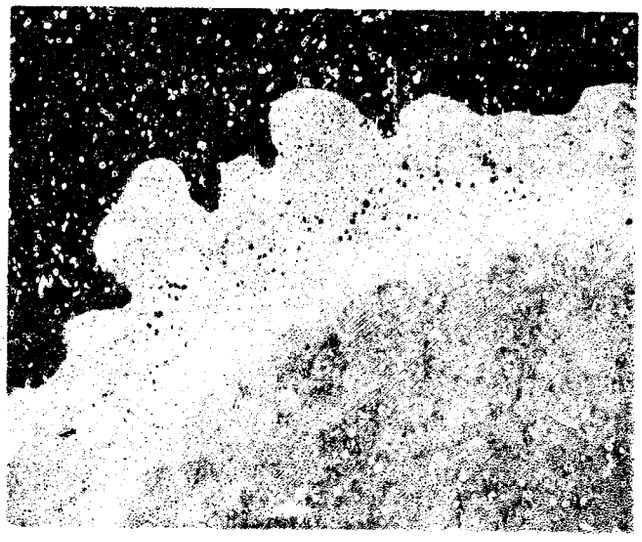

Dendritic vanadium deposit on D43 from large low pressure pack

Magnification: 250X

FIGURE 141.

DENDRITIC VANADIUM DEPOSIT ON D43 ALLOY FROM LARGE LOW-PRESSURE PACK

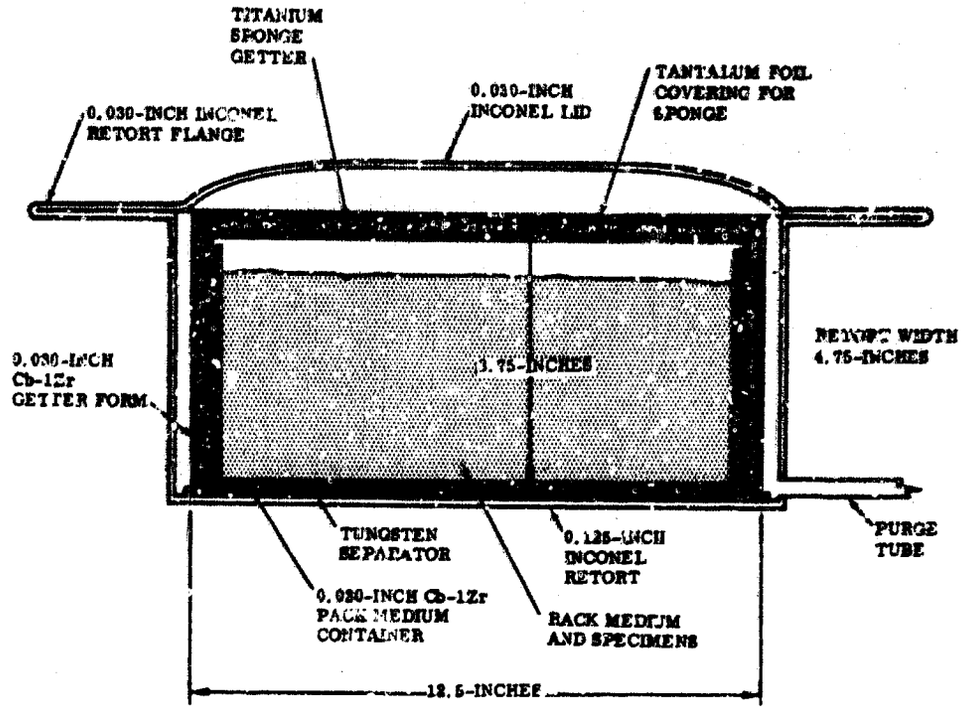

FIGURE 142. HIGH-PRESSURE ARGON RETORTS FOR COATING PHASE II AND III SPECIMENS

Chrome-Titanium

The retorts used to deposit chrome-titanium onto Phase II and III specimens were similar to the low-pressure retorts described under vanadizing. Some early difficulty occurred with the large low-pressure chrome-titanium packs. An unforseen high-temperature reaction occurred between the pack medium and activator, causing an unexpectedly high retort pressure. The latter bulged the walls of the rather weak Cb-1Zr retorts and allowed the pack medium to shift during the run. This resulted in spotty deposits on the specimens. To remedy the problem, liners were constructed for the retorts to eliminate the pressure effects and the pack media was tamped around the specimens. The difficulty was totally eliminated. Because of the large packs used, the cycle time was extended three to five hours to allow for heatup. A coating of approximately 11mg/cm^2 was generally deposited in one 13- to 15-hour 2300 F cycle. Although activator concentration did not appear to affect the deposition rate, 0.1 wt % NaF was added to the pack before each use to exclude any unexpected drop in the deposition rate.

Silicon

Packs of (-200) mesh silicon powder were used throughout the siliciding of the Phase II and III specimens. Retorts used were similar to the one shown in Figure 101. An early practice was to add 1 wt % NaF activator to the silicon packs before each use. This practice was discontinued after several groups of specimens showed severe edge cracking after siliciding. The final procedure adopted added only 1 wt % NaF initially and relied upon the residual to maintain pack activity in the subsequent runs. A cycle time and temperature of three hours at 1950 F was used consistently for all specimens. The deposit weight obtained during the cycle depended largely on the deposit weight of chrome-titanium. Table LXXIII lists the average deposition weight gains for the various types of Phase II and III specimens. A number of the specimens have an unusually heavy deposit of chrome-titanium. These specimens were recycled to remedy a spotty initial deposit.

A description of the performance of these coated specimens is contained in Parts II and III of this report.

TABLE LXXIII

DEPOSITION WEIGHT GAINS FOR V-(Cr-Ti)-Si COATED PHASE II AND III SPECIMENS

Specimen Type (in.)	Alloy	Number Coated	Average Deposit Weight		
			V	Cr-Ti	Si
0.5 by 0.75 by 0.012	Cb752	80	8.0	18.5	19.0
Oxidation tabs	D43	80	9.0	13.0	12.0
0.75 by 1.0 by 0.030	Cb752	40	7.5	16.0	18.0
Oxidation tabs	D43	40	9.0	13.5	12.0
2.0 by 2.0 by 0.012	Cb752	2	6.5	11.0	11.5
Torch test	D43	2	7.0	11.0	7.5
3.0 by 3.0 by 0.030	Cb752	9	6.5	16.0	18.0
Thermal fatigue	D43	9	9.5	12.5	10.0
0.75 by 5.0 by 0.012	Cb752	27	7.0	15.5	15.5
Fatigue	D43	27	7.0	11.5	10.0
0.75 by 5.0 by 0.030	Cb752	27	5.5	15.0	15.5
Fatigue	D43	27	12.0	10.0	12.5
0.75 by 7.0 by 0.012	Cb752	6	7.0	15.5	16.5
Tensile	D43	6	7.0	10.0	11.0
0.75 by 9.0 by 0.012	Cb752	18	7.0	15.5	17.0
Creep	D43	18	8.5	16.0	12.0
0.75 by 11.0 by 0.012	Cb752	16	7.5	15.0	16.0
Environmental	D43	16	8.5	16.0	13.0
0.5 by 3.0	Cb132M	18	8.0	11.0	11.0
Erosion bars	D43	18	9.5	11.0	10.0

VI. CONCLUSIONS

6.1 DIFFUSION BARRIER FOR THE Ti-Cr MODIFIER

Tungsten, molybdenum, tantalum, and vanadium were studied as diffusion barriers for the Ti-Cr modifier (Ti-33Cr alloys were used) on the Cb752, D43 and B66 alloys. The barriers were interdiffused for 100 hours at 2400 F. On a weight/unit area basis, tantalum and vanadium were less effective than a comparable amount of substrate alloy. Tungsten was six times as effective as the D43 or Cb752 substrate, but only slightly more effective than the B66 substrate. Molybdenum was by far the most effective barrier on the B66 alloy, and also was three times as effective as a comparable weight of either the D43 or Cb752 alloy.

The use of a barrier in an actual coating system was not studied because of practical application difficulties. That is, not only does the application of tungsten or molybdenum present a major application problem, but the slow diffusion of titanium and chromium into these elements would greatly retard the rate of deposition of Ti-Cr by pack cementation, which is a diffusion-controlled process. It was concluded that a better approach to controlled diffusion appeared to be the minimization of titanium in the coating.

6.2 SUBSTITUTION OF MOLYBDENUM FOR CHROMIUM IN THE Ti-Cr MODIFIER LAYER

One of the failure mechanisms in (Cr-Ti)-Si coating is the slow loss of chromium by vaporization. The substitution of molybdenum for chromium would eliminate this problem and should also improve oxidation resistance, decrease interdiffusion, and improve the expansion match. The application of the Ti-Mo modifier proved essentially impossible by the conventional pack technique; however, by vacuum sintering of a slurry applied coating, compositions of 95Mo-5Ti could readily be applied.

After siliciding, these compositions consistently lasted for more than 200 one-hour cycles at 2400 F, but 1600 F performance was poor. Glass impregnation or small additions of iron to the modifier eliminates the 1600 F problem without loss of 2400 F protection.

The effect of these high-molybdenum coatings on the mechanical properties of duplex treated D43 and Cb752 alloys was not determined; however, due to the increased partial molal free energy of formation of carbon and oxygen solutions compared to 60Cr-40Ti, the coatings should have little tendency to remove these elements from the substrates. Loss of mechanical properties should, therefore, be negligible.

6.3 SUBSTITUTION OF VANADIUM FOR TITANIUM IN THE Ti-Cr MODIFIER LAYER

The substitution of vanadium for titanium in the Ti-Cr modifier had two objectives--elimination of the MCr_2 laves phase and elimination of the interstitial sink effect.

Attainment of a (V-Cr)-Si coating was not accomplished because of:

- Slow deposition rate of vanadium from packs and severe sintering
- Severe embrittlement of the substrate due to the transport of oxygen from the chromium and to a lesser extent vanadium from the pack media.

A compromise coating was developed based on the initial application of vanadium followed by 80Cr-20Ti and silicon. This coating has a much lower titanium content than the 60Cr-40Ti coating and should have less effect on interstitial element migration.

Application of the V-(Cr-Ti)-Si coating to D43 and Cb752 alloys provided over 500 hours of protection at 1600 F. Some D43 specimens were also protected for more than 500 hours at 2400 F.

The coating does have its problems in application as a result of sintering of the vanadium pack media and embrittlement of the Cb752 alloy through oxygen transport; however, the compositional concept has been proved. Better application techniques using materials of higher purity are required. Duplex slurry techniques such as those used for the (95Mo-5Ti)-Si coating should be explored for this composition.

6.4 VANADIUM MODIFIED COATINGS

Vanadium disilicide is extremely oxidation resistant and exhibits no pest oxidation at low temperatures. A duplex coating, V-Si, was applied to the Cb752 alloy and evaluated at 1600 and 2400 F. The coating exhibited failure in less than 48 hours at 1600 F, but performed quite well at 2400 F (up to 131 hours). The performance did not justify continued process development.

The poor performance of the V-Si system is believed to be the result of the high expansion of VSi_2 and rapid oxidation rate of vanadium and V-Cb alloys. Protection at the base of craze cracks would rely on V_2C_5 modified glass only. This appears to be an inadequate protection mechanism at 1600 F. Alloying with titanium and chromium greatly enhances the low-temperature oxidation resistance of the alloy beneath the silicide and is probably responsible for the improved oxidation resistance of the V-(Cr-Ti)-Si coating.

6.5 GAMMA SUBLAYER ALUMINIDE COATINGS

Gamma titanium aluminide (TiAl) has fair oxidation resistance and some ductility. Property studies showed that the addition of molybdenum or tantalum improved the oxidation resistance at 1600 to 2400 F. Attempts to demonstrate that the relatively oxidation resistant sublayers, high in titanium and molybdenum, could be developed into a coating system were not successful. Maximum life attained with a Ti-Al coating on a Cb-15Mo alloy was 43 hours at 2400 F. Very early failures were also noted with this system. The potential for long-term protection was not indicated and the all-aluminide systems were abandoned.

6.6 DUCTILE METALLIC COATING SYSTEM

The one truly ductile system investigated used the Fe-25Cr-5Al outer layer with various diffusion barriers to separate this alloy from the columbium substrate, and also to minimize crystallographic changes at the interface between surface layers. The coating receiving the most detailed evaluation consisted of Cb-Mo-Cr (Fe-25Cr-5Al) and was formed by solid state diffusion bonding. The evaluation of the coating at 2300 and 2500 F in air showed that an extremely hard phase developed between the chromium and molybdenum as a result of iron diffusion. Diffusion of iron through the chromium and molybdenum produced secondary phases (probably $CbFe_2$) in the columbium alloy. Oxygen also appeared to diffuse through the coating, producing internal oxidation of the columbium alloy.

Although for short periods of time, e.g., up to 10 hours at 2300 F, this type of coating may be the most reliable of all coatings on columbium alloys, a great deal of basic diffusion work must be performed before this type of coating can be used for long periods of time at this temperature. Both oxygen and iron diffusion barriers are required.

6.7 THE COMBINATION ALUMINUM-SILICON COATING

Alloys containing aluminum, e.g., Cb-Ti-Al, and Cb-Ti-Cr-Al were quite oxidation resistant at 1600 F and ductile. By combining these alloys as sublayers with a disilicide primary oxygen barrier, it was hoped that the best feature of the aluminum and silicon coating could be combined. Considerable experimentation on various sublayers showed that a coating of the following type provided the most satisfactory performance:

- Cb-V-(80Cr-20Ti)-Al-Diffusion-Silicon

The coating required two extra processing steps over the V-(80Cr-20Ti)-Si coating (aluminizing and diffusion), but had only comparable life at 1600 and 2400 F and was not, therefore, developed into a major coating system. Performance of the coating was quite interesting in that, although a defect might develop in the coating at 80 hours, catastrophic oxidation would not occur for up to 40 or 50 additional one-hour cycles. That is to say, the oxide appeared to have remarkable self-healing properties.

6.8 THE CERAMIC COATING OVERLAY

Ceramic coatings of the silica-base type were applied over a silicided columbium alloy. The silicide was used to prevent oxygen ingress to the columbium and the overlay was to seal cracks and provide a controlled composition coating independent of the composition of the silicide.

Standard ceramic coatings for superalloys were used which, even with large mill additions, were too soft at 2400 F to prevent reaction with the support media. Compatibility plagued the evaluation of this system. The coatings would protect the substrates, up to 12 hours at 2400 F but compatibility with the silicide at craze cracks was poor. Major crack enlargement was noted.

To investigate effectively the potential of this type of system, studies will be required to determine chemical compatibility of the silicide with the ceramic coatings, and new, more refractory coatings will be required to minimize mobility at 2400 F.

6.9 GENERAL CONCLUSIONS ON PROPERTY MEASUREMENT RELATIVE TO COATING PERFORMANCE

- Significance of Expansion Match of MSi_2 and M_5Si_3 with Columbium Alloys - Expansion matching, although possibly desirable, is far overshadowed by the oxidation resistance of sublayers, the type of oxide formed, and the oxidation resistance of the disilicide. The (95Mo-5Ti)-Si and V-(Cr-Ti)-Si coatings afford comparable protection to columbium alloys, but one is closely matched and one has a 50 to 60 percent higher expansion than the columbium alloys.

- Oxidation Resistance of Disilicides - Correlation of 2400 F oxidation resistance as a coating is very good with oxidation resistance of the monolithic disilicide. At 1600 F mismatch in expansion overshadows simple oxidation resistance.

- Oxidation Resistance of the M_5Si_3 Silicide - There does not appear to be a requirement for oxidation resistance of the M_5Si_3 silicide to produce a good coating if the disilicide is sufficiently protective.

- Oxidation Resistance of a Ductile Sublayer - Oxidation resistance at low temperatures of silicide coatings appears to correlate well with oxidation resistance of the sublayer. The (Cr-Ti)-Si, V-(Cr-Ti)-Si have good oxidation resistance at 1600 F; while the (95Mo-5Ti)-Si has problems. The problem appears traceable to sublayer oxidation resistance.

REFERENCES

1. Holloway, J. F. Jr., et al, Coatings for Cb Alloy Gas Turbine Engine Components. AF33(615)-2117.

2. Girard, E. H., et al, Ductile Coatings for the Oxidation Protection of Cb and Mo Alloys. Final Report, BuWeps Contract NOw 65-0340-F (May 1966).

3. Moore, V.S. and Stetson, A.R., Evaluation of Coated Refractory Metal Foils. RTD-TDR-63-4006, AF33(657)-9443 Part I and II (1963 and 1964).

4. Hansen, M., et al, Constitution of Binary Alloys, 2 ed., McGraw-Hill, New York (1958).

5. Stein, B. A. and Lisagor, W. B., Oxidation and Embrittlement in Silicide Coated Columbium Alloys and Aluminide Coated Tantalum-Alloy Sheet. Presented at the AIME Meeting, French Lick, Indiana (October 1965).

6. Stetson, A.R., An Analysis of the (Cr-Ti)-Si Coating Chemistry and Modification for the Protection of Columbium-Base Alloy. Presented to the Tenth Meeting of the Refractory Composites Working Group, Atlanta, Georgia (April 1965).

7. Metcalfe, A. G. and Dunning, J.S., Interstitial Sink Effect in the Refractory Metals. Presented at the AIME Meeting, French Lick, Indiana (October 1965).

8. Sheely, W. F. and Wilson, J. L., "The Properties of Columbium-Aluminum-Vanadium Alloys, Part II, Mechanical Properties". Columbium Metallurgy, Vol. 20, Interscience, New York (1960) pp. 585-595.

9. Hubbard, R. J. J. and Minton, C. D. T., "Protective Coatings for Niobium and Its Alloys". Metals for the Space Age (Plansee Proceedings, 1964) pp 444-459, Springer Volage, Wien 1965.

10. Carlson, R. G., "Oxidation Resistance of Aluminum Dip Coated Columbium Alloys, "Columbium Metallurgy, Interscience Publishers, New York, 1960.

11. Rausch, J. J., Low-Temperature Disintegration of Intermetallic Compounds. ARF-2981-4, August 31, 1961.

12. Sama, L. and Ludkins, M.F., Preparation and Properties of $CbAl_3$. General Telephone and Electronic Laboratories, Inc., Bayside, New York.

13. Wukusick, C. S., Oxidation Behavior of Intermetallic Compounds in the Cb-Ti-Al System. GEMP-218, July 31, 1963.

REFERENCES (Contd)

14. Bartlett, R. W., Investigation of Mechanisms for Oxidation Protection and Failure. Final Report ASD-TDR-63-753, Part III (September 1965).

15. Passmore, E. M., Investigation of Diffusion Barriers for Refractory Metals, Contract No. AF33(616)-6354, ASD-TDR-62-432 (July, 1962).

16. Hill, V. L. and Rausch, J. J., Protective Coatings for Tantalum-Base Alloys. Contract No. AF33(615)-3071, to be published.

17. Wimber, R. T., and Stetson, A. R., "Coatings for Tantalum Alloy Nozzle Vanes" Final Report in preparation, Solar Report Number RDR1396-3 (NASA Contract NAS3-7276).

18. Stetson, A. R., Cook, A. A., Moore, V. S.. "Development of Protective Coatings for Tantalum Alloys" AFML TR-65-205 Part I, Contract AF33(657)-11259 (June 1965).

19. Alden, T et al., Solubility of Nickel and Chromium in Molten Lead, Transaction of AIME (Feb. 1958).

20. Wlodek, S. T. and Wulff, I., Growth of Chromium Coatings from Liquid Metallic Solutions. Transaction AIME (August 1960).

21. Mellors, G. W. and Senderoff, S., Electrodeposition of Coherent Deposits of Refractory Metals. 1. Niobium. Journal of the Electromechanical Society p 266-272 (March 1965).

APPENDIX

Two tasks are described in the Appendix that, although significant technically, were not pursued in sufficient detail during the course of the program to warrant inclusion in the body of the report. These tasks are:

- Purification of vanadium/chromium alloy
- Fused salt deposition of vanadium and chromium

PREPARATION OF VANADIUM/CHROMIUM PACK ALLOYS

A number of methods were investigated for the preparation of vanadium/chromium pack alloys. A major problem involved the production of alloy powders having a low oxygen content, because oxygen is readily transferred to columbium alloys from the pack material. Embrittlement of the columbium alloys can be expected if there is an excessive transfer of oxygen. Vanadium/chromium pack alloys are particularly difficult to prepare with a low oxygen content, because the commercial grades of these metals contain relatively large amounts of this element. Methods of removing oxygen from vanadium/chromium alloys were investigated as well as means of tying it up in solution, thereby preventing its transfer to the base metal during the coating process.

The diffusion of oxygen into columbium alloy substrates during coating produces interstitial embrittlement in these metals and, therefore, pack alloys having a low oxygen content are to be desired. Commercial grades of vanadium contain typically about 1000 ppm oxygen. Commercial grade chromium will generally contain from 2000 to 5000 ppm oxygen. Higher purity metals are available at a greatly increased cost; however, purification of commercial quality material appears to represent a more feasible approach. Typical prices for commercial grade and ultrapure vanadium and chromium metals are shown in Table LXXIV.

TABLE LXXIV

TYPICAL PURITIES AND COST COMPARISONS FOR VARIOUS GRADES OF VANADIUM AND CHROMIUM

Production Process	Overall Purity (%)	Interstitual Level (ppm)	Cost/Pound ($)
Chromium			
Electrolytic	99.2	C -- N -- O 5000	1.25
Iodide	99.997	C 10 N 5 O 10	120.00 to 130.00
Vanadium			
Unknown	91.0	-- N 300 O 800	6.00 to 7.00 40.00 to 50.00
Unknown (Electrolytic nondimensional)	99.9	C 300 N 200 O 300	90.00 to 110.00

Methods of removing oxygen from vanadium/chromium alloys by the addition of gettering agents were investigated. A series of 100-gram arc melts was made containing small additions of mischmetal[1] (MM), carbon, tungsten, and zirconium. The mischmetal additions were effective in reducing the oxygen content as determined initially by microhardness readings on the as-cast structure and by chemical analysis. The hardness correlation for the nominal 50V-50Cr alloys studied is shown in Figure 143. The composition of all gettered melts and their respective oxygen analyses after double arc melting are shown in Table LXXV. (Retained mischmetal and oxide in the alloy will increase the analyzed oxygen content so that the amount in the vanadium/chromium alloy must be less than the analyzed amount.) Arc melts were

1. Rare earth metal comprised principally of Ce (50%), La (25%). Purchased from Ronson Metals Corporation, Newark, N.J.

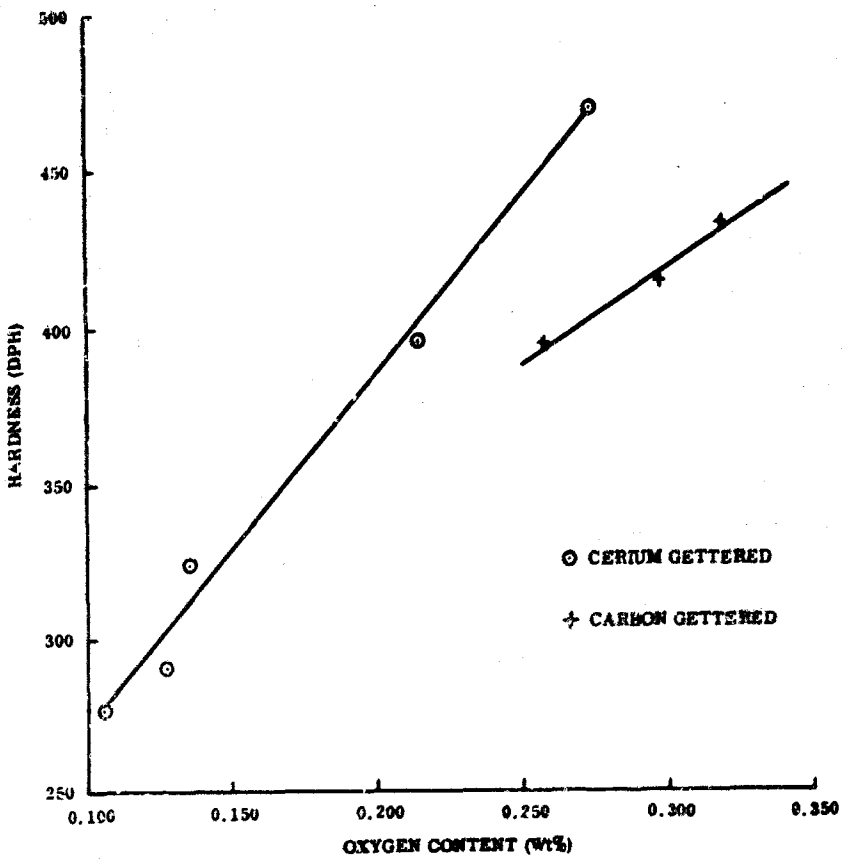

FIGURE 143. HARDNESS VERSUS OXYGEN CONTENT IN ARC-MELTED V-50 Cr ALLOY

TABLE XV

ARC-MELTED, NOMINAL 50V-50Cr ALLOYS SHOWING EFFECT OF GETTERING AGENTS ON RESIDUAL OXYGEN CONTENT AND HARDNESS OF AS-CAST STRUCTURE

Alloy Composition (wt %)	Oxygen Content (wt %)	Hardness (DPH)
V-50Cr	0.291	381
V-49.8Cr-0.5MM	0.272	470
V-49.5Cr-1.0MM	0.213	396
V-49Cr-2.0MM	0.136	322
V-47.5Cr-5.0MM	0.128	290
V-45Cr-10MM	0.107	277
V-49.9Cr-0.20C	0.295	417
V-49.8Cr-0.40C	0.317	432
V-49.8Cr-0.20C-0.20Zr	0.257	396
V-45Cr-10W	0.295	439
V-45Cr-10Ti	0.337	389

conducted in argon at a chamber pressure of approximately 200 Torr. Mischmetal was the most effective scavenger of oxygen of all the addition elements tried. The major amount of the gettering action was achieved after a two-percent addition; however, further small reductions in oxygen occurred up to the maximum amount used of 10 percent. Residual oxygen contents, as a function of the amount of mischmetal added, are shown in Figure 144. The rare earth oxide, which is formed, tends to separate on the surface of the ingot as a thin glassy layer and can be removed by sandblasting. The residual mischmetal separates on the bottom of the ingot in a fairly discrete layer since it has very little solubility in the vanadium/chromium alloy. Although sandblasting could be used to remove residual rare earth metal on the outside of the ingot, a small amount remains dispersed in the alloy. Figure 145 shows the appearance of an ungettered V-50Cr melt. Photomicrographs of melts, which were gettered with mischmetal are shown in Figures 146 through 150. There is a decreasing amount of second-phase impurity with increasing amounts of mischmetal. The small spherodial particles are believed to be occluded rare earth metal. The dark precipitates in segregate regions are believed to be oxides and other interstitial impurities.

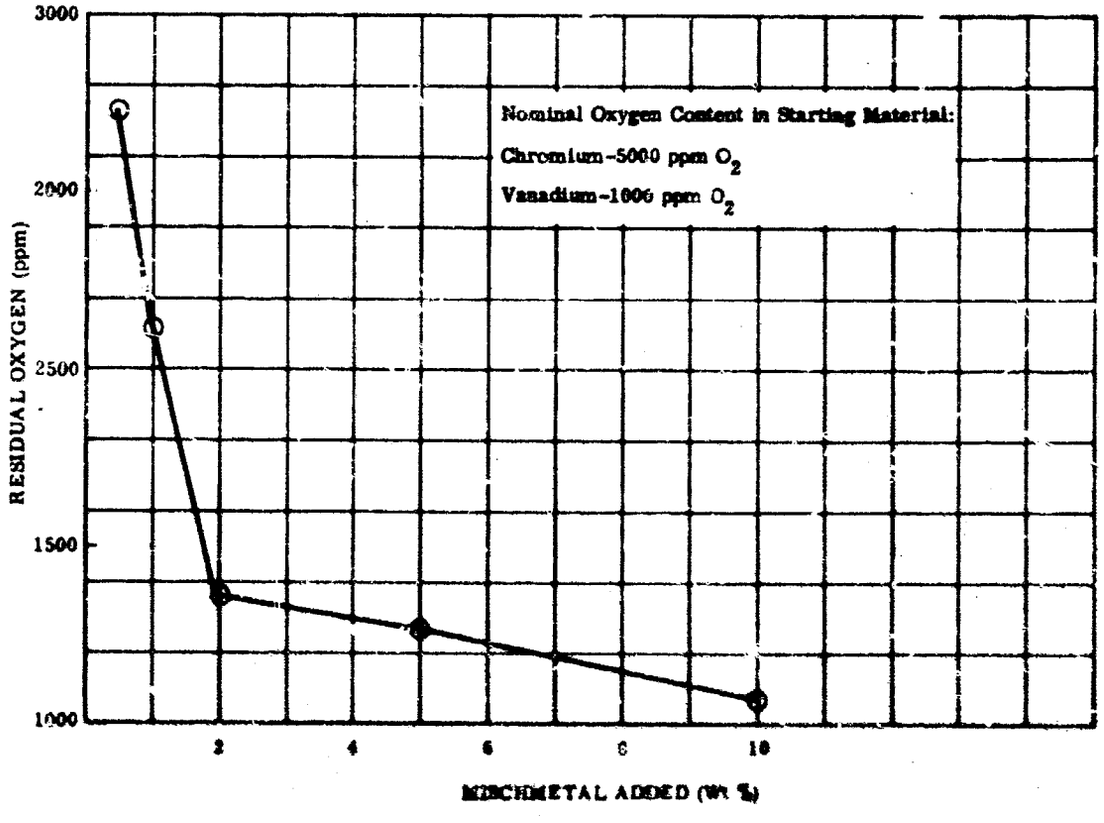

FIGURE 144. DEOXIDIZING EFFECT OF MISCHMETAL IN ARC-MELTED 50V-50Cr ALLOY

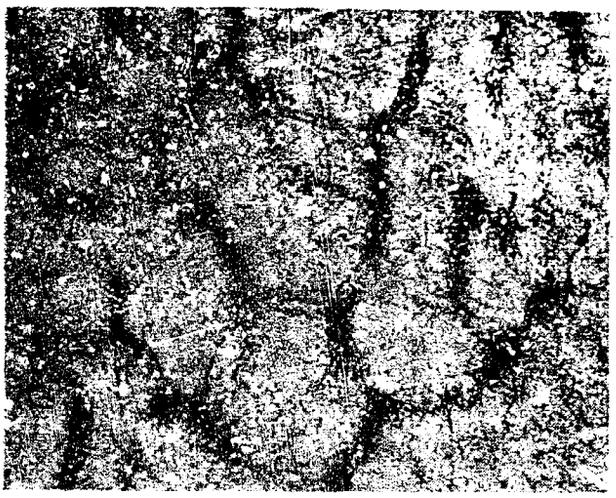

Ungettered, showing second phase contamination.

Magnification: 250X

FIGURE 145.

ARC MELTED V-50Cr-ALLOY

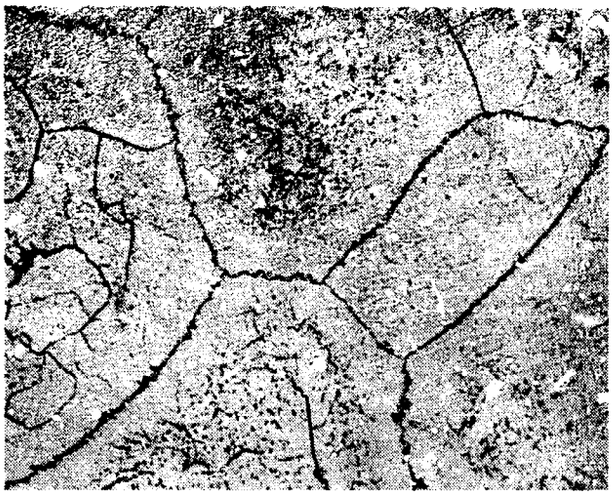

Mischmetal addition too small to show any visible scavenging

Magnification: 250X

FIGURE 146.

ARC MELTED V-49.8Cr-0.5 MM ALLOY

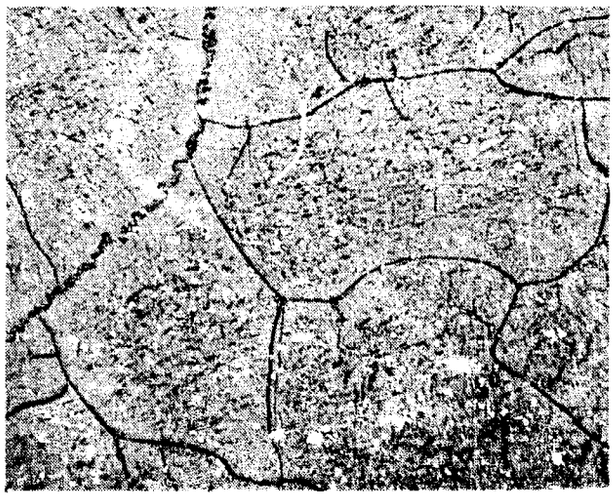

Gettering effect of mischmetal becoming evident by decreasing segregation.

Magnification: 250X

FIGURE 147.

ARC MELTED V-49.5Cr-1.0 MM ALLOY

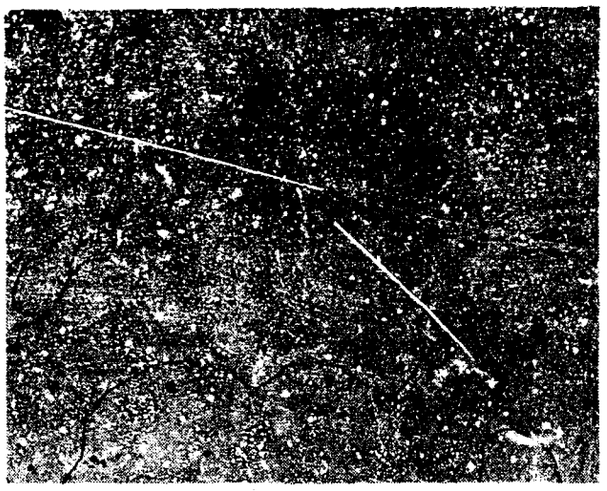

Visible contamination has been virtually eliminated.

Magnification: 250X

FIGURE 148.

ARC MELTED V-49Cr-2.0 MM ALLOY

Spheroidal particles are believed to be occluded mischmetal.

Magnification: 250X

FIGURE 149.

ARC MELTED V-47.5Cr-5.0 MM ALLOY

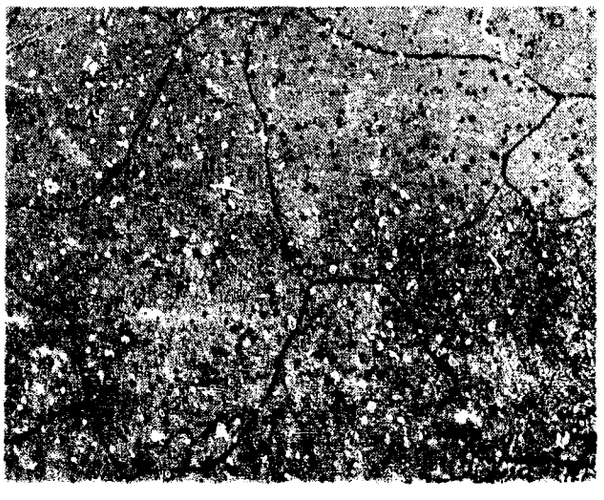

Magnification: 250X

FIGURE 150.

ARC MELTED V-45Cr-10 MM ALLOY

There was a possibility that oxygen transfer to metal substrates in packs can be avoided if the oxygen in the pack material can be combined with an element having a higher negative partial molal free energy of solution of oxygen than the metal being coated. Titanium was added to study this approach. Partial molal free energies of solution of oxygen in titanium and columbium are shown in Figure 151 at a typical pack temperature of 2200 F. A nominal V-45Cr-10Ti alloy was prepared to determine if titanium could be used as a gettering agent, whereby the oxygen is not removed but merely prevented from transferring. The as-cast structure of the V-45Cr-10Ti pack alloy is shown in Figure 152. Table LXXV shows that this alloy contains the highest oxygen content as determined by chemical analysis.

Deposition Experiments

A number of alloy compositions were selected from the previous series of arc melts to evaluate their coating properties. They were chosen to determine the effect of high and low oxygen content, and also to evaluate the effectiveness of titanium to retain dissolved oxygen and prevent its transfer to the part being coated. The extent of oxygen transfer was determined metallographically and by a bend test. The sheet material used for coating specimens was 0.006-inch thick Cb752 alloy. This

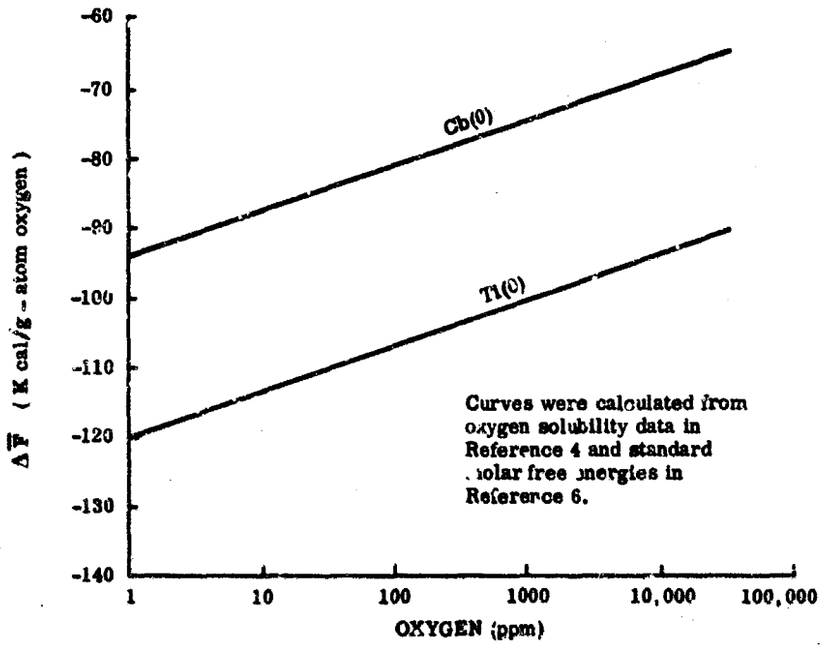

FIGURE 151. PARTIAL MOLAR FREE ENERGY OF SOLUTION OF OXYGEN IN TITANIUM AND COLUMBIUM AT 2200 F

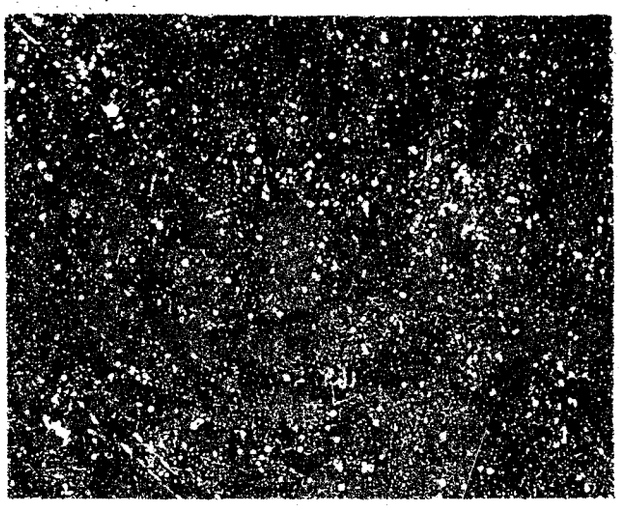

Magnification: 500X

FIGURE 152. ARC-MELTED V-45Cr-10Ti ALLOY

alloy is very sensitive to embrittlement by oxygen. Bend testing provided a simple means for judging the amount of oxygen transfer to the base metal. Two packs of specimens were run. Test parameters were the same for both with the exception that an activator (0.1 wt% NaCl) was used in one of the packs and time at temperature was increased to 15 hours compared to 6 hours for the first pack. The results of these experiments show that the pack alloys that were gettered with large amounts of mischmetal, and consequently contained the lowest amount of oxygen, caused the least amount of embrittlement to the substrate. The titanium gettered material also produced very little embrittlement to the substrate, but was less effective than the mischmetal gettered alloys. In contrast, the ungettered 50V-50Cr alloy, which contained roughly three times as much oxygen as the best mischmetal melt (2910 ppm versus 1070 ppm), gave a very brittle substrate. The use of small carbon additions was not effective in removing oxygen during arc melting, and pack material containing carbon, which analyzed at 2170 ppm oxygen, also produced very brittle substrates. Coating data and bend test results are summarized in Table LXXVI.

TABLE LXXVI

COATING RESULTS WITH VANADIUM/CHROMIUM POWDERS ON Cb752 SUBSTRATE AT 2200 F

Pack Alloy Nominal Composition	Oxygen Content (wt %)	Deposit (mg/cm^2)	90-degree Room Temperature Bend Test	Surface Condition
V-50Cr	0.291	0.35(1)	Failed	Clean
		1.30(2)	Failed	Clean
V-49Cr-(2.0MM)	0.136	0.17(1)	Partial failure	Clean
		0.50(2)	Failed	Mottled
V-47.5Cr-(5.0MM)	0.128	0.18(1)	Passed	Mottled
		0.06(2)	Passed	Mottled
V-45Cr-(10MM)	0.107	0.29(1)	Passed	Slight sinter
		0.60(2)	Passed	Mottled
V-49.8Cr-0.4C	0.317	0.72(1)	Failed	Clean
		1.50(2)	Failed	Mottled
V-45Cr-10Ti	0.337	0.31(1)	Partial failure	Very clean
		1.20(2)	Failed	Clean

Coating parameters: 1. 6 hours - no activator
2. 15 hours - 0.10 weight percent NaCl activator

The following conclusions can be drawn on the basis of work that was conducted:

- Mischmetal was a relatively effective getter of oxygen in vanadium/chromium alloys as evidenced by a reduction of oxygen levels from approximately 3000 to 1000 ppm in arc-melted alloys.
- The use of mischmetal as a gettering agent for pack alloys will reduce oxygen embrittlement of columbium-base substrates, but methods for removing residual mischmetal from pack alloys to prevent its codeposition with other pack constituents are required.

- Small amounts of titanium will getter oxygen and reduce embrittlement to the Cb752 substrate, and are effective in absorbing relatively large amounts of oxygen in pack alloys and preventing transfer during coating.

- The pack codeposition of V-Cr or V-Cr-Ti is extremely slow and would preclude use of this technique to develop coatings at least 0.002 inch in thickness at practical temperatures.

The use of codeposition of vanadium and chromium was dropped due to slow deposition, but the use of titanium as an internal getter was retained. Subsequent use of vanadium deposition followed by 80Cr-20Ti used titanium to prevent oxygen transfer from the chromium and to remove oxygen transferred in the vanadizing step.

FUSED SALT DEPOSITION OF VANADIUM AND CHROMIUM

Compounds of most of the Group IV-B, V-B, and VI-B metals can be reduced to metal in molten salts but generally in the form of powder or dendrites. Mellors and Senderoff (Ref. 21) have reported that coherent deposits of chromium, hafnium, molybdenum, columbium, tantalum, tungsten, vanadium, and zirconium can be produced on several substrates by a general method of molten salt electrolysis involving dissolution of the refractory metal fluoride or chloride in mixtures of alkali metal fluorides or chlorides. Experience at Solar in the development of an all-fluoride titanium electrolytic plating bath (U.S. Patent No. 3,024,174) indicated that a plating rate of 0.002 inch/hour is readily obtained. Emphasis in this program was on the deposition of vanadium to minimize the sintering problem in packs, and on chromium to hopefully minimize the embrittlement of the columbium alloy substrate.

Equipment

The fused salt plating cells used in the program are shown schematically in Figure 153. The cells consist of a heated crucible with provisions for specimen support, manipulation, and maintenance of predetermined temperatures and atmosphere. Heating is provided by a natural gas/air burner projecting a flame tangentially on an Inconel retort which is protected with an oxidation-resistant ceramic coating. The top portion of the cell is water-cooled stainless steel. A graphite crucible contains the salt. This crucible is separated from the Inconel wall by tungsten or

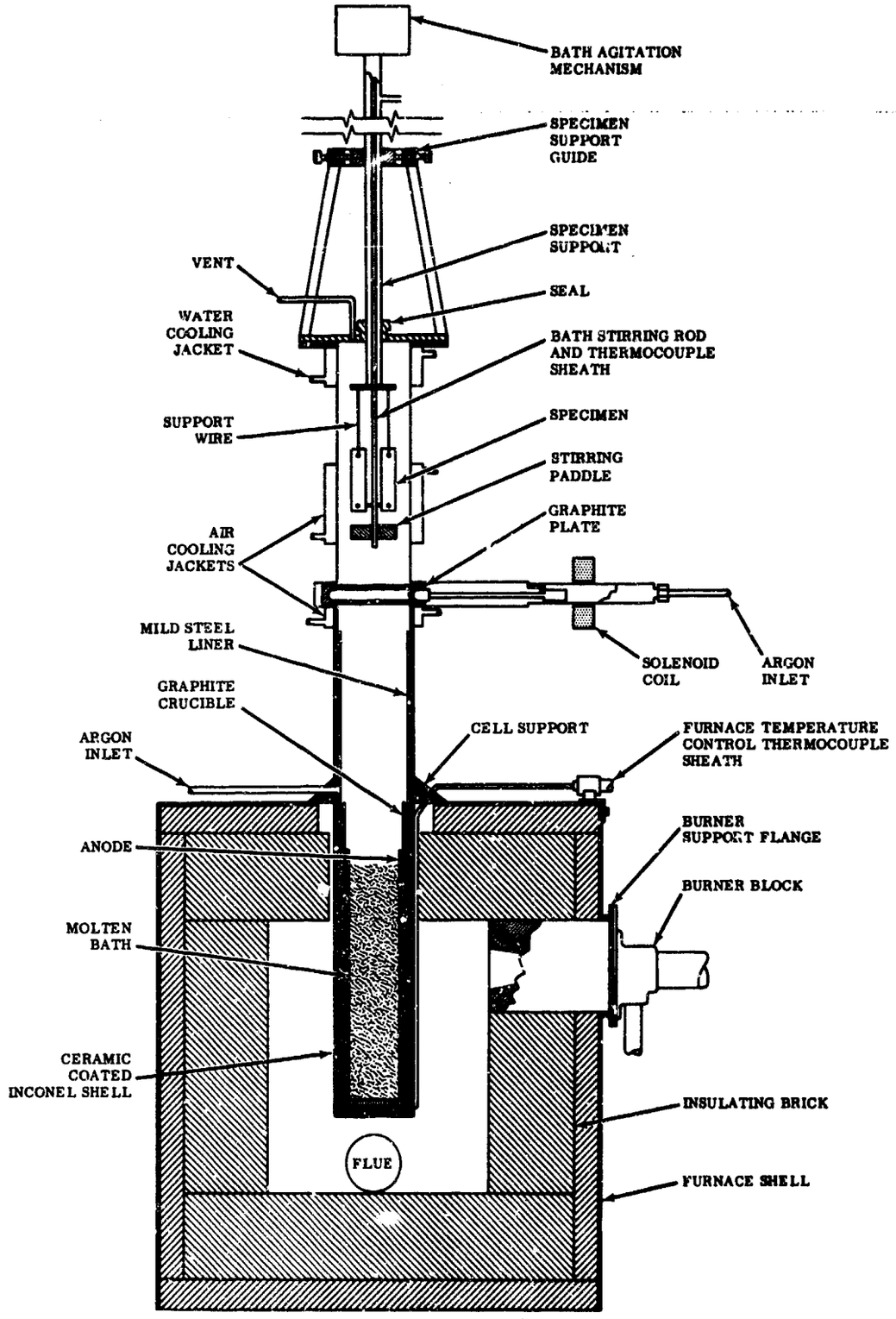

FIGURE 153. SCHEMATIC DIAGRAM OF FUSED SALT PLATING CELL

molybdenum sheet. Specimens are supported in the bath with tungsten wire which is fastened to a stainless steel ring. The ring is welded on a stainless steel tube which enters the cell through a Teflon-sealed fitting, permitting vertical adjustment of the support tube and electrical insulation from the anodic retort. A stainless steel sheathed chromel-alumel thermocouple passes through a Teflon-sealed fitting in the support tube and is used to continuously monitor bath temperature. The portion of the thermocouple actually in the bath is tantalum sheathed. Argon is continuously admitted to the cell in the cooling and plating chambers. Furnace temperature is controlled by a proportional-type temperature controller with a stainless steel sheathed chromel-alumel thermocouple as a sensing element. A Kepco power supply was used as the source of constant current and voltage, and has a maximum output of 2 amperes at 36 volts with less than 1 millivolt noise and ripple. Bath potentials are measured with a Welch Model 3060 K voltmeter.

Materials

The sodium, lithium, potassium fluoride, and chloride solvents currently being used were all reagent grade and meet ACS specifications. The salts were vacuum dried for 16 hours at 250 F prior to use.

The potassium vanadium pentafluoride, potassium chromium hexafluoride, and potassium molybdenum hexachloride salts were prepared at Solar by the following techniques:

Potassium Vanadium Pentafluoride (K_2VF_5) Preparation (Section V)

Potassium Chromium Hexafluoride (K_3CrF_6) Preparation

- Mix $K_2CrF_5 \cdot xH_2O$ (B and A technical) is dried in hydrogen fluoride gas.
- Heat in completely argon-purged retort for 2 hours at 900 F.
- Cool in argon.

Chemical analyses of the vanadium and chromium, used as anode material are contained in Table LXXVII. Vanadium is added to the plating bath in the form of -20 +50 mesh granules. Chromium fines are sintered in an argon atmosphere (16 hours at 2000 F) in a suitable mold to produce a cylindrical anode 2.5 inches OD by 2.25 inched ID by 6 inches high.

Also contained in Table LXXVII is the analysis of the 0.012-inch Cb752 substrate alloy being used in the study. Specimens were fabricated from 0.75-inch wide roll stock to 0.5 inch by 0.75 inch dimensions. A 0.125-inch support hole was drilled at each end of each specimen. All specimen corners were rounded in a suitable jig to a 0.125-inch radius on a rubber abrasive wheel. Specimen edges were uniformly radiused and deburred in a standard pebble-cleaning solution (Oakite Hi-Lite) media. The specimens were tumbled in the media until sufficient radiusing occurred and all scratches and nicks were removed.

TABLE LXXVII

CHEMICAL ANALYSES OF THE METAL ANODE MATERIALS AND Cb752 SUBSTRATE ALLOY

Metal	Source	Composition (wt %)											
		V	Cr	Mo	Cb	Zr	W	Fe	Ni	O	C	H	N
Vanadium	Union Carbide Corp.	99.8	--	0.025	--	--	--	0.015	0.020	0.077	0.027	0.0012	0.006
Chromium	Union Carbide Corp.	--	99.75	--	--	--	--	0.004	--	0.080	0.020	0.006	0.001
Cb752 Alloy	Union Carbide Crop.	--	--	--	88.3	2.7	9.0	--	--	0.022	0.010	0.0005	0.011

OPERATING PROCEDURES

The initial bath additions were computed on a 1000-gram basis. The required amounts of solvent salt, active metal salt, and metal granules (in the case of vanadium) were weighed separately. The solvent salt was added to the graphite crucible, and the cell purged with laboratory grade argon (99.99%) for 10 to 15 minutes before igniting the gas-fired furnace. The argon atmosphere was maintained throughout the entire operation of the bath. Following liquation of the solvent salt, the cell was allowed to cool to below 100 F before the addition of the active metal salt and metal is made. The cell was fired to melt the active metal salt and the bath held above the remelt temperature for approximately 16 hours. A pre-electrolysing run of four hours at 50 ma/cm^2 was used to establish the correct valence state required for deposition prior to actual experimental runs. The Cb752 specimen surfaces were prepared by etching in a $4H_2O$-$2HNO_3$-$1HF$-$1H_2SO_4$ solution, water rinsing, acetone rinsing, and drying in a nitrogen gas blast. Each specimen was individually weighed on a Mettler Type H15 balance. Four specimens were used in each plating run and were suspended in the bath with 0.010-inch tungsten wire. Prior to insertion of the

specimens, the bath depth was determined by inserting a clean stainless steel rod into the bath for approximately five seconds and quickly removing the rod to freeze the adhered molten salt. The specimen support tube is then adjusted so that the specimens are suspended midway in the bath. Where electrolytic deposition is being studied, the specimens enter the bath with an applied voltage.

After the desired plating cycle, the specimens were allowed to cool in the upper portion of the cell for approximately 10 minutes before removal. Adhered salt was removed from the plated specimens by soaking in hot water to loosen the salts followed by light brushing of the specimen surfaces. The specimens were acetone rinsed, dried with a nitrogen blast, and weighed to determine the weight change attributable to the plating run.

EVALUATION TECHNIQUES

Deposition is determined by specimen weight gain/unit area and metallographic coating thickness. One specimen from each run was subjected to a simple bend test to ascertain the retention or loss of ductility as a result of the coating process. Microhardness traverses were employed as a measure of possible coating and substrate contamination from interstitials. Coating composition was qualitatively determined by X-ray fluorescent analysis.

EXPERIMENTAL RESULTS

Vanadium Deposition

Vanadium was deposited from a bath containing 69 weight percent NaF, 15.5 weight percent K_2VF_5, and 15.5 weight percent vanadium metal. A current density of 78 ma/cm^2 and a deposition temperature of 1900 F yielded average deposits of 5.30, 6.46, 9.02, and 11.35 mg/cm^2 on the Cb752 substrate alloy after plating times of 50, 60, 80, and 120 minutes, respectively. A deposition/time plot of these data is approximately linear indicating that deposition obeys Faraday's Law of electrolysis with an indicated cathode current efficiency of 12 to 14 percent. The deposit itself was extremely hard (600 to 1000 KHN, 50-gram load) and the vanadium-Cb752 composite was brittle. X-ray fluorescent analyses of the vanadium plate did not indicate the transfer of tramp elements such as iron and nickel, and embrittlement was probably due to oxygen and hydrogen pickup from the plating materials and from normal operation of the cells by the entering and exiting of the specimens.

The throwing power of the vanadium bath was poor. Bottom and outward surfaces were preferentially plated which necessitate the use of half cycles at which time specimens were inverted to produce a uniform deposit. The use of a cylindrical vanadium anode in contact with the walls of the graphite crucible should minimize this directional plating effect.

Forty 0.500-inch by 0.750 inch by 0.012 inch Cb752 specimens were vanadized. Two cycles of 30 minutes each at 1900 F with a current density of 78 ma/cm^2 were used. An average of 6.55 mg/cm^2 of vanadium was deposited on the specimens. Thirty-seven of the vanadized specimens were subsequently vacuum annealed for six hours at 2500 F at 10^{-6} Torr.

Chromium Deposition

Chromium deposition was investigated from two bath compositions (Table LXXVIII). The first bath (C1) contained 41.3 weight percent KF, 20.4 weight percent LiF, 8.3 weight percent NaF, 15 weight percent K_3CrF_6, and 15 weight percent chromium metal in granular form. A current density of 50 ma/cm^2 and a deposition temperature of 1800 F yielded average deposits of 2.65, 6.04, 9.02, and 17.92 mg/cm^2 on the Cb752 substrate alloy after plating times of 8, 20, 30, and 60 minutes, respectively. A deposition/time plot of these data was linear indicating that deposition conforms to Faraday's law of electrolysis with an indicated cathode current efficiency of 55 to 62 percent. The deposit itself was soft (123 KHN, 50-gram load), but the chromium-Cb752 composite was brittle. X-ray fluorescent analysis of the chromium deposit did not indicate transfer of metal elements other than chromium. The bath material was extremely hygroscopic and, therefore, especially prone to moisture contamination. The gradual buildup of dissolved H_2O during normal cell operation may explain the inconsistent deposition and fine-grained deposits that resulted with the C1 bath.

The second chromium bath (C2) contained 85.0 weight percent NaCl, 15 weight percent K_3CrF_6, and a sintered chromium cylindrical anode. At a deposition temperature of 1800 F and a current density of 50 ma/cm^2, average deposits of 2.57, 6.57, and 13.53 mg/cm^2 were obtained on the Cb752 substrate after plating times of 15, 30, and 60 minutes, respectively. A plot of these data was linear and a cathode current efficiency of 32 to 43 percent was indicated. The C2 plating bath, because of its consistent deposition rate and nonhygroscopic nature, was selected to chromize the previously vanadized specimens.

TABLE LXXVIII

FUSED SALT DEPOSITION OF CHROMIUM ON Cb752 ALLOY

Bath No.	Bath Composition (wt %)						Process Conditions			Deposition (mg/cm^2)	Cathode Current Efficiency (%)
	KF	LiF	NaF	NaCl	K_2CrF_6	Cr	Temperature (F)	Time (min)	Current Density (ma/cm^2)		
C1	41.3	39.4	3.8	—	15	15	1800	8	50	2.65	61.5
								20	50	6.04	56.0
								30	50	9.62	55.7
								60	50	17.32	50.3
C2	—	—	—	—	15	Sintered Anode	1800	15	50	7.37	51.7
								30	50	4.97	40.5
								60	50	13.53	41.6

The throwing power of the chromium bath containing the sintered chromium cylindrical anode was sufficient to uniformly coat the entire surface of the 0.5 inch by 0.75 inch specimen in a single cycle.

Twenty-four of the vanadized and annealed Cb752 specimens were chromized in the C2 bath. A plating cycle of 120 minutes at 1800 F with a current density of 50 ma/cm^2 produced an average of 22.84 mg/cm^2 of chromium deposit on the specimens. Eighteen of the chromized specimens were subsequently annealed for 16 hours at 2200 F in gettered argon.

To determine the oxidation resistance of vanadium- and chromium-modified Cb752 substrate, selected specimens were oxidized for 1 and 4 hours at 1600 F in slowly moving air. The results of these tests are listed in Table LXXIX and shown graphically in Figure 154. Chromium by itself did not appear to improve the oxidation resistance of the Cb752 substrate at 1600 F for exposures greater than 1 hour, but considerable improvement through 4 hours was obtained by vanadium modification of the Cb752 alloy surface prior to chromium deposition. Oxidation resistance also appeared to be sensitive to the relative amounts of vanadium and chromium in the surface alloy, and adequate oxidation resistance for the 4-hour period required larger quantities of vanadium and chromium in the coating. The specimens that were annealed after chromizing sustained little surface oxidation damage.

TABLE LXXIX

OXIDATION TEST RESULTS OF VANADIUM AND CHROMIUM SURFACE MODIFIED Cb752 SUBSTRATE ALLOY AT 1600 F

Material	Amount of Deposit (mg/cm^2)			Oxidation Weight Gain (mg/cm^2)		Comments
	Vanadium	Chromium	V/Cr Ratio	1 hour	4 hours	
Cb752 Uncoated	--	--	--	32.00	64.00	Rapid oxidation and defoliation; white oxide.
Cb752 + Vanadium + Anneal(1) + Chromium	6.00	5.40	1.11	1.27	37.85	Slow oxidation and green discoloration up to 1 hour. Rapid oxidation and dark oxide thereafter.
Cb752 + Vanadium + Anneal(1) + Chromium	6.32	22.00	0.29	4.67	5.31	Slow oxidation and green discoloration. Specimens intact after 4 hours.
Cb752 + Vanadium + Anneal(1) + Chromium + Anneal(2)	5.81	21.66	0.27	0.63	0.90	Very slow oxidation and green discoloration. Specimens intact after 4 hours.
Cb752 + Chromium	--	20.79	--	8.83	59.10	Slow oxidation and green discoloration up to 1 hour. Rapid oxidation later and dark oxide.

1. Vacuum annealed for 6 hours at 2500 F at 10^{-6} Torr
2. Gettered argon annealed for 16 hours at 2200 F

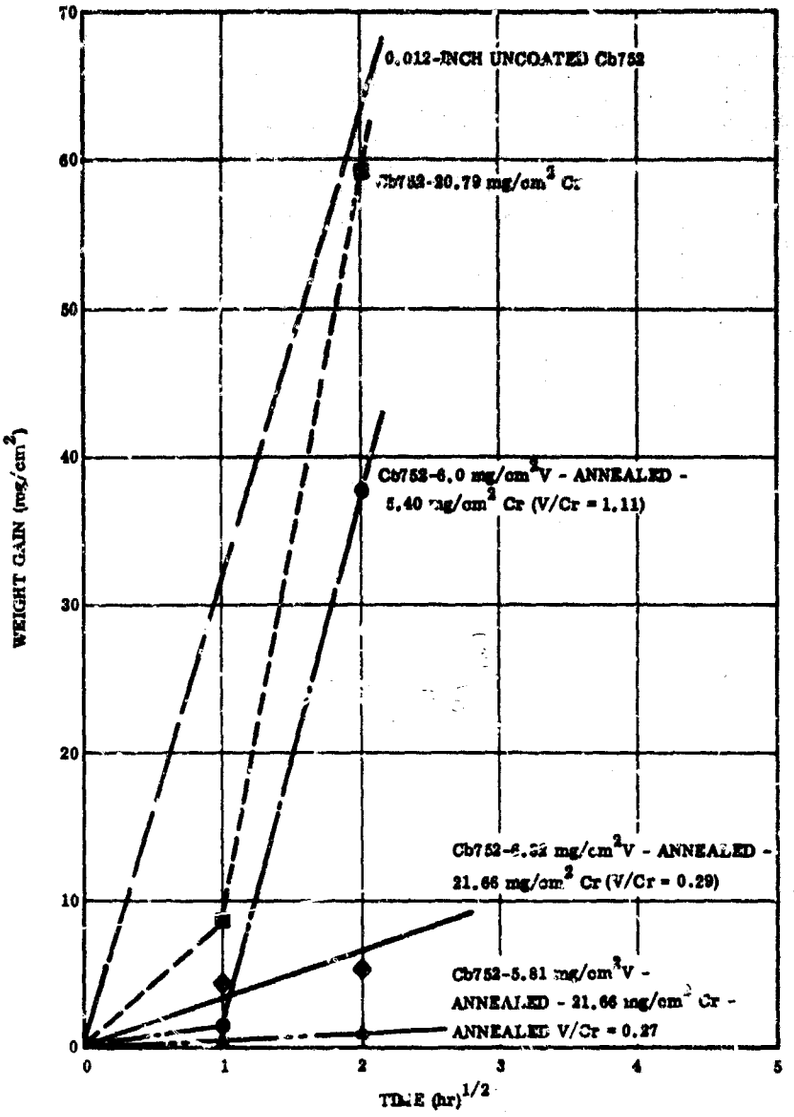

FIGURE 154. OXIDATION RATE OF VANADIUM AND CHROMIUM SURFACE MODIFIED Cb752 SUBSTRATE ALLOY

CONCLUSIONS

Relatively rapid deposition rates for both chromium and vanadium were obtained with current efficiencies of 12 to 14 percent for vanadium and 30 to 60 percent for chromium. Deposition from both baths, however, produced severe substrate embrittlement due apparently to absorption of oxygen from the bath. An extensive development program would be required to refine the plating bath chemicals to eliminate the oxygen problem. This was beyond the scope of this program; consequently, work with these promising deposition techniques was suspended.

Oxidation results of interdiffused vanadium and chromium-plated Cb752 alloy after exposure for up to 4 hours at 1600 F indicated that the oxidation rate was extremely low. This rate was very sensitive to both the amount of chromium and vanadium and the ratio of the two elements as shown in Table LXXIX. Although the fused salt deposition technique was not used to process program specimens due to substrate embrittlement, the excellent substrate oxidation resistance of the V-Cr coating lent support for the V-(Cr-Ti)-Si coating that was finally selected.

UNCLASSIFIED

Security Classification

DOCUMENT CONTROL DATA - R&D

(Security classification of title, body of abstract and indexing annotation must be entered when the overall report is classified)

1. ORIGINATING ACTIVITY (Corporate author)
Solar Division
International Harvester Company
San Diego, California 92112

2a. REPORT SECURITY CLASSIFICATION
UNCLASSIFIED

2b. GROUP

3. REPORT TITLE
Development of Coatings for Columbium-Base Alloys Part I - Basic Property Measurements and Coating System Development

4. DESCRIPTIVE NOTES (Type of report and inclusive dates)
Summary Technical Report - 1 July 1964 - 31 October 1966

5. AUTHOR(S) (Last name, first name, initial)
Stetson, A. R.
Metcalfe, Dr. A. G.

6. REPORT DATE	7a. TOTAL NO. OF PAGES	7b. NO. OF REFS
March 1967	202	21

8a. CONTRACT OR GRANT NO.	9a. ORIGINATOR'S REPORT NUMBER(S)
AF33(615)-1598	AFML-TR-67-139 Pt I
b. PROJECT NO. 7312	
c. Task No. 731201	9b. OTHER REPORT NO(S) (Any other numbers that may be assigned this report)
d.	RDR 1380-6

10. AVAILABILITY/LIMITATION NOTICES This document is subject to special export controls and each transmittal to foreign governments or foreign nationals may be made only with prior approval of the Metals and Ceramics Division (MAM), Air Force Materials Laboratory, Wright-Patterson AFB, Ohio 45433.

11. SUPPLEMENTARY NOTES

12. SPONSORING MILITARY ACTIVITY
Air Force Materials Laboratory, Research & Technology Division, AF Systems Command
Wright-Patterson AFB, Ohio 45433

13. ABSTRACT

The program was designed to originate protective coating concepts for columbium-base alloys for applications in aerospace environments and gas turbine engines. Thermal expansion and oxidation resistance was determined on potential ductile sublayer alloys, MA1 and M Al_3 aluminides, and MSi_2 and M_5Si_3 silicides.

Diffusion barriers between the Ti-Cr modifier and substrate were also evaluated. Coating systems evolved from the studies included the V-(80Cr-20Ti)-Si, (94Mo-5Ti)-Si, Mo-Cr-(Fe-25Cr-5Al) ductile all bcc system, V-(Cr-Ti)-Al-Si and other systems of lesser importance. The V-(80Cr-20Ti)-Si system was the most extensively studied. It exhibited the potential for 500 plus hours of protection at 1600 and 2400 F. This system was extensively evaluated for re-entry (Part II) and turbojet (Part III) applications.

"This abstract is subject to special export controls and each transmittal to foreign governments or foreign nationals may be made only with prior approval of the Metals and Ceramics Division (MAM), Air Force Materials Laboratory, Wright-Patterson AFB, Ohio 45433."

DD FORM 1 JAN 64 1473

UNCLASSIFIED

Security Classification

14. KEY WORDS	LINK A		LINK B		LINK C	
	ROLE	WT	ROLE	WT	ROLE	WT

INSTRUCTIONS

1. ORIGINATING ACTIVITY: Enter the name and address of the contractor, subcontractor, grantee, Department of Defense activity or other organization *(corporate author)* issuing the report.

2a. REPORT SECURITY CLASSIFICATION: Enter the overall security classification of the report. Indicate whether "Restricted Data" is included. Marking is to be in accordance with appropriate security regulations.

2b. GROUP: Automatic downgrading is specified in DoD Directive 5200.10 and Armed Forces Industrial Manual. Enter the group number. Also, when applicable, show that optional markings have been used for Group 3 and Group 4 as authorized.

3. REPORT TITLE: Enter the complete report title in all capital letters. Titles in all cases should be unclassified. If a meaningful title cannot be selected without classification, show title classification in all capitals in parenthesis immediately following the title.

4. DESCRIPTIVE NOTES: If appropriate, enter the type of report, e.g., interim, progress, summary, annual, or final. Give the inclusive dates when a specific reporting period is covered.

5. AUTHOR(S): Enter the name(s) of author(s) as shown on or in the report. Enter last name, first name, middle initial. If military, show rank and branch of service. The name of the principal author is an absolute minimum requirement.

6. REPORT DATE: Enter the date of the report as day, month, year, or month, year. If more than one date appears on the report, use date of publication.

7a. TOTAL NUMBER OF PAGES: The total page count should follow normal pagination procedures, i.e., enter the number of pages containing information.

7b. NUMBER OF REFERENCES: Enter the total number of references cited in the report.

8a. CONTRACT OR GRANT NUMBER: If appropriate, enter the applicable number of the contract or grant under which the report was written.

8b, 8c, & 8d. PROJECT NUMBER: Enter the appropriate military department identification, such as project number, subproject number, system numbers, task number, etc.

9a. ORIGINATOR'S REPORT NUMBER(S): Enter the official report number by which the document will be identified and controlled by the originating activity. This number must be unique to this report.

9b. OTHER REPORT NUMBER(S): If the report has been assigned any other report numbers *(either by the originator or by the sponsor)*, also enter this number(s).

10. AVAILABILITY/LIMITATION NOTICES: Enter any limitations on further dissemination of the report, other than those imposed by security classification, using standard statements such as:

(1) "Qualified requesters may obtain copies of this report from DDC."

(2) "Foreign announcement and dissemination of this report by DDC is not authorized."

(3) "U. S. Government agencies may obtain copies of this report directly from DDC. Other qualified DDC users shall request through _____."

(4) "U. S. military agencies may obtain copies of this report directly from DDC. Other qualified users shall request through _____."

(5) "All distribution of this report is controlled. Qualified DDC users shall request through _____."

If the report has been furnished to the Office of Technical Services, Department of Commerce, for sale to the public, indicate this fact and enter the price, if known.

11. SUPPLEMENTARY NOTES: Use for additional explanatory notes.

12. SPONSORING MILITARY ACTIVITY: Enter the name of the departmental project office or laboratory sponsoring *(paying for)* the research and development. Include address.

13. ABSTRACT: Enter an abstract giving a brief and factual summary of the document indicative of the report, even though it may also appear elsewhere in the body of the technical report. If additional space is required, a continuation sheet shall be attached.

It is highly desirable that the abstract of classified reports be unclassified. Each paragraph of the abstract shall end with an indication of the military security classification of the information in the paragraph, represented as *(TS)*, *(S)*, *(C)*, or *(U)*.

There is no limitation on the length of the abstract. However, the suggested length is from 150 to 225 words.

14. KEY WORDS: Key words are technically meaningful terms or short phrases that characterize a report and may be used as index entries for cataloging the report. Key words must be selected so that no security classification is required. Identifiers, such as equipment model designation, trade name, military project code name, geographic location, may be used as key words but will be followed by an indication of technical context. The assignment of links, rules, and weights is optional.